HARNESSING ONCOLYTIC VIRUS-MEDIATED ANTI-TUMOUR IMMUNITY

By

Chantal Lemay

A thesis submitted in partial fulfillment of the requirements for the degree of

Doctor of Philosophy, Specialization in Biochemistry

University of Ottawa

Faculty of Medicine

May 24, 2012

Supervisor

Dr. John C Bell, PhD

Abstract

Treatment of permissive tumours with the oncolytic virus (OV) VSV-Δ51 leads to a robust anti-tumour T cell response, which contributes to efficacy; however, many tumours are not permissive to *in vivo* treatment with VSV-Δ51. In an attempt to channel the immune stimulatory properties of VSV-Δ51 and broaden the scope of tumours that can be treated by an OV, a potent oncolytic vaccine platform was developed, consisting of tumour cells infected with VSV-Δ51. I demonstrate that prophylactic immunization with this infected cell vaccine (ICV) protected mice from subsequent tumour challenge, and expression of GM-CSF by the virus (VSVgm-ICV) increased efficacy. Immunization with VSVgm-ICV in the VSV-resistant B16-F10 model induced maturation of dendritic cells, natural killer (NK) cells, and T cells. I demonstrate that this approach is robust enough to control the growth of established and spontaneous tumours. This strategy is broadly applicable because of VSV's extremely broad tropism, allowing nearly all cell types to be infected at high MOIs *in vitro,* where the virus replication kinetics outpace the cellular IFN response. It is also personalized to the unique tumour antigen(s) displayed by the cancer cell.

Histone deacetylase inhibitors (HDIs) can augment viral replication, making them particularly interesting complements to OV therapy. However, the impact of HDIs on the generation and re-stimulation of immune responses remains to be clearly elucidated. Along with my collaborators at McMaster University, I demonstrate that MS-275, but not SAHA, selectively depletes naïve and regulatory lymphocytes. Memory lymphocytes that are being boosted remain unscathed and even have enhanced cytokine production, potentially as a

consequence of the depleted lymphocyte compartment. This leads to a delay in anti-VSV neutralizing antibodies and T cell responses. Interestingly, HDI treatment of B16-F10 cells appears to inhibit VSV replication but allows for a longer persistence within the tumour. When used in an oncolytic prime/boost vaccination model, MS-275 potently enhanced survival. Though the anti-tumour immune response is enhanced, a near complete reduction in autoimmune vitiligo is observed with MS-275 administration. Therefore, this HDI uniquely modulates the immune response to enhance anti-tumour immunity and decrease the anti-viral response, while also decreasing autoimmune sequelae.

Acknowledgements

I would like to thank my supervisor Dr. John Bell for his support, words of wisdom, and encouragement, even when the immunology was threatening to drown us both. As well, I must thank Dr. Kelley Parato for being my immunology mentor and for always knowing the perfect thing to say when I needed it.

I would also like to thank everyone in the Bell/Auer/Atkins labs for their continued support, technical assistance, and good times. Special thanks to Theresa and Christiano for their help with animal work, Lee for helping me do a chromium release assay, and definitely Julia for her boundless encouragement, comfort in tough times, and willingness to help. Together you have all made this a journey to enjoy instead of an obstacle to overcome.

In addition, I would like to thank my family. Their unfaltering enthusiasm and encouragement made this possible. Lastly, I thank Dan for everything. His support, understanding, care, and love continue to bring me strength and warmth.

Table of Contents

List of Abbreviations

Ab = Antibody
ACT = Adoptive cell transfer
ADCC = Antibody dependent cytotoxicity
APC = Antigen presenting cell
ATP = Adenosine triphosphate
BCG = Bacillus calmette-guerin
BM = Bone marrow
BM-DC = Bone marrow-derived dendritic cell
CD = Cluster of differentiation
CDC = Complement dependent cytotoxicity
CFSE = Carboxyfluorescein succinimidyl ester
CTLA4 = Cytotoxic T-lymphocyte antigen 4
DAMP = Damage associated molecular pattern
DC = Dendritic cell
DCT = dopachrome tautomerase
EGFR = Epidermal growth factor receptor
FLuc = Firefly luciferase
GFP = Green fluorescent protein
GM-CSF = Granulocyte-monocyte colony stimulating factor
HDAC = Histone deacetylase
HDI = Histone deacetylase inhibitor
HLA = Human leukocyte antigen
HMGB1 = High mobility group protein B1
HSV = Herpes simplex virus
ICV = Infected cell vaccine
IDO = Indoleamine 2,3-dioxegenase
IFN = Interferon
IHC = Immunohistochemistry
IL = Interleukin
IP = Intraperitoneal
irrB16 = gamma-irradiated B16-F10 cells
IV = Intravenous
LIGHT = TNFSF14, homologous to **L**ymphotoxins exhibits **I**nducible expression and competes with HSV **G**lycoprotein D for **H**VEM, a receptor expressed by **T**-lymphocytes
MDSC = Meyloid-derived suppressor cells
MHC = Major histocompatibility complex
MISIIRTAg = Muellerian inhibiting substance type II receptor promoter driving the SV40 large T antigen

MOI = Multiplicity of infection
NDV = Newcastle disease virus
NK = Natural killer
ORFV = Orf virus
OV = Oncolytic Virus
OVA = Ovalbumin
PAMP = pathogen associate molecular pattern
PBMC = Peripheral blood mononuclear cells
PBS = Phosphate-buffered saline
PCR = Polymerase chain reaction
Pfu = Plaque forming units
PRR = Pattern recognition receptors
RFP = Red fluorescent protein
SMNC = Splenic mononuclear cells
TAA = Tumour associated antigen
TAP = Transporters associated with antigen processing
TDLN = Tumour-draining lymph node
TGFβ = Transforming growth factor β
TIL = Tumour infiltrating lymphocyte
TK = Thymidine kinase
TLR = Toll-like receptor
TNF = Tumour necrosis family
TRAIL = TNF-related apoptosis inducing ligand
Treg = Regulatory T cell
VACV = Vaccinia virus
VEGF = Vascular endothelial growth factor
VSV = Vesicular stomatitis virus
VSVgm = VSV-Δ51-GMCSF
WT or wt = Wild type
β-gal = β-galactosidase

List of Figures and Illustrations

1 Introduction

1.1 Cancer

In Canada, 40% of women and 45% of men will develop cancer during their lifetime, and approximately 1 in 4 Canadians will die from cancer(1). These shocking statistics reveal the devastating effect this disease has on our society and why research into better therapeutics is important.

The overarching definition of a cancer cell is one that gains the ability, through genetic and epigenetic alterations, to grow and divide uncontrollably(164). However, this process is far from simple. Tumorigenesis requires mutations to occur in genes involved in crucial checkpoint, survival, and metabolic pathways, among others, to allow for the evolution of a malignant cellular collective(66, 164). This collective is shaped and evolves through its requirements for oxygen, nutrients, and waste disposal. In addition, cells that can evade death or senescence signals are selected for, which ultimately leads to cells that are sufficient in growth signals and unresponsive to the natural mechanisms that regulate cellular growth and death(66). In 2000, Hanahan and Weinberg(65) formulated and described a list of the known hallmarks that characterize malignant cells. Since then, many breakthroughs have helped refine and expand these hallmarks, allowing for a more in-depth understanding of the cellular and systemic processes that are often implicated in cancer initiation and progression(66).

1.2 Cancer Immune Surveillance

Though the immune system was previously thought to be a driving force in tumorigenesis through the workings of chronic inflammation(30), it is now also seen as a

vital source of natural anti-tumour defences that must be overcome or suppressed during neoplastic transformation(85, 155, 160). Research into cancer immunoediting, the process of shaping the cancer cell collective through immune pressures, has made great strides in detailing mechanisms of anti-tumour immune functions and immune resistance employed by tumours.

It is now widely understood that the immune system has multiple tools in its arsenal against cancer. Though the immune system can detect and kill tumour cells, this has the potential to select for variants that are more immune evasive and suppressive. This reciprocal interplay between the immune system and cancer is termed cancer immunoediting and has been divided into three distinct steps known as the three Es: elimination, equilibrium, and escape(160) (**Figure 1.1**). The initial step of elimination describes the process of immune surveillance, whereby the immune system can recognize nascent tumours and exert various effector functions to suppress or kill these cells(39). It is hypothesized that this occurs at a low background rate and is corroborated by data of immunosuppressed patients having a higher rate of cancer incidence(22). Recognition of cancer cells can be through the release of endogenous damage-associated molecular patterns (DAMPs)(53), the increase in activating natural killer (NK) cell ligands or the decrease in inhibitory NK ligands (26, 114), and the expression of altered self-proteins that can be recognized by cells of the adaptive immune system(24).

Dendritic cells (DCs) and other antigen presenting cells (APCs) will generally initiate the process of immune surveillance through the phagocytosis of dying tumour cells. However, DCs require danger signals to initiate their activation and maturation(48). Danger signals can be DAMPs or pathogen-associated molecular patterns (PAMPs) that ligate

Figure 1.1 – The three Es of cancer immunoediting

Overview of the impact that the immune system has on cancer progression and clearance. In the "elimination" phase, innate and adaptive immune effectors recognize nascent tumours based on tumour antigens and activating NK cell ligands. This then leads to tumour cell destruction. Non-immunogenic tumour cells are selected for and eventually escape and suppress immune surveillance mechanisms. Reproduced with permission from Vesely *et al*(160)

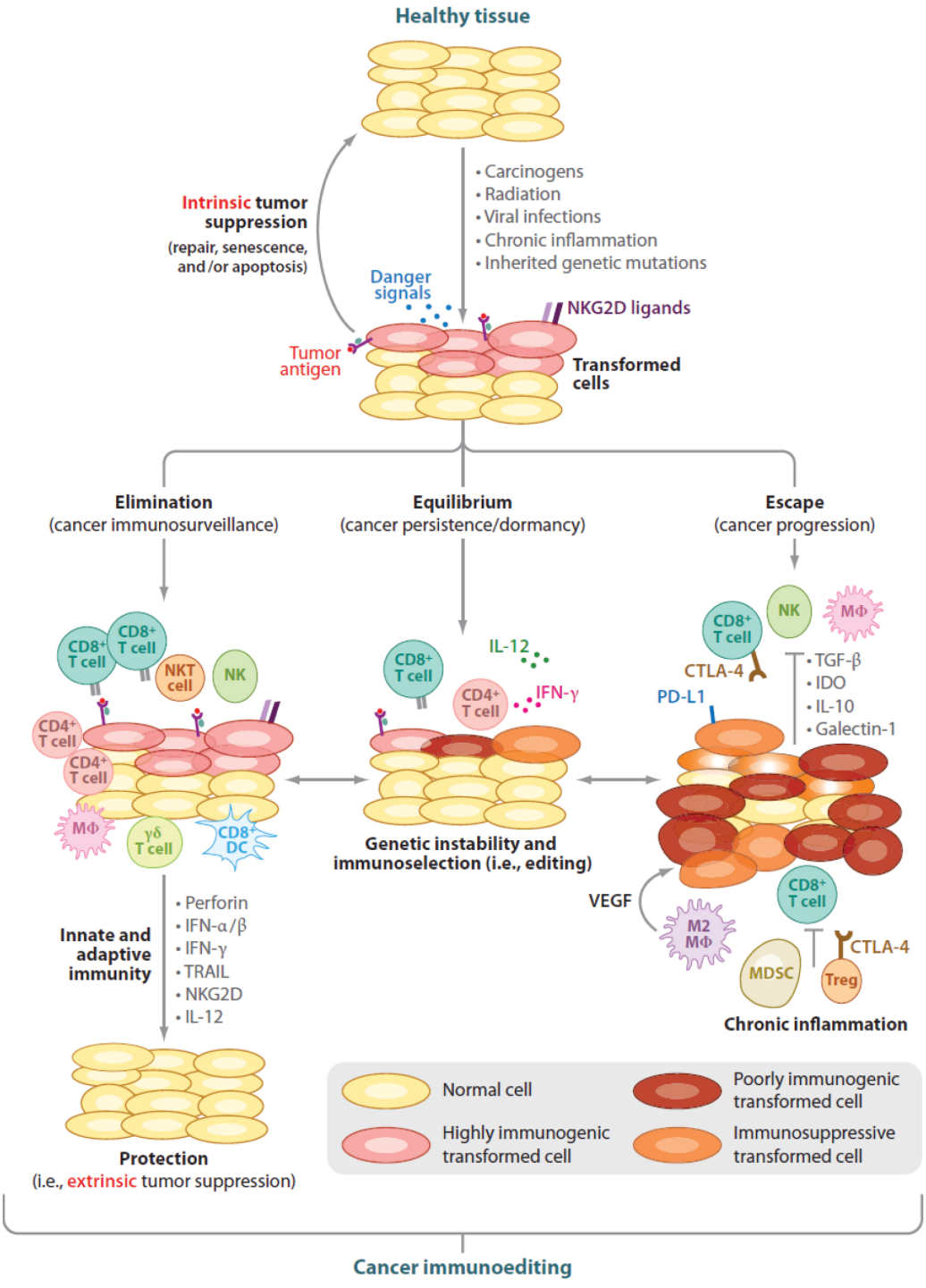
Healthy tissue
• Carcinogens
• Radiation
• Viral infections
• Chronic inflammation
• Inherited genetic mutations
Intrinsic tumor suppression
(repair, senescence, and/or apoptosis)
Danger signals
NKG2D ligands
Tumor antigen
Transformed cells
Elimination
(cancer immunosurveillance)
Equilibrium
(cancer persistence/dormancy)
Escape
(cancer progression)
CD8+ T cell
CD8+ T cell
NKT cell
NK
CD4+ T cell
CD4+ T cell
MΦ
γδ T cell
CD8+ DC
IL-12
CD8+ T cell
CD4+ T cell
IFN-γ
Genetic instability and immunoselection (i.e., editing)
NK
MΦ
CD8+ T cell
CTLA-4
PD-L1
• TGF-β
• IDO
• IL-10
• Galectin-1
VEGF
M2 MΦ
CD8+ T cell
MDSC
Treg
CTLA-4
Chronic inflammation
Innate and adaptive immunity
• Perforin
• IFN-α/β
• IFN-γ
• TRAIL
• NKG2D
• IL-12
Protection
(i.e., extrinsic tumor suppression)
Normal cell
Poorly immunogenic transformed cell
Highly immunogenic transformed cell
Immunosuppressive transformed cell
Cancer immunoediting

pattern recognition receptors (PRRs) on or in DCs(53, 152). Without such activating signals, the DC does not upregulate the expression of co-stimulatory molecules such as CD40, CD80, and CD86, nor does it secrete pro-inflammatory cytokines such as IL-12 and interferons (IFN)(9). In addition, though the immature DC expresses low levels of MHC class I and II, these are upregulated following maturation, to further promote antigen presentation to T cells. Without the presence of danger signals, uptake of tumour cells by DCs can lead to either no antigen presentation or a tolerogenic/suppressive T cell response(48). Ideally, DCs will phagocytose dying tumour cells that are releasing DAMPs like HMGB1 or ATP, which lead to proper DC maturation and movement to the draining lymph node(53) (**Figure 1.2**). The DC digests tumour proteins and presents these as peptides on both MHC class I and II along with co-stimulatory molecules. In addition, the release of pro-inflammatory cytokines such as IL-12 and type I IFNs allows for proper T cell maturation(9). From here, the DC interacts with $CD4^+$ T helper cells, which release important cytokines and survival signals. These "license" the APC to continue driving the pro-inflammatory process, and $CD8^+$ effector cells, which gain the ability to secrete cytokines such as TNFα and IFNγ, and kill tumour cells in an antigen-dependent manner(48, 57). These DCs can also enhance NK cell responses through the release of IL-2, IL-12, IL-15, and type I IFNs(15, 53).

Many immune effectors have means to recognize and kill tumour cells. NK cells recognize the increase in activating ligands, like NKG2D ligands, which can be induced through bacterial or viral infection or through cellular transformation(114). They also recognize the loss of inhibitory ligands, like MHC class I, which is the basis of the "missing self" hypothesis(163). The role of B cells in anti-tumour surveillance is still quite controversial, with reports indicating both pro- and anti-tumour activities. However, there is

Figure 1.2 – The generation of an anti-tumour immune response

Simplified diagram from Gabrilovich *et al*(48) demonstrating the process of generating a T cell anti-tumour immune response. Dendritic cells must phagocytose dying tumour cells and become activated, upregulating MHC II and co-stimulatory molecules. These DCs must then traffic to draining lymph nodes and present antigen to tumour-specific CD4 and CD8 T cells, leading to the T cell activation and cytokine secretion. This process licences the CD8 T cells that can now traffic to the tumour and kill the tumour cells in an antigen-dependent manner. Reproduced with permission.

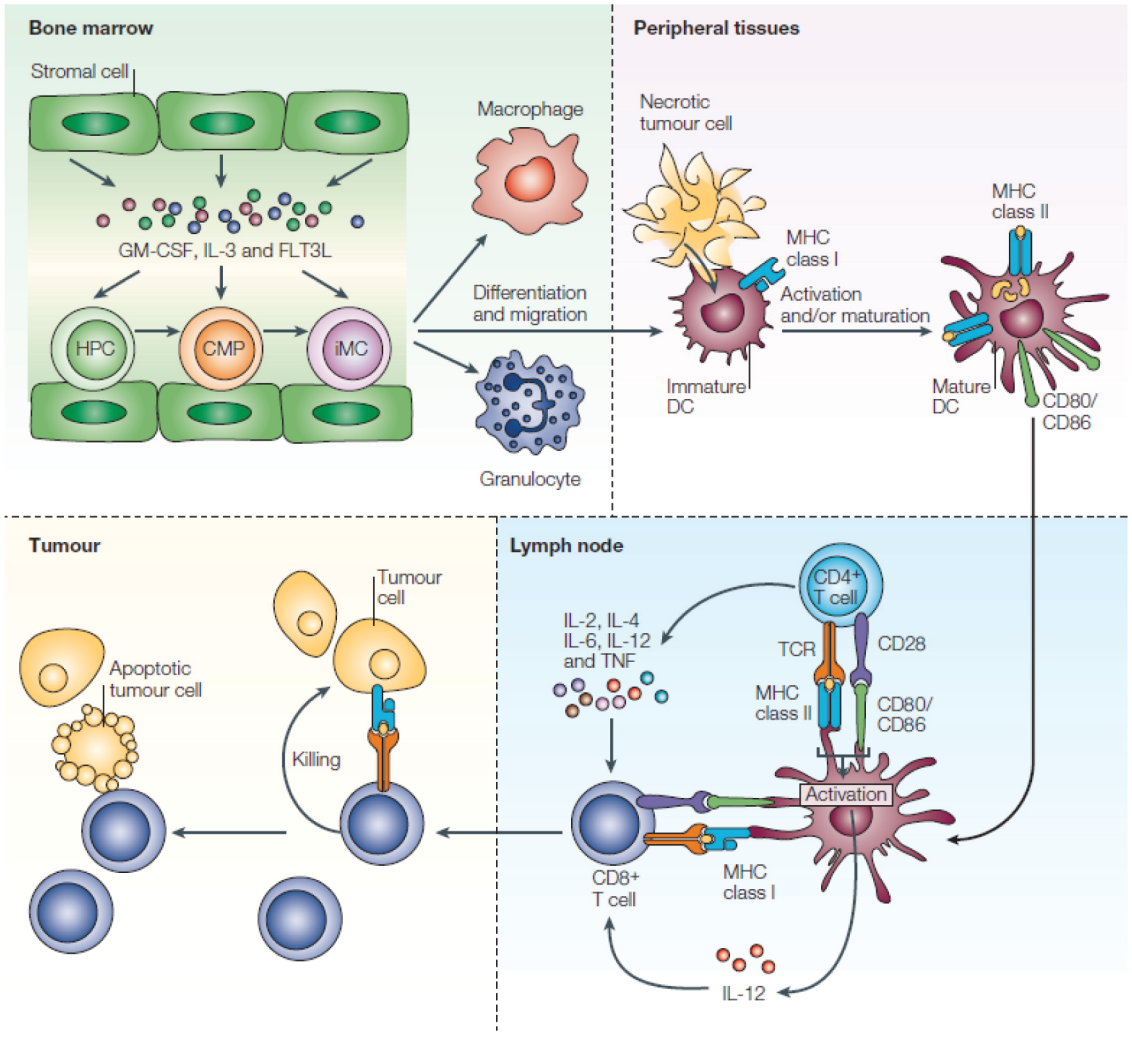
Bone marrow
Stromal cell
GM-CSF, IL-3 and FLT3L
HPC
CMP
iMC
Macrophage
Granulocyte
Differentiation and migration
Peripheral tissues
Necrotic tumour cell
MHC class I
Activation and/or maturation
Immature DC
MHC class II
Mature DC
CD80/ CD86
Tumour
Tumour cell
Apoptotic tumour cell
Killing
Lymph node
CD4+ T cell
IL-2, IL-4 IL-6, IL-12 and TNF
TCR
CD28
MHC class II
CD80/ CD86
Activation
CD8+ T cell
MHC class I
IL-12

evidence that B cells can play an important role in the rejection of cancer. One study found that B16-F10 tumours grew faster in B cell depleted hosts. B cells have been observed to be APCs that lead to $CD8^+$ T cell stimulation, produce anti-tumour antibodies, and even lead to direct cytotoxicity, though the mechanism of killing in not known. Tumour-specific antibodies can lead to cancer cell death through the blockade of important cellular receptors, antibody-dependent cytotoxicity (ADCC), or complement-dependent cytotoxicity (CDC)(113). Activated $CD8^+$ T cells recognize tumour cells based on the expression of altered proteins that are presented via MHC class I. Genetic mutations that arise due to genetic instability are an important source of tumour associated antigens (TAAs), which in some cases can lead to tumour-specific immune responses(24). These TAAs are important targets as most proteins in tumours are "self" antigens, subject to tolerance mechanisms that limit immune reactivity towards them(23).

Though NK cells and $CD8^+$ T cells recognize their targets in very different ways, they both kill tumour cells using similar mechanisms. The release of perforin from the immune effectors forms a pore in the target cell. This allows the entry of Granzyme B, a proteolytic enzyme that activates caspases, thereby initiating apoptosis(154). In addition, both NK and $CD8^+$ T cells can express FasL and TRAIL(26, 160) on their surface and ligate cognate death receptors on their targets to initiate apoptosis. Also, both NK and T cells produce an array of cytokines that have immune modulating and direct anti-cancer functions. Interferon gamma (IFNγ), the only type II IFN, is a very important cytokine with potent anti-tumour effects and is widely produced by activated NK and T cells, among others. This cytokine targets tumour cells as well as the tumour's stromal counterparts, such as endothelial cells and immune cells. Through direct interaction with tumour cells, IFNγ has been demonstrated to increase

MHC class I expression(78, 136), thereby augmenting tumour cell immunogenicity and potential interaction with T cells. There is evidence of anti-proliferative effects, through the induction of cell cycle inhibitors, as well as pro-apoptotic effects, through the induction of caspases, Fas, and FasL. In addition, IFNγ can induce the production of chemokines like CXCL9 and CXCL10, attracting T cells, NK cells, DCs, and macrophages(99) and leading to anti-angiogenic effects on endothelial cells(39). Finally, IFNγ is vital to the skewing of the immune response towards a Th1 pro-inflammatory phenotype(39). The exact immune response required to clear a tumour will likely strongly depend on the exact genetic and antigenic characteristics of the tumour and the host's immune system.

Type I IFNs (IFNα and IFNβ especially) also play an important role in cancer rejection and are produced by most cells following ligation of PRRs by viral or bacterial components. Type I IFNs can lead to increased DC phagocytosis, maturation, and antigen presentation, in addition to increasing B cell maturation and antibody production. These cytokines also enhance NK cell effector functions. It is thought that these IFNs target the hematopoietic system as opposed to tumour cells directly, however, there have been observations of increased sensitivity to apoptosis and antiangiogenic effects that could also play a role in tumour control(159). In addition, type I IFNs can upregulate MHC class I expression, making them more visible to T cell scrutiny(134).

1.3 Cancer immune subversion and escape

Though the immune system has means of recognizing and killing tumour cells, it is not always successful in halting the progression of the disease. Cancer is rapidly evolving and, consequently, it can adapt to the immune pressures to continue to survive. It is postulated that during this period of adaptation there is a moment of balance between tumour growth

and immune-mediated killing. This is referred to as the equilibrium phase by Schreiber *et al* and can correlate with an apparent dormancy in the tumour(39, 85).

The elimination and equilibrium phases of immunoediting generally occur before diagnosis, potentially taking years to progress. However, a growing tumour commonly represents a malignant collective that has adapted to the immune system. It has been shaped through the natural selection of cancer cell variants that could grow and survive in the presence of an immune response(39). This is achieved through many mechanisms, and though many of these immune resistance mechanisms have been examined and described in the literature, there are certainly many more that remain to be discovered. A common mechanism of adaptive immune evasion is the downregulation of the antigen presentation machinery. A large body of research demonstrates that anywhere from 40-90% of tumours lack HLA class I molecules(39), in addition to common losses in the pathways required for proper antigen presentation. These include the transporters associated with antigen processing (TAP) molecules, immunoproteasome components, and IFN receptors that can lead to the induction of antigen presentation(58, 128, 160, 179, 180). However, the loss of MHC molecules should lead to a heightened sensitivity to NK-mediated recognition on the basis of the "missing self" hypothesis(62, 163). For NK cell recognition and killing, in addition to a loss of inhibitory receptors like MHC class I, target cells must express activating receptors induced through cellular stress, transformation, or infection. As well, Toll-like Receptor (TLR) ligands and pro-inflammatory cytokines such as type I and II IFNs and IL-2 increase the potential for NK activation(15, 62). These requirements allow a window of opportunity for tumour cells to adapt. It follows that the downregulation of NK cell activating receptors(160), in addition to a loss in the expression of pro-inflammatory

cytokines like type 1 IFNs, has been noted in many tumour types(153). Another way of thwarting the apoptosis inducing mechanisms of many immune cells is through the production of decoy death receptors, the acquisition of mutations leading to defective death receptors, or mutations in the apoptosis cascade leading to an anti-apoptosis bias(160, 180).

Cancers can also employ immune suppressive tactics, producing anti-inflammatory or regulatory proteins that thwart immune-mediated anti-tumour destruction. Transforming Growth Factor beta (TGFβ)(126) and IL-10(160) are commonly expressed by tumour cells and play an important role in inhibiting immune cell activation or maintenance of activation. Tumour-derived TGFβ represses DCs, NK cells, T cells, and macrophages. It reduces cytokine secretion and proliferation of these cells and reduces responsiveness to the important survival cytokine IL-2(126). IL-10 inhibits Th1 pro-inflammatory T cell functions, including cytokine secretion and proliferation, and it downregulates MHC expression on tumour cells. In addition, TGFβ and IL-10 can work together to promote regulatory T cell (Treg) generation from an effector T cell(62).

Other commonly employed immunosuppressive tactics include the production of molecules that impede upon the maintenance of T cell activation and survival. One such molecule is indoleamine 2,3-dioxygenase (IDO), which catalyzes the breakdown of tryptophan, an essential amino acid for T cells, into kynurenine, a toxic metabolite to T cells. This leads to the inhibition of $CD8^+$ T cell functions and proliferation and the apoptosis of $CD4^+$ T cells(62, 180). Other immune suppressive molecules are the programmed cell death ligands (PDL-1 and PDL-2), which bind to the programmed cell death receptor (PD-1) on T cells, inducing their anergy(157). Indeed, tumours often express the PD-1 ligands, and their expression correlates with poor prognosis in cancer patients(62).

Through the secretion of chemokines and anti-inflammatory proteins, tumours also induce the recruitment of suppressive cells, like Tregs, myeloid-derived suppressor cells (MDSCs), and M2 macrophages(128). M2 macrophages can be induced through the expression of anti-inflammatory proteins, like IL-4 and IL-13, and recruited through chemokines such as Vascular Endothelial Growth Factor (VEGF). These suppressive macrophages secrete TGFβ and IL-10, as well as Platelet-derived Growth Factor (PDGF) and VEGF, which promote angiogenesis(160). These are in contrast to the tumouricidal M1 macrophages that secrete IL-12 and TNFα(148, 180). M2 macrophages also secrete CCL22, which recruits Tregs(148).

Recently there have been observations of two types of regulatory T cells, either natural or induced (nTregs or iTregs), though both express the transcription factor X-linked forkhead/winged helix transcription factor 3 (Foxp3). nTregs mature in the thymus and retain their suppressive function throughout their life cycle. In contrast, iTregs are generated from naïve T cells that receive weak ligation of their T cell receptor (TCR) without co-stimulation but with suppressive cytokine stimulation(62). Other regulatory T cell subsets have been proposed, and the various immune suppressive strategies described to date might represent the heterogeneity in this population. However, all regulatory T cells appear to create a tolerogenic environment within the tumour, inhibiting T cell, NK cell, and DC functions(32). This is achieved by the production of TGFβ and IL-10 and the competitive consumption of IL-2 and ATP(128). They also inhibit DC activation by expressing inhibitory ligands for receptors on DCs, such as CTLA4, which binds CD80 and CD86(180, 181). Tregs have also been observed directly killing DCs and T cells through perforin and Granzyme release(181).

Lastly, there are the myeloid-derived suppressor cells (MDSCs), which represent a heterogeneous population of immature myeloid cells that suppress T cell functions through both antigen-dependent and independent means. They deplete arginine and secrete reactive oxygen species, to which effector T cells have a heightened sensitivity that leads to their anergy or apoptosis(62, 128, 148). MDSCs also produce TGFβ and IL-10(62), reflecting the critical role of these cytokines.

1.4 Cancer Immunotherapy

Though cancers evolve mechanisms to evade and suppress the immune system, there are indications that productive anti-tumour immune responses can occur and have a large benefit. A landmark study by Galon *et al* demonstrated that a Th1-biased immune cell infiltration was more prognostic of patient survival than the currently used histological methods in colorectal cancer(49). Many studies have investigated other cancer types and found similar prognostic value of $CD8^+$ T cells(112, 140, 146) and NK cells(47, 170). This suggests that the immune system can have a large impact on tumour progression and that, across multiple tumour types, patients that have a strong immune effector presence in their tumour will fare better than those that do not.

With this in mind, the goal of cancer immunotherapy is to initiate, restore, or augment these natural immune mechanisms to mediate tumour rejection(109). If successful, immunotherapy leads to the induction of immunological memory that can not only lead to ongoing tumour clearance, but also protect from future recurrence(93). For the purposes of this introduction, immunotherapeutic interventions will be divided into specific or non-specific.

1.4.1 Non-specific cancer immunotherapy

Non-specific cancer immunotherapies are those that seek to generally augment various aspects of the immune system to lead to a greater anti-tumour immune response. This includes the use of immune stimulatory cytokines, like IL-2 and IFNα, which are already in use in the clinic(109, 167). Other cytokines are in clinical testing, like GM-CSF and IL-21, which seek to enhance APC and T cell activation, respectively. However, all of these treatments induce serious side-effects that, in some cases, can limit treatment use(167). The use of monoclonal antibodies and single chain antibodies as either agonists or antagonists has also become quite popular. Agonistic antibodies have been made against the pro-inflammatory receptor CD40, to boost APC function and promote a more robust T cell response. In addition, agonists to OX40, which boost T cell activation and survival, have been produced and are in clinical testing(167, 169).

Antagonistic antibodies are also being investigated for the ability to block important immune regulatory receptors, the most well-known of which is CTLA-4. Blockade of CTLA-4 with the clinical candidate ipilimumab is thought to unrestrain effector T cell functions while inhibiting Treg functions. Ipilimumab demonstrated modest responses in clinical testing and was granted FDA approval in March 2011 for use in metastatic melanoma, however, on-target toxicities from systemic inflammation can be severe(109). Though responses were modest, ipilimumab is the first treatment to deliver a survival benefit in advanced metastatic melanoma(93). Many other antibodies are being developed to trigger activating receptors like 4-1BBL or to antagonize inhibitory receptors like PD-1 and IDO(109).

Another strategy uses TLR agonists to deliver a danger signal to the immune system, thus potentially helping to prime a more robust anti-tumour immune response. The use of Bacillus Calmette-Guérin (BCG) is a common treatment in bladder cancer(109) and imiquimod, a TLR7 agonist, has been used in clinical testing as well, though it demonstrates limited efficacy(125).

1.4.2 Targeted cancer immunotherapy: lymphocyte adoptive cell transfer

Specific, or targeted, immunotherapies seek to generate or enhance a tumour-specific immune response through the use of vaccination or adoptive cell transfer (ACT) protocols. ACT using tumour infiltrating lymphocytes (TILs) has been most commonly used and has largely been developed by Dr. Rosenberg and colleagues. Though still in clinical testing, significant responses have been observed, mostly in metastatic melanoma, with up to 50 percent of patients having objective responses. The treatment consists of harvesting tumour sections, isolating lymphocytes and culturing these with tumour cells, and then assessing which lymphocytes are tumour-reactive by cytokine secretion analysis. These tumour-reactive cells are expanded in culture and then re-infused into the patient. Unfortunately, this process takes 4-5 weeks, making it quite costly. In addition, the patient is lymphodepleted prior to infusion and then treated with pro-inflammatory cytokines to better encourage cell engraftment(109, 138). The cost and time that this protocol requires is prohibitive, and strategies to reduce the culturing time or the amount of lymphodepletion and total body irradiation are currently under investigation.

Strategies to alter the T cell specificity have been developed, most notably through the use of virally-transduced T cell receptors, bi-valent antibodies, or chimeric antigen receptors. These approaches allow peripheral blood T cells to be harvested and their antigenic affinity

re-targeted to the tumour. Chimeric antigen receptors allow T cells to recognize tumour targets through an antibody in addition to their native T cell receptor and have achieved encouraging results in neuroblastoma and lymphoma(138).

Adoptive transfer of NK cells has also been investigated as a cancer treatment. NK cells can be expanded and activated *in vitro* through the use of feeder layers and the pro-survival cytokines IL-15 and IL-2. In addition, it is hypothesized that NK cells mediate graft versus leukemia rejection during haploidentical bone marrow transfer. Consequently, allogeneic NK cells have also been examined and found to be able to mediate anti-tumour killing. However, both of these methods are fraught with the same issues as with the T cell ACT. They require time- and cost-consuming *in vitro* expansion protocols to generate pure, specific, and activated cells for transfer. An option that might lower this cost is the use of NK cell lines instead of allogeneic cells, however, the efficacy and feasibility of this approach still need to be demonstrated(26).

1.4.3 Targeted cancer immunotherapy: dendritic cell adoptive transfer

The use of autologous DCs is also being investigated with various protocols currently in use. The assumption is that there is insufficient PRR stimulation *in vivo* when DCs naturally encounter tumour antigens, which leads to the induction of tolerance. Through the *ex vivo* culturing, loading, and priming of DCs, the optimal APC can be generated to produce potent innate and adaptive responses following infusion. However, it is still unclear what culture conditions lead to the most robust and long-lived DCs. Though most protocols use cytokines for maturation, the use of TLR agonists seem to be more effective. Indeed, the maturation of DCs *in vivo* is a complex and concerted process, and recent data indicate that different PRRs can initiate different maturation phenotypes. It is important that the DCs generated express

co-stimulatory molecules (CD40, CD80, CD86), secrete cytokines (IL-12 and type I IFNs), and express the chemokine CCR7, which allows for trafficking to the draining lymph node. In addition, antigen presentation through both MHC class I and class II will allow for "licencing" by $CD4^+$ T cells, which enhances cytokine secretion, and interaction with $CD8^+$ T cells(57). In addition to priming T cell responses, DCs can prime NK cell responses. The expression of type I IFNs by DCs enhances NK cytotoxicity, the expression of IL-12 and IL-18 enhances IFNγ production by NK cells, and the trans-presentation of IL-15 by DCs enhances NK survival. As a consequence of MHC upregulation, activated DCs also become protected from NK-mediated killing(10).

Developing a maturation protocol for generating DCs is only half the battle, and the choice of antigen can have a significant impact on the outcome of DC adoptive transfer strategies. Several approaches to antigen selection and loading have been investigated, and no clear winner has been declared to date. Some researchers have opted for loading DCs with only one or very few tumour antigens, while others have examined the use of whole tumour cell lysates; each approach has pros and cons. The use of a few TAAs allows for a closer examination of the immune response in the patient following vaccination, because there only a few epitopes, which have already been defined, to follow. However, tumours are genetically unstable and demonstrate a large diversity in their antigens, both between tumours(67) and even within a given tumour(52). This heterogeneity must inform how cancer vaccines are made, but the full examination of the antigen pool of every tumour is not feasible. Therefore, if only one or a few TAA are used, it is possible that the antigens chosen for immunization will not represent viable targets in all patients. A meta-analysis of 173 publications determined that vaccination with whole tumour lysates produced a larger

clinical response than with one or a few antigens only(109). There are several possible reasons for this. Presenting multiple tumour antigens allows for the potential to target multiple cancer cells, decreasing the likelihood of escape variants. In addition, this strategy allows for the presentation of both $CD4^+$ and $CD8^+$ T cell epitopes, which could lead to stronger responses. Also, using whole tumour cells as the antigen source bypasses the need to determine the specific antigens found in each patient's tumour. Consequently, many researchers have attempted to use whole tumour cells to load DCs. However, this is not the end of the story. The means by which these tumour cells are killed has also been determined to be an important factor in the DC maturation process and subsequent efficacy(68).

The DC-based cancer immunotherapy Provenge received FDA approval in April 2010 and received a lot of attention for being the first specific cancer immunotherapy to receive approval. This treatment consists of a mixture of autologous, peripheral blood mononuclear cells cultured with a fusion protein of GM-CSF and prostatic acid phosphatase, a prostate cancer antigen. Results from the Phase III clinical trial demonstrated little to no tumour size decrease, though patient survival was increased by 4 months with Provenge treatment. This discrepancy has been widely observed with immunotherapies and is attributed mainly to two factors. The first is that this delay in efficacy reflects the time required to generate an anti-tumour immune response. The second is that this immune response can lead to oedema and inflammation, which can make the tumour appear to be growing when tumour cells are actually being killed. Indeed, this phenomenon was also seen in the ipilimumab (anti-CTLA4 antibody) trial, where 10 percent of patients that were scored as having progressive disease later demonstrated tumour stabilization and even prolonged survival(109).

1.4.4 Targeted cancer immunotherapy: vaccines

Another approach to generating an anti-tumour immune response is to initiate DC priming *in vivo*, by providing a vaccine that delivers relevant TAAs in an inflammatory context. The theory behind vaccination is that the cytokines and helper cells required for proper DC priming and T cell activation are all found *in vivo*. Also, because DC maturation is a stepwise process that remains incompletely understood, it is likely to be most productive in its native environment(119). In addition, vaccination bypasses expensive cell culture procedures required for ACT. There are two components to any vaccine: the antigen and the immune stimulator; each needs to be carefully optimized.

Antigen selection has been discussed in the section regarding the adoptive transfer of DCs and holds true for vaccines as well. Small peptide, whole protein, mRNA, DNA, and whole cell vaccines are all under investigation, though most have shown limited clinical efficacy(61). Though many tumour antigens have been identified, research suggests that most patients have unique tumour antigens as a result of genetic instability, and that many of these unique antigens can elicit protective immune responses if used in a vaccine(16, 24, 52, 67). Interestingly, a recent study also observed variation in antigen expression within a given tumour, demonstrating that generating an immune response against only one antigen may not lead to the complete destruction of an entire tumour(52). The use of allogeneic or autologous tumour cells allows for a more multivalent vaccine. The use of allogeneic tumour cell lines allows for the production of "off-the-shelf" vaccines, however, this approach has generated poor clinical results. This is exemplified by the recent failure of Canvaxin, a mixture of three irradiated allogeneic cell lines mixed with BCG. Though the use of autologous tumour cells adds a level of complexity to vaccine manufacturing, it

appears to generate more meaningful responses. OncoVax, a vaccine composed of irradiated autologous cells mixed with BCG, demonstrated impressive decreases in the risk of recurrence and is currently approved in Europe and Switzerland(61, 93). One of the down-falls of using allogeneic cell lines is that along with the relevant tumour antigens, the patient's immune system is also being presented a myriad of irrelevant proteins. Autologous vaccines present only the proteins that are found within that given tumour.

The immune stimulator must induce the recruitment of APCs to the vaccination site, the engulfment of the antigen components, and then lead to the proper maturation and trafficking of the APC. Finding an adjuvant or protein mixture that can accomplish each of these important steps is currently a challenge, and much of the disappointing results from previous cancer vaccine attempts have been attributed to poor understanding of DC maturation requirements and the use of inadequate adjuvants(61, 93). Viruses have been investigated as vaccine vectors because of their inherent immune stimulatory properties. Indeed viruses are immunogenic, and replicating viruses offer constant PRR stimulation during the infection, which is required to break tolerance in the presence of Tregs(175).

1.5 Oncolytic Viruses

Oncolytic viruses (OVs) are replication-competent, tumour-selective viruses that lead to cancer cell death during their life cycle. Based on early observations in the 1900s of patients having cancer remission following certain viral infections, clinical trials with wild-type viruses were attempted in the middle of the 20th century. Despite promising efficacy, the side-effects of infecting cancer patients with pathogenic viruses led to serious complications(80). The idea of using viruses against cancer was re-visited at the end of the 20th century, when knowledge of viruses and cancer had reached a point that allowed for the

rational choice and design of cancer-specific strains. The oncolytic virus field has progressed rapidly in the last 10 years with important milestones having been reached(17). Many different types of OVs have been developed to date, and clinical trials have begun on a handful of these.

1.5.1 Background on VSV, VACV, and ORFV

Three OVs were used in this thesis work, so they will be discussed to a greater extent in this dissertation. Vesicular Stomatitis Virus (VSV) is a small negative-sense RNA virus of the Rhabdoviridae family. It has five genes: N, P, L, G, and M. The gene product of G, the glycoprotein, determines the tropism of the virus. Its cognate receptor on cells remains elusive; however, it has an extremely broad tropism, able to infect nearly all mammalian cells in addition to insect cells(12, 137). The matrix protein, the M gene product, has been studied extensively for its role in blocking nuclear transport of mRNAs into the cytoplasm, which inhibits the production of antiviral mediators like type I IFNs. A mutant was created with a deletion in methionine 51 of the M protein (VSV-Δ51). It cannot block nuclear export, leading to the release of cytokines from infected cells. In cells that are capable of secreting type I IFNs, which is most or all normal cells, over 300 genes are produced that rapidly blunt the virus life cycle. Interestingly, 80 percent of the NCI 60 panel of human cancer cell lines is unable to respond to type I IFNs, making them susceptible to VSV-Δ51(153).

Vaccinia virus (VACV) and Orf Virus (ORFV) are both poxviruses, having large double stranded DNA genomes with approximately 200 genes. These viruses encode many immune modulatory genes that allow them to inhibit the production or function of common cytokines and chemokines, especially type I IFNs(144). Both of these viruses are able to

infect most, if not all, mammalian cells through the binding of heparin sulfate on target cells(141). Research into VACV safety in humans is extensive as it was effectively used in millions of people worldwide as the vaccine against smallpox and continues to be used in the US military for bioterrorism purposes(115). Many oncolytic strains of VACV have been engineered to allow for tumour-specificity; however, the most common alteration in the clinical candidates is a deletion in the thymidine kinase (TK) gene, forcing the virus to preferentially replicate in cells that are rapidly dividing. In addition, VACV appears to have a natural propensity for cells with an activated epidermal growth factor receptor, and it is estimated that over 90 percent of cancer cells are of this phenotype(121). Clinical investigations with the oncolytic vaccinia mutant JX-594 (Jennerex Biotherapeutics Inc.) has progressed rapidly and demonstrated promising results after intratumoural (IT)(69, 100, 122) and intravenous (IV)(17) administration. Moreover, during the recent clinical testing of IV administration of JX-594, delivery to the tumour and replication within were demonstrated, representing an important milestone for the OV field(17).

Limited research has been performed on ORFV, however, there have been reports of human infections, which all resolve rapidly, demonstrating low human pathogenicity. ORFV has been investigated as a vaccine vector and recently as an oncolytic with the ability to stimulate both DC and NK cell responses(135).

A new wave of targeted therapeutics are being brought to the clinic in the hopes of killing tumour cells in a more specific and robust manner. Though there are a few cancers that are driven by very specific oncogenes, this is not the case for most. Recent work suggests that tumours often have a myriad of mutations, and many are not shared among most cancer patients(24, 52, 67). Instead, there appear to be common pathways that are

affected, but the genes mutated within these pathways vary between people. Therefore, successful cancer treatments will broadly target biological pathways, instead of focusing on one aberrant protein(76). Herein lies the strength of the oncolytic virus platform. These viruses target entire oncogenic pathways, like overactive EGFR signaling or inhibited type I IFN signaling, no matter the specific genetic alterations involved, allowing for broadly targeted and efficient therapeutics.

1.5.2 The multi-modal nature of oncolytic viruses

Oncolytic viruses have emerged as a promising anti-cancer treatment platform able to specifically replicate in and kill cancer cells while leaving normal cells unharmed. Though engineered for tumour-specific lysis, the multi-modal nature of this platform is currently being revealed. Many of these viruses can be delivered systemically to reach distant tumour beds(17), be targeted to induce tumour vascular shutdown (18, 100), and can be engineered to carry genetic payloads. Importantly, pre-clinical and clinical evidence for oncolytic virus-mediated anti-tumour immunity is emerging (108).

Our immune system has evolved to recognize and kill pathogenic intruders. Through the use of many PRRs, the presence of a virus is rapidly recognized, and a strong inflammatory response ensues(171). The premise of using OVs to generate a long-term anti-tumour immune response is to usurp these viral "danger signals" to activate the immune system against the cancer. As previously discussed, the immune system requires two signals. The first signal is the foreign antigen, which in this case is the TAA. The second signal is a molecular signal that warns of tissue stress or pathogen invasion through the ligation of PRRs. Through the encouragement of phagocytosis of dying, infected cancer cells, both signals can be satisfied and immune-mediated tumour destruction can proceed(111).

1.5.3 OVs create the "perfect inflammatory storm"

Many OVs have demonstrated the ability to stimulate dendritic cell (DC) maturation upon incubation with infected tumour cells(14, 42, 51, 72, 130). Likewise, many OVs have been found to stimulate T cell activation(51, 63, 130) and, in some cases, to depend on T cells for efficacy *in vivo(35, 151)*.

In addition, some groups have begun investigating the role and efficacy of oncolytic viruses in stimulating natural killer (NK) cells, with encouraging results. A few OVs, namely Reovirus, Newcastle Disease Virus, parvovirus, VACV, ORFV, and VSV, have demonstrated the ability to stimulate IFNγ secretion and tumouricidal functions by NK cells(11, 15, 27, 75, 131, 135, 173). Specifically, wild-type VSV (wtVSV) leads to innate immune cells secreting IL-28, which acts upon IL-28R-expressing tumour cells and leads to their NK-mediated lysis(173). In addition, VSV-Δ51 infection of DCs leads to the secretion of type I IFNs and IL-15, which stimulates NK cells and leads to *in vivo* efficacy(15).

1.5.4 Pouring Gas on the Fire – OVs and immunotherapies

A popular strategy for boosting the virotherapy-induced anti-tumour immune response is to engineer the virus to express a cytokine or chemokine. Granulocyte/monocyte colony-stimulating factor (GM-CSF) has been the most commonly used, having been engineered into VSV(133), NDV(73), HSV (86, 105), vaccinia strains JX-963(156) and JX-594(121), among others. GM-CSF is potent in the recruitment, maturation, and activation of antigen presenting cells and has been used extensively in vaccine protocols (133, 149). However, many other cytokines and chemokines have been successfully introduced into oncolytic viral genomes, such as IL-12(28, 147), a potent Th1-promoting cytokine that activates NK and T cells, as well as IL-2(74), the T cell chemokine RANTES (CCL5)(91,

94), MIP-1a, FLT3L(40), and interleukin-23(110). These viruses are all found to be more robust than their parental counterparts in the therapeutic treatment of cancer. This strategy manages to harness the strength of the immune system while mitigating side effects that might arise from systemic administration of the cytokine, as seen with IL-2 and vascular leak syndrome(74). OVs will only express these cytokines where they can productively replicate, *i.e.* in the tumour microenvironment.

In addition, OV treatment has been used in conjunction with DC vaccination and adoptive T cell therapy. When preceding DC vaccination, hTERT-Ad is able to induce tumour-specific IFNγ production by splenocytes and lead to better tumour control. This OV-induced inflammation could not be substituted with TLR ligands, demonstrating the strength of the inflammatory response generated by replicating viruses(172). Boudreau *et al* demonstrated that VSV-Δ51 is a potent activator of DCs, and that these VSV-transduced DCs can lead to tumour regression when injected into a tumour-bearing animal. This protocol is even more efficient when VSV is engineered to express the model antigen OVA, and efficacy can be abrogated by the depletion of $CD8^+$ T cells or NK cells(14). As alluded to previously, T cell adoptive therapies are gaining ground as a profound cancer treatment. Though more recent work from Dr. Vile's lab uses T cells as carriers for VSV(87), previous work demonstrates that intratumoural delivery of VSV in conjunction with intravenously delivered tumour-specific T cells could lead to significant tumour control, with 75% of mice demonstrating long term responses(35).

A novel strategy that is gaining momentum is the encoding of TAAs into the OV genome(14, 56, 174). This strategy has been elegantly utilized by Bridle *et al*, in which wtVSV expressing the human melanoma antigen dopachrome tautomerase (hDCT) is used to

boost a pre-existing anti-DCT response generated with a replication deficient adenovirus. This heterologous, antigen-specific boost with an oncolytic vector leads to enormous anti-tumour T cell responses that delay the growth of aggressive B16-F10 brain tumours(21). In addition, by specifically boosting the anti-DCT response with VSV-hDCT, the anti-VSV response is decreased. Another interesting take on this strategy is offered by Kottke *et al*. They have incorporated a cDNA library from a normal human prostate into VSV. Surprisingly, this treatment led to significant prostate tumour control with no autoimmunity(88). In addition, both Bridle *et al* and Kottke *et al* use xenogenic antigens in order to more successfully break tolerance.

2 Materials & Methods

Cell lines and mice

Vero, HeLa, CT26.WT and CT26.LacZ (also known as CT26.CL25) colon carcinoma, 4T1 breast cancer, and B16-F10 melanoma cells were purchased from the American Type Culture Collection. B16-F10.LacZ were a gift from Dr. Anne Chambers. All cells were cultured in HyQ Dulbecco's modified Eagle medium (High glucose) (HyClone) supplemented with 10% fetal bovine serum (CanSera, Etobicoke, Canada). 6048R cells (gift from Dr. Vanderhyden) were grown in αMEM with 10% FBS, 2.08 ug/mL EGF (R&D systems, Minneapolis, MN), 1x of ITSS (Roche), Gentamicin, and Penicillin/Streptomycin (Invitrogen).

Female 6-week old Balb/C, C57BL/6, and CD1 Nude mice were purchased from Charles River Laboratories (Wilmington, MA). Female 8-week old FVB/N MISIIRTAg transgenic mice (line tg4568, a gift from Dr. Vanderhyden) were generated using the transgene described by Connolly *et al(31)*. These mice develop bilateral ovarian tumours of epithelial origin with full penetrance and typically endpoint at 14 weeks of age. All experiments were conducted with the approval of the University of Ottawa Animal Care and Veterinary Service. Tumour area was calculated by multiplying the width by the length of the tumour.

Viruses

VSV-Δ51-GFP , VSV-Δ51-GMCSF, and wtVSV were grown in Vero cells and purified by centrifugation or sucrose gradient banding and centrifugation. VSV-GLess was grown on 293G cells. Virus stocks were aliquoted in PBS, kept at -80˚C, used once, and then discarded. VSV-Δ51-GMCSF was cloned using PCR primers to murine GMCSF and amplified off the pcDNA4.1-GMCSF vector. GM-CSF was cloned into the VSV-Δ51 vector

at the XhoI and NheI sites between the G and L genes and rescued in BHK-T7 cells. Vaccinia virus used was the Wyeth strain with a deletion in the thymidine kinase (TK) and vaccinia growth factor (VGF) genes. Virus was grown in HeLa cells and was purified on a 36% sucrose cushion and resuspended in PBS. ORFV was grown in OA3.T cells, purified by sucrose cushion, and resuspended in PBS. Ad-DCT was provided by Dr. Bridle and grown as previously published(20).

Tumour models and immunohistochemistry

Subcutaneous tumours were established by injecting $1x10^5$ or $3x10^5$ CT26.LacZ or B16-F10 cells in PBS on the hind flank of the mouse. Systemic dissemination models were seeded at cell concentrations described in figure captions through intravenous administration in the tail vein. B16-F10.LacZ-tumour bearing lungs were stained for β-galactosidase activity to visualize tumour nodules(135).

To analyze VSV replication in CT26.LacZ and B16-F10 tumours following intravenous delivery, Balb/c or C57BL/6 mice were implanted with tumours subcutaneously, and tumours were allowed to grow until reaching a sufficient size to dissect. Mice were then injected IV with $5x10^8$ pfu/100uL. 48 hours after injection, mice were euthanized; tumours were excised and frozen in Shandon Cryomatrix freezing medium (TermoElectron, Waltham, MA) in liquid nitrogen. 5μm sections were stained by immunohistochemistry with rabbit anti-serum raised against VSV (gift of Dr. Earl Brown) at a 1/5000 dilution for 30min. Secondary antibody and ABC reagents were used as directed from the Vectastain ABC kit, and Horseradish peroxidase activity was assessed using a Diaminobenzene-HRP kit (KPL Biosciences, Guelph, Canada). Nuclei were counterstained with hematoxylin. Images were obtained using an Epson Perfection 2450 Photo Scanner.

Splenocyte transfer

Mice were treated as in the direct oncolysis model with 6 doses of VSV at $5x10^8$ pfu/100uL intravenously once tumours were palpable (as in Figure 3.1). Mice that had complete responses were kept for at least 3 months to ensure long term responses. Splenocytes were harvested and purified by Lympholyte-M gradient from mice that were naive, had a tumour but received no treatment, or cured by VSV treatment. $5x10^7$ of these isolated splenocytes were transferred to naive mice IV, and these mice were then challenged 48 hours later with $3x10^5$ CT26.LacZ cells on the right hind flank or 4T1 cells on the left flank. Tumour outgrowth was monitored.

Infected cell vaccine

Tumour cells were harvested from tissue culture and aliquoted in Eppendorf tubes at $2x10^7$ cells / 200uL in PBS. These were irradiated for 30 Gy (CT26.wt), 45 Gy (6048R), or 60 Gy (B16-F10) in a Pantak HF320 X-Ray machine. Virus or PBS was added to the tubes at $2x10^8$ pfu in 200uL of PBS and incubated at 37˚C for 2 hours, unless otherwise stated. The mixture was then injected in mice, 100uL intraperitoneally, thereby giving each mouse $5x10^6$ irradiated cells and $5x10^7$ pfu of virus per dose. For **figure 3.7**, the "irrB16 → F/T + VSVgm" sample was irradiated, then subjected to 3 freeze/thaw cycles in a dry ice bath and 42˚C water bath. Cells were then mixed with VSVgm before injection into the animal. For the "VSVgm-ICV → F/T" sample, the ICV was made as usual and following the 2 hour infection the mixture was subjected to 3 freeze/thaw cycles before injection as detailed above. In the prophylactic model, mice were immunized on days -14 and -7, and then challenged with $1x10^5$ live tumour cells subcutaneously on day 0.

In subcutaneous models, tumour measurements were determined with callipers until end point was reached. In intravenous models, endpoint was reached when the mouse demonstrated severe respiratory distress, had a mass larger than 15x15mm, or pre-determined experimental endpoint was reached. Lungs were removed and fixed in 10% formalin for at least 3 days. These were then blotted dry and weighed. Lungs were then paraffin embedded and slices were analyzed by hematoxylin and eosin staining. Pictures were taken on the Aperio ScanScope (Axiovision Technologies) and analyzed using Aperio ImageScope software.

Flow Cytometry

Spleens and blood were harvested from mice at indicated timepoints, red blood cells were lysed using ACK lysis buffer, and resuspended in RPMI+10% FBS. Tumour draining lymph nodes were strained through a 100μM filter and washed in PBS. For examination of DC maturation, cells were stained with cell surface antibodies for CD11c-PE-Cy7 (clone N418, eBioscience), CD86/B7-1 (clone GL1, eBioscience), CD80 (clone 16-10A1, eBioscience), CD40 (clone 1C10, eBioscience), and MHC class II-FITC (clone M5/114.15.2, eBioscience). For early lymphocyte activation, splenocytes were stained with CD3-PerCP (clone 17A2, R&D systems), NK1.1-PE (clone PK136, BD Bioscience), and CD69-FITC (clone H1.2F3, BD Biosciences). For IFNγ, TNFα, or IL-12 intracellular staining, cells were first surface stained with the above antibodies or antibodies against CD3-PE (clone 17A2, BD Bioscience) or CD8-PECy5.5 (clone 53-6.7, BD Bioscience). Cells were then permeabilized and fixed using the BD Cytofix/Cytoperm kit (BD Bioscience) and then stained with antibodies against IFNγ-FITC (clone XMG1.2, eBioscience) or TNFα-FITC (clone MP6-XT22, eBioscience) and IL-12-APC (clone 15.6, BD Bioscience). For the examination of

NK cell activation, splenocytes were re-stimulated for 1.5 hours with PMA and Ionomycin; during the last hour GolgiPlug (BD Biosciences) was added. These cells were then stained with antibodies against CD3-PerCP, DX5-PE, Granzyme-B-PE-Cy7 (clone 16G6, eBioscience), and IFNγ-FITC and examined by flow cytometry.

All flow cytometry was performed on a Beckman Coulter CyAn and data analyzed with Kaluza v1.1 software or FlowJo software 7.6.5.

Examination of cellular infiltrate of matrigel challenge tumour

Following the regular prophylactic immunization schedule, mice were challenged with $3x10^5$ B16-F10 cells resuspended in 300uL of matrigel (BD Biosciences). Three days after tumour challenge, mice were euthanized. Six hours before euthanasia, mice were treated IV with 0.25mg Brefeldin A (Sigma), as previously published(45). Mice were euthanized and matrigel plugs were excised from the flank, cut into approximately 1-3mm^3 pieces, and disaggregated for 1-2 hours using a cocktail of collagenase type IV (Cooper Biomedical), Dispase, and DNase I (Invitrogen) resuspended in HBSS at 37˚C. This mixture was then washed and stained for flow cytometry as described above.

Depletion studies

C57BL/6 mice were depleted of $CD8^+$ cells with an anti-CD8 antibody that was supplied by Dr. B Lichty (McMaster University). The mice were given 250μg of depleting antibody IP on days -2 and 0 and 200μg on days 4, 8, 11, and 15. Depletions were confirmed by flow cytometry by taking saphenous bleeds on day 4 and staining for CD3 and CD8, as well as examining 4 spleens at endpoint.

NK cell depletions were first performed with an anti-NK1.1 antibody from Dr. Lichty. Mice were given 250μg of depleting antibody IP on days -2 and 0 and then 200μg on day 4. Depletions were confirmed using an anti-DX5 antibody to avoid epitope masking complications on day 4 using PBMCs from saphenous bleeds. A second attempt at NK depletion was performed using the commercially available anti-asialo antibody (Cedarlane, Asialo GM1). The antibody vial was resuspended in 2mL of ddH_2O and mice were treated with 50μL IV on days -3, -1, 1, 4, 8, and 11. Depletions were confirmed by saphenous bleeds on day 7 and staining with an anti-NK1.1 antibody. Mice began getting slow and ill after antibody treatments as of day 11 and all mice were euthanized on day 14 after one mouse was found dead.

T cell activity assays

Ex vivo peptide restimulation: Blood or spleen was harvested and processed with ACK lysis buffer. Cells were stimulated with the VSV N peptide, the DCT peptide, or the GP100 peptide, as described by Bridle *et al(21)*. Cells were stained with antibodies against CD3 and CD8 and then intracellular staining was performed with an antibody against IFNγ.

In vivo CTL assay: donor splenocytes from C57BL/6 mice were stained with 0.5μM CFSE and left unpulsed or they were stained with 5μM CFSE and pulsed for 30 minutes at 37˚C with 10μM DCT and 10μM GP100 peptides. Both cell populations (pulsed and unpulsed) were mixed 1:1 and then $2x10^7$ were injected IV to the mice. These mice were euthanized 24 hours later; their spleens were processed by ACK lysis, and then examined for the numbers of CFSE-positive cells by flow cytometry. Percent specific lysis = [1-[($CFSE^{low}/CFSE^{hi}$ in PBS mice)/($CFSE^{low}/CFSE^{hi}$ in treated mice)]]x100.

IFNγ ELISA: Blood was harvested and processed with ACK lysis buffer. Two days before harvest $5x10^3$ B16-F10 cells were plated in each well of a 96-well plate. $4.7x10^5$ peripheral blood mononuclear cells (PBMCs) were incubated with nothing, or these B16-F10 cells, or with a mixture of DCT and GP100 peptides and 0.4uL/100uL anti-CD28 antibody (clone 37.1, eBioscience) for two days. Supernatants were collected and assayed with a mouse IFNγ Quantikine ELISA (R&D Systems).

Chromium release assay: spleens from 3 mice per group were harvested and processed by ACK lysis buffer. $CD8^+$ T cells were isolated by untouched mouse $CD8^+$ isolation kit (Miltenyi Biotec) on an Automacs Pro cell sorter (Miltenyi Biotec) and counted by ViCell (Beckman Coulter). B16-F10 cells were labeled with Chromium-51 (Perkin Elmer) in the form of Na_2CrO_4 at 100 μCi for 60 minutes at 37°C. Targets (B16-F10 cells) were washed and resuspended at a concentration of $5x10^4$ cells/mL and incubated for 4 hours at 37°C with various effector:target ratios. Supernatants were analyzed for chromium release by gamma counter (Perkin Elmer).

***Ex vivo* dendritic cell assay**

The extraction of mouse bone marrow and culture of monocyte derived dendritic cells was performed according to a previously published procedure(13). Briefly, C57BL/6 mouse bone marrow was extracted and cultured for 6 days in RPMI with 50μM 2-mercaptoethanol and pen/strep with either 10ng/mL of rmGM-CSF or 10ng/mL rmGM-CSF and 20ng/mL rmIL-4. These were then counted and incubated for 16 hours with either nothing (negative control), 2μg/mL CpG-ODN 1826 (positive control), virus at an MOI of 3, or 1:1 ratio of B16-F10 cells with virus at an MOI of 3. These were then washed, stained with antibodies

against CD11c along with CD86 and CD40 or with TNFα and IL-12, and examined by flow cytometry.

Prime/boost vaccination model

Tumour implantation and vaccination was performed as previously published(21). Briefly, under anaesthesia, an incision was made on the mouse head and $1x10^3$ B16-F10 cells in 2μL PBS were injected directly in the brain at approximately 2mm to the right and 0.5mm above bregma. The hole was plugged with bone wax and the scalp incision was closed with skin glue. Mice were primed with $1x10^8$ pfu of the Ad-hDCT intramuscularly on day 5 and then boosted on day 19 with $2x10^9$ pfu wtVSV-hDCT IV.

Histone deacetylase inhibitors

For *in vivo* use, HDIs were resuspended in 30% EtOH, 5% DMSO, and 65% distilled water. For *in vitro* use they were resuspended in pure DMSO. Vehicles were always the same as what the drug was resuspended in for that experiment. Mice were injected with 0.2mg of SAHA and Oxamflatin, and 0.1mg of MS-275, unless otherwise stated.

Neutralizing antibody assay

Anti-VSV neutralizing antibodies were titered by doing serial dilutions of mouse plasma, starting at 1:50 and doing 1:2 dilutions from then on. These dilutions were incubated with $2x10^5$ pfu of VSV for 1 hour and then incubated for 48 hours at 37˚C on a monolayer of Vero cells plated in a 96-well plate. Cell viability was assessed using Alamar Blue (Invitrogen) and detected using a Fluoroskan reader (Thermo). The titer was defined as the plasma dilution at which cell viability was 50 percent of the cells only control.

Statistical Analysis

All statistical analyses were determined using GraphPad Prism 5.0 software. Where applicable, data are presented as mean + SEM and significance of variance was determined by two-tailed T-test with Welch's correction, unless otherwise stated.

3 Harnessing Oncolytic Virus-Mediated Antitumour Immunity in an Infected Cell Vaccine

3.1 Introduction: infected cell vaccines

Though the strategy described by Kottke *et al*(88) is an effective multivalent vaccine, it would be quite laborious to make a personalized library of recombinant viruses for every patient. Another strategy that has been explored by a few research groups for decades is the idea of infecting tumour cells with viruses *ex vivo* and giving this back to the patients. This has been termed an "oncolysate" by some groups or "virally-augmented tumour cells" by others. The premise for this strategy is that virus infection of tumour cells increases their immunogenicity, which is clearly demonstrated by the immune activation seen with OV infections(14, 42, 51, 88). Many protocols of virus-infected tumour cell vaccines have been attempted and with very different viruses. Initially wild-type viruses were used including Influenza A by the Lindenmann group(97) and the Vaccinia smallpox vaccine strain by the Wallack group(166). These studies, however, used long infection times and further lysed cells by freeze/thaw and homogenization. Previous research from other groups has determined that the immunogenicity of intact cells, healthy or UV-inactivated, is higher than that of cellular lysates(143, 158). Moreover, cell lysates, as opposed to intact cells, inhibited DC responsiveness to TLR ligands(158).

Another problem with previously used infected-cell vaccine platforms is the choice of virus. The non-lytic Newcastle Disease Virus (NDV) used by the Schirrmacher group is not immunogenic enough to lead to DC maturation on its own, instead it requires co-incubation with LPS(46). The same has been found with adenovirus(142) and the Western Reserve(41, 71, 176), Copenhagen(38), and modified virus Ankara(71) strains of Vaccinia virus. Though

this last result seems in contrast to the use of VACV as a vaccine vector against smallpox, it was determined that VACV can lead to $CD8^+$ T cell responses through the infection of already mature DCs(176). However, this would not be amenable for an infected cell vaccine platform that requires active uptake by the DC, a trait largely down-regulated in mature DCs(9). A virus that can stimulate DCs would be hypothesized to lead to a much greater anti-tumour immune response when mixed with tumour cells. Of note, Livingston *et al* used wtVSV to infect melanoma cell lines to create a vaccine but observed very limited responses. However, in this case the infected cells were swelled, homogenized, enucleated, and the virus UV-inactivated before treatment(101). It is reasonable to hypothesize that actively replicating virus is more immunogenic than inactivated virus, as our immune system would have evolved mechanisms of ensuring that potentially dangerous pro-inflammatory responses do not occur without good reason.

The addition of cytokines into the genomes of viruses used in infected cell vaccines has been noted to increase immune stimulation in some cases(55). The inclusion of IL-2 into NDV enhanced cytokine secretion and cytotoxic functions of $CD8^+$ T cells(74). Another cytokine often used in autologous tumour cell vaccines is GM-CSF(77). Though few studies have examined the mechanisms behind the efficacy achieved with GM-CSF, the use stems largely from research published in 1993 by Dranoff *et al*(37). They determined that GM-CSF expression from irradiated B16-F10 cells led to a more potent whole cell vaccine, and that this cytokine was better than nine other cytokines, including IL-2, IFNγ, and TNFα. It was determined that this was CD4 and CD8 T cell dependent and also worked in numerous other tumour cell lines(37). A study comparing a whole cell vaccine infected with vaccinia virus to the same vaccine made with a GM-CSF-expressing vaccinia virus determined that

there were profound impacts on peritoneal macrophages. Macrophages from GM-CSF vaccine-treated mice expressed higher levels of nitrite and TNFα, in addition to having higher cytotoxic functions. In addition, peripheral blood lymphocytes and splenocytes demonstrated higher cytolysis of tumour targets following GM-CSF vaccine treatment(77).

As discussed previously, many OVs have been reported to stimulate anti-tumour immune responses, but these studies have largely been undertaken in tumour models permissive to *in vivo* infection. However, not all tumours will be permissive to *in vivo* oncolysis by OVs. For example, IFN responsive tumours will rapidly blunt the replication and spread of most viruses. Conversely, the extremely broad tropism afforded by the glycoprotein of VSV makes it able to infect nearly all mammalian cells when given at a high multiplicity of infection (MOI) *in vitro.* In such a situation, the rapid replication kinetics of the virus can outpace the cellular IFN response.

3.2 Hypothesis & Objectives

Hypothesis

I hypothesize that an infected cell vaccine made with an oncolytic VSV would lead to potent DC stimulation and downstream NK and T cell anti-tumour responses. This vaccine would protect mice from a later tumour challenge following prophylactic vaccination but would also slow tumour growth in a therapeutic treatment setting. Because of the vast number of immunomodulatory genes expressed by poxviruses, these will not lead to anti-tumour responses when used in an infected cell vaccine.

Objectives

1. Determine the importance of replication and T cells in the efficacy achieved by VSV.
2. Optimize a VSV infected cell vaccine for use in prophylactic murine tumour models.
3. Optimize a VSV infected cell vaccine for therapeutic treatment use in multiple tumour models.
4. Determine the ability of poxviruses to perform in an infected cell vaccine.

3.3 Results

3.3.1 T cells and viral replication are required for VSV-mediated long-term tumour regression

I examined the role of the T cell compartment in oncolytic VSV-Δ51 treatment of cancer. A VSV-sensitive clone of CT26.LacZ, a colon carcinoma, was established in immunocompetent and athymic nude mice. Mice were then treated with six intravenous (IV) doses of VSV-Δ51-GFP, UV-inactivated VSV-Δ51, or PBS. In the immune-competent mice, only those treated with VSV-Δ51-GFP had measurable responses, with 60 percent of the mice demonstrating complete tumour clearance (**Figure 3.1a,b**). The athymic nude mice initially responded to VSV treatment, demonstrating stable tumour sizes, but showed marginal long term efficacy, with only 1 out of 10 mice having a durable response (**Figure 3.1c,d**).

Subsequently, immune competent mice demonstrating long-term complete responses were used as splenocyte donors in an adoptive cell transfer. Naive immune-competent mice that received splenocytes from VSV-treated and cured mice were not susceptible to CT26.LacZ tumour growth, but were susceptible to syngeneic 4T1 growth (**Figure 3.1e**).

Figure 3.1 – T cells are required for VSV-mediated long-term tumour regression

Balb/C (**a, b**) or athymic nude (**c, d**) mice were injected subcutaneously with $3x10^5$ CT26.LacZ cells. Immune competent Balb/C mice were treated starting on day 14 post tumour implantation and nude mice were treated on day 10 to reflect a slightly faster onset of tumour development. Mice were injected 6 times every 2 days with $5x10^8$ pfu of VSV-Δ51-GFP IV or equivalent amount of UV-inactivated VSV-Δ51 or phosphate buffered saline (PBS). (**a**) Kaplan-Meier survival analysis of VSV-Δ51-GFP treatment in Balb/C mice. N=8 per group. Statistical significance verified by the log rank test, where $p<0.0001$. (**b**) Tumour area growth over time plotted only for VSV-Δ51-GFP treated mice. (**c**) Kaplan-Meier survival analysis of VSV-Δ51-GFP treatment in nude mice. N=10 for each group. Statistical significance verified by the log rank test, where $p<0.0001$. (**d**) Tumour area growth over time plotted only for VSV-Δ51-GFP treated mice. (**e**) Splenocytes were harvested from either naïve mice, CT26.LacZ tumour-bearing mice, or CT26.LacZ tumour-bearing mice cured with 6 doses of VSV-Δ51-GFP. These splenocytes were injected IV into naïve Balb/C mice, which were challenged subcutaneously 48 hours later with CT26.LacZ cells. The table demonstrates the percent of mice that grew a tumour. (**f**) Balb/C mice bearing CT26.LacZ subcutaneous tumours were injected IV with $5x10^8$pfu of VSV-Δ51. Two days later, mice were euthanized; tumours were harvested, and frozen. Sections were stained by IHC for VSV.

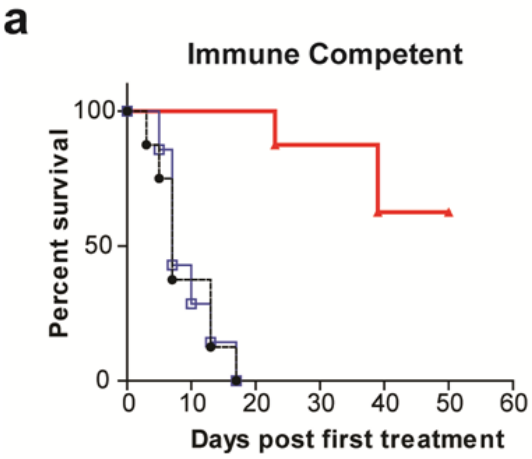

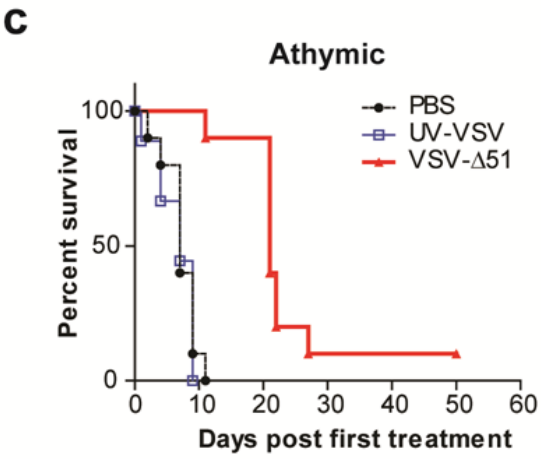

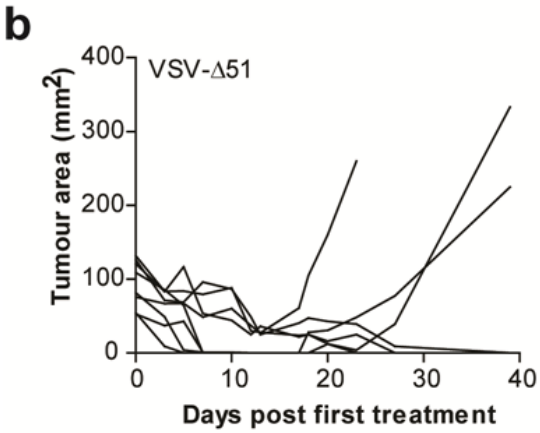

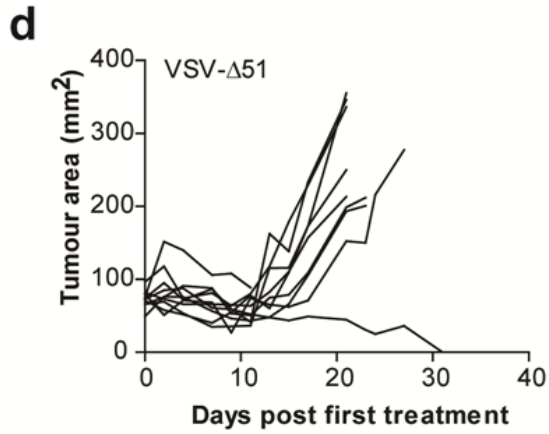

e

	Splenocyte Source		
	Naïve Control	CT26 Bearing	CT26 + VSV Cured
CT26	75	100	0
4T1	100	100	100

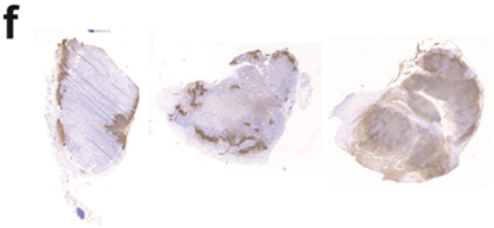

Splenocytes from naïve mice and CT26.LacZ tumour-bearing, but untreated, mice were not able to protect against subsequent tumour challenge.

UV-inactivated VSV was not able to induce any efficacy in the CT26 subcutaneous model (**Figure 3.1a**). This leads me to reason that VSV replication in the tumour cells may be necessary for immune stimulation. CT26.LacZ tumours are very sensitive to VSV and demonstrate robust infection by immunohistochemistry at 24 hours following IV administration (**Figure 3.1f**).

B16-F10 cells have been observed to be moderately type I IFN responsive and, as such, might demonstrate poor VSV susceptibility at the low doses achieved during IV delivery. It was determined that giving $1x10^5$ B16-F10 cells subcutaneously led to consistent tumour growth and endpoint (**Figure 3.2**). B16-F10 cells do not demonstrate any VSV replication in IV-treated tumours (**Figure 3.3a**) and B16-F10 tumour-bearing mice have no response to VSV-treatment (**Figure 3.3b,c**), further demonstrating the importance of replication in efficacy.

Though no VSV replication is detected in the B16-F10 tumours, a minimal amount of replication is hypothesized to occur briefly after delivery. In an attempt to boost the anti-tumour immune response generated from this minimal replication, the cytokines GM-CSF and LIGHT were cloned into the VSV genome. GM-CSF is a potent immunostimulating cytokine able to increase monocyte and macrophage migration and activation (149). LIGHT (TNFSF14, homologous to **L**ymphotoxins exhibits **I**nducible expression and competes with HSV **G**lycoprotein D for **H**VEM, a receptor expressed by **T**-lymphocytes) is part of the tumor necrosis factor superfamily and delivers potent co-stimulatory signals to naïve T cells.

Figure 3.2– Optimizing the B16-F10 subcutaneous model

C57BL/6 mice were implanted with either 10^3, 10^4, 10^5, or 10^6 B16-F10 cells in 100uL PBS subcutaneously. (**a**) Mice were monitored for tumour growth and (**b**) survival.

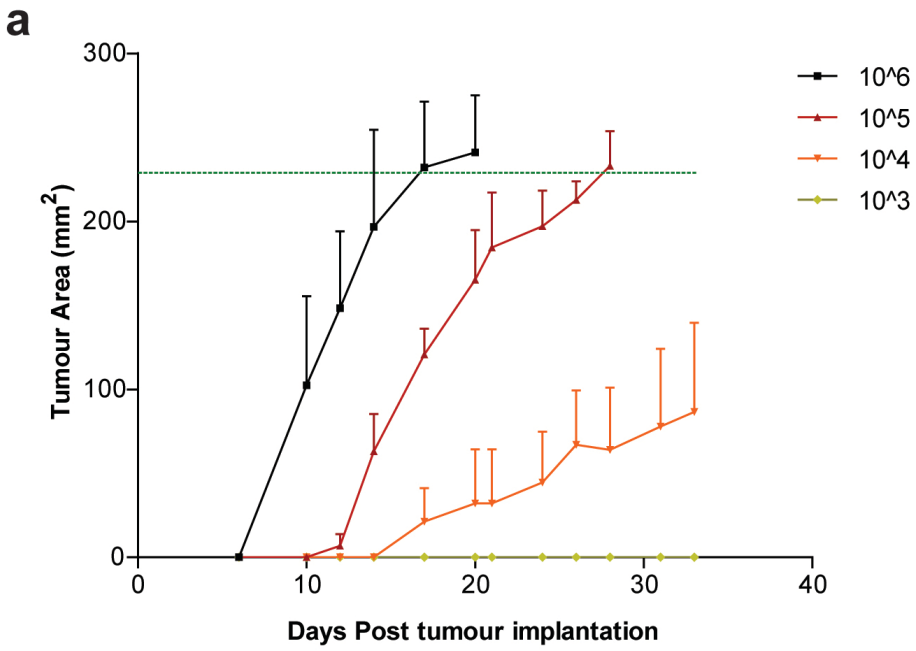
a
300
200
100
0
Tumour Area (mm2)
0
10
20
30
40
Days Post tumour implantation
10^6
10^5
10^4
10^3

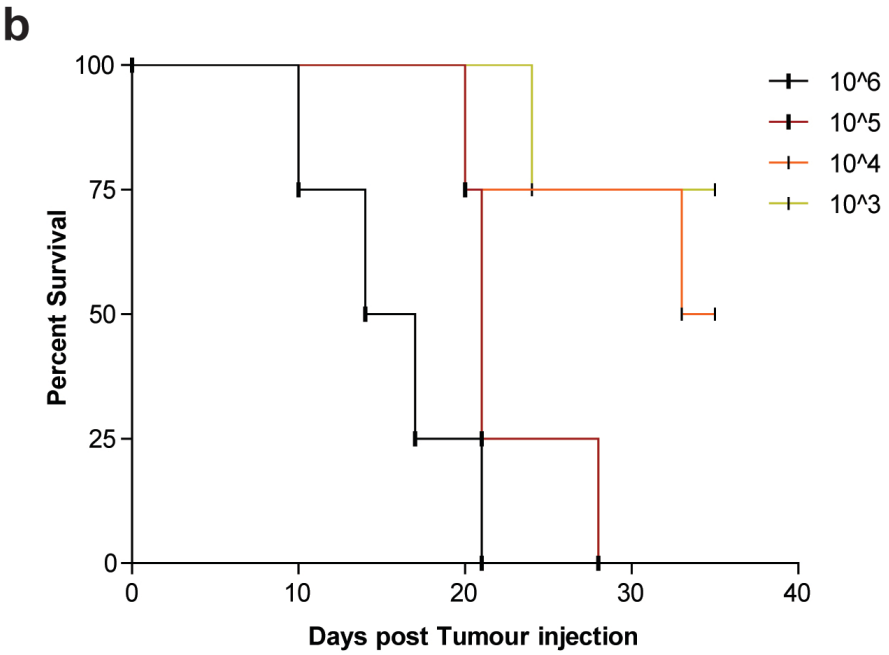
b
100
75
50
25
0
Percent Survival
0
10
20
30
40
Days post Tumour injection
10^6
10^5
10^4
10^3

Figure 3.3 – VSV replication is poor in B16-F10 tumours and leads to no efficacy

(**a**) C57BL/6 mice bearing B16-F10 subcutaneous tumours were injected IV with $5x10^8$pfu of VSV-Δ51. Two days later, mice were euthanized, and tumours were harvested and frozen. Sections were stained by IHC for VSV. (**b**) C57BL/6 mice bearing B16-F10 subcutaneous tumours were injected 3 times a week starting on day 6 with 6 doses of VSV-Δ51 IV. Tumour area growth over time plotted for PBS (in black) and VSV-Δ51 treated (in red). N=6 per group. (**c**) Kaplan-Meier survival analysis with statistics examined by log rank test where p>0.2. (**d**) Kaplan-Meier survival analysis of B16-F10 subcutaneous tumour-bearing mice treated with $5x10^8$ pfu VSV-Δ51-GFP, VSV-Δ51-GMCSF, VSV-Δ51-LIGHT, or PBS starting on day 8. Treatments continued every second day for a total of 5 doses, all were given IV. Number of mice per group was as follows: PBS n=7, VSV-GFP n=8, VSV-GMCSF n=8, VSV-LIGHT n=9. Statistics verified by Log Rank test.

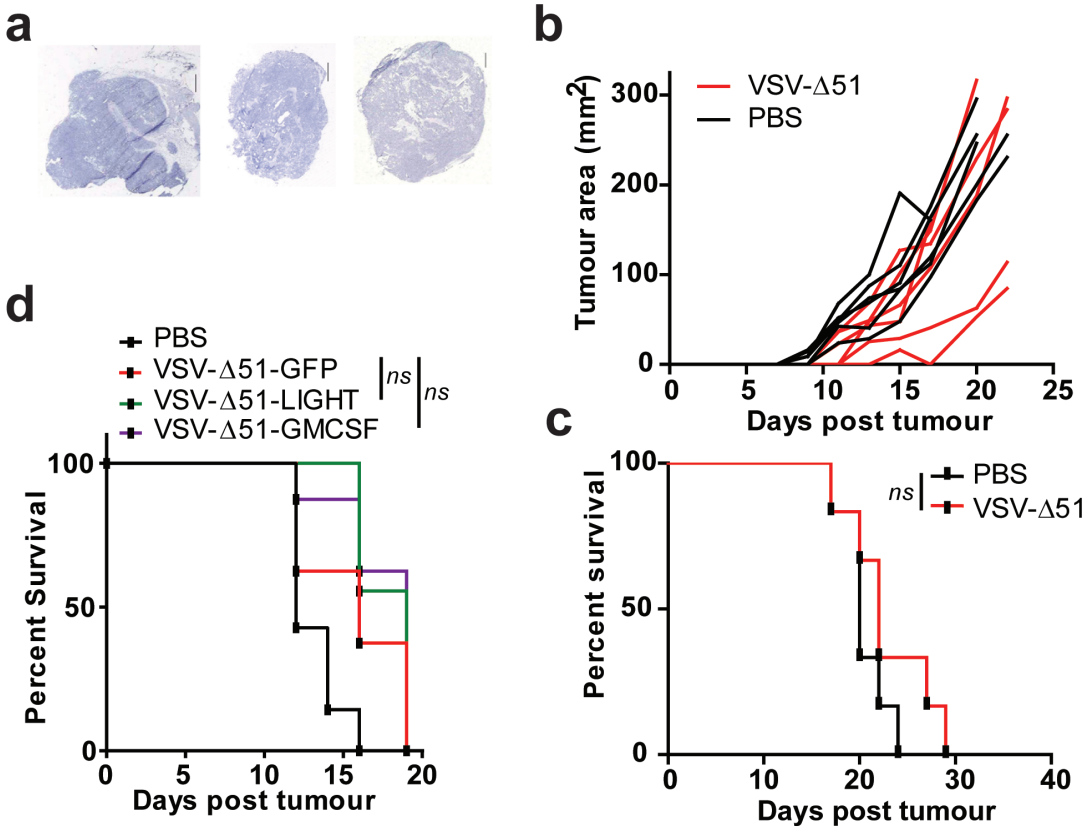
a
b
VSV-Δ51
PBS
Tumour area (mm2)
300
200
100
0
0
5
10
15
20
25
Days post tumour
c
100
50
0
Percent survival
ns
PBS
VSV-Δ51
0
10
20
30
40
Days post tumour
d
PBS
VSV-Δ51-GFP
VSV-Δ51-LIGHT
VSV-Δ51-GMCSF
ns
ns
100
50
0
Percent Survival
0
5
10
15
20
Days post tumour

One study found that the expression of LIGHT on tumour cells initiated the recruitment and activation of naïve T cells that led to tumour rejection(177). However, neither of these viruses performed better than VSV expressing GFP (**Figure 3.3d**).

3.3.2 VSV infection is a potent immune stimulator in a prophylactic ICV

The results so far demonstrated that VSV replication in a permissive tumour can elicit a therapeutic anti-tumour T cell response. I examined whether I could generate a sufficiently robust therapeutic response in VSV-resistant B16-F10 cells by infecting them *ex vivo* and presenting this cocktail as an infected cell vaccine (ICV). This would bypass the necessity for *in vivo* replication to mount an anti-tumour immune response. Though B16-F10 cells are not readily permissive to VSV following IV delivery, complete infection can be achieved by infecting the cells *in vitro* at a high MOI (**Figure 3.4a**).

As a safety measure, the cancer cells would be irradiated before infection to ensure that no cell would have the means of dividing and initiating a new tumour after injection into the animal. It was determined that 50 Gy was sufficient to inhibit cellular outgrowth in a colony forming assay (**Figure 3.4b**). In addition, 60 Gy of gamma irradiation did not hinder viral growth or release from these cells (**Figure 3.4c**).

As a means of determining the immunogenicity of such a vaccine, irradiated tumour cells were infected and assessed for their ability to provide protection against a future tumour challenge (**Figure 3.5a**). This VSV-infected cell vaccine (VSV-ICV) was administered intraperitoneally (IP) to mice on days -14 and -7, with a tumour challenge on day 0 (**Figure 3.5b**).

Figure 3.4 – Optimizing the irradiation of B16-F10 cells

(**a**) B16-F10 cells were infected at an MOI of 10 with VSV-Δ51-GFP. GFP and bright field microscope pictures taken at 24hrs post infection. (**b**) Colony forming assay to determine the potential for cell division following various doses of gamma irradiation. 10, 100, or 1000 B16-F10 cells were plated following gamma irradiation or no irradiation (mock) and two weeks later colony outgrowth was evaluated. All samples were done in duplicate, except for mock that had 4 replicates. Data are mean + SEM. (**c**) B16-F10 cells were gamma irradiated with 0 or 60Gy and then infected *in vitro* at an MOI of 10 with VSV-Δ51-GFP. Supernatants were harvested 48 hours later and the titer was determined on Vero cells by plaque assay. Average titer of 3 wells in pfu/mL + SEM.

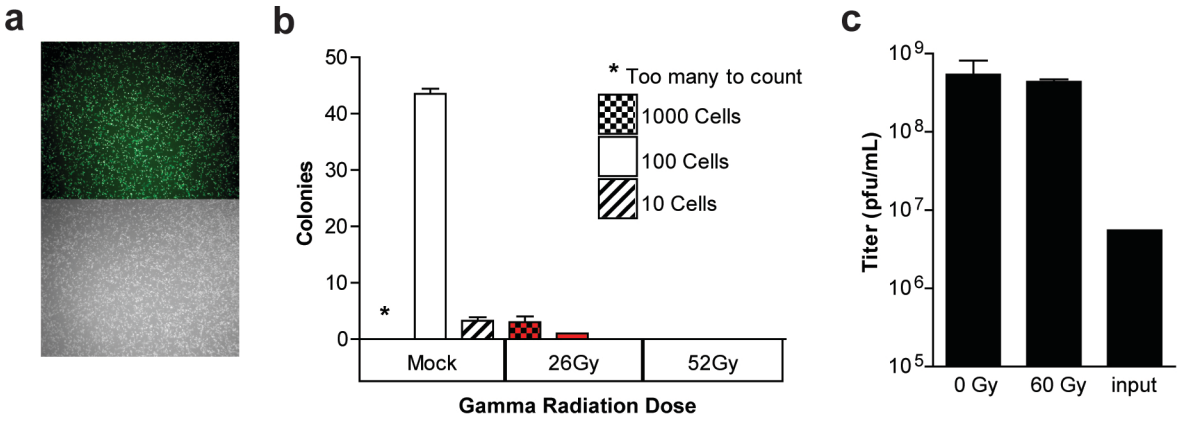
a
b
c
50
40
30
20
10
0
Colonies
* Too many to count
1000 Cells
100 Cells
10 Cells
*
Mock
26Gy
52Gy
Gamma Radiation Dose
10^9
10^8
10^7
10^6
10^5
Titer (pfu/mL)
0 Gy
60 Gy
input

Figure 3.5 - VSV acts as a potent adjuvant in a prophylactic B16-F10 infected cell vaccine

(**a**) Schematic representing preparation of infected cell vaccine. (**b**) Prophylactic ICV treatment timeline in days. (**c**) C57BL/6 mice were immunized with various control or vaccine preparations according to the timeline in panel (b). They were then challenged with $1x10^5$ B16-F10 cells subcutaneously and tumour outgrowth was monitored. Shown is the weighted mean + weighted standard deviation of final tumour outgrowth for each group, averaged from results from multiple experiments. The total number of mice tested, with the fraction exhibiting tumour growth, is listed below the graph. (**d**) Balb/C mice were immunized with PBS, gamma-irradiated CT26.wt cells, or a VSV-ICV made from CT26.wt cells according to the protocol and timeline in (a) and (b). Mice were then challenged with CT26.wt cells and outgrowth was monitored. Average of 2 independent experiments, N and proportion of mice that grew a tumour are denoted below the bars on the graph.

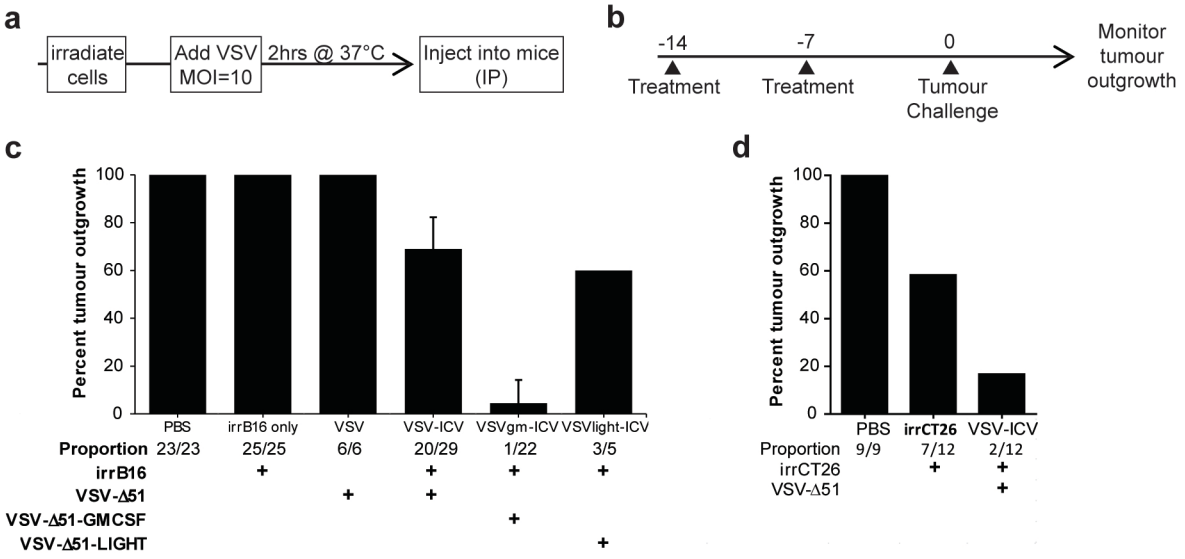
a
irradiate cells
Add VSV MOI=10
2hrs @ 37°C
Inject into mice (IP)
b
-14
-7
0
Treatment
Treatment
Tumour Challenge
Monitor tumour outgrowth
c
Percent tumour outgrowth
100
80
60
40
20
0
PBS
irrB16 only
VSV
VSV-ICV
VSVgm-ICV
VSVlight-ICV
Proportion 23/23 25/25 6/6 20/29 1/22 3/5
irrB16 + + + +
VSV-Δ51 + +
VSV-Δ51-GMCSF +
VSV-Δ51-LIGHT +
d
Percent tumour outgrowth
100
80
60
40
20
0
PBS
irrCT26
VSV-ICV
Proportion 9/9 7/12 2/12
irrCT26 + +
VSV-Δ51 +

The immunization of mice with irradiated B16-F10 cells infected with VSV-Δ51-GFP was able to completely protect 30% of mice tested (9 protected/29) from later live cell challenge (**Figure 3.5c**). Control groups immunized with PBS or irradiated B16-F10 cells alone demonstrated complete susceptibility to the tumour challenge. These results were also verified in a different mouse strain with the parental CT26.wt cell line (**Figure 3.5d**). Like the B16-F10 cells, and unlike the clone CT26.LacZ, the parental CT26.wt cells are resistant to VSV infection *in vivo*.

To increase the immune stimulatory properties of this vaccine, the preparation was made with either the VSV-Δ51-GMCSF (VSVgm-ICV) or the VSV-Δ51-LIGHT (VSVlight-ICV) viruses. The VSVgm-ICV prevented B16-F10 tumour engraftment in over 95 percent of mice tested (21 protected/22) (**Figure 3.5c**). However, the VSVlight-ICV did not improve efficacy beyond what was afforded by the VSV-ICV. Due to the heightened efficacy of the VSVgm-ICV, the VSV-Δ51-GMCSF virus was used for further characterization.

Gamma irradiation has previously been demonstrated to induce immunogenic cell death in CT26 cells(117, 118) and to marginally increase the levels of MHC class I and II on B16-F10 cells(2). The impact of altering the dose of gamma irradiation on the therapeutic outcome of the VSV-ICV was investigated. Though 30 Gy was inadequate to completely halt cellular division in B16-F10 cells, this dose coupled to VSV infection was enough to inhibit the outgrowth of the vaccine. However, mice that received uninfected 30 Gy irradiated B16-F10 cells succumbed to large masses in the abdomen from outgrowth of those cells (data not shown). No difference was observed between 30 and 60 Gy in the VSVgm-ICV in the B16-F10 model (**Figure 3.6a**).

Figure 3.6 – Examining the impact of the dose of gamma irradiation on the VSV-ICV efficacy

(**a**) C57BL/6 mice were immunized with a B16-F10 VSVgm-ICV made with 30 Gy, 45 Gy, or 60 Gy of gamma irradiation. Percent outgrowth of the challenge tumour is depicted with an N of 6 mice per group. (**b**) Balb/C mice were immunized with a CT26.wt VSV-ICV as per the usual protocol and timeline as depicted in Figure 2.5a,b. Vaccine was made with cells gamma irradiated with 30Gy, 45Gy, or 60Gy and there were 5 mice per group, except for the 60Gy ICV that had 6. Percent outgrowth was monitored (**c**) along with survival. *P* values, * $P<0.05$, ** $P<0.005$.

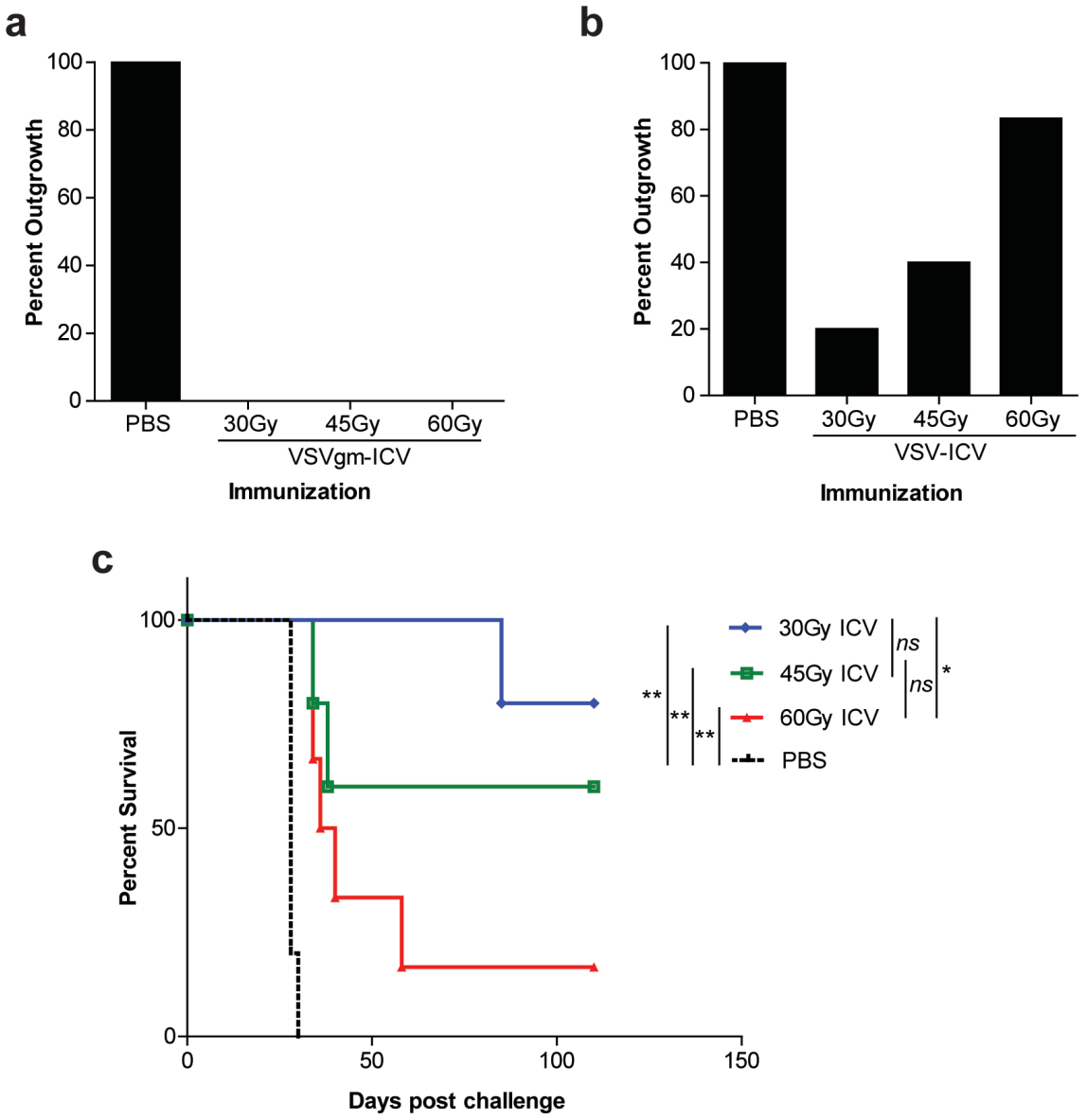
a
Percent Outgrowth
100
80
60
40
20
0
PBS
30Gy
45Gy
60Gy
VSVgm-ICV
Immunization
b
Percent Outgrowth
100
80
60
40
20
0
PBS
30Gy
45Gy
60Gy
VSV-ICV
Immunization
c
Percent Survival
100
50
0
0
50
100
150
Days post challenge
30Gy ICV
45Gy ICV
60Gy ICV
PBS
**
**
**
ns
ns
*

A difference was observed in the CT26.wt model. Cellular division of these cells was completely inhibited with 30 Gy of gamma irradiation (data not shown). Interestingly, although 30 Gy irradiated VSV-ICV was able to protect the mice from tumour rechallenge, there was a dose response whereby 45 Gy was not as effective and 60 Gy was even less effective (**Figure 3.6b,c**).

Virus replication and spread or tumour cell integrity were examined for their importance for ICV efficacy in the B16-F10 model. UV-inactivated VSV lacks the ability to express any gene products and was unable to confer any protection (**Figure 3.7a**). G-Less VSV is a recombinant that lacks the gene encoding the glycoprotein but is grown in cells expressing VSV G. This virus infects cells and expresses N, M, L, and P genes. It can package new virions, but these are not infectious(137). This virus was able to protect the same proportion of mice as the VSV-ICV in this experiment (**Figure 3.7a,b**). These viruses were compared to VSV-Δ51-GFP because neither UV-inactivated nor G-Less virus expresses GM-CSF. To determine the importance of cellular integrity for the efficacy of the vaccine, vaccine preparations were attempted by two other methods. Irradiated B16-F10 cells were first freeze/thawed multiple times before being mixed with VSV-Δ51-GMCSF (irrB16 --> F/T + VSVgm). This preparation was not able to protect any of the 6 mice treated. Alternatively, the VSVgm-ICV was made as per usual but was freeze/thawed multiple times before injection (VSVgm-ICV --> F/T). This preparation protected 4 out of 7 mice.

Taken together, these results indicate that in two VSV-resistant cancer models tumour cells infected with VSV-Δ51 can stimulate an anti-tumour immune response that is capable of protecting mice from a later tumour challenge. In addition, the expression of

Figure 3.7 – Deconstructing the VSV-ICV to better understand the role of viral replication and cellular integrity

C57BL/6 mice were immunized with various preparations of B16-F10 VSV-ICV. (**a**) Shown is the percent outgrowth from the one experiment in which that condition was tested. (**b**) The Kaplan-Meier curve from one experiment.

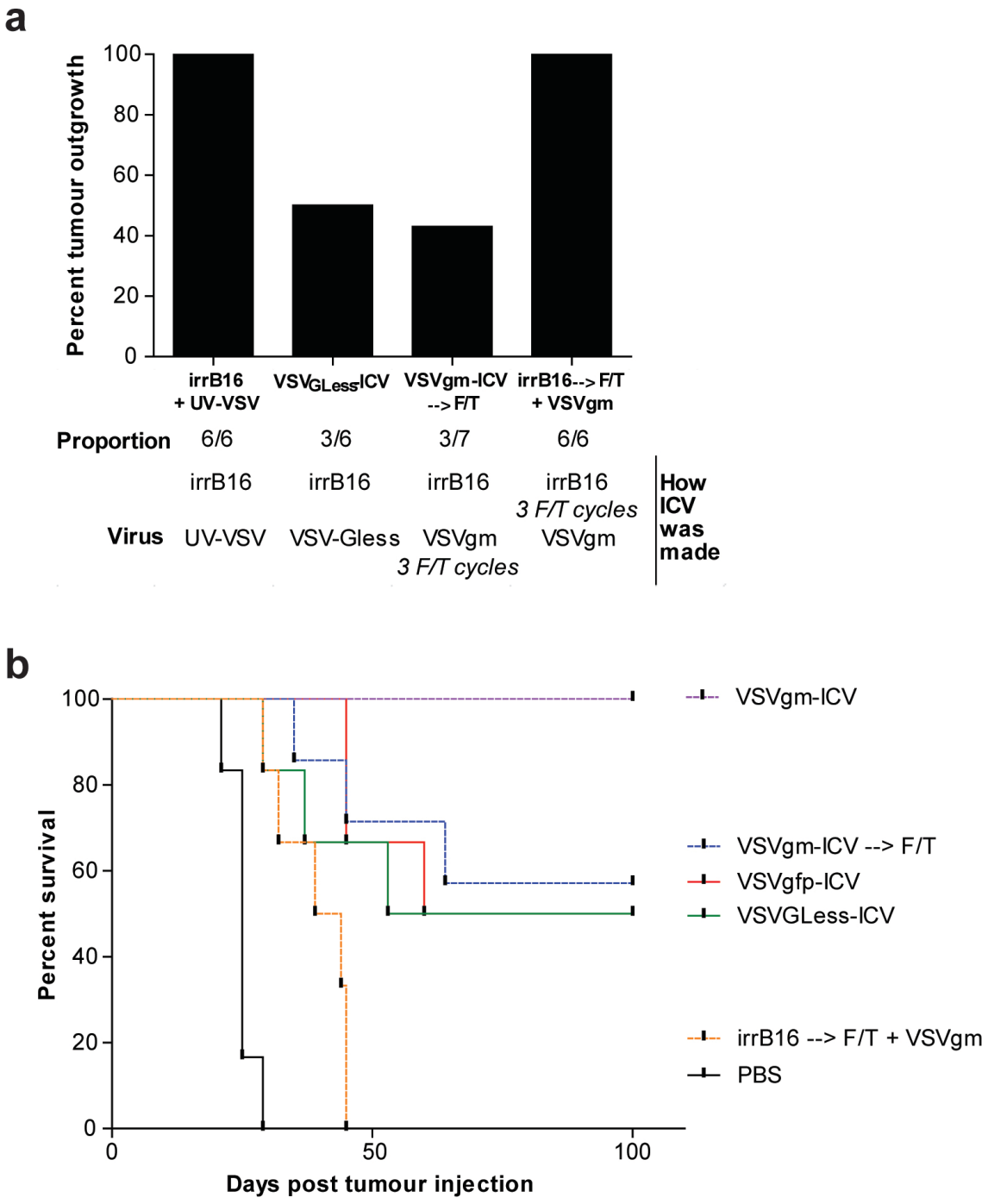
a
Percent tumour outgrowth
100
80
60
40
20
0
irrB16 + UV-VSV
VSVGLessICV
VSVgm-ICV --> F/T
irrB16--> F/T + VSVgm
Proportion
6/6
3/6
3/7
6/6
irrB16
irrB16
irrB16
irrB16
3 F/T cycles
Virus
UV-VSV
VSV-Gless
VSVgm
3 F/T cycles
VSVgm
How ICV was made
b
Percent survival
100
80
60
40
20
0
0
50
100
Days post tumour injection
VSVgm-ICV
VSVgm-ICV --> F/T
VSVgfp-ICV
VSVGLess-ICV
irrB16 --> F/T + VSVgm
PBS

GM-CSF from infected cells greatly increased the immunization capabilities of the ICV in the B16-F10 model. Interestingly, it seems that cellular integrity is important in conferring immunological protection with this vaccine but virus need not replicate beyond the cells that constitute the vaccine, as demonstrated by the VSV_{GLess}-ICV.

3.3.3 VSVgm-ICV induces rapid innate immune activation

The activation of early innate immune cells following VSVgm-ICV treatment was examined. Splenocytes were harvested at 24 hours post treatment and DCs were evaluated for markers of activation. Mice treated with either VSVgm alone or VSVgm-ICV had a higher proportion of activated DCs. This is demonstrated by a higher frequency of cells expressing MHC II, CD80, and CD86, as well as higher expression levels of these maturation markers (**Figure 3.8a-c**). In addition, a higher frequency of DCs in the blood were observed to express CD80 (**Figure 3.8d**) and to have a higher overall expression of the co-stimulatory molecule (**Figure 3.8e**).

Bone-marrow derived DCs produced both TNFα and IL-12 following VSV or VSV-ICV stimulation (**Figure 3.9a-d**). However, the presence of GM-CSF in the VSV genome did not enhance cytokine secretion by the DCs.

Splenic lymphocytes were examined for early activation through CD69 expression 15 hours after treatment with the VSVgm-ICV. CD69 is a marker of early lymphocyte activation and is not found on naive lymphocyte populations(98, 127). NK and T cells from VSVgm-ICV-treated mice demonstrate dramatically higher degrees of early activation than control animals (**Figure 3.10a**). In keeping with this finding, at 24 hours post treatment, a

Figure 3.8 - The VSVgm-ICV leads to dendritic cell and lymphocyte early activation within 24hrs of vaccination.

C57BL/6 mice were immunized with the VSVgm-ICV or relevant controls IP and euthanized 24hrs later. (**a-c**) Splenocytes or (**d-e**) PBMCs were stained and examined by flow cytometry for dendritic cell markers of maturation. (**a**) Percent of $CD11c^+$ cells that express MHC II and/or CD86 and/or CD80. (**b**) Mean fluorescence intensity of CD86 and CD80 staining on $CD11c^+$ cells normalized to PBS levels. (**c**) Mean fluorescence intensity of MHC II staining on $CD11c^+$ cells. N=3 mice per group, except for VSVgm-ICV that had 4 mice. (**d**) Percent of CD11c+ cells in the blood expressing CD80 and the (**e**) mean fluorescent intensity of the staining. All data presented as mean + SEM with 3 mice per group. *P* values, * $P<0.05$, ** $P<0.005$, *** $P\leq0.0001$

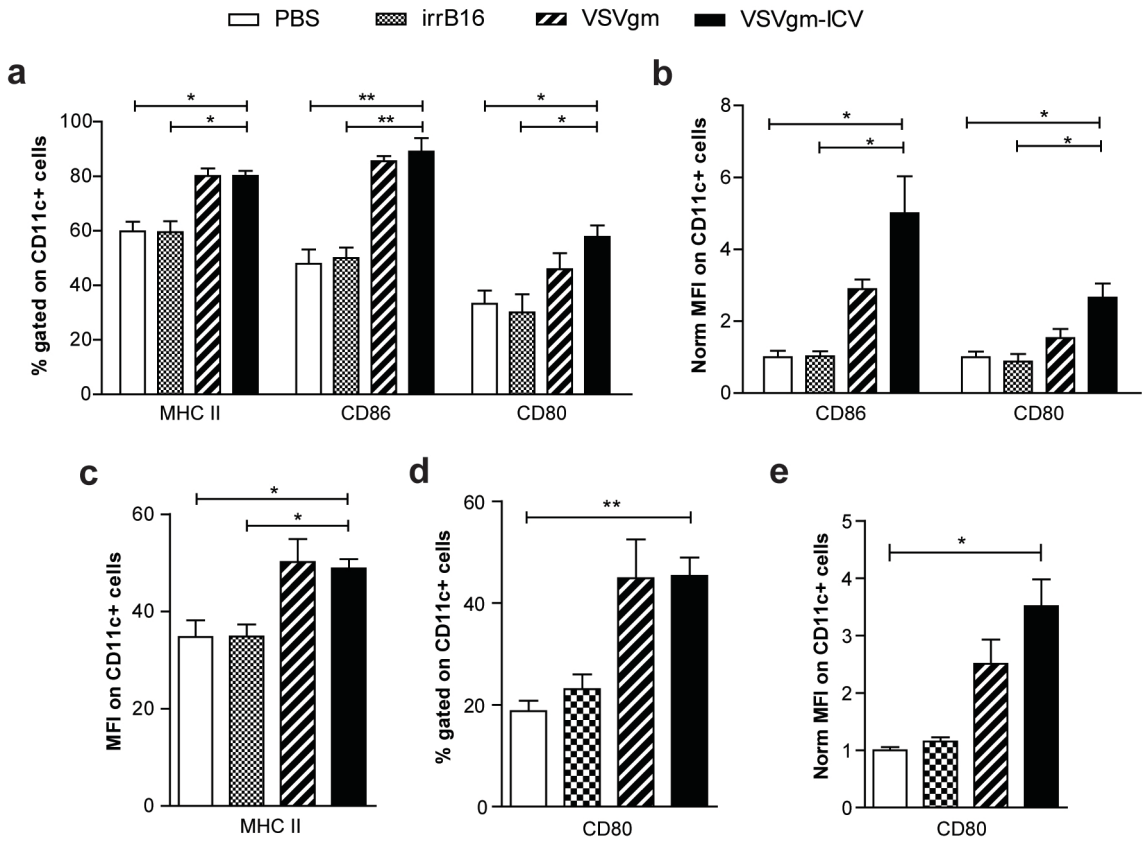
PBS
irrB16
VSVgm
VSVgm-ICV
a
% gated on CD11c+ cells
MHC II
CD86
CD80
b
Norm MFI on CD11c+ cells
CD86
CD80
c
MFI on CD11c+ cells
MHC II
d
% gated on CD11c+ cells
CD80
e
Norm MFI on CD11c+ cells
CD80

Figure 3.9 – *in vitro* DC stimulation with the VSV-ICV demonstrates cytokine secretion

DCs were generated from C57BL/6 mouse bone marrow and incubated for 16 hours with various ICV preparations or controls. Cells were stained for CD11c and then intracellular staining was performed for TNFα and IL-12. Percent of $CD11c^+$ cells that were positive for (**a**) TNFα or (**c**) IL-12. Mean fluorescent intensity of (**b**) TNFα or (**d**) IL-12 on $CD11c^+$ cells. Cells were assayed in duplicate and presented as mean + SEM. *P* values; * $P<0.05$ as compared to all VSV or VSV-ICV bars.

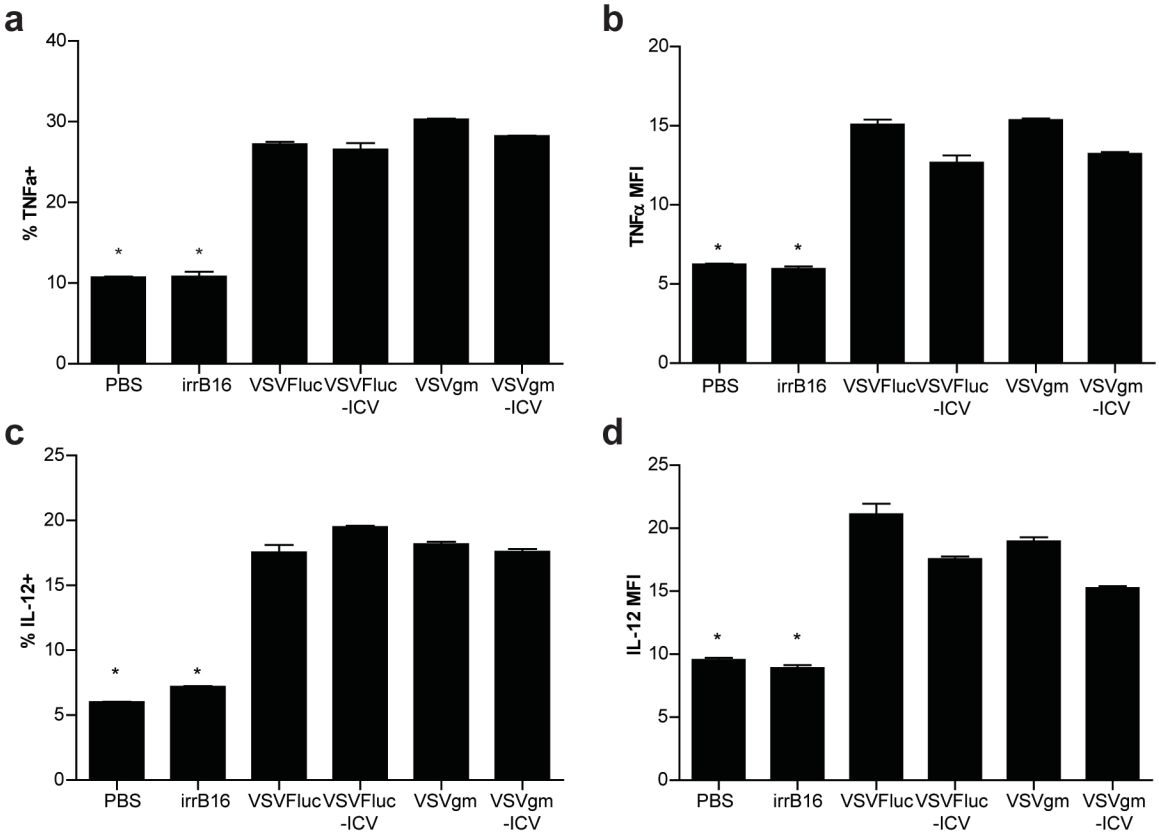
a
% TNFa+
40
30
20
10
0
*
*
PBS
irrB16
VSVFluc
VSVFluc -ICV
VSVgm
VSVgm -ICV
b
TNFα MFI
20
15
10
5
0
*
*
PBS
irrB16
VSVFluc
VSVFluc -ICV
VSVgm
VSVgm -ICV
c
% IL-12+
25
20
15
10
5
0
*
*
PBS
irrB16
VSVFluc
VSVFluc -ICV
VSVgm
VSVgm -ICV
d
IL-12 MFI
25
20
15
10
5
0
*
*
PBS
irrB16
VSVFluc
VSVFluc -ICV
VSVgm
VSVgm -ICV

Figure 3.10 – The VSVgm-ICV activates blood and splenic NK cells

(**a**) C57BL/6 mice were immunized with the VSVgm-ICV or relevant controls and euthanized 15hrs later. Splenocytes were stained and examined by flow cytometry for NK1.1 and CD3 in addition to CD69. Percent of indicated cells that express CD69 is demonstrated. (**b-c**) C57BL/6 mice were immunized IP with the VSVgm-ICV or relevant controls and euthanized 24hrs later. PBMCs were stained and examined by flow cytometry for $CD3^{-}NK1.1^{+}$ cells and IFNγ. Data are presented as mean + SEM with 3 mice per group, except for VSVgm-ICV that had 4 mice. (**d-e**) C57BL/6 mice were immunized IP with the VSVgm-ICV or relevant controls on days -14 and -7 and then euthanized on day 1, at which point blood was harvested and stained for $CD3^{-}NK1.1^{+}$ cells and IFNγ. (**b,d**) Percent of $CD3^{-}NK1.1^{+}$ cells that express IFNγ. (**c,e**) Mean fluorescence intensity of IFNγ staining on $CD3^{-}NK1.1^{+}$ cells normalized to PBS levels. All data presented as mean + SEM with 3 mice per group (unless otherwise stated). *P* values, * $P<0.05$, ** $P<0.005$, *** $P\leq0.0001$

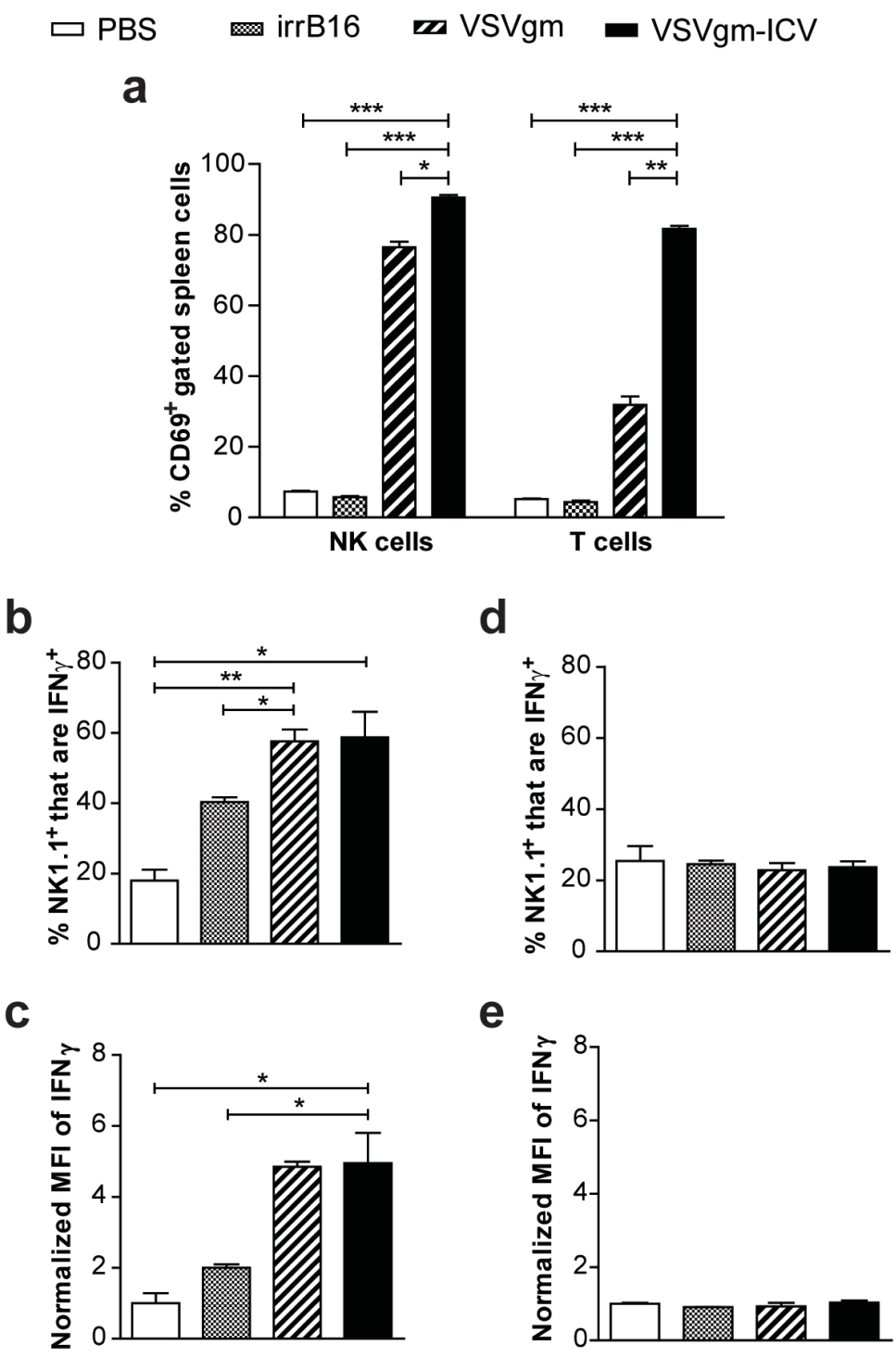
PBS
irrB16
VSVgm
VSVgm-ICV
a
% CD69+ gated spleen cells
NK cells
T cells
b
% NK1.1+ that are IFNγ+
d
% NK1.1+ that are IFNγ+
c
Normalized MFI of IFNγ
e
Normalized MFI of IFNγ

higher frequency of blood NK cells from VSVgm or VSVgm-ICV-treated mice expressed IFNγ and more of the cytokine was expressed per cell (**Figure 3.10b,c**). However, NK cells no longer express IFNγ in the blood on the day of tumour challenge (**Figure 3.10d,e**).

3.3.4 VSVgm-ICV treatment increases activated T and NK cell tumour infiltration

To understand what cell types are responsible for tumour rejection in the prophylactic B16-F10 model following VSVgm-ICV treatment, I implanted the challenge tumour in matrigel, thereby allowing me to easily resect and disaggregate the tumour after 3 days (**Figure 3.11a**). Mice were injected with Brefeldin A 6 hours before tumour harvest. This allowed me to determine the expression profiles of tumour infiltrating cells while they are in the tumour environment. T cells were 10 times more numerous in the tumour following vaccination with the VSVgm-ICV than with irradiated cells alone or VSVgm (**Figure 3.11b,c**). This difference is even larger when compared to the PBS treated mice, with 30 times more T cells in the treated tumour. Indeed, over 8% of the tumour cellular content was T cells, equal to a ratio of one T cell for every 12.5 tumour cells (**Figure 3.11d**). There was also a much greater number of $CD3^{+}IFN\gamma^{+}$ cells in the tumour following VSVgm-ICV than in any control group (**Figure 3.11b,e,f**).

Though no NK cells were observed to be activated in the blood at the time of challenge (**Figure 3.10d,e**), VSVgm-ICV-immunized mice had 4- to 13-fold more NK cells in their tumours than control treated animals (**Figure 3.12a**). There were more NK cells expressing both IFNγ and Granzyme B (**Figure 3.12b**) and more NK cells producing either cytokine individually (**Figure 3.12c**). Likewise, tumour-resident DCs demonstrated a more mature phenotype with VSVgm-ICV treatment (**Figure 3.12d,e**).

Figure 3.11 - Prophylactic immunization with the VSVgm-ICV leads to robust activated T cell infiltration of the challenge tumour

(**a**) C57BL/6 mice were prophylactically immunized as described earlier with VSVgm-ICV or controls. B16-F10 cells in matrigel were subcutaneously injected on day 0. Tumours were resected on day 3 for enzymatic disaggregation and flow cytometric analysis. (**b**) Representative dot plots demonstrating $CD3^+$ cells expressing IFNγ. (**c**) The total number of $CD3^+$ cells per tumour in each group. (**d**) The percent of $CD3^+$ cells in the tumour. (**e**) The total number of $CD3^+$ $IFN\gamma^+$ cells per tumour in each group. (f) The percent of $CD3^+$ cells that were $IFN\gamma^+$. All data are presented as mean + SEM with 5 mice per group. *P* values, * $P<0.05$, ** $P<0.005$.

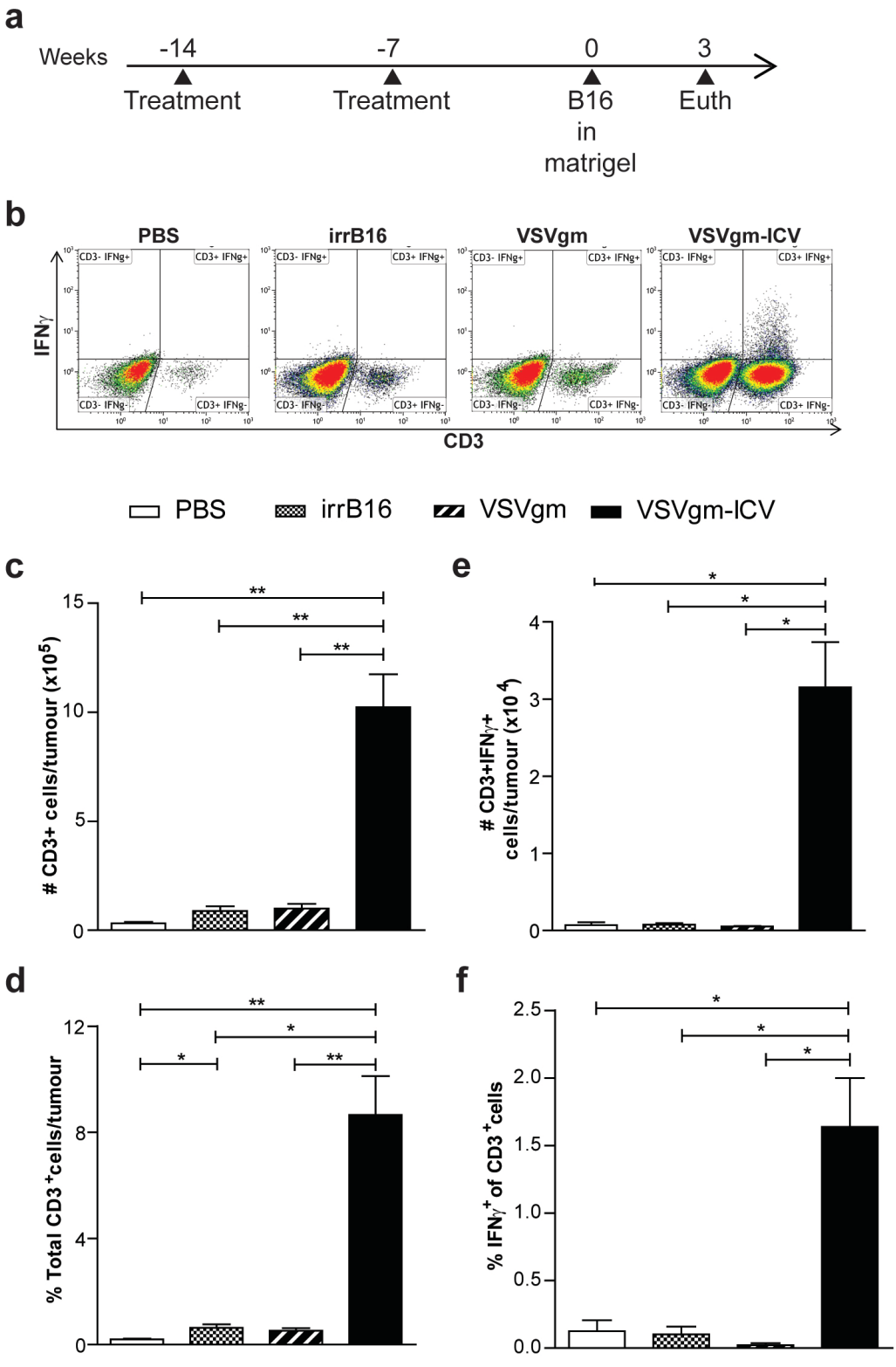
a
Weeks
-14
-7
0
3
Treatment
Treatment
B16 in matrigel
Euth
b
PBS
irrB16
VSVgm
VSVgm-ICV
IFNγ
CD3
PBS
irrB16
VSVgm
VSVgm-ICV
c
CD3+ cells/tumour (x10^5)
d
% Total CD3+cells/tumour
e
CD3+IFNγ+ cells/tumour (x10^4)
f
% IFNγ+ of CD3+cells

Figure 3.12 – NK cells and DCs are also more numerous in the challenge tumour following VSVgm-ICV treatment

NK cell and DC flow cytometric analysis of the tumours described in **Figure 3.11** further characterizing the cellular infiltrate in challenge tumour. (**a**) The total number of $NK1.1^+$ cells per tumour in each group. (**b**) The total number of $NK1.1^+IFN\gamma^+GranzymeB^+$ cells per tumour in each group. (**c**) The total number of $NK1.1^+IFN\gamma^+$ cells and $NK1.1^+GranzymeB^+$ cells per tumour in each group. (**d**) The total number of $CD11c^+CD86^+$ cells and (**e**) the percent of $CD11c^+$ cells that expressed CD86. *P* values, £, †, ‡, ∫, §, and € are all *P≤0.005.* All data are presented as mean + SEM with 5 mice per group. *P* values, * *P*<0.05, ** *P*<0.005, *** *P*≤0.0005

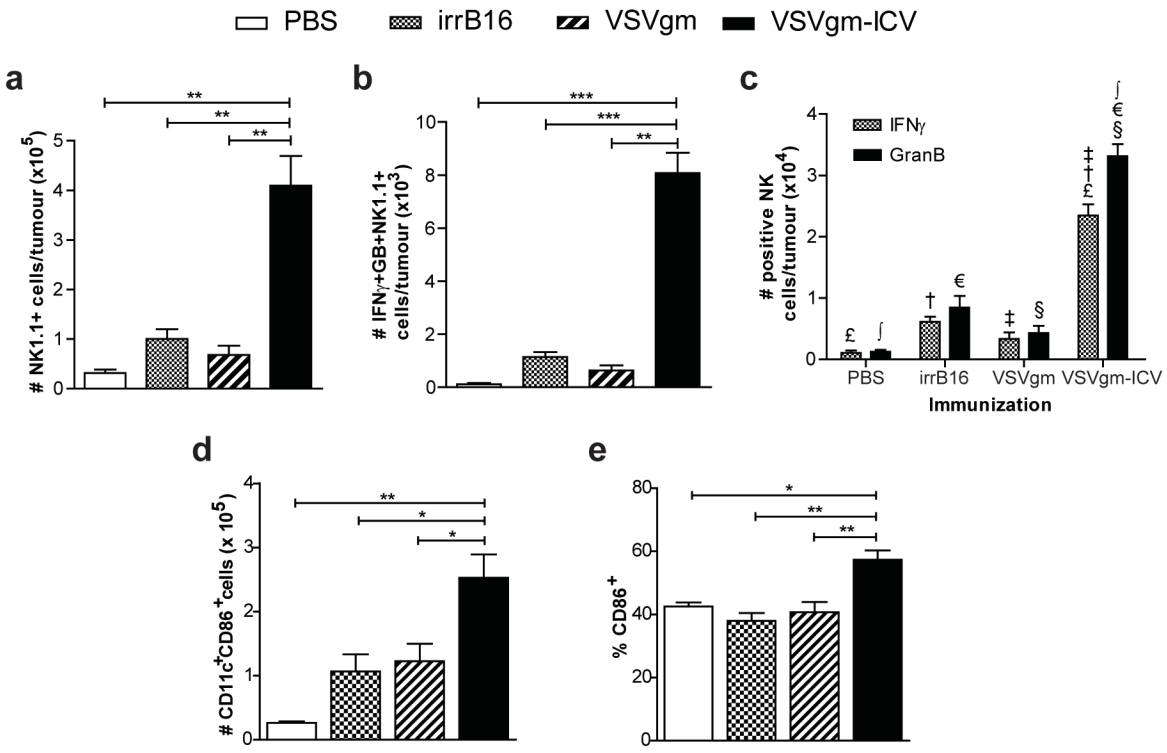
PBS
irrB16
VSVgm
VSVgm-ICV
a
NK1.1+ cells/tumour (x10^5)
b
IFNγ+GB+NK1.1+ cells/tumour (x10^3)
c
IFNγ
GranB
positive NK cells/tumour (x10^4)
PBS
irrB16
VSVgm
VSVgm-ICV
Immunization
d
CD11c+CD86+cells (x 10^5)
e
% CD86+

3.3.5 VSVgm-ICV leads to innate immune activation in the therapeutic setting

By means of investigating whether similar immune activation could occur in the therapeutic setting, B16-F10 tumour-bearing mice were immunized with the VSVgm-ICV or relevant controls. DCs in tumour-draining lymph nodes (TDLN) were assayed for maturation phenotypes following VSVgm-ICV treatment (**Figure 3.13**). More DCs expressed MHC class II as well as CD80 and CD86 upon VSVgm-ICV treatment (**Figure 3.13a,b,c**), and the TDLN DCs also had a higher expression level of all three activation markers. Similar profiles were seen in the spleen of VSVgm-ICV treated mice, where a higher proportion of DCs expressed CD80, CD86, and IL-12 (**Figure 3.13d-f**). In addition, a higher proportion of blood NK cells were expressing IFNγ (**Figure 3.13g**). Interestingly, whereas splenic expression of maturation markers was statistically equivalent between VSVgm and VSVgm-ICV-treated mice, TDLN responses were more pronounced with VSVgm-ICV treatment.

3.3.6 The VSVgm-ICV reduces tumour burden in the therapeutic setting

Having demonstrated that the VSVgm-ICV can protect mice from a tumour challenge, the vaccine's potency in treating established tumours was examined. Various VSVgm-ICV treatment protocols were examined for the ability to delay tumour growth of established B16-F10 subcutaneous tumours (**Appendix I**). From these experiments a successful treatment protocol was established that consisted of treatments on days 1, 8, and 20 after inoculation of the tumour (**Figure 3.14a**). C57BL/6 mice bearing B16-F10 subcutaneous tumours were treated IP with VSVgm-ICV, irrB16, VSVgm, or PBS control. Animals treated with the VSVgm-ICV had a dramatic delay in tumour growth. In contrast, treatment with oncolytic VSV-Δ51-GMCSF resulted in similar tumour growths as seen in PBS-treated animals (**Figure 3.14b**). Treatment with irradiated B16-F10 cells led to

Figure 3.13 – The VSVgm-ICV leads to innate immune cell activation in B16-F10 tumour-bearing mice

C57BL/6 mice bearing 3 day old subcutaneous B16-F10 tumours were inoculated with one dose of the VSVgm-ICV or a control. 24hrs later inguinal and axillary lymph nodes, spleen, and blood were harvested. (**a-c**) Percent of $CD11c^+$ cells expression activation marker and MFI of marker on $CD11c^+$ cells in the lymph nodes. (**d-f**) Percent of splenic $CD11c^+$ cells expression co-stimulatory molecules or cytokines. (**g**) Percent of $NK1.1^+CD3^-$ cells that expressed IFNγ. All data are mean + SEM, with an N of 3 mice per group. *P* values, * $P<0.05$, ** $P<0.005$.

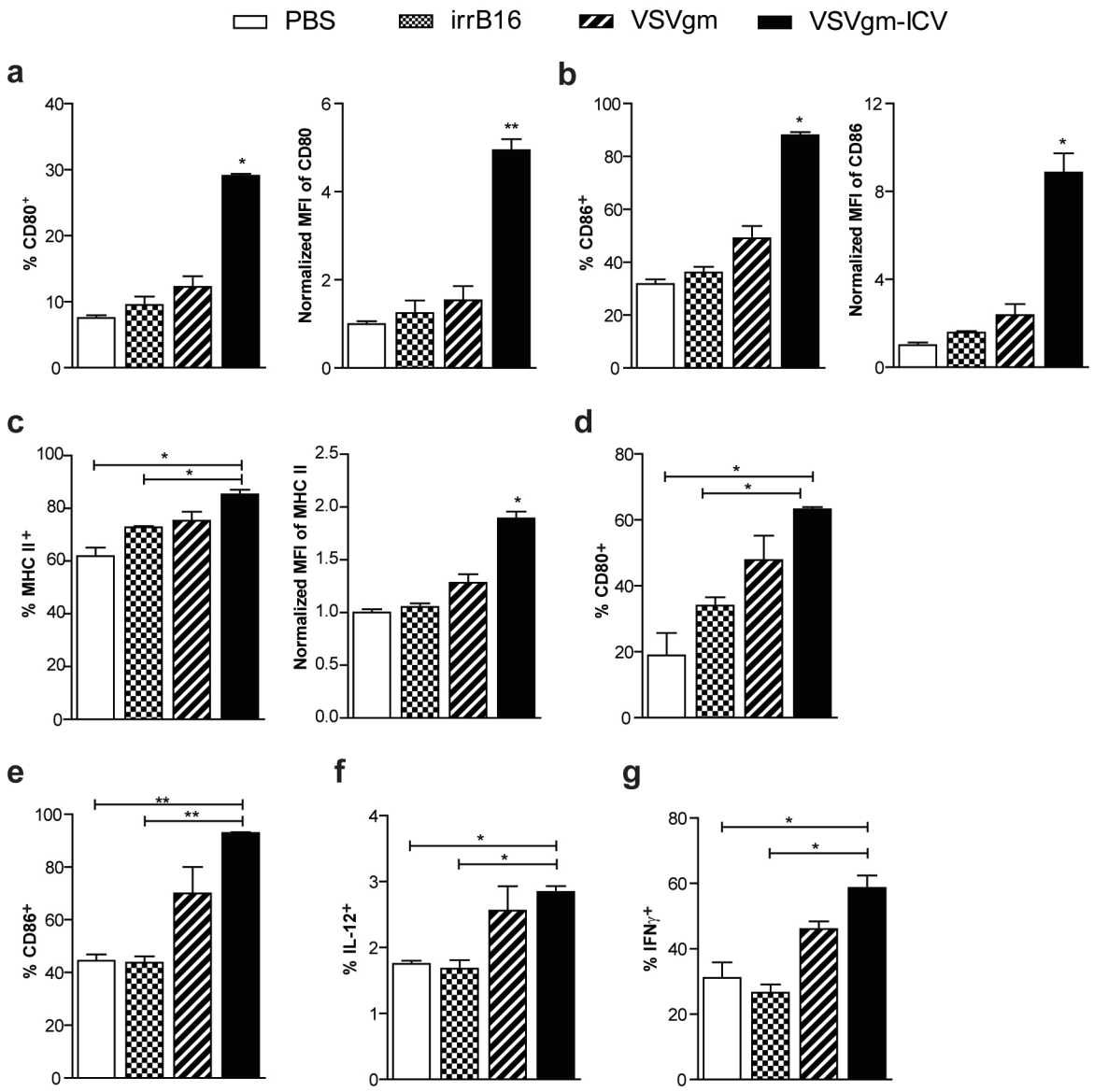
PBS
irrB16
VSVgm
VSVgm-ICV
a
% CD80+
Normalized MFI of CD80
b
% CD86+
Normalized MFI of CD86
c
% MHC II+
Normalized MFI of MHC II
d
% CD80+
e
% CD86+
f
% IL-12+
g
% IFNγ+

Figure 3.14 – Treatment with the VSVgm-ICV significantly delays tumours growth in a subcutaneous model of B16-F10

(**a**) C57BL/6 mice were implanted with $1x10^5$ B16-F10 subcutaneous tumours and treated IP according to the presented timeline. (**b**) Tumour area was monitored and is shown in days following tumour implantation as mean + SEM with 5 mice per group, except for the VSVgm only group that had 4. *P* values, * $P<0.05$, ** $P<0.005$, *** $P\leq0.0001$

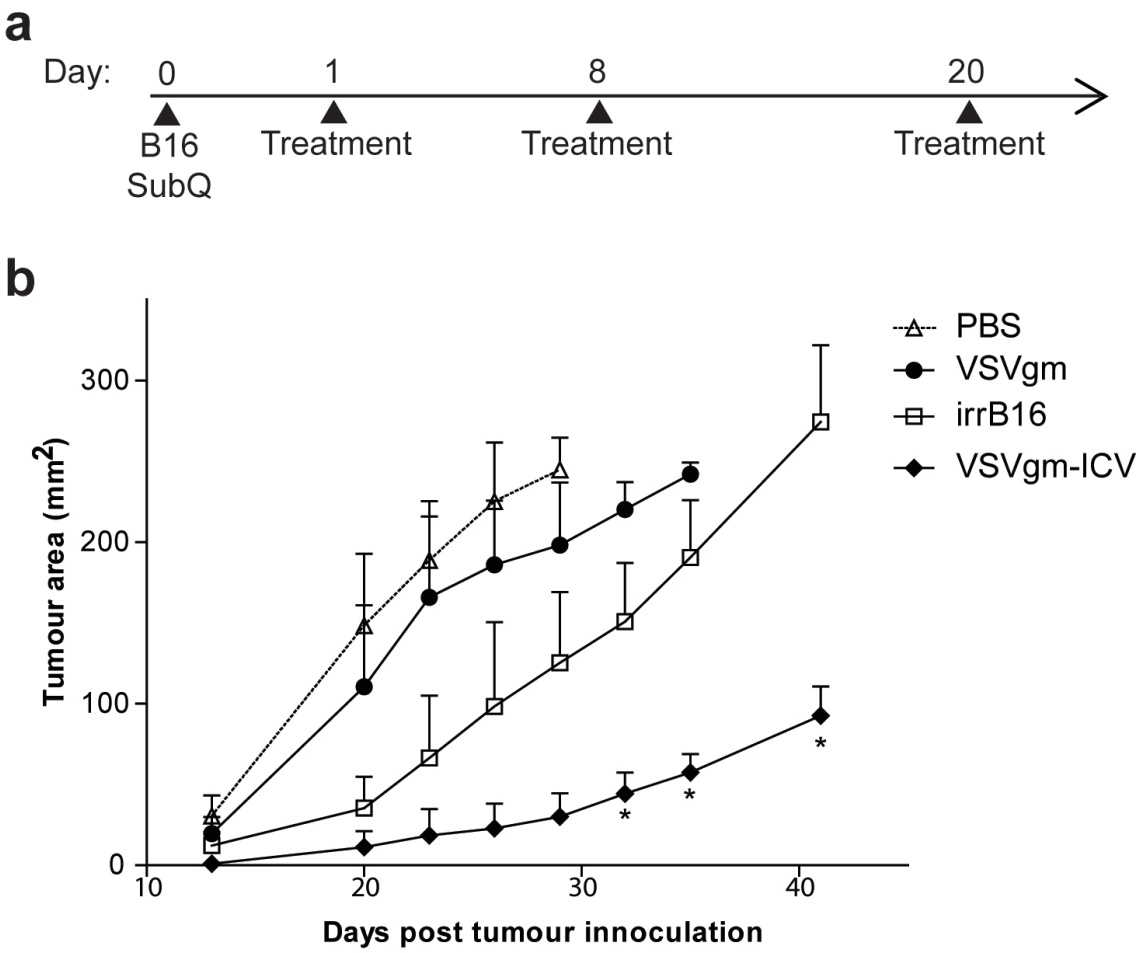
a
Day:
0
1
8
20
B16
SubQ
Treatment
Treatment
Treatment
b
PBS
VSVgm
irrB16
VSVgm-ICV
Tumour area (mm2)
300
200
100
0
10
20
30
40
Days post tumour innoculation
*
*
*

marginally delayed tumour growth compared to the other control groups, though this was not statistically significant.

A disseminated lung cancer model was also undertaken to examine the potency of this vaccine. First the model was attempted with the B16.LacZ cell line, which would allow for optimal visualization of the tumour burden. C57BL/6 mice were injected IV with B16.LacZ cells, leading to tumour seeding in the lung. A similar treatment schedule as used with the subcutaneous model was employed (**Figure 3.15a**). Mice were euthanized on day 28 to examine tumour burden through β-galactosidase staining. Lungs from VSVgm-ICV-treated mice had a very low tumour burden, a substantial difference from control-treated lungs (**Figure 3.15b**). However, irrB16-treated lungs also demonstrated a lower tumour burden than VSVgm or PBS-treated lungs, though still higher than vaccine-treated lungs. It was hypothesized that this was an artifact of the exogenous β-gal transgene in those cells, which might be leading to heightened immunization. Concomitantly, the efficacy achieved through the VSVgm-ICV was examined when initial treatment was started either on day 3 or 4 following tumour inoculation. This was compared to the tumour burden of irrB16-treated mice. In both situations, the VSVgm-ICV was better able to reduce tumour burden, even when treatment was delayed by 4 days (**Figure 3.15c**).

As a consequence of the potential artifacts created by the presence of the β-gal transgene, a similar experiment was undertaken with the parental B16-F10 cell line. Mice were given B16-F10 cells IV, leading to tumour seeding mostly in the lung, though macroscopic tumours can also occur in the thymus, kidneys, and ovaries. Treatments were initiated the following day and all mice were euthanized on day 22 to examine tumour burden (**Figure 3.16a**). Treatment with VSVgm-ICV lead to undetectable tumour

Figure 3.15 – Treatment with the VSVgm-ICV reduces tumour burden in a systemic model of B16-F10.LacZ

(**a**) $8x10^4$ B16-F10.LacZ cells were administered IV and then mice were treated according to the timeline with PBS, VSVgm, irrB16 cells, or the VSVgm-ICV. (**b**) On day 28, all mice were euthanized, at which point lungs were harvested and stained for β-galactosidase. Pictures were then taken using a macro setting on a digital camera. (**c**) The first treatment was postponed until day 3 or 4 and all subsequent treatments moved down as well. All animals were euthanized on day 28 and visualized as above.

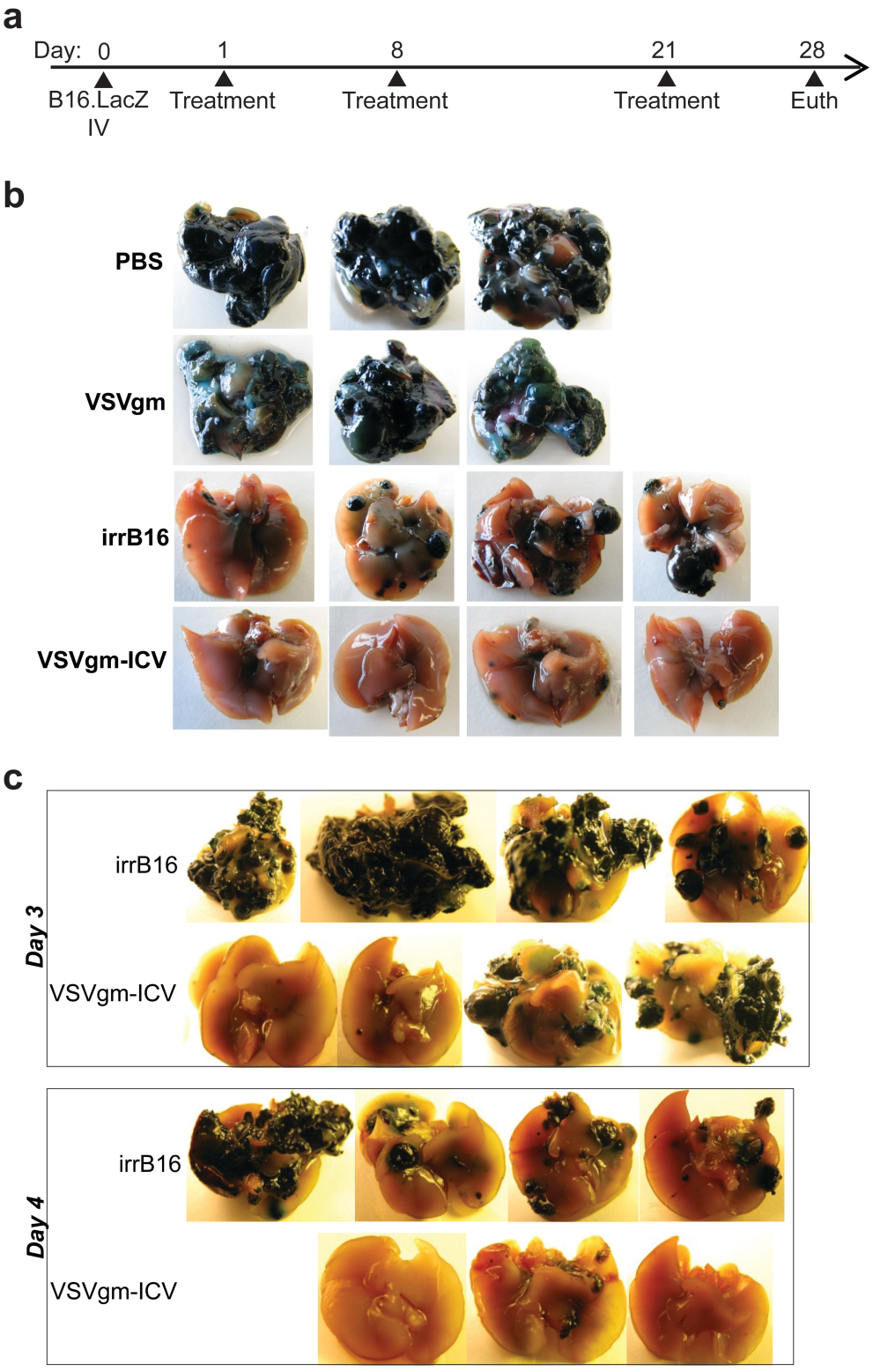
a
Day: 0
1
8
21
28
B16.LacZ IV
Treatment
Treatment
Treatment
Euth
b
PBS
VSVgm
irrB16
VSVgm-ICV
c
Day 3
irrB16
VSVgm-ICV
Day 4
irrB16
VSVgm-ICV

Figure 3.16 – Treatment with the VSVgm-ICV in the B16-F10 systemic dissemination model leads to decreased tumour burden and normal lung weights

(**a**) C57BL/6 mice were injected IV with B16-F10 cells and treated according to presented timeline with the VSVgm-ICV or controls. Mice were euthanized on day 22, and their lungs were weighed and fixed in 10% formalin. Lungs were then sliced and analyzed by hematoxylin and eosin (H&E) staining. (**b**) H&E staining of all mice in one experiment with representative sections demonstrating tumour burden at endpoint. All lungs are on the same scale, with black bar indicating 2 millimeters. A higher magnification of a representative vaccine and control-treated lung are presented on the right. One PBS mouse had the heart buried in tumour, and so the organ could not be removed. A few control mice had tumours in their thymus and so these organs were kept in the H&Es and weights. (**c**) Lung weights shown are pooled from 2 separate experiments and presented as mean + SEM with variance analysis by Mann-Whitney test. Normal lungs are those from mice that have not received any lung tumours or treatments. *P* values, * $P<0.05$, ** $P<0.005$, *** $P\leq0.0001$

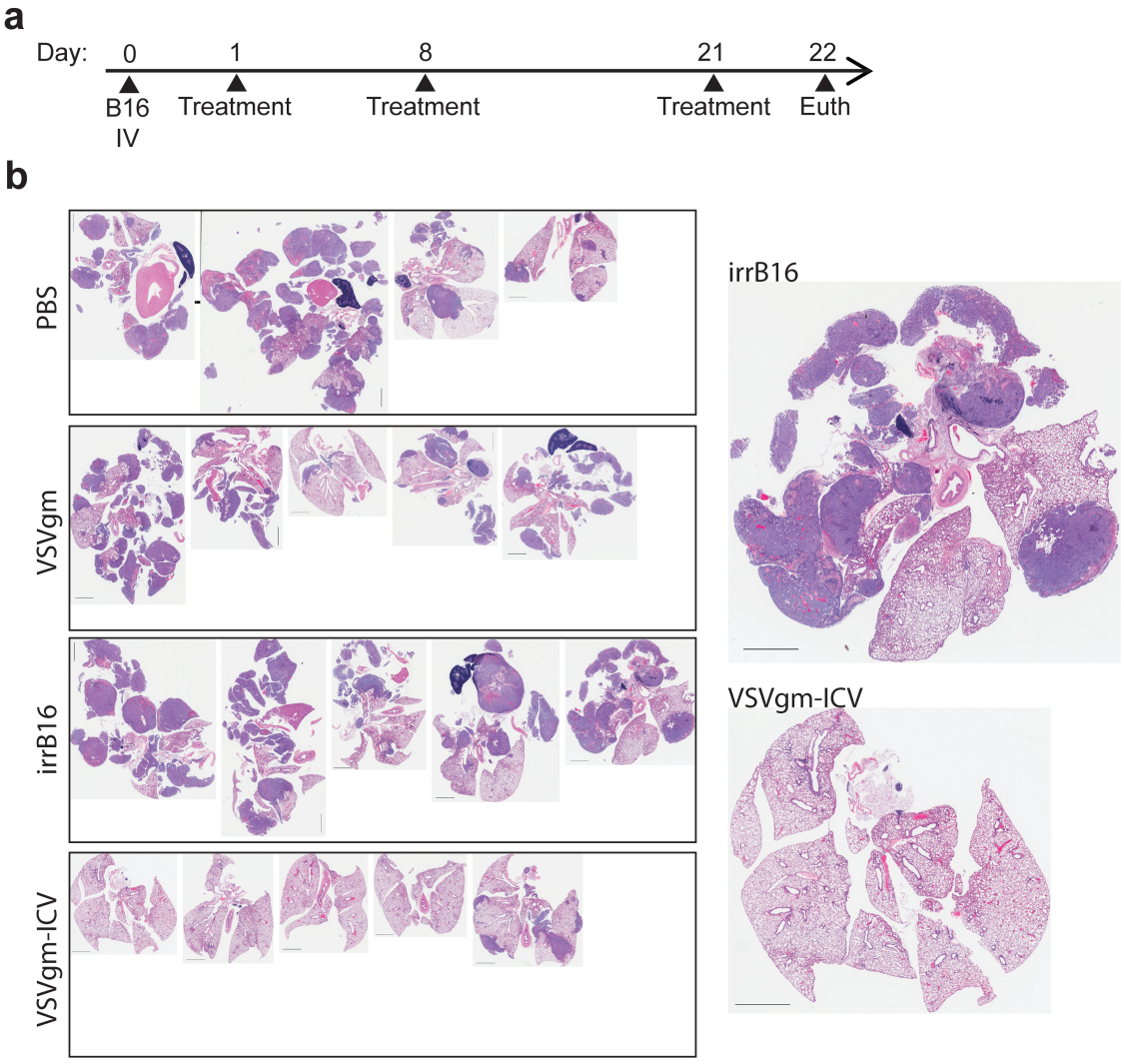
a
Day: 0 1 8 21 22
B16 IV
Treatment
Treatment
Treatment
Euth
b
PBS
VSVgm
irrB16
VSVgm-ICV
irrB16
VSVgm-ICV
c
***
**
**
ns
900
600
300
0
Lung weights (mg)
PBS VSVgm irrB16 VSVgm-ICV Normal
N = 13 5 5 14 4
Treatment

burden in 80 percent of mice and no other tumours were found in any of the animals. In contrast, control-treated mice demonstrate heavy tumour burden, with one PBS-treated mouse found dead before scheduled culling, in addition to 3 other PBS-treated mice, 1 VSVgm-treated mouse, and 1 irrB16-treated mouse having large growths in locations other than the lung (**Figure 3.16b,c**). Lung weights demonstrated that the VSVgm-ICV-treated mice had a much lower tumour burden than controls, identical to non-tumour bearing mouse lungs.

This result highlights the strength of this vaccine platform; it is able to initiate anti-tumour immune responses that are potent enough to slow the progression of a highly aggressive, immunosuppressive, and VSV-resistant tumour.

The therapeutic VSVgm-ICV was also attempted in the CT26.wt tumour model. Balb/C mice bearing CT26.wt flank tumours were treated on day 3 with the VSVgm-ICV, irrCT26.wt, VSVgm, or PBS, all given IP. On day 15 mice were boosted (**Figure 3.17a**). In addition to the homologous prime and boost with the ICV, priming with irrCT26.wt cells followed by a boost with an ICV was also attempted (**Figure 3.17b**). This might lead to a selective anti-tumour boost while only priming an anti-viral response. Intratumoural treatments were also examined as a strategy in the boost situation (**Figure 3.17c**). However, only 2 groups demonstrated significant survival enhancement compared to PBS-treated animals: the mice that were primed with irrCT26.wt or with VSVgm-ICV and then boosted with VSVgm-ICV. A moderate delay in tumour growth was also observed for these two groups compared to PBS (**Figure 3.17d**).

Figure 3.17 – The VSVgm-ICV can delay tumour growth in a therapeutic model of CT26.wt

(**a**) Balb/C mice bearing CT26.wt subcutaneous tumours were treated according to the following timeline with various priming or boosting immunizations. (**b**) Kaplan Meier survival curve of treatments comprising a boost immunization delivered IP. Groups are named according to "prime → boost" strategy. *P* Values; **P*<0.05. (**c**) Kaplan Meier survival curve of treatments comprising a boost immunization delivered intratumourally. Same PBS group as in (b) for reference. There were 5 mice per group, except for the VSVgm-ICV → VSVgm-ICV group and the irrCT26 → VSVgm-ICV, which had 7. Data points are mean + SEM with *P* Values; * *P*<0.05 "irrCT26 → VSVgm-ICV" as compared to PBS group, # *P*<0.05 "VSVgm-ICV → VSVgm-ICV" as compared to PBS group, ** *P*<0.005 as compared to PBS group.

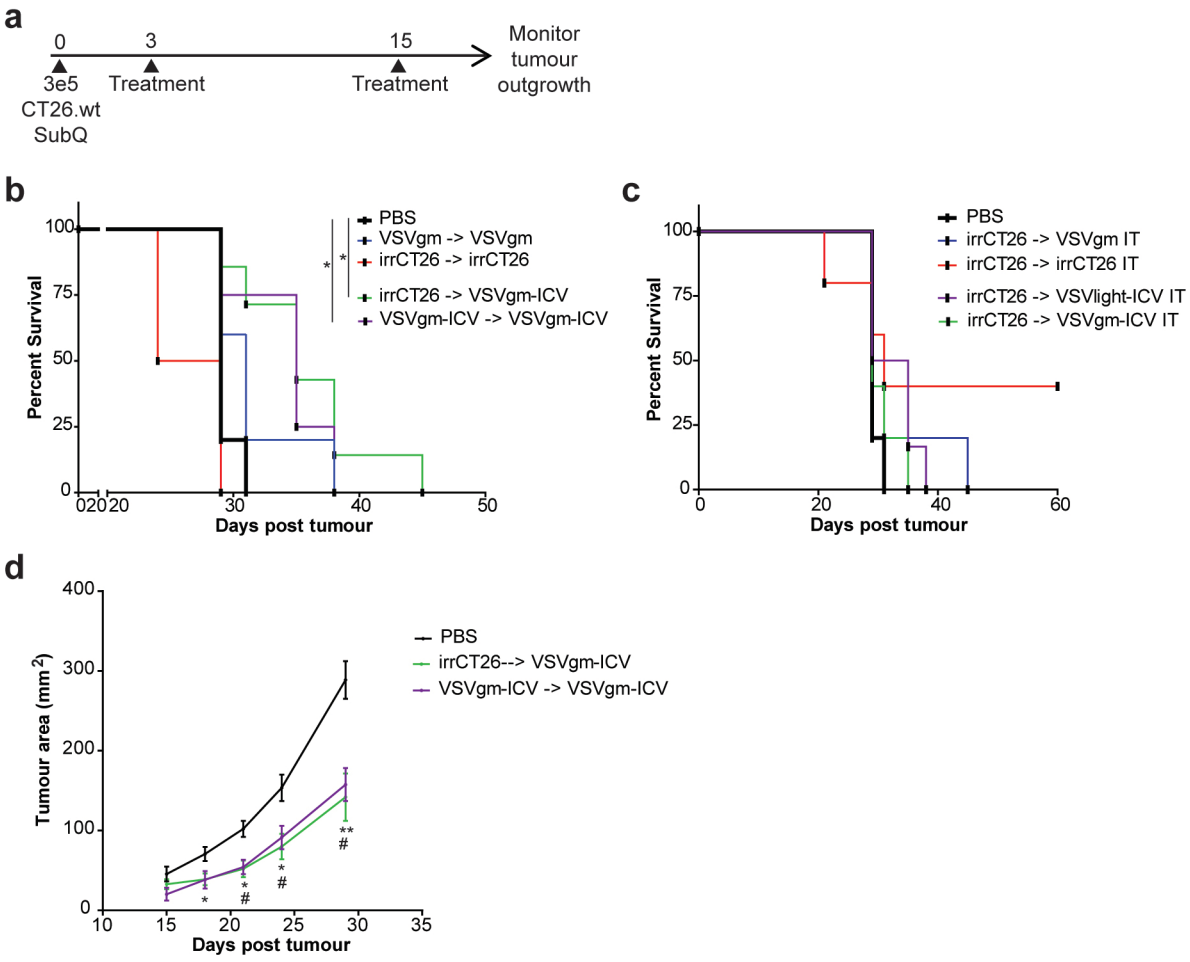
a
0
3
15
Monitor tumour outgrowth
3e5 CT26.wt SubQ
Treatment
Treatment
b
Percent Survival
Days post tumour
PBS
VSVgm -> VSVgm
irrCT26 -> irrCT26
irrCT26 -> VSVgm-ICV
VSVgm-ICV -> VSVgm-ICV
c
Percent Survival
Days post tumour
PBS
irrCT26 -> VSVgm IT
irrCT26 -> irrCT26 IT
irrCT26 -> VSVlight-ICV IT
irrCT26 -> VSVgm-ICV IT
d
Tumour area (mm 2)
Days post tumour
PBS
irrCT26--> VSVgm-ICV
VSVgm-ICV -> VSVgm-ICV

The therapeutic efficacy of the VSVgm-ICV was also investigated in a spontaneous model of ovarian cancer. This model, herein named the MISIIRTAg model, is characterized by bilateral ovarian tumours of epithelial origin that are very resistant to VSV-Δ51 (personal communication with Dr. B Vanderhyden). These FVB/N-MISIIRTAg mice consistently reach endpoint at approximately 14 weeks of age due to large ovarian tumours and ascites. One such tumour had previously been harvested and a cell line was established: the 6048R cell line, which was used to make the infected cell vaccine. A small pilot study indicated that the VSVgm-ICV could have efficacy in this model (**Figure 3.18a,b**). A more extensive study was performed to investigate the efficacy of the VSVgm-ICV as well as determine if IP treatment with VACVgm could enhance the efficacy of the vaccine (**Figure 3.18c)**. Unpublished research from the Bell lab indicates that VACV replicates very well in these tumours, but VSV-Δ51 does not, however, neither virus had efficacy in reducing tumour burden or increasing survival. In addition, VACV replication can enhance VSV replication through the secretion of B18R(92). The only groups demonstrating a statistically significant decrease in tumour burden were the VSVgm-ICV and VSVgm-ICV + VACVgm treated mice (**Figure 3.18c,d**). However, all treatment groups appear to trend towards lower tumour burden as compared to PBS treated mice.

Antibody binding to tumour cells has been shown to increase phagocytosis and lead to antigen presentation by APCs through binding of their Fc receptors(169). It was postulated that antibody binding to the infected cell in the ICV might, therefore, enhance the efficacy. To investigate this possibility, mice bearing B16-F10 flank tumours were treated with the VSVgm-ICV or relevant controls. Anti-VSV antibody was generated through immunization, either passive by serum transfer or active, with the goal of these antibodies

Figure 3.18 – The VSVgm-ICV reduces tumour burden in the MISIIRTAg model of spontaneous ovarian cancer

(**a**) Trangenic MISIIRTAg mice previously confirmed to be homozygous for SV40 Tag expression were treated with the VSVgm-ICV made with 6048R cells or PBS according to the indicated timeline and euthanized at week 14. (**b**) Ovaries were harvested at necropsy and weighed. Total ovary weight per mouse is graphed. (**c**) A follow-up experiment with more controls was undertaken. Mice were treated according to the timeline with the VSVgm-ICV or relevant controls. In addition, a VACVgm IP treatment was assessed for its ability to enhance the vaccine effect and was given 3 days before the vaccine dose. All mice were born within 2 weeks of each other. *P* Values; **P*<0.05.

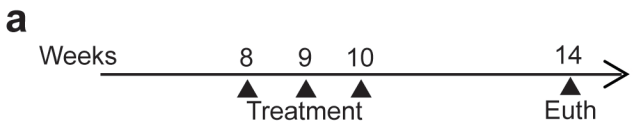
a
Weeks
8
9
10
14
Treatment
Euth

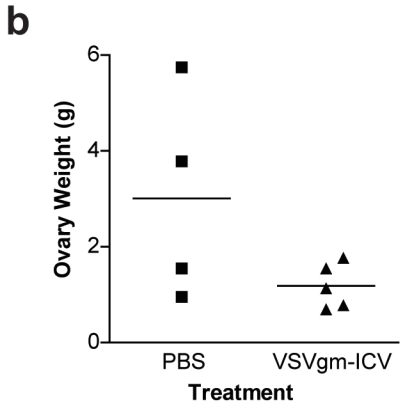
b
Ovary Weight (g)
6
4
2
0
PBS
VSVgm-ICV
Treatment

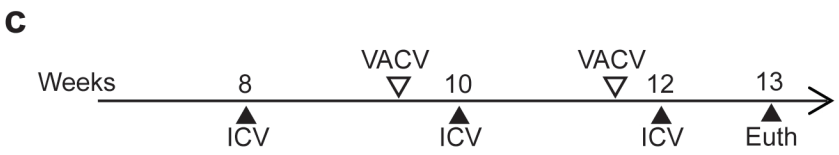
c
Weeks
8
VACV
10
VACV
12
13
ICV
ICV
ICV
Euth

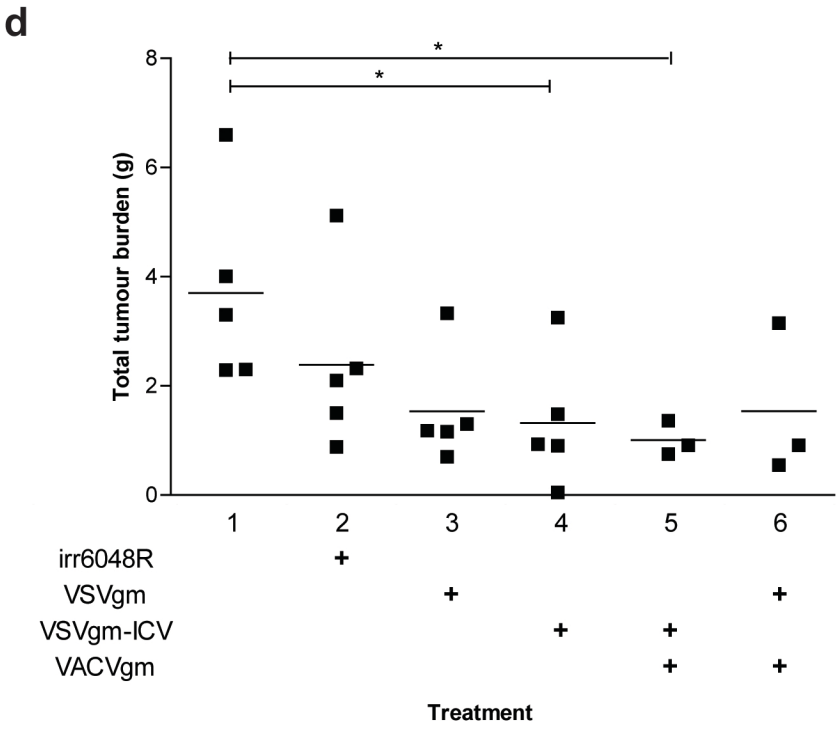
d
Total tumour burden (g)
8
6
4
2
0
*
*
1
2
3
4
5
6
irr6048R
VSVgm
VSVgm-ICV
VACVgm
Treatment

coating the VSV infected cells. In addition, one group received VSVgm-ICV that was *ex vivo* incubated with anti-VSV serum. Notably, all three groups that had anti-VSV antibodies demonstrated a significant decrease in efficacy compared to the VSVgm-ICV (**Figure 3.19**).

3.3.7 Examining the role of NK and T cells in the efficacy achieved with the VSVgm-ICV

To investigate the role of NK cells in the therapeutic efficacy of VSVgm-ICV, the B16-F10 IV model described in **Figure 3.16** was established in mice depleted of NK cells using NK1.1 antibody. To simplify the model, only one dose of the ICV was administered and animals were euthanized on day 16 (**Figure 3.20a**). Confirmation of depletion was done on day 4 on saphenous bleeds by flow cytometry after staining with anti-DX5. Only a slight depletion in NK cells (**Figure 3.20b**). Though the flow cytometric examination of the depletion did not yield statistically significant results, the mice demonstrated a large increase in tumour burden in both the lung and the liver, which was never noted in the undepleted mice (**Figure 3.20c**). Surprisingly, the VSVgm-ICV was still able to debulk a large proportion of the tumours in the face of a partial NK depletion and with only one dose (**Figure 3.20d**).

Another NK depletion was undertaken using a commercial anti-asialo depleting antibody and mice were treated with two doses of ICV **(Figure 3.21a)**. Depletions were monitored at day 4 as before (**Figure 3.21b**) and at endpoint by examining the spleen (**Figure 3.21c**); both demonstrating a good depletion of NK cells. Mice treated with the anti-asialo antibody had a similar tumour burden as those depleted with the anti-NK1.1 antibody (**Figure 3.20c**). However, mice treated with the anti-asialo antibody did not tolerate the treatment beyond the first 10 days and had to be euthanized early because of declining health due to the antibody

Figure 3.19 – The presence of anti-VSV plasma reduces ICV efficacy

This experiment is the same as the one presented in Figure 2.14 but with three extra groups. The active immunization group was immunized with $5x10^8$ pfu VSVgm 10 days prior to B16-F10 implantation. The passive immunization group received 120uL of immune plasma from mice actively immunized one day prior to their first and second VSVgm-ICV dose. The "VSVgm-ICV + Ab ex vivo" group had their ICV made as per the usual protocol for a 2 hour incubation, then 400uL of ICV was incubated for 1 hour with 120uL immune serum at 37C. To accommodate this preparation, all ICV preparations were extended to 3 hour incubations. There were 5 mice per group.

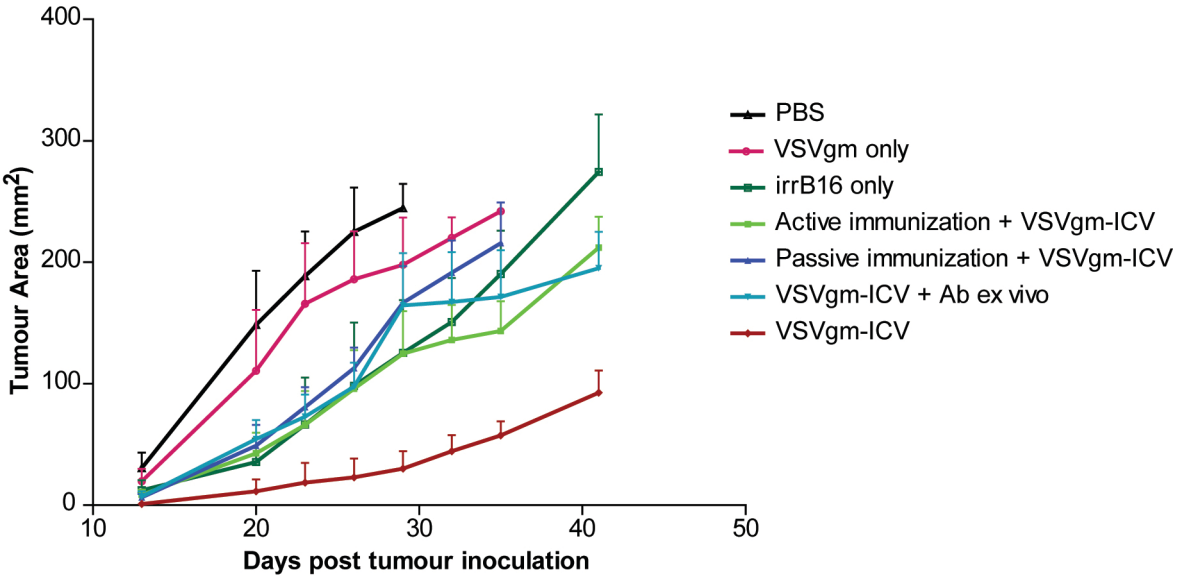
400
300
200
100
0
Tumour Area (mm2)
10
20
30
40
50
Days post tumour inoculation
PBS
VSVgm only
irrB16 only
Active immunization + VSVgm-ICV
Passive immunization + VSVgm-ICV
VSVgm-ICV + Ab ex vivo
VSVgm-ICV

Figure 3.20 – One dose of the VSVgm-ICV can impede tumour growth in the face of a partial NK depletion

(**a**) C57BL/6 mice were treated with an anti-NK1.1 antibody and the VSVgm-ICV or PBS. Mice were injected IV with $7x10^4$ B16-F10 tumours on day 0. (**b**) Confirmation of depletion on day 4 using anti-DX5 antibody using 3 mice per group. (**c**) Tumour burden in the livers and lungs in PBS + anti-NK1.1-treated mice. (**d**) Tumour burden in the livers and lungs of VSVgm-ICV + anti-NK1.1-treated mice.

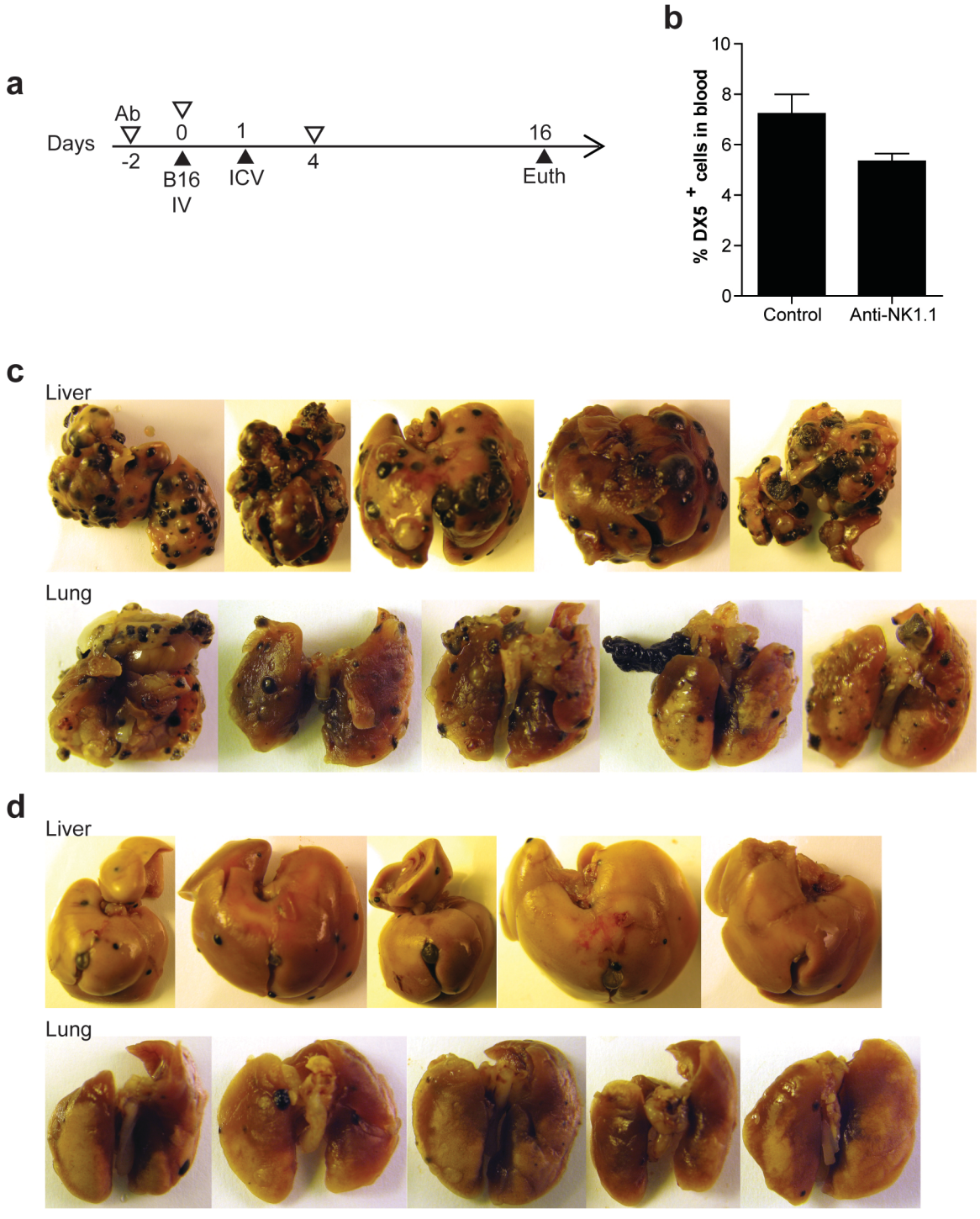
a
Days
Ab
-2
0
B16
IV
1
ICV
4
16
Euth
b
% DX5 + cells in blood
10
8
6
4
2
0
Control
Anti-NK1.1
c
Liver
Lung
d
Liver
Lung

Figure 3.21 – The VSVgm-ICV maintains moderate efficacy despite NK depletion

(**a**) C57BL/6 mice were treated with an anti-asialo antibody or nothing and immunized with the VSVgm-ICV or PBS according to the given timeline. (**b**) Depletions were confirmed on day 7 using an anti-NK1.1 antibody on PBMCs with 2 mice per group. (**c**) Splenic NK1.1 content at endpoint in VSVgm-ICV-treated mice. (**d**) Livers were examined for tumour burden in the anti-asialo treated mice and enumerated under dissecting microscope. (**e**) Lungs were examined for tumour burden in the anti-asialo-treated mice. Tumour nodules were too numerous to count in the PBS-treated group.

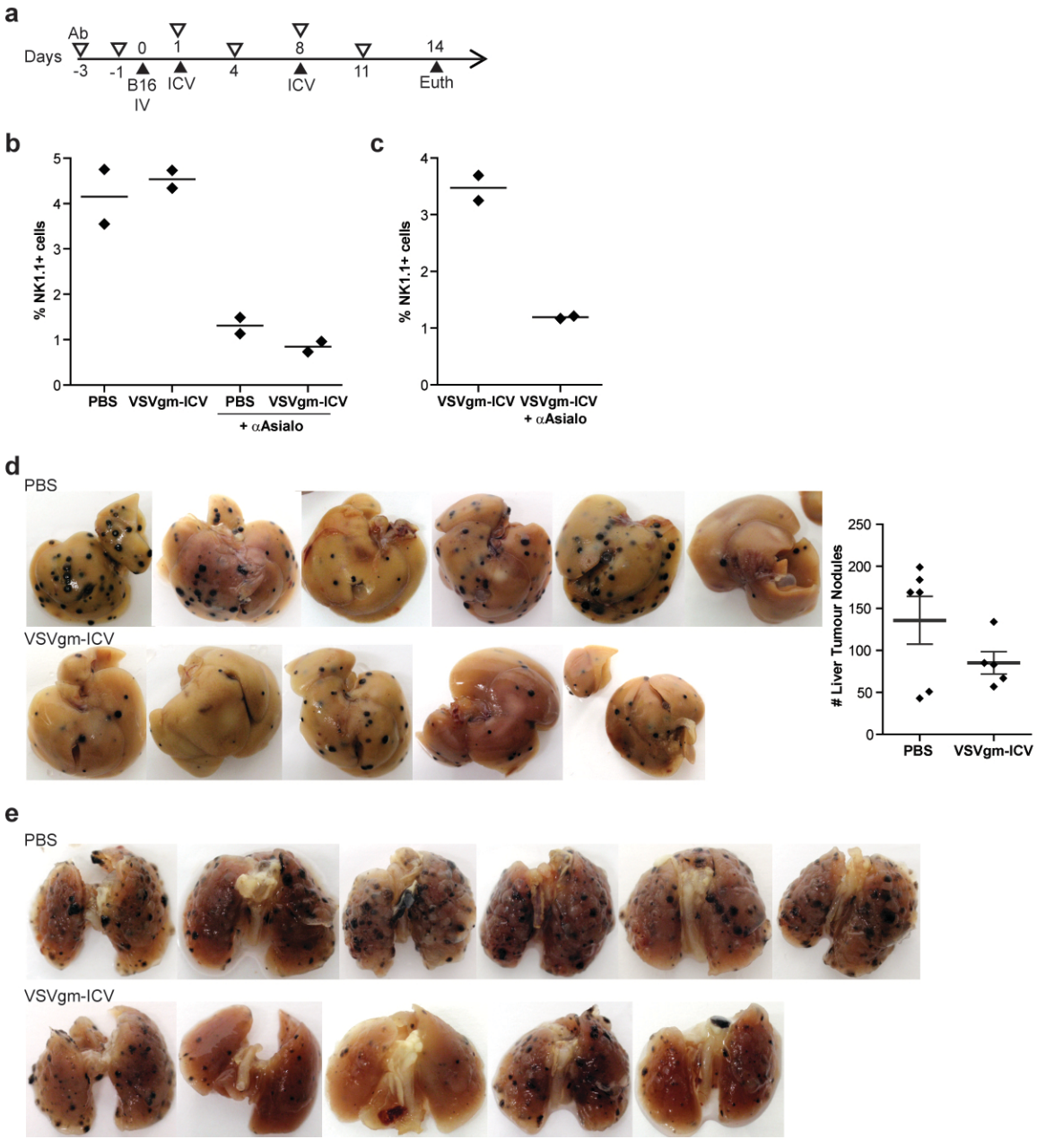
a
Ab
Days
-3
-1
0
1
4
8
11
14
B16 IV
ICV
ICV
Euth
b
% NK1.1+ cells
PBS
VSVgm-ICV
PBS
VSVgm-ICV
+ αAsialo
c
% NK1.1+ cells
VSVgm-ICV
VSVgm-ICV
+ αAsialo
d
PBS
VSVgm-ICV
Liver Tumour Nodules
PBS
VSVgm-ICV
e
PBS
VSVgm-ICV

injections. The VSVgm-ICV was still able to decrease tumour burden in the depleted mice, though to a lesser extent than what was previously seen (**Figure 3.21d**).

To determine the contribution of $CD8^+$ T cells in the therapeutic efficacy of the VSVgm-ICV, experiments were undertaken in the presence or absence of anti-CD8 depleting antibody (**Figure 3.22a**). The depletion was first confirmed at day 4 on saphenous bleeds by flow cytometric analysis (**Figure 3.22b,c**) and then again at sacrifice on splenocytes (**Figure 3.22d**). The CD8 depletion was confirmed to be potent and long-lasting. Pictures and weights of the harvested lungs and other tumours reveal a slight decrease in efficacy of the vaccine in 3 of the 8 mice treated with the VSVgm-ICV+αCD8 (**Figure 3.22e,f**), though no statistical significance was achieved in the tumour weights ($p=0.1246$). The same four normal lung weights from Figure 2.16 are represented here for comparison.

An additional group was treated with the VSVgfp-ICV to allow for examination of the impact of GM-CSF in the therapeutic efficacy of the VSV-ICV in this model. As opposed to the decrease in efficacy seen in the prophylactic ICV, the VSVgfp-ICV suffered no loss in efficacy as compared to the VSVgm-ICV (**Figure 3.22f**).

Peptide-based T cell assays were used to measure the cytokine secretion abilities of $CD8^+$ T cells following VSVgm-ICV. Mice bearing B16-F10 subcutaneous tumours and treated as in **Figure 3.14** had blood harvested on day 10 post tumour inoculation (**Figure 3.23a**). PBMCs were re-stimulated for 5 hours with either VSV N peptide or both the GP100 and DCT peptides, to measure anti-B16-F10 immune responses. IFNγ intracellular staining was then performed on these cells. Though a robust anti-VSV response was measured (**Figure 3.23b**), no anti-GP100/DCT response was observed (**Figure 3.23c**).

Figure 3.22 – The VSVgm-ICV maintains efficacy despite a strong CD8 depletion

(**a**) C57BL/6 mice were used in the B16-F10 systemic dissemination model as described previously and treated with an anti-CD8 antibody IP following the specified timeline. (**b**) Flow cytometry dot plots of the depletion confirmation on day 4 PBMCs using anti-CD3 and anti-CD8 antibodies. (**c**) Summary of findings from (b) denoting percent of PBMCs that are $CD3^{+}CD8^{+}$. (**d**) CD8 flow cytometry on spleens at endpoint. (**e**) Pictures of lungs and systemic tumours demonstrating tumour burden. (**f**) The total weight of systemic tumour burden with mean + SEM. N was 8 mice per group, except for VSVgfp-ICV that had 9. Normal non-tumour bearing lungs are included for comparison. *P* Values; **P*<0.05.

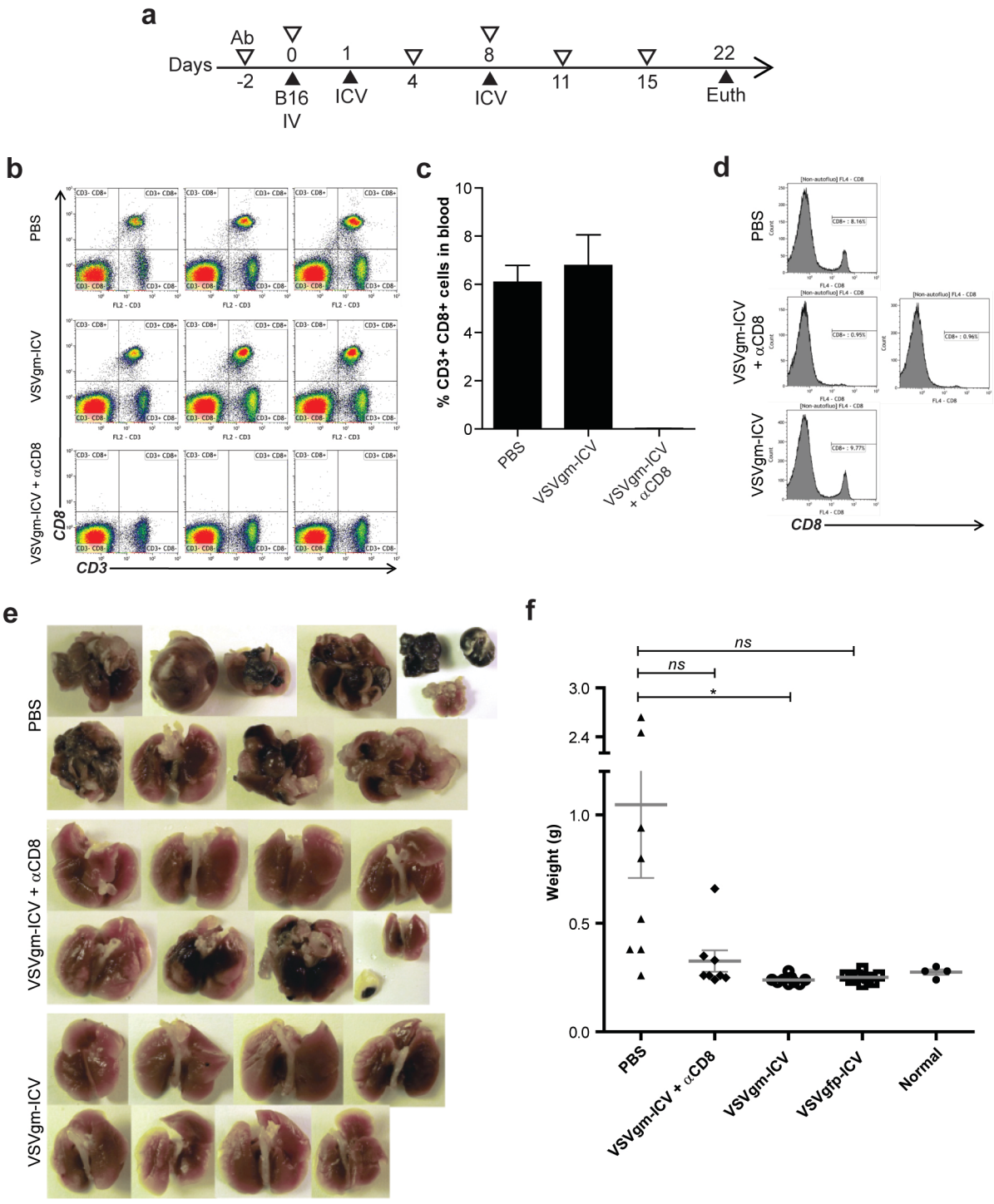
a
Ab
Days
-2
0
B16
IV
1
ICV
4
8
ICV
11
15
22
Euth
b
PBS
VSVgm-ICV
VSVgm-ICV + αCD8
CD8
CD3
c
% CD3+ CD8+ cells in blood
PBS
VSVgm-ICV
VSVgm-ICV + αCD8
d
PBS
VSVgm-ICV + αCD8
VSVgm-ICV
CD8
e
PBS
VSVgm-ICV + αCD8
VSVgm-ICV
f
ns
ns
*
Weight (g)
PBS
VSVgm-ICV + αCD8
VSVgm-ICV
VSVgfp-ICV
Normal

Figure 3.23 – T cell assays using DCT/GP100 peptides

(**a**) C57BL/6 mice from **figure 2.14** treated according to the specified timeline were bled on day 10 and their PBMCs assessed for reactivity against the (**b**) VSV N or the (**c**) DCT/GP100 peptides by IFNγ intracellular staining. (**b-c**) Following *in vitro* stimulation with either no peptide, the VSV N peptide, or the B16 peptides (DCT/GP100), PBMCs were assessed for percent of $CD3^{+}CD8^{+}$ cells that were expressing IFNγ. There were 5 mice per group. (**d**) *In vivo* CTL assay performed on mice treated according to the specified timeline. (**e**) Percent specific lysis of the $CFSE^{high}$ + peptide labeled splenocytes in all groups. There were 4 mice per group, except the PBS group that had 3. No statistical significance was achieved for any group.

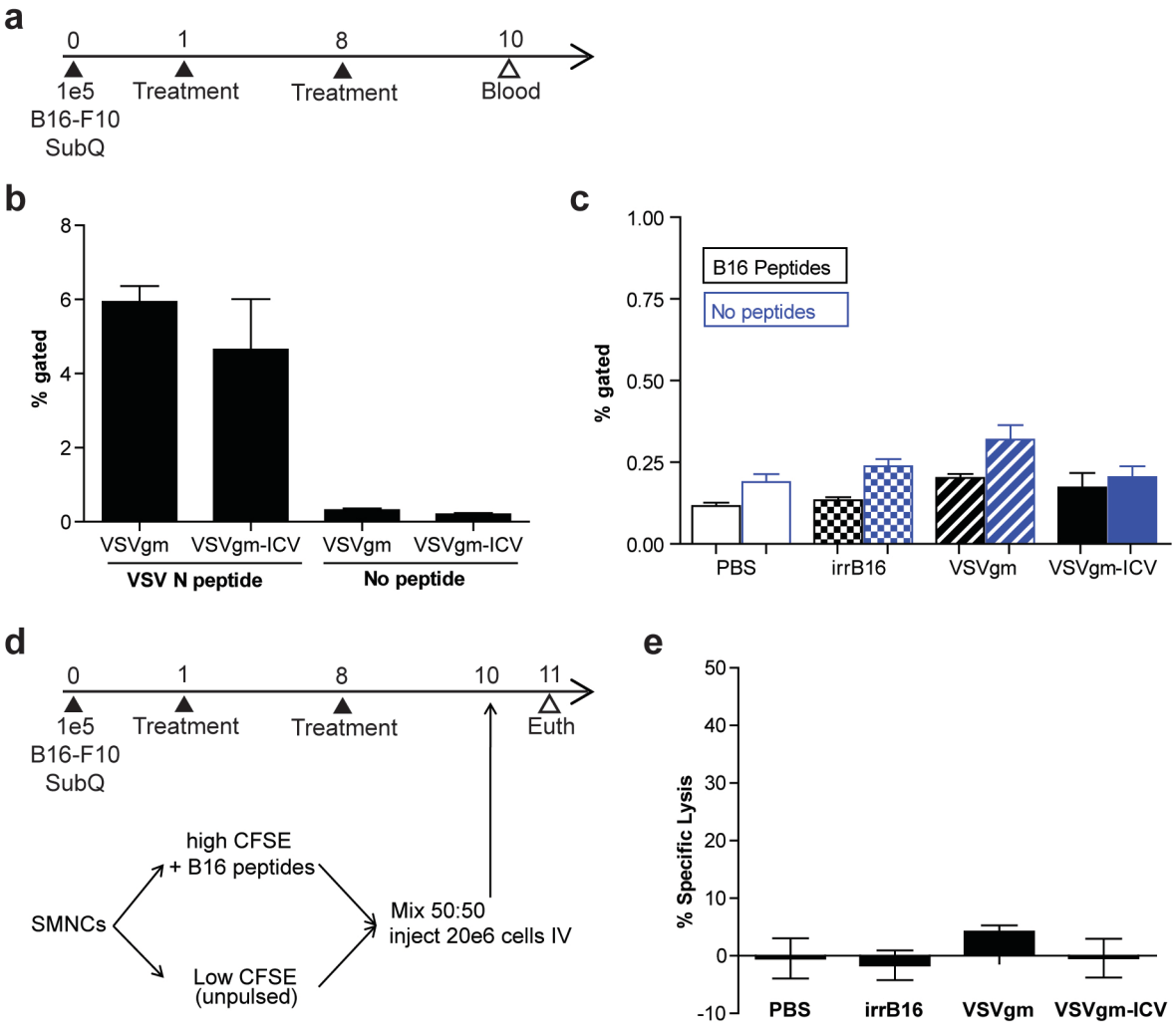
a
0
1
8
10
1e5
B16-F10
SubQ
Treatment
Treatment
Blood
b
% gated
VSVgm
VSVgm-ICV
VSVgm
VSVgm-ICV
VSV N peptide
No peptide
c
% gated
B16 Peptides
No peptides
PBS
irrB16
VSVgm
VSVgm-ICV
d
0
1
8
10
11
1e5
B16-F10
SubQ
Treatment
Treatment
Euth
high CFSE
+ B16 peptides
SMNCs
Low CFSE
(unpulsed)
Mix 50:50
inject 20e6 cells IV
e
% Specific Lysis
PBS
irrB16
VSVgm
VSVgm-ICV

The previous assay required the isolation of immune cells from the animal and assumed that the tumour reactive T cells were in the blood. To bypass this assumption an *in vivo* CTL assay was performed in the therapeutic B16-F10 flank model. Splenocytes from naïve syngeneic donors were harvested and labeled with low CFSE or high CFSE plus the peptides of interest, which in this case were the GP100 and DCT peptides (**Figure 3.23d**). These were injected into tumour-bearing treated mice. The ratio of recovered cells correlates to the immune activation targeting those antigens; no responses were observed against GP100 or DCT (**Figure 3.23e**).

Both previous assays relied on the re-stimulation of $CD8^+$ T cells with peptides, assuming that the response against those peptides would be strong enough to measure. To circumvent this potential problem, two assays were undertaken against whole B16-F10 targets, vastly increasing the number of antigens presented to the effectors. IFNγ production was examined from whole PBMCs incubated with B16-F10 cells for 48 hours. These PBMCs were from the mice treated in **Figure 3.22** and the cells were harvested on day 22, when lungs were examined. The results demonstrate a strong trend towards increased IFNγ production in the PBMCs from VSVgm-ICV treated mice, though not only dependent upon *ex vivo* re-stimulation (**Figure 3.24a**). Baseline cytokine secretion was increased in the VSVgm-ICV mice, however, there appears to be a moderate decrease in IFNγ production in mice whose $CD8^+$ cells were depleted (**Figure 3.24b,c**). The difference between unstimulated and whole B16-F10 cell-stimulated PBMCs demonstrates a statistically significant increase in IFNγ secretion for VSV-ICV-treated PBMCs (**Figure 3.24c**). In addition, VSVgm-ICV PBMCs have slightly increased IFNγ secretion following

Figure 3.24 – T cell assays using whole B16-F10 cells as targets

(**a**) Mice from **figure 3.22** had their blood taken at endpoint and PBMCs were incubated for 48 hours with nothing, whole B16-F10 cells, or a mix of DCT/GP100 peptides and anti-CD28. Supernatants were then assayed for IFNγ by ELISA. There were 8 mice per group, except for VSVgfp-ICV that had 9. (**b**) Graph depicting the IFNγ production on a per mouse basis during PBMC incubation with nothing or with whole B16-F10 cells, showing an upward trend. (**c**) Mean +SEM difference between PBMCs incubated with nothing and those incubated with whole B16-F10 cells. (**d-e**) Chromium release assay against B16-F10 targets on the $CD8^+$ cells of undepleted mice from **figure 3.21**, 3 mice per group. (**d**) The percent of $CD8^+$ cells following magnetic selection in both groups. (**f**) The average percent killing of B16-F10 targets by $CD8^+$ effectors at various effector to target ratios. Data points are mean of 3 mice + SEM, *P* Values; $*P<0.05$.

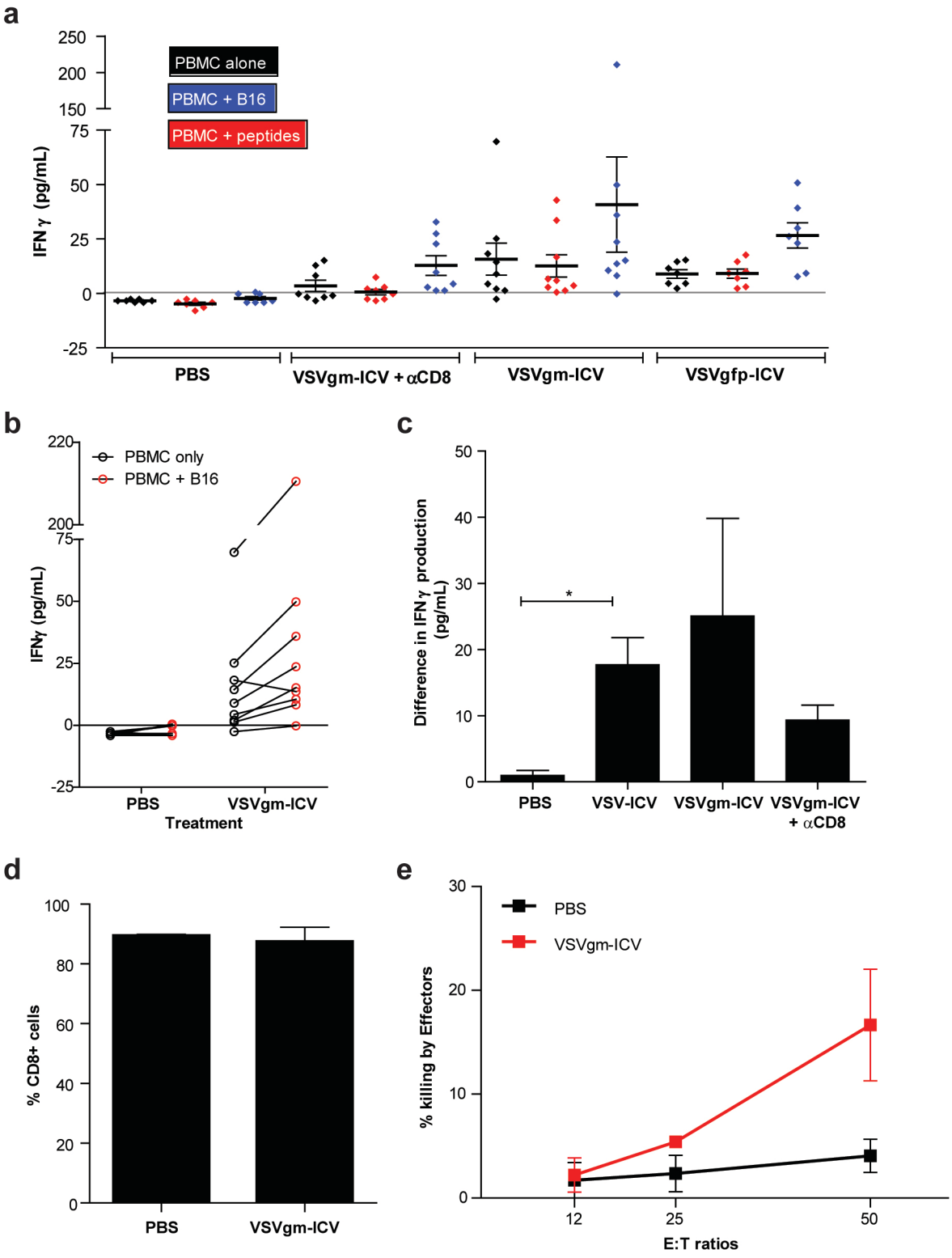
a
PBMC alone
PBMC + B16
PBMC + peptides
IFN γ (pg/mL)
250
200
150
75
50
25
0
-25
PBS
VSVgm-ICV + αCD8
VSVgm-ICV
VSVgfp-ICV
b
PBMC only
PBMC + B16
IFNγ (pg/mL)
220
200
75
50
25
0
-25
PBS
VSVgm-ICV
Treatment
c
Difference in IFN γ production (pg/mL)
50
40
30
20
10
0
*
PBS
VSV-ICV
VSVgm-ICV
VSVgm-ICV + αCD8
d
% CD8+ cells
100
80
60
40
20
0
PBS
VSVgm-ICV
e
PBS
VSVgm-ICV
% killing by Effectors
30
20
10
0
12
25
50
E:T ratios

re-stimulation with whole B16-F10 cells when compared to unstimulated PBMCs. PBS-treated mice have no IFNγ production, with or without re-stimulation.

A chromium release assay was also used to examine the anti-B16-F10 response of $CD8^+$ splenocytes. In this case, spleens were harvested from the mice in **Figure 3.21** on day 16 post B16-F10 cell injection. $CD8^+$ cells were isolated through negative selection (**Figure 3.24d**) and were incubated with $chromium^{51}$-labeled B16-F10 cells. The results demonstrated a trend towards increased B16-F10 death only when targets were incubated with the $CD8^+$ cells from VSVgm-ICV-treated mice (**Figure 3.24e**).

3.3.8 Poxviruses do not exhibit immune stimulatory capabilities in an ICV platform

ORFV has been demonstrated to stimulate both DCs and NK cells, leading to robust immune responses against viral pathogens(168) and cancer(135). However, the mechanism of this anti-cancer response is not fully understood, though it does appear to be partially NK-dependent(135). To determine if ORFV could perform as VSV does in the ICV, a prophylactic B16-F10 vaccination was performed with ORFV (**Figure 3.25a**). The cell number was decreased to $5x10^5$ to better suite the titers of available ORFV stocks and a VSV-ICV was made in the same way for comparison. While a delay in tumour growth was achieved by immunizing with $5x10^5$ VSV-infected cells (**Figure 3.25b**), it is not as protective as with $5x10^6$ cells, which protects approximately 30% of immunized mice from tumour growth (**Figure 3.5**). However, the ORFV-ICV failed to protect the mice against the tumour challenge, leading to tumour growth and survival identical to control-treated animals.

In addition to the prophylactic ICV, a therapeutic ORFV-ICV was performed to rule out its potential in eliciting a protective NK cell response during ICV immunization

Figure 3.25 – An ORFV-ICV does not protect from tumour growth in prophylactic or therapeutic B16-F10 models.

(a) C57BL/6 mice were treated with gamma-irradiated B16-F10 cells (irrB16), the ORFV-ICV, or the VSV-ICV made the same way as the ORFV-ICV for comparison. There were 5 mice per group, except for the PBS group that had 6. (b) Graph of the mean tumour area over time + SEM. (c) B16-F10 tumour-bearing mice were treated according to the timeline with PBS, irrB16 only, ORFV, or an ORFV-ICV. (d) Kaplan Meier survival plot with 6 mice per group, except for irrB16 only that had 7 and *P* Values are **P*<0.05, ***P*<0.005.

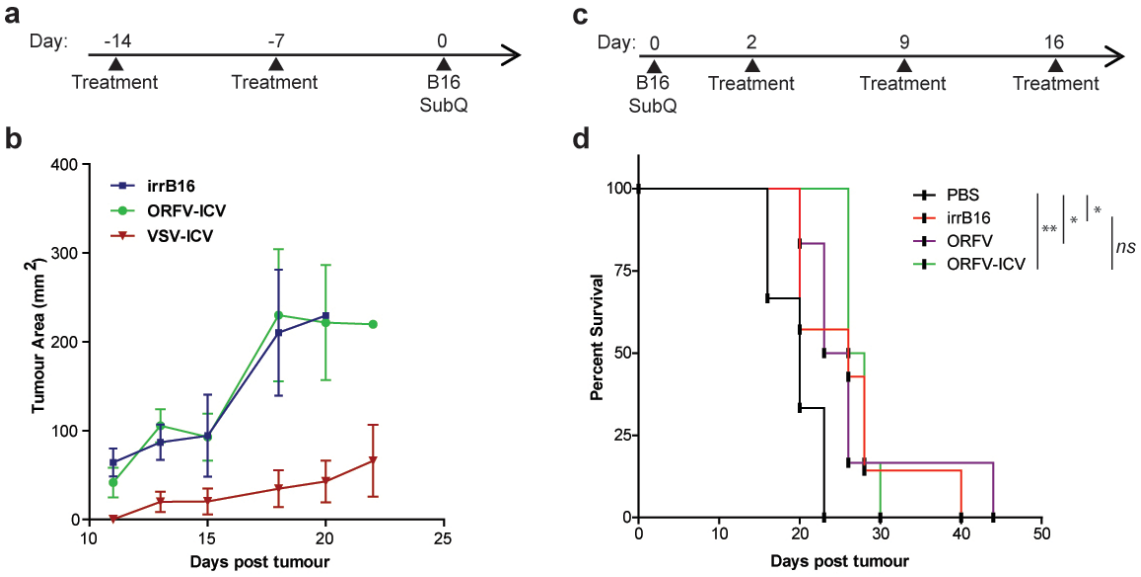
a
Day:
-14
-7
0
Treatment
Treatment
B16
SubQ
b
irrB16
ORFV-ICV
VSV-ICV
Tumour Area (mm 2)
Days post tumour
c
Day:
0
2
9
16
B16
SubQ
Treatment
Treatment
Treatment
d
PBS
irrB16
ORFV
ORFV-ICV
**
*
*
ns
Percent Survival
Days post tumour

(**Figure 3.25c**). To increase the efficacy of the vaccine, $5x10^6$ cells were used per dose and cells were infected with an MOI of 3 instead of 10, which should infect most or all cells nonetheless. However, the ORFV-ICV was unable to enhance the slight delay in tumour growth achieved with irrB16 cells only (**Figure 3.25d**).

Vaccinia virus is a current oncolytic clinical candidate and is demonstrating great promise as a robust anti-cancer agent(17, 69, 100, 122). This virus has also been widely used as the vaccine for smallpox and (115). However, these Vaccinia uses differ from the ability to induce a protective immune response when replicating in a tumour cell, as is necessary in an ICV. The mutant Vaccinia used in the following studies has a deletion in the TK gene and was engineered to express human or murine GM-CSF. Because human and mouse GM-CSF are species specific, the human GM-CSF-expressing virus is considered to be null for GM-CSF in the mouse(145). A prophylactic VACV-ICV was performed to examine the immunization capabilities of such a vaccine. The vaccine was also attempted with Vaccinia expressing murine GM-CSF (VACVgm). Neither virus was able to protect mice against B16-F10 challenge (**Figure 3.26a**), though a very slight delay in tumour growth was observed with the VACVgm-ICV (**Figure 3.26b**). As with ORFV, VACVgm was also not able to delay tumour growth in a therapeutic model of B16-F10 (**Appendix II**). A comprehensive optimization of the VACVgm-ICV was undertaken to determine if therapeutic efficacy could be augmented through alterations in the ICV protocol. An initial experiment was performed where each ICV preparation differed from the last in only one way, to better assess the impact of each alteration. A trend towards fewer lung tumours is observed when the VACVgm-ICV was allowed to infect for 24 hours instead of 2 hours.

Figure 3.26 – A VACV-ICV does not enhance tumour protection in a prophylactic model of subcutaneous B16-F10

(**a**) C57BL/6 mice were treated according to the regular prophylactic protocol. VACV either expressing human GM-CSF (VACV-ICV) or the murine GM-CSF (VACVgm-ICV) was used. Kaplan Meier survival curve with 5 mice per group, except for the VACVgm-ICV, which had 6. (**b**) Average day to tumour outgrowth for all groups + SEM, with *P* Value; **P*<0.05.

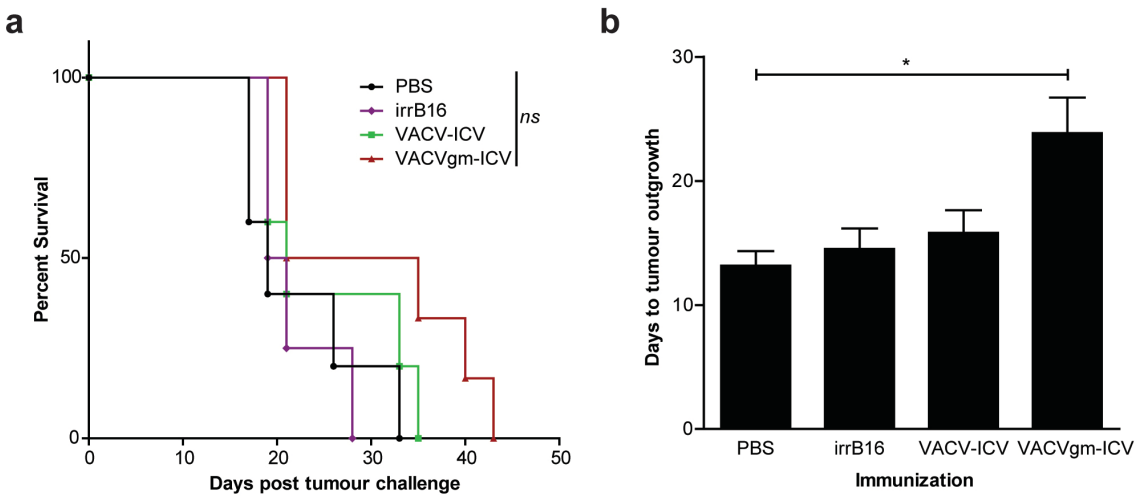
a
100
50
0
0
10
20
30
40
50
Percent Survival
Days post tumour challenge
PBS
irrB16
VACV-ICV
VACVgm-ICV
ns
b
30
20
10
0
*
Days to tumour outgrowth
PBS
irrB16
VACV-ICV
VACVgm-ICV
Immunization

The model was repeated with an earlier first treatment to favour therapeutic efficacy with the vaccine but the results did not show the trend previously observed (**Appendix II**).

The impact of VSV, VACV, and ORFV on DCs has been previously investigated in the literature; however, they have never been compared to understand their relative impact. In addition, there are conflicting reports as to the ability of VACV to induce DC maturation (70, 71, 176), though many publications do not indicate which strain of VACV they were using. To determine the impact of these viruses on DC maturation, an *in vitro* stimulation assay was performed with bone-marrow derived DCs (BM-DCs). The BM-DCs were incubated for 16 hours with no stimulation (negative control), CpG (positive control), or each virus at an MOI of 3. The BM-DCs were then analyzed by flow cytometry. Previous publications have noted the ability of VSV-Δ51 to induce DC maturation (14), and this finding was corroborated (**Figure 3.27**). Upon incubation with BM-DCs, vaccinia virus was unable to increase the expression of the co-stimulatory molecules CD40 or CD86 (**Figure 2.27a-d**). ORFV demonstrated an intermediate phenotype between VSV and VACV.

To better understand the BM-DC response when virus is in the context of an immunosuppressive tumour, B16-F10 cells were co-incubated with BM-DCs with or without a VSV or VACV infection. Interestingly, adding B16-F10 cells to the BM-DCs greatly reduced the background level of CD40 and CD86 (**Figure 2.27e-h**). Upon addition of VSV, the mean expression level of CD86 returned to baseline on the BM-DCs, and more of these cells were positive for this protein. CD40 expression increased moderately above baseline. Surprisingly, when VACV was added to the B16-F10 and BM-DC co-culture, the expression of CD40 and CD86 decreased even further.

Figure 3.27 – *In vitro* DC maturation assay demonstrates potent VSV immunogenicity

DCs were matured *in vitro* and incubated for 16 hours with various stimulants and then assayed for the expression of CD86 or CD40 by flow cytometry. (**a, c, e, g**) Percent of CD11c+ cells expressing co-stimulatory marker. (**b, d, f, h**) Mean fluorescence intensity of co-stimulatory expression on $CD11c^+$ cells. All samples were performed in duplicate.

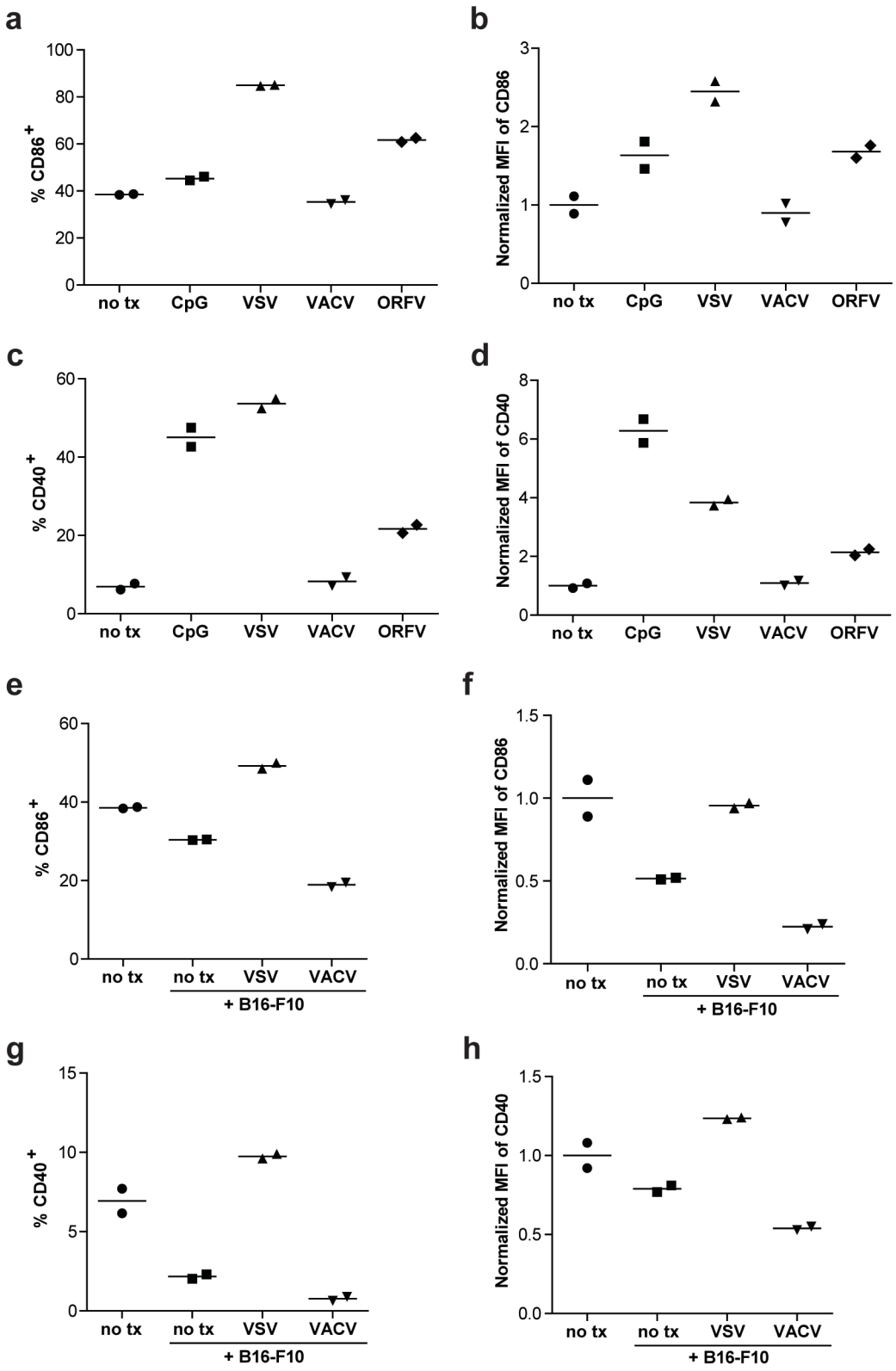
a
% CD86+
100
80
60
40
20
0
no tx
CpG
VSV
VACV
ORFV
b
Normalized MFI of CD86
3
2
1
0
no tx
CpG
VSV
VACV
ORFV
c
% CD40+
60
40
20
0
no tx
CpG
VSV
VACV
ORFV
d
Normalized MFI of CD40
8
6
4
2
0
no tx
CpG
VSV
VACV
ORFV
e
% CD86+
60
40
20
0
no tx
no tx
VSV
VACV
+ B16-F10
f
Normalized MFI of CD86
1.5
1.0
0.5
0.0
no tx
no tx
VSV
VACV
+ B16-F10
g
% CD40+
15
10
5
0
no tx
no tx
VSV
VACV
+ B16-F10
h
Normalized MFI of CD40
1.5
1.0
0.5
0.0
no tx
no tx
VSV
VACV
+ B16-F10

3.4 Discussion

Oncolytic viruses are emerging as promising clinical candidates that target tumours on multiple fronts. Importantly, many have been observed to stimulate anti-tumour immune responses when replicating in susceptible tumours(108). However, not all tumours are susceptible or permissive to these viruses. I sought to optimize and test an OV vaccine that could be used with all tumour types, regardless of *in vivo* permissivity for the virus, harnessing the anti-tumour immune response generated when an immunogenic virus replicates in tumour cells.

I chose VSV-Δ51 for several reasons. Firstly, VSV has an extremely broad tropism, perhaps one of the broadest. Its glycoprotein can bind most or all mammalian cells(137). Though many tumours may not be permissive to *in vivo* infection with VSV-Δ51 due to an intact IFN response, nearly all cells are permissive when infected at a high MOI *in vitro*. In this situation the virus can easily replicate and kill the cells before the IFN response takes hold. Another reason for using VSV is its strong immunogenicity. VSV-Δ51 has been published to infect DCs *in vitro*, and those infected DCs stimulate the activation of NK and T cells(14). In addition, this NK cell stimulation depends on the production of type I IFNs(15), indicating that VSV-Δ51 may be more stimulatory to NK cells than wtVSV. Similarly, the Δ51M mutation means that this virus does not inhibit cytokine production by infected cells. A similar VSV-M mutant was shown to induce more potent conventional DC stimulation than wtVSV(3). Indeed, many large viruses express immunomodulatory proteins that suppress pro-inflammatory cytokines and cells(144). These would arguably not perform as well in a vaccine of this sort. VSV-Δ51 was also chosen because it can be engineered to

express a foreign transgene, and it is safer than wtVSV, having a 4.5 log higher LD50 in immune competent mice following intranasal administration(153).

The efficacy obtained with VSV-Δ51 in the permissive CT26.LacZ colon cancer model was observed to be largely dependent on an intact T cell compartment and that mice cured with this OV treatment generated a robust anti-tumour immune response (**Figure 3.1**). In addition, a UV-inactivated virus performed identically to PBS, indicating that replication is required for long term complete response. Moreover, this efficacy did not translate to tumours that are resistant to *in vivo* infection following systemic delivery of VSV (**Figure 3.3**). I propose that the deficit in efficacy due to the lack of *in vivo* replication could be overcome by infecting irradiated tumour cells *in vitro,* and then injecting this ICV into the mouse. In fact, an ICV using VSV-Δ51-GFP was able to protect 30% of mice from future B16-F10 tumour challenge, and 80% of mice from CT26.wt tumours in a prophylactic setting (**Figure 3.5c,d**). I hypothesize that this is through multiple mechanisms. Firstly, once the infected tumour cell is phagocytosed by a DC, viral RNA can bind to several PRRs (namely TLR7(3) and RIG-I(79)) to stimulate maturation. Unlike TLR agonists, viruses deliver a sustained TLR signal allowing for activation even in the presence of regulatory cells(175). It is also possible that VSV infection alters the immunogenicity of the cancer cells, either through triggering an upregulation of MHC I through the IFN pathway(134) (in IFN-responsive cells), or through the induction of immunogenic cell death. Immunogenic cell death requires the presentation of calreticulin (CRT) on the cell surface, as well as the release of ATP and HMGB1 from the dying cells(6, 54, 118).

3.4.1 What does GM-CSF contribute to the VSV-ICV?

Interestingly, cloning the cytokine GM-CSF into the viral genome greatly increased the potency of the ICV. Specifically, the VSVgm-ICV protected 95% of mice from future tumour challenge (**Figure 3.5c**). Previous research into this cytokine can offer insight into what may be happening. GM-CSF enhances the recruitment and maturation of monocytes and granulocytes(149). A previous group had made a recombinant wtVSV with GM-CSF in the first position of the genome. However, having a transgene at this position greatly impairs viral replication kinetics, decreasing viral gene transcription by 30 percent and leading to 2 logs lower viral yields(133). To avoid viral attenuation, GM-CSF was cloned into the fourth position, between the G and L genes. In this way, viral gene transcription of all genes but L is not affected, and viral titers are not hampered(89). Interestingly, though replication attenuated viruses usually elicit lower CD8 T cell responses, the GM-CSF expressing wtVSV was still able to elicit strong responses, perhaps indicating that GM-CSF enhances T cell activation. A larger anti-VSV N memory T cell population was also observed in mice primed with wtVSV-GMCSF, and those memory cells expanded to a much greater extent following a VSV N boost. Therefore, GM-CSF expression in wtVSV appears to enhance both memory T cell production and recall within the mouse. No difference in neutralizing antibody production was detected, however, a greater macrophage infiltration of the lung was seen specifically with GM-CSF production(133). There have also been observations that type I IFNs can enhance GM-CSF-mediated DC maturation and subsequent Th1 T cell responses(139), leading me to believe that VSV-Δ51-GMCSF might be even more potent at DC stimulation than wtVSV-GMCSF. Previously discussed research also implicated macrophages in the effects seen with GM-CSF; these macrophages demonstrated increased

TNFα production and cytolytic functions(77). Therefore, it is possible that the VSV-derived GM-CSF leads to enhanced DC, macrophage, and neutrophil recruitment to the site of ICV delivery, which in this case is the peritoneum. In addition, GM-CSF could improve DC and macrophage maturation, promoting more robust CD4 and CD8 T cell responses and memory phenotypes. However, these speculations remain to be proven.

3.4.2 Deconstructing the VSV-ICV

Though UV-inactivated VSV does not lead to sufficient immune stimulation, a G-Less VSV was able to recapitulate the tumour protection achieved with fully replication-competent virus (**Figure 3.7**). Therefore, a basal level of viral replication is required, though it need not replicate beyond the initially infected cells that constitute the vaccine. A requirement for cellular integrity was also observed. There was a decrease in efficacy when the VSVgm-ICV is fragmented by freeze and thaw cycles before injections. This may reflect the greater immunogenicity of intact cells as compared to lysed cells(158). However, efficacy decreased much more dramatically when freeze and thaw cycles were done before the addition of VSVgm to the irrB16 cells (irrB16→F/T + VSVgm). Lysing cells before virus would preclude viral infection. Consequently, the inability of this preparation to stimulate a protective immune response may point to the importance of the tumour cell being infected, and not simply admixed with replication competent virus. Thus, it is reasonable to hypothesize that this vaccine does not simply present viral danger signals in the context of tumour antigens. Instead, it is speculated that viral infection of cells initiates critical immunogenic processes that, coupled with tumour-associated antigens, lead to robust immune activation. What these immunological processes are remains to be determined. The examination of known immunogenic cell death signals, like cell surface calreticulin

exposure, or HMGB1 and ATP release may be a good starting point(6, 54, 118). In addition, viral infection of an intact cell is quite immunologically relevant, offering persistent toll-like receptor ligation required for a robust immune response(175).

The dose of irradiation used to stop cell division also had a large impact on the efficacy of the VSV-ICV in the CT26.wt model (**Figure 3.6b,c**). Though no impact was observed on the B16-F10 cells, they also required a much higher dose of radiation to halt cell division. 60 Gy was required to stop colony formation in the B16-F10 cells, whereas less than 30 Gy was required for the CT26.wt cells to observe the same cellular phenotype. Accordingly, a decrease in efficacy may have been observed in the B16-F10 cells had the dose of radiation been increased higher than the dose required to stop cell division, as was used in the CT26.wt cells. Though research suggests that the dose of irradiation can alter the immunogenicity of cells, it is generally observed that higher doses of radiation lead to stronger anti-tumour responses through the induction of immunogenic cell death(44). It is currently unknown by what mechanism(s) increased radiation is decreasing vaccine effectiveness in this model.

3.4.3 The VSVgm-ICV stimulates innate immune effectors

Treatment with the VSVgm-ICV leads to the maturation of DCs in the spleen and blood of tumour naïve animals and is also observed through *in vitro* assays (**Figure 3.8 and 3.9**). Not surprisingly, VSVgm and the vaccine lead to the same level of early immune activation. VSV has previously been reported to potently activate DCs *in vitro.* Injected IP, VSV will productively infect the first cells it encounters; thereby initiating immune activation due to viral infection. However, no anti-tumour immune responses were detected at late timepoints with VSVgm alone (**Figure 3.11, 3.12, 3.15, and 3.16**) and, importantly,

no auto-immune sequelae have ever been observed with VSVgm treatment, whether IP or IV (data not shown). Interestingly, in tumour-bearing mice, only treatment with the VSVgm-ICV led to enhanced DC maturation in the TDLN (**Figure 3.13**). However, similar DC maturation in the spleen was observed for VSVgm and the VSVgm-ICV.

NK cells are becoming increasingly studied for their important role in tumour rejection. They have the ability to recognize and kill tumours cells, and their activation and tumour infiltration has also been associated with clinical benefit (47, 102). Importantly, the VSVgm-ICV is observed to activate NK cells. Though the VSVgm-ICV is demonstrated to activate NK cells 24 hours after prophylactic vaccination, they do not likely play a role in challenge tumour rejection as tumour implantation occurs after NK cells have returned to baseline (**Figure 3.10b-e**). Though seemingly related to the vaccination, I propose that the NK cell infiltration and activation observed in the challenge tumour following VSVgm-ICV is in fact a consequence of activated T cell infiltration (**Figures 3.11 and 3.12**). Previous research indicates that T cells can activate NK cells in this manner(43). Importantly, NK cell activation following VSVgm-ICV was observed in the therapeutic setting (**Figure 3.13g**) and should have a significant role in this situation through the early tumour cell killing and through the induction of inflammation at the tumour site. NK cells have been demonstrated to be important in mediating early tumour killing and cytokine secretion, which further amplifies Th1 responses(106, 150, 162). Certainly, the large quantity and activated nature of the T cells observed infiltrating the B16-F10 challenge tumour only 3 days after implantation indicates that the VSVgm-ICV initiates an effective Th1 T cell response.

3.4.4 Therapeutic efficacy achieved with the VSVgm-ICV

The strength of this vaccine is highlighted by its significant impact in therapeutic models of cancer (**Figures 3.14-3.18**). Notably, therapy could be delayed to 4 days after systemic dissemination of tumours while still providing a therapeutic benefit (**Figure 3.15**). In some cases, the vaccine was delivered in a completely separate anatomical compartment and still led to significant tumour clearance.

Though the virus alone (VSVgm) seemed to have a similar impact on the tumour growth in the MISIIRTAg model (**Figure 3.18d**), it is important to note that no efficacy has ever been observed with VSV-Δ51 or wtVSV in this model no matter what route of virus administration is used, and VSV-Δ51 replicates very poorly in this model (personal communication with Dr. Vanderhyden). Therefore, the effect observed might be due to immune recruitment by GM-CSF because the VSVgm could be infecting cells of the ovary after IP injection. Further studies on this model could focus on understanding the effect that VSVgm is having beyond what VSVgfp can offer. In addition, starting vaccination earlier may provide more time for the immune response to develop and, in turn, to more robust tumour killing.

The experiment depicted in **Figure 3.19** was originally undertaken as a pilot study to examine the impact of antibodies bound to the cell surface of the ICV. It was hypothesized that these antibodies might enhance phagocytosis of the vaccine through Fcγ receptors on NK cells and antigen presenting cells(169) or FcRn on DCs(132). This was shown to be an important mediator of the efficacy with the clinical Her2 antibody Herceptin(123). However, a decrease in efficacy was observed with all of the antibody-generating protocols

attempted. One difference in this pilot experiment was that the antibodies used were all against VSV. This may have had strong negative effects as these antibodies could have significantly redirected the immune response away from the tumour antigens and towards the viral proteins. This process, often called "original antigenic sin", has been observed in influenza infections, where immune responses to a new strain will be highly skewed towards epitopes shared by previously encountered strains(84). While the idea that antibody coating the outside of the ICV could enhance phagocytosis and antigen presentation may still hold true, it should be repeated with an anti-tumour antibody. An interesting idea might be to use tumour cells that are known to express Her2/neu and use the original mouse antibody from which Herceptin was derived, called 7.16.4, which binds to the ectodomain of both human and rat Her2/neu(178). One such cancer model that has been well characterized is the MMTV-neu-p53 mouse from Dr. Nelson's lab. These transgenic mice develop mammary tumours expressing the full length rat neu protein harbouring the ovalbumin model epitopes of OT-I and OT-II(165). Preliminary work suggests that cell lines that have been made from these tumours are only permissive to VSV-Δ51 infection at high MOIs *in vitro* (data not shown). These cell lines could be used to make an ICV coated with the 7.16.4 antibody to investigate the usefulness of the abovementioned strategy. From previous work, it is already known that the 7.16.4 antibody is able to mediate FcγR-mediated cytotoxicity and phagocytosis(123).

To better understand the immune mediators of the efficacy observed with the VSVgm-ICV in the B16-F10 model, multiple experiments were undertaken to selectively deplete NK or CD8 T cells. The first NK depletion experiment was with an anti-NK1.1 antibody that has been successfully used in the past with a similar treatment schedule and

mouse strain(33). In these studies NK depletion was confirmed with an anti-NK1.1 antibody. However, to avoid epitope masking, we used an anti-DX5 antibody to confirm depletion in these mice and observed only a slight decrease in $DX5^+$ cells in the anti-NK1.1 treated animals (**Figure 3.20b**). However, depleted mice demonstrated a very striking increase in tumour burden compared to undepleted mice and had to be euthanized at day 16 because of animal distress. Indeed these animals had a large number of tumour nodules on their livers, which have never been observed in undepleted mice (**Figure 3.20c**). It is likely that these mice did have sufficient NK depletion to impact tumour growth. Another experiment was undertaken with an anti-asialo antibody, which allowed me to compare the depletion with both NK1.1 and DX5 antibodies. While a clear depletion is observed using the NK1.1 antibody, the DX5 antibody demonstrated only a very small decrease, quite similar to what was observed in **Figure 3.20** (data not shown). Therefore, it is likely that the anti-NK1.1 depletion was successful but was not confirmed with an appropriate antibody.

The results from both NK depletion experiments indicate that tumour burden increased dramatically upon NK depletion, an observation that has been made by the Bell lab in the past. In addition, though a much larger tumour burden had to be controlled, the VSVgm-ICV still demonstrated efficacy in most mice depleted of NK cells. However, 2 of the 5 mice in the anti-asialo depletion had lung tumour burden similar to PBS-treated animals, though their livers had a lower tumour burden. This may indicate an important role for NK cells in ICV-mediated efficacy, but these experiments do not rule out that another cell type may also be important.

An anti-CD8 depletion was then used to examine the role of these T cells (**Figure 3.22a**). This depletion was very successful and led to a near complete depletion of $CD8^+$

cells in the blood at day 4 (**Figure 3.22b,c**) and a sustained depletion in the spleen (**Figure 3.22d**). However, tumour burden in VSVgm-ICV + anti-CD8 treated mice remained undetectable in 5 of the 8 mice, indicating that $CD8^+$ T cells were not absolutely necessary for tumour clearance by the VSVgm-ICV (**Figure 3.22e,f**). Nevertheless, three mice did demonstrate an increase in tumour burden as compared to CD8 sufficient mice, indicating that these cells may play an important role. It is likely that both NK and CD8 T cells are involved in the efficacy seen with this vaccine. If activated to a sufficient extent, each effector could compensate for the other when it is depleted, reflecting my observations. To rule this out, a double depletion with the anti-asialo and the anti-CD8 antibodies could be undertaken. If the VSVgm-ICV can still decrease tumour burden in the face of a double NK and CD8 cell depletion, this would indicate that another cell type is involved in the efficacy observed in this model.

Because a clear role for CD8 T cells was not observed in the previous experiment, studies were carried out to measure T cell activation following VSVgm-ICV treatment in the B16-F10 therapeutic models. Perhaps not surprisingly, no anti-DCT or gp100 responses were detected in either experiment (**Figure 3.23**). The ICV is a whole tumour cell vaccine, so the immune system is being presented with potentially thousands of proteins and epitopes to target. In addition, although gp100 and DCT are common epitopes examined in B16-F10 research, they may not be the immunodominant epitopes targeted after exposure to irradiated and infected cells. Therefore, experiments were attempted against whole B16-F10 cells to greatly increase the number of epitopes used as targets. The first experiment demonstrates that the PBMCs from ICV-treated animals have a higher production of IFNγ at baseline, without stimulation (**Figure 3.24a,b**). Because this experiment was done using all PBMCs,

this could be from any number of IFNγ producing cells, including macrophages, NK cells, and T cells. MHC class I-specific peptides used here did not increase the amount of IFNγ, in keeping with previous results. However, incubation with B16-F10 cells did increase IFNγ production in 7 of 8 mice treated with the VSVgm-ICV. In addition, the average increase in IFNγ production (from unstimulated PBMCs to B16-F10 cell stimulated) was significantly increased in VSV-ICV-treated mice (**Figure 3.24c**). The high variability observed with the VSVgm-ICV decreased the statistical significance of the response, however, there is a clear trend demonstrating IFNγ production and a concomitant decrease in cytokine production from CD8-depleted PBMCs. As a more direct examination of CD8 T cell cytotoxic responses following VSVgm-ICV treatment, the chromium release assay used isolated CD8+ cells as the effectors. Though statistical significance was not achieved, there is an indication that PBMCs from VSVgm-ICV-treated mice have a stronger cytotoxic response to B16-F10 cells than do PBS-treated mice (**Figure 3.24e**).

3.4.5 Poxviruses may encode genes that interfere with the generation of an anti-tumour immune response

The results delineated in **Figures 3.25, 3.26, and Appendix II** demonstrate that neither ORFV nor VACV stimulate an anti-tumour immune response when given in the context of an ICV. Interestingly, when VACV and VSV ICVs were mixed before injection, the tumour growth kinetics mirror the VACV-ICV more closely (**Appendix III**). This might indicate that not only is the VACV-ICV not stimulating the immune system to the same extent as the VSV-ICV does, but it might be actively inhibiting what the VSV-ICV stimulates. Vaccinia immunomodulatory genes have been extensively studied and are

known to express inhibitors for a wide range of cytokines and chemokines, including type I and II IFNs, TNFα, IL-1β, IL-18, and many CC chemokines(4, 8). In addition, vaccinia has been reported to inhibit ligand binding to MHC class II, leading to poor CD4 T cell responses, and the virus encodes several proteins that inhibit NF-κB induction of pro-inflammatory genes(8, 95). Therefore, it is conceivable that one or several of these proteins interferes with the induction of anti-tumour immune responses in the context of an infected cell vaccine. However, there is evidence that oncolytic vaccinia treatment in patients can lead to an anti-tumour immune response. In melanoma patients a vaccinia encoding GM-CSF led to increased immune cell infiltration into tumours and responses in non-injected tumour(107). One can stipulate that part of that response is attributable to the GM-CSF, but at the very least it can be said that vaccinia infection did not inhibit this response. Further research might focus on if and how vaccinia virus treatment of an established tumour generates an anti-tumour immune response and how this situation differs from the ICV. Understanding how vaccinia can induce such an immune response is critical to properly designing therapeutic strategies that fully harness the immune stimulating potential of this OV.

3.4.6 Potential of the VSV-ICV

This vaccine platform would be best coupled to a cytotoxic treatment that might also stimulate the immune system. Local tumour irradiation may help with tumour killing and has been demonstrated to increase inflammation in the tumour environment(34), leading to enhanced immunotherapeutic responses(25, 64). An ideal scenario might include first surgically removing the tumour, using this tumour bulk to create the VSV-ICV, and then treating the patient to reduce metastatic recurrence.

The infected cell vaccine is a promising immunotherapeutic platform that achieves potent stimulation of antigen presenting cells, leading to the activation of innate and adaptive immune effectors (**Figure 3.28**). It is well documented that tumours create a tolerogenic environment which leads to the inhibition of DC maturation and the generation of immune tolerance. However, when VSV is replicating in a permissive tumour, the immune system will now induce NK and T cell activation. The potency of the ICV is highlighted by the significant impact it has on the progression of an aggressive and immunosuppressive tumour. In addition, the use of autologous tumour cells leads to a personalized vaccine that can potentially present the full range of a patient's unique tumour antigens.

Recently, Castle *et al*(24) have shown that the B16-F10 tumour cell line has acquired over 500 somatic mutations that could, in principle, encode numerous novel immunogenic epitopes. Despite this, irradiated B16-F10 cells alone are ineffective in stimulating anti-tumour immunity, probably due to a lack of robust danger signals. Here we show that infection of B16-F10 cells makes them a very potent vaccine platform that has the capacity to induce both a protective and therapeutic immune response. Since the B16-F10 cell line expresses a vast array of potential neo-antigens, perhaps many of these could now be made visible to the immune system when presented as an ICV. It is possible that because of this, the ICV has the potential to induce a broadly active T cell response against a spectrum of neo-antigens. Currently, I have no data to support this idea; however, future studies are aimed at determining if the breadth of the T cell response elicited by the VSVgm-ICV is larger than that generated with other vaccination strategies that only use one antigen, like a VSV encoding DCT. It remains possible that the ICV approach simply focuses a robust response on a single or limited number of tumour antigens.

In addition, many other melanoma vaccines induce autoimmune conditions such as vitiligo. Conversely, the VSVgm-ICV has not led to any signs of autoimmunity. This suggests that the VSVgm-ICV offers a physiologically safer immunization, perhaps through the allowance of the animal's immune system to react only to those antigens which exist within the confines of its natural tolerance mechanisms. Potentially, only those antigens that are both immunogenic enough and are not currently inhibited by peripheral tolerance will be selected to further elicit adaptive immune responses.

Figure 3.28 – Model of the generation of OV-mediated anti-tumour immunity

A- In tumours that are non-permissive to *in vivo* infection by VSV or in uninfected tumours, tumour antigens are presented to the immune system without any danger signals to help with DC maturation.

B- Immature DCs express low MHC, no co-stimulatory molecules, and no pro-inflammatory cytokines. Immature DCs therefore present the tumour antigens in a toleragenic manner, leading to either no T cell response or a regulatory T cell response.

C- This generates immune tolerance towards tumour antigens, perpetuating the anti-inflammatory and suppressive tumour microenvironment.

D- In tumours that allow for robust VSV infection *in vivo* (like the CT26.LacZ) or in the case of a VSV-ICV treatment, tumour antigens are presented to the immune system in a stimulatory environment. Viral PAMPs are plentiful and viral infection may also lead to the release of DAMPs from infected cells, such as ATP or HMGB1. These lead to potent DC maturation, with the upregulation of MHC class II, co-stimulatory molecules like CD40, CD86, and CD80, and the production of inflammatory cytokines like TNFa and IL-12.

E- There is a heightened presentation of tumour antigens by DCs to naïve T cells because of the increased MHC expression. The pro-inflammatory environment leads to the successful generation of activated CD4 and CD8 T cells, able to secrete inflammatory IFNγ and lead to tumour cell killing.

F- The pro-inflammatory environment also leads to NK cell activation, with IFNγ and Granzyme B production. This NK activation may result from the infected cells, from the DCs that phagocytosed the infected cells, or both.

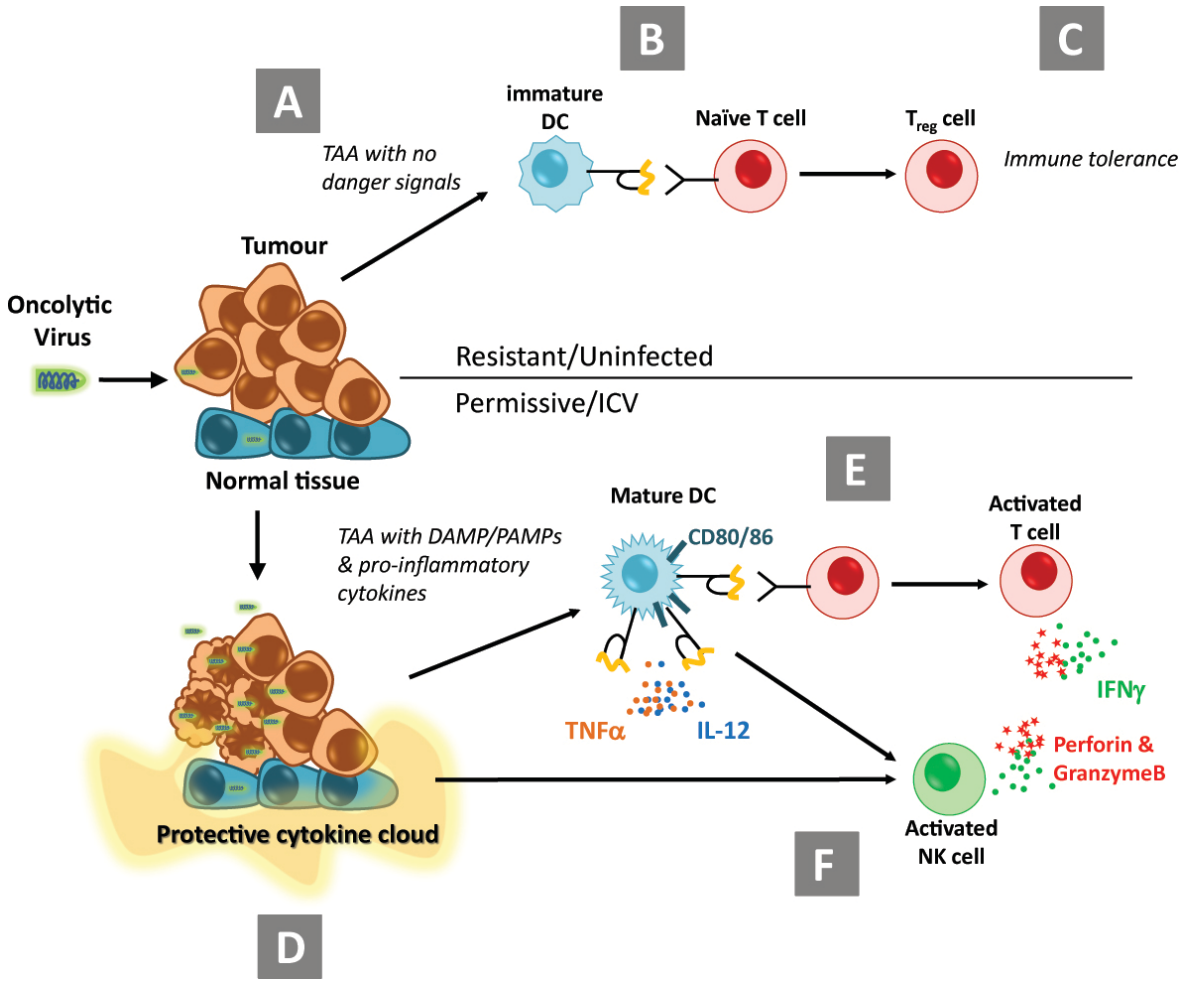
A
B
C
immature DC
Naïve T cell
T_{reg} cell
Immune tolerance
TAA with no danger signals
Tumour
Oncolytic Virus
Resistant/Uninfected
Permissive/ICV
Normal tissue
E
Mature DC
CD80/86
Activated T cell
TAA with DAMP/PAMPs & pro-inflammatory cytokines
IFNγ
TNFα
IL-12
Perforin & GranzymeB
Activated NK cell
F
Protective cytokine cloud
D

4 Investigating the immune modulating effects of MS-275 and its impact on an oncolytic prime/boost vaccination model

4.1 Introduction

4.1.1 Oncolytic Prime & Boost Model

Recently, Bridle *et al* published several papers describing an oncolytic prime/boost strategy that allows for robust anti-tumour immune responses to develop in an aggressive B16-F10 brain tumour model(20, 21). This platform relies on a replication deficient adenovirus expressing the human DCT protein (Ad-hDCT) as a priming vector, and then uses wt-VSV expressing human DCT (wtVSV-hDCT) given IV two weeks later as a boost. The wtVSV-hDCT dose fulfills multiple functions. It specifically boosts the anti-DCT immune response, leading to an impressive 20 percent of blood CD8 T cells demonstrating reactivity to DCT. In addition, the oncolytic virus itself allows for tumour killing, and though insufficient to affect survival on its own, it could greatly help in conjunction with an ongoing immune response. Also, because the immune response is being skewed towards the pre-immunized DCT antigen, the anti-VSV response here is significantly decreased(21). Another interesting aspect of this platform is the use of the xenoantigen, in this case immunizing with the human DCT counterpart in the mouse. This has been demonstrated to overcome CD4 T cell tolerance and lead to 5-10 fold higher CD8 T cell activation levels(82). This immunization strategy leads to remarkable T cell responses and a very significant extension in animal survival, yet rarely leads to curative responses(21).

4.1.2 Histone Deacetylase Inhibitors

Histone deacetylases (HDACs) are enzymes that catalyze the removal of acetyl groups from lysines in both histone and non-histone proteins. Research on lysine acetylation has uncovered a wide range of regulatory functions for this post-translational modification. The most widely studied is histone acetylation, which leads to the uncoiling of chromatin and increased access to genetic sequences, generally resulting in increased gene expression. In addition, many non-histone proteins are regulated by lysine acetylation, including p53. HDACs can be pharmacologically inhibited by a diverse family of small molecules termed HDAC inhibitors (HDIs). HDIs are subdivided into classes based on their structural properties. These include hydroxamic acids, benzimides, cyclic peptides, and aliphatic acids(36). These HDIs have demonstrated utility in a range of human diseases, including cancer, autoimmunity, Parkinson's, and Alzheimer's disease(7, 29).

Many HDIs demonstrate anti-cancer properties, though the exact mechanisms by which they exert this function remains only partly understood. It is known, however, that HDACs are required for cell cycle progression, and their inhibition induces cell cycle arrest. HDI treatment also promotes cell differentiation and apoptosis. Decreased histone acetylation has been noted in many cancers, leading to the transcriptional silencing of tumour suppressors, cell cycle inhibitors, and apoptosis inducers. In addition, altered acetylation in cancer can lead to increased angiogenesis, as well as cellular migration and invasion. Not surprisingly, decreased acetylation in cancer has been correlated to both increased HDAC expression and negative clinical outcome(60). The HDI suberoylanilide hydroxamic acid (SAHA, also known as Vorinostat) has been approved for the treatment of cutaneous T cell lymphoma(81). SAHA, of the hydroxamic acid class of HDIs, is a broad spectrum inhibitor

of class I and class II HDACs, which includes HDACs 1 through 10. MS-275 (also known as Entinostat, SNDX-275, or NOX-275) is a benzamide HDI that selectively inhibits HDAC1, and to a lesser extent HDACs 2 and 3(36, 83).

Of particular interest to the OV field, HDIs inhibit the transcriptional response to type I IFNs. Treatment with various HDIs, including SAHA and MS-275, significantly augments VSV replication in cancer cells and enhances efficacy *in vivo*(116). Consequently, many papers now demonstrate that HDI treatment of cancer cells enhances the replication of many other OVs, including vaccinia virus(104) and herpes virus(120). Though enhanced efficacy was observed in two different *in vivo* models, there was concern that HDI treatment might negatively affect the anti-tumour immune response that is generated through VSV treatment of tumours. This might then hamper the long term control of tumour growth.

Many HDIs have demonstrated anti-inflammatory properties and usefulness in treating autoimmune disorders(7). However, research remains sparse on the impact of HDIs on the generation or homeostasis of immune responses(161). In addition, some research suggests that HDIs would be pro-inflammatory. For example, the RelA subunit of NF-κB is regulated by two acetylation sites and both require acetylation for full gene transcription functionality. Therefore, HDI treatment would inhibit the deacetylation of these sites, allowing for full NF-κB functions. In addition, many groups have observed that HDI treatment augments MHC class I and II expression on cancer cells, in addition to co-stimulatory molecules and NK cell activating ligands. Together these properties could lead to stronger anti-tumour immune responses. Conversely, treatment with MS-275 or SAHA leads to the induction of FOXP3 and TGFβ expression in human and mouse cells, leading to regulatory T cell generation. Moreover, HDI treatment has been observed in multiple

models to suppress the expression of pro-inflammatory cytokines leading to reduced endotoxemia following LPS administration and ConA-mediated liver injury in mice, among others(103).

4.2 Hypothesis & Objectives

Hypothesis

Enhanced oncolytic virus replication by HDAC inhibitors will lead to a more pronounced anti-tumour immune response in models that are only moderately permissive to VSV infection due to their intact IFN response.

Objectives

1. Assess the impact of the MS-275 and SAHA HDIs on the generation of an immune response using the anti-VSV response as a model.
2. Examine the effect of HDIs on the anti-tumour immune response in the non-permissive B16-F10 model, using the oncolytic prime/boost vaccination model.
3. Examine the overall efficacy that is achieved when HDIs are coupled to VSV in the prime & boost vaccination model.

The results that are presented in the section below first delineate preliminary studies to investigate the impact of HDIs on the anti-VSV immune response. These results led to a collaboration with Dr. Bridle and Dr. Lichty at McMaster University. The initial experiments of this collaboration were performed to probe the mechanisms of efficacy in the oncolytic prime/boost vaccination model. However, many of the experiments that further elucidate the mechanism were undertaken by the lab at McMaster. These results will only be

briefly discussed and readers are referred to the manuscript in **Appendix V** to examine those figures.

4.3 Results

4.3.1 Impact of MS-275 on the anti-VSV immune response

To assess the impact of MS-275 on the adaptive immune response, a simple model was established whereby naïve mice were treated with vehicle or MS-275 IP and $1x10^7$ pfu of VSV-Δ51 IV 2-4 hours later. Treatments with vehicle or MS-275 continued daily for a total of 5 doses, and the animals were euthanized to assess cellular anti-VSV responses on day 5 (**Figure 4.1a**). A striking difference in the size of the spleen was observed, which is reflected in the cellular content of the organs (**Figure 4.1b**). VSV treatment led to an increase in cell numbers in the spleen, however, MS-275 treated mice had fewer cells in their spleens, and mice treated with both MS-275 and VSV had even fewer cells. The composition of the spleen was also altered, leading to a higher proportion of $CD3^+$ T cells with MS-275 treatment, and more so with VSV and MS-275 treatment (**Figure 4.1c**). Conversely, the absolute number of $CD3^+$ T cells in the spleen decreased with both MS-275 treatments (**Figure 4.1d**). Splenocytes harvested from these animals were incubated with VSV N peptide, and IFNγ production was assessed by flow cytometry to determine the anti-VSV T cell response. A significant response to VSV N was detected in the $CD8^+$ T cells of VSV-treated animals, however, a blunted response was observed in mice treated with VSV and MS-275 (**Figure 4.1e**). Though T cell numbers dropped following MS-275 treatment, they became over-represented, potentially indicating that other cell types in the spleen were also depleted.

Figure 4.1 – MS-275 treatment in Balb/C mice leads to splenic cellular loss

(**a**) Balb/C mice were treated with vehicle or 0.1mg of MS-275 IP followed by $1x10^7$ pfu VSV-Δ51-DsRed IV. Animals received MS-275 or vehicle IP for 5 consecutive days and were euthanized on day 5. (**b**) At endpoint, spleens were processed and the number of cells per spleen counted on the ViCell. (**c-d**) SMNCs were stained with CD3 and percent and number $CD3^+$ assessed by flow cytometry. (**e**) SMNCs were incubated for 5 hours with the Balb/C-reactive VSV N peptide and IFNγ intracellular staining was performed to assess the number of $CD3^+CD8^+$ that secrete IFNγ upon stimulation with the VSV peptide. There were 5 mice per group and *P* Values are $*P<0.05$, $**P<0.005$, $***P\leq0.0001$.

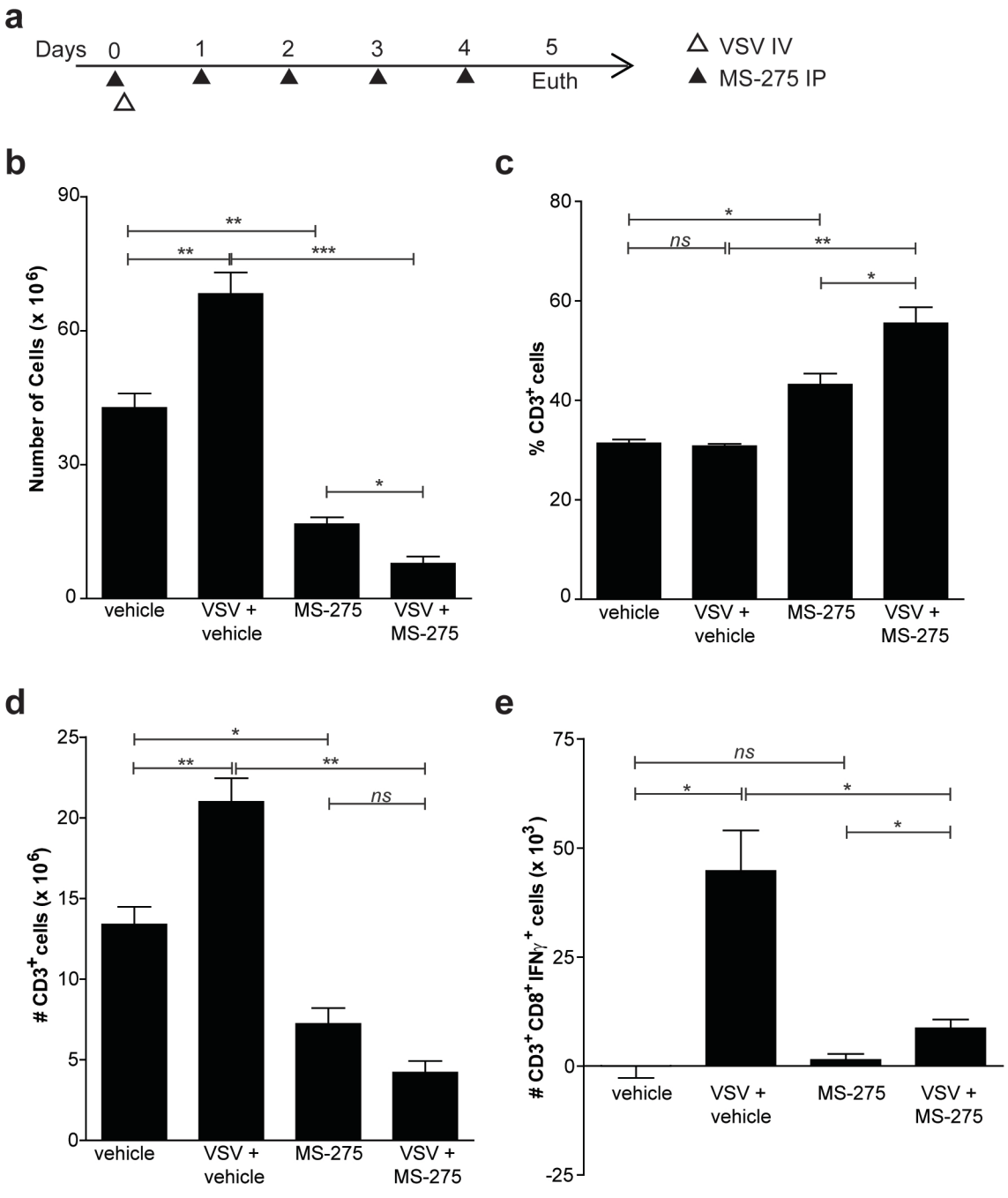
a
Days 0 1 2 3 4 5
Euth
VSV IV
MS-275 IP
b
Number of Cells (x 10^6)
vehicle
VSV + vehicle
MS-275
VSV + MS-275
c
% CD3+ cells
ns
d
CD3+ cells (x 10^6)
e
CD3+ CD8+ IFNγ+ cells (x 10^3)

This observation led to the investigation of B cells and to the confirmation of these results in C57BL/6 mice, a strain more commonly used in immune phenotyping. The same treatments and schedule were used in C57BL/6 mice as in **Figure 4.1a**. The C57BL/6 mice demonstrated a similar splenic response to MS-275, with a loss of over half of the cells in the spleen by day 5 (**Figure 4.2a**). Although both $CD3^+$ and $CD19^+$ cells decreased upon MS-275 treatment, $CD19^+$ cells decreased by a greater extent (**Figure 4.2b**). Similarly, the proportion of $CD3^+$ cells remained unchanged during MS-275 treatment, however, the proportion of $CD19^+$ cells decreased with MS-275 treatment and more so with VSV and MS-275 treatment (**Figure 4.2d**). T cells were assayed for IFNγ production following stimulation with VSV N peptide and, as with Balb/C mice, there was a decrease in the anti-VSV $CD8^+$ T cell response with MS-275 treatment, however, a small response remained (**Figure 4.2c**). The number of $CD19^+$ cells was also dramatically decreased in the blood following MS-275 treatment (**Figure 4.2e**).

To evaluate B cell functionality during MS-275 treatment, mice were treated as in **Figure 4.2** and plasma was quantified for VSV neutralizing antibodies. Although MS-275 treatments ended on day 4, a significant delay in the production of neutralizing antibodies against VSV was detected upon MS-275 treatment until day 7 (**Figure 4.3**). Importantly, titers returned to control levels by day 16 and remained normal at day 56. A higher dose of MS-275 was also attempted, and while this led to a more robust delay in antibody titers, mice weight decreased significantly and they suffered from severe dehydration (data not shown). Therefore the dose of 0.1mg was maintained for future studies as this caused only minimal weight loss in mice. The hydroxamic acid HDI Oxamflatin was also used in this experiment.

Figure 4.2 – MS-275 + VSV treatment in C57BL/6 mice leads to significant B cell depletion

C57BL/6 mice were treated with vehicle or 0.1mg of MS-275 IP followed by $1x10^7$ pfu VSV-Δ51 IV in the afternoon. Animals received MS-275 or vehicle IP for 5 consecutive days and were euthanized on day 5. (a) Mean number of cells per spleen. (b) Mean number of $CD3^+$ or $CD19^+$ cells per spleen. (c) SMNCs were incubated for 5hrs with the C57BL/6-reactive VSV N peptide and IFNγ production was assessed by intracellular staining and flow cytometry. (d) Percent of SMNCs that are $CD3^+$ or $CD19^+$. (e) Number of $CD19^+$ cells per mL of blood. There were 6 mice per group, except the MS-275+VSV group that had 7. All data points are mean + SEM, with *P* Values; where $*P<0.05$, $**P<0.005$, $***P\leq0.0001$.

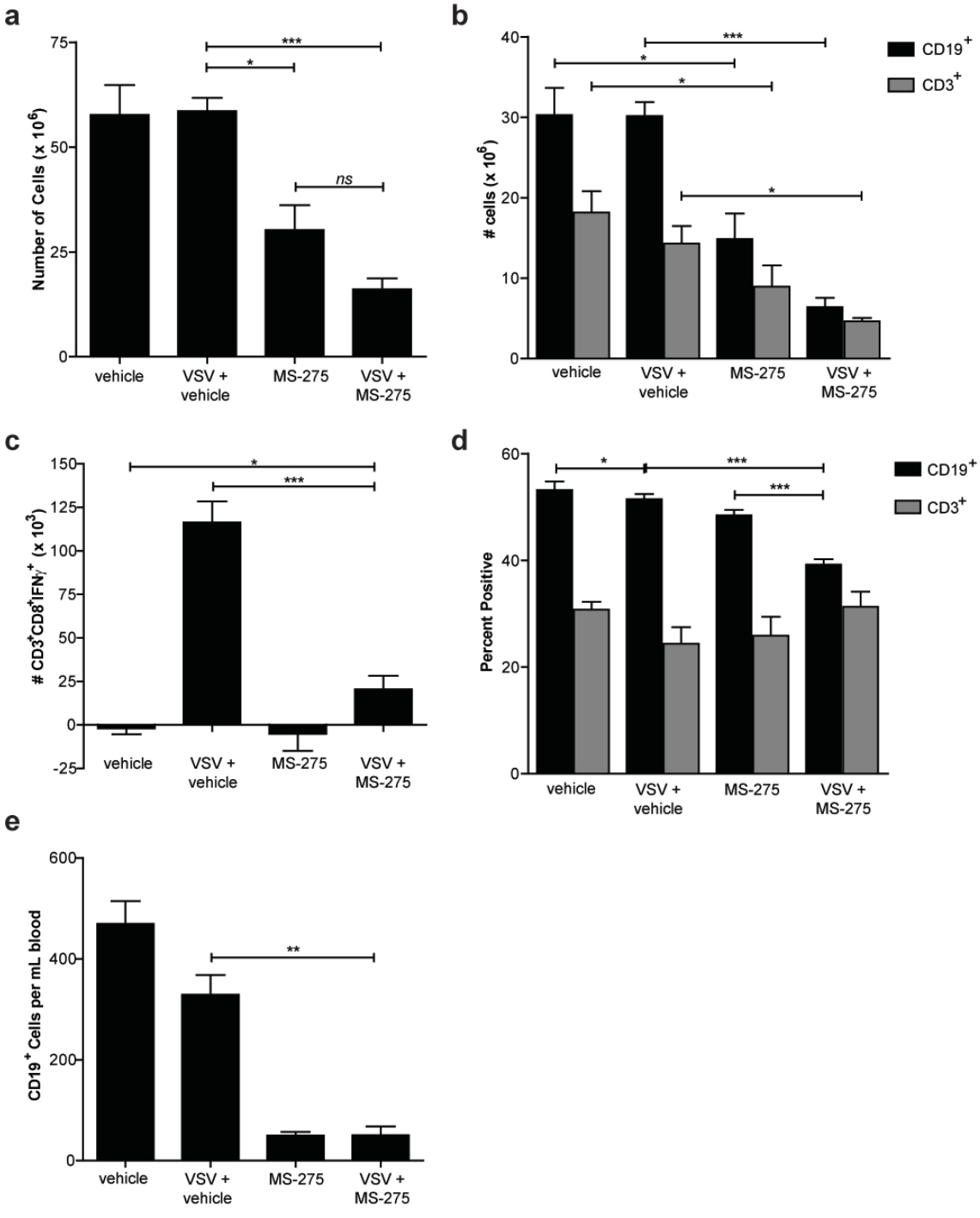
a
Number of Cells (x 10^6)
75
50
25
0
***
*
ns
vehicle
VSV + vehicle
MS-275
VSV + MS-275
b
cells (x 10^6)
40
30
20
10
0
CD19+
CD3+
c
CD3+CD8+IFNγ+ (x 10^3)
150
125
100
75
50
25
0
-25
d
Percent Positive
60
40
20
0
e
CD19+ Cells per mL blood
600
400
200
0
**

Figure 4.3 – Anti-VSV neutralizing antibody generation delayed with MS-275 treatment

C57BL/6 mice treated as in **figure 4.2** had blood drawn by saphenous bleed on indicated days. Plasma was used to assay the anti-VSV neutralizing antibody titer. Data is mean + SEM with *P* Values; where **P*<0.05, ***P*<0.005.

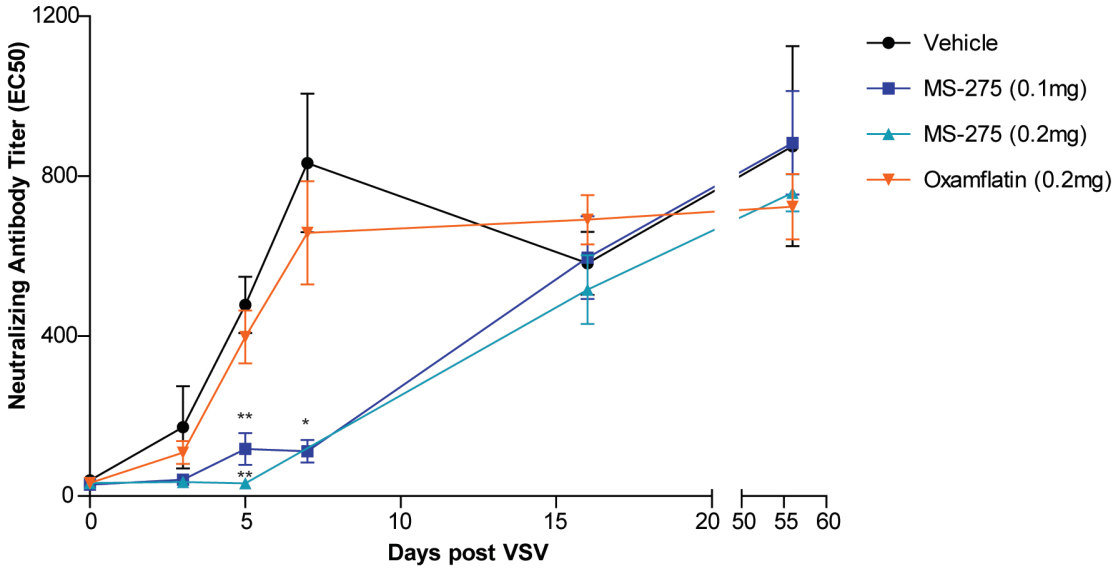
1200
800
400
0
Neutralizing Antibody Titer (EC50)
**
*
**
0
5
10
15
20
50
55
60
Days post VSV
Vehicle
MS-275 (0.1mg)
MS-275 (0.2mg)
Oxamflatin (0.2mg)

Surprisingly, no change in the levels of anti-VSV neutralizing antibody was detected with this drug. These results initiated a collaboration with Dr. Byram Bridle from McMaster University to treat mice with MS-275 in their oncolytic prime/boost vaccination model(21). This model allows for the examination of the impact of MS-275 on T cell function, as efficacy is dependent upon the anti-tumour T cell response. In addition, the delay in anti-VSV antibody production might play a role in this model in further allowing the replication of VSV. The result of the addition of MS-275 to this vaccination protocol was a dramatic enhancement in survival, leading to a 60 percent rate of complete responses (see **Appendix V: Figure 1**). This model uses wtVSV and immune phenotyping performed by Dr. Bridle demonstrates that MS-275 treatment with wtVSV leads to similar lymphotoxicity. Further studies revealed that MS-275 specifically depletes naïve and regulatory lymphocytes while leaving memory lymphocytes unscathed (**Appendix V: Figure 2**). Ensuing studies used wtVSV in the oncolytic prime & boost model when possible to further determine how MS-275 treatment enhances efficacy.

To better understand the time-line of the lymphodepletion, mice were euthanized either on days 1, 2, 3, or 5 to examine $CD3^+$ and $CD19^+$ cell levels. Total splenocyte counts in the spleen begin dropping as early as day 2 post MS-275 treatment and reach their lowest point by day 3 (**Figure 4.4a**). $CD3^+$ cell numbers have a much less striking decrease in the spleen that is at its lowest on day 2, after which levels begin to rise (**Figure 4.4b**). $CD19^+$ cells, however, have a large decrease that resembles the total splenocyte decrease, with a lowest point at day 3 and no increase by day 5 (**Figure 4.4c**). Blood was examined on day 5 for total white blood cell counts, and results indicate a similar loss of immune cells as in the spleen (**Figure 4.4d**).

Figure 4.4 – Timeline of lymphodepletion demonstrates peak decrease in B cells at day 3

C57BL/6 mice were given 0.1mg of MS-275 or vehicle IP and then $1x10^9$ pfu of wtVSV IV a few hours later. Daily MS-275 or vehicle treatments were maintained until day 4. Animals were euthanized on days 1, 2, 3, and 5 and SMNCs (**a**) counted by ViCell or assessed by flow cytometry for (**b**) the number of $CD3^+$ cells or (**c**) the number of $CD19^+$ cells. Untreated mice were used to determine control levels (shown in red on day 0). (**d**) The total number of PBMCs in the blood on day 5 was counted by ViCell. There were 3 mice per group per timepoint except for day 5 VSV+vehicle, which had 4. Data points are all mean + SEM with *P* Values; where $*P<0.05$, $**P<0.005$.

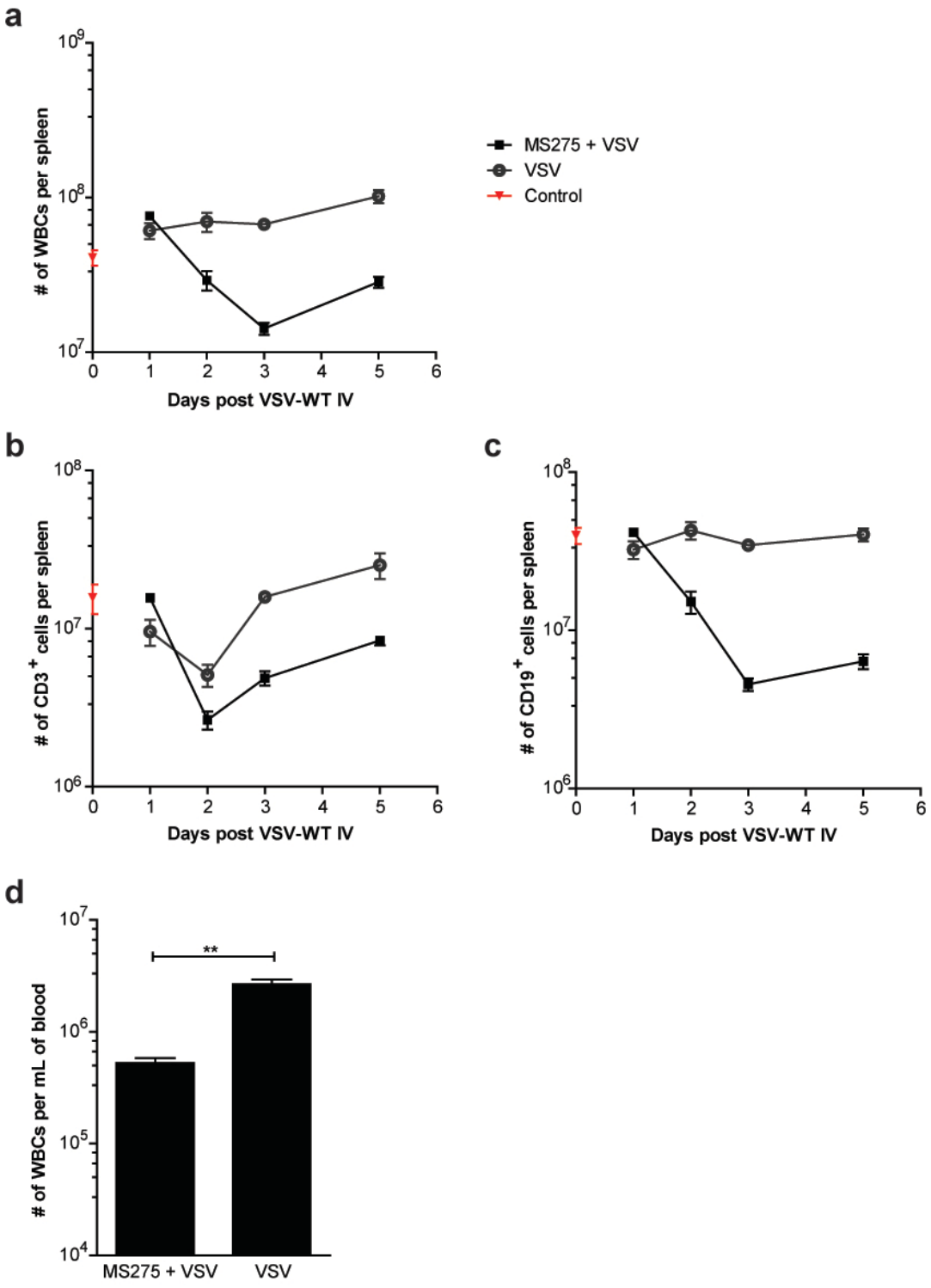
a
# of WBCs per spleen
Days post VSV-WT IV
MS275 + VSV
VSV
Control
b
# of CD3+ cells per spleen
Days post VSV-WT IV
c
# of CD19+ cells per spleen
Days post VSV-WT IV
d
# of WBCs per mL of blood
**
MS275 + VSV
VSV

4.3.2 SAHA does not lead to lymphodepletion

Oxamflatin did not lead to a delay in production of anti-VSV neutralizing antibodies (**Figure 4.3**). This observation led to the examination of SAHA, another hydroxamic acid and a current cancer treatment. Using the same experimental timecourse as in **Figure 4.1**, mice were treated with VSV and then given a 5 day course of SAHA at 0.2mg per dose, a high concentration that was well tolerated by the mice. Results of this experiment further verified that hydroxamic acids do not appear to have the same effect on the immune system as does MS-275, a benzamide HDI (**Figure 4.5**). The number of cells in the spleen was unchanged with SAHA treatment and increased upon co-treatment of VSV and SAHA (**Figure 4.5a**). In addition, the proportion of T and B cells in the blood increased upon SAHA treatment (**Figure 4.5b,c**). Interestingly, VSV treatment enhanced the proportion of B cells in the blood, but the addition of SAHA did not lead to a further increase (**Figure 4.5c**). Also, the proportion and number of T cells did not change in the spleen of SAHA-treated mice (**Figure 4.5d,e**). The anti-VSV N $CD8^+$ T cell response was measured through peptide-stimulation and IFNγ intracellular staining. Though 5 days is early to measure an anti-VSV T cell response, a significant response was measured after VSV treatment with or without SAHA (**Figure 4.5f**). Though no statistical difference was observed, half of mice treated with SAHA and VSV appear to have a higher IFNγ production following VSV stimulation than those treated with VSV only. SAHA did not alter the proportion or number of B cells in the spleen (**Figure 4.5g,h**), and no difference was observed in the neutralizing antibody response to VSV (**Figure 4.5i**).

Figure 4.5 – SAHA, a hydroxamic acid HDI, does not modulate the anti-VSV immune response like MS-275

C57BL/6 mice were treated with 0.2mg of SAHA IP and then with $1x10^7$ pfu VSV-Δ51 IV. SAHA treatments continued daily for 4 more days. (**a**) Splenocytes were assessed for total numbers by ViCell. (**b-c**) The percent CD3 and CD19 content of the blood was examined by flow cytometry, as well as (**d, g**) the percent CD3 and CD19 content of the spleen. (**e, h**) The total number of $CD3^+$ or $CD19^+$ cells in the spleen was also examined. (**f**) Splenocytes were assayed for responsiveness to the VSV N peptide by intracellular cytokine staining for IFNγ following *in vitro* restimulation. (**i**) The neutralizing antibody titer against VSV of the plasma was determined as previously described. There were 5 mice per group except for the PBS group that had 4 and the SAHA+VSV group that had 6. All data points are mean + SEM with *P* Values; where $*P<0.05$.

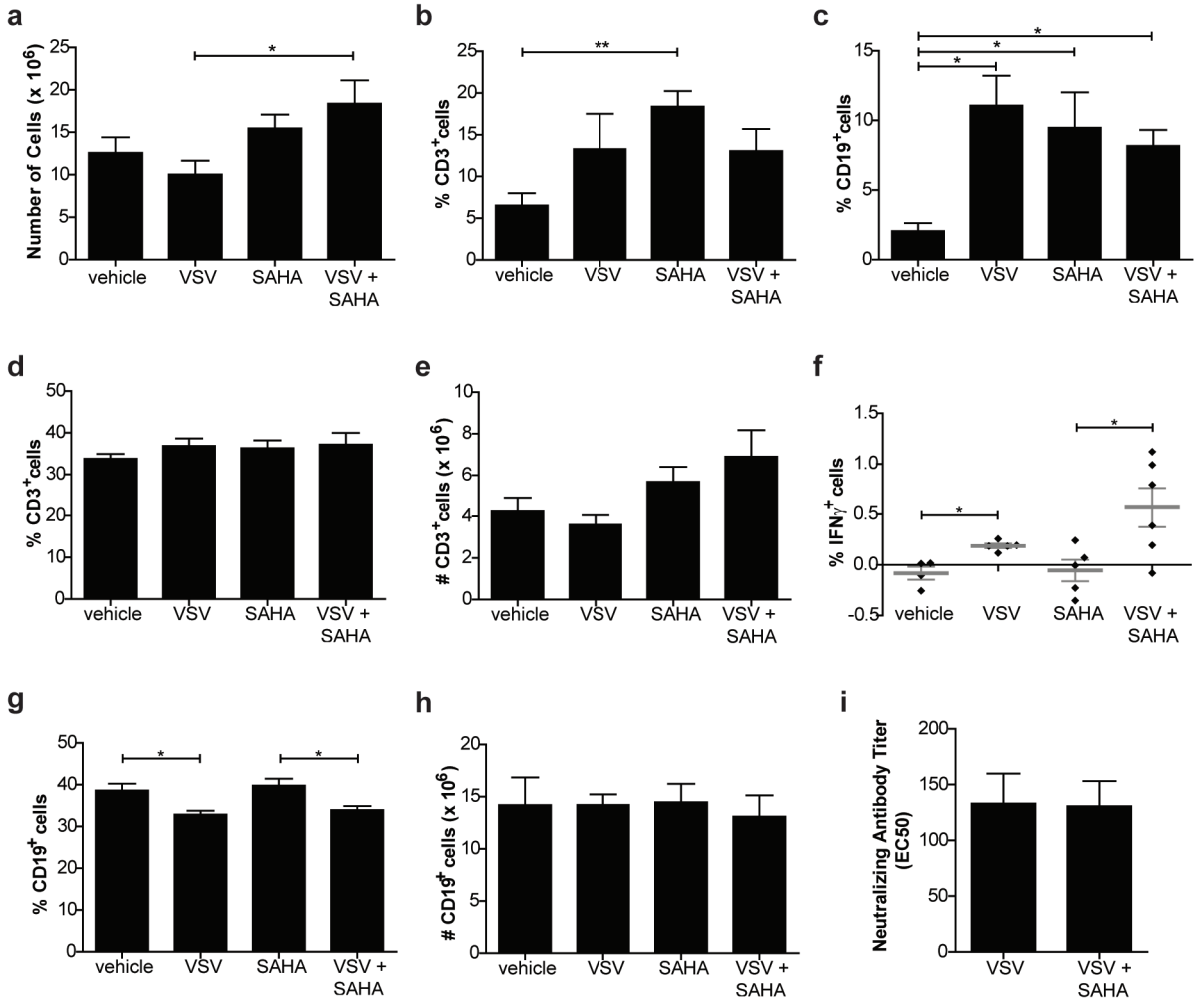
a
Number of Cells (x 10^6)
25
20
15
10
5
0
*
vehicle
VSV
SAHA
VSV + SAHA
b
% CD3+cells
25
20
15
10
5
0
**
vehicle
VSV
SAHA
VSV + SAHA
c
% CD19+cells
15
10
5
0
*
*
*
vehicle
VSV
SAHA
VSV + SAHA
d
% CD3+cells
50
40
30
20
10
0
vehicle
VSV
SAHA
VSV + SAHA
e
CD3+cells (x 10^6)
10
8
6
4
2
0
vehicle
VSV
SAHA
VSV + SAHA
f
% IFNγ+cells
1.5
1.0
0.5
0.0
-0.5
*
*
vehicle
VSV
SAHA
VSV + SAHA
g
% CD19+cells
50
40
30
20
10
0
*
*
vehicle
VSV
SAHA
VSV + SAHA
h
CD19+cells (x 10^6)
20
15
10
5
0
vehicle
VSV
SAHA
VSV + SAHA
i
Neutralizing Antibody Titer (EC50)
200
150
100
50
0
VSV
VSV + SAHA

4.3.3 HDIs do not enhance viral replication or cell death in immune cells

To determine if MS-275 is leading to an increase in VSV replication in immune cells, bone marrow (BM) and splenocytes were harvested and incubated with VSV-Δ51and MS-275, SAHA, or Oxamflatin. All three HDIs induced cell death in a subset of BM cells, however, the addition of VSV did not increase cell death (**Figure 4.6a**). Splenocytes incubated for 24hrs with HDIs had no increase in cell death with or without VSV (**Figure 4.6b**). In addition, GFP levels, used as a correlate of VSV-Δ51-GFP replication, indicate that splenocytes are likely not being infected to any significant extent (**Figure 4.6c**).

HDIs have previously been noted to augment the replication of OVs through the inhibition of the type 1 IFN response(116). Therefore, the increase of VSV replication in B16-F10 cells could be an important source of enhancement in this model. Mice bearing B16-F10 intracranial tumours were treated with wtVSV-FLuc followed by MS-275 or vehicle for 5 days. Unexpectedly, MS-275 appears to inhibit VSV replication in B16-F10 tumours initially (**Figure 4.7a**). However, VSV persisted longer in tumour treated with MS-275, leading to a higher viral load on days 4 and 5. These results were confirmed by titering the brains of mice at 48hrs post VSV, demonstrating that no increase was found with MS-275 treatment (**Figure 4.7b**). In addition, B16-F10 cells in culture were less susceptible to both wtVSV and VSV-Δ51 when treated with MS-275 or SAHA (**Figure 4.8a-c**).

4.3.4 MS-275 and then anti-tumour immune response

The oncolytic prime/boost vaccination strategy relies heavily on the induction of a strong anti-tumour immune response(21). The recruitment of T and NK cells to the brain was quantified following vaccination with or without MS-275 treatment. Though statistical

Figure 4.6 – HDI and VSV *in vitro* treatment of immune cells does not explain *in vivo* phenomenon

Bone marrow and spleens were harvested from C57BL/6 animals and cultured *in vitro* in RPMI + 8% FBS with or without HDIs. HDIs were all used at 4μM and VSV-Δ51-GFP infection was initiated 2 hours later at an MOI of 0.01. (**a**) Bone marrow cell viability was assessed by PI uptake after 48 hours of incubation. (**b**) Splenocytes were examined after 24 hours of incubation for PI uptake and (**c**) for GFP expression. Splenocytes were run in duplicate and bone marrow in singlet. Data points are mean + SEM for splenocytes.

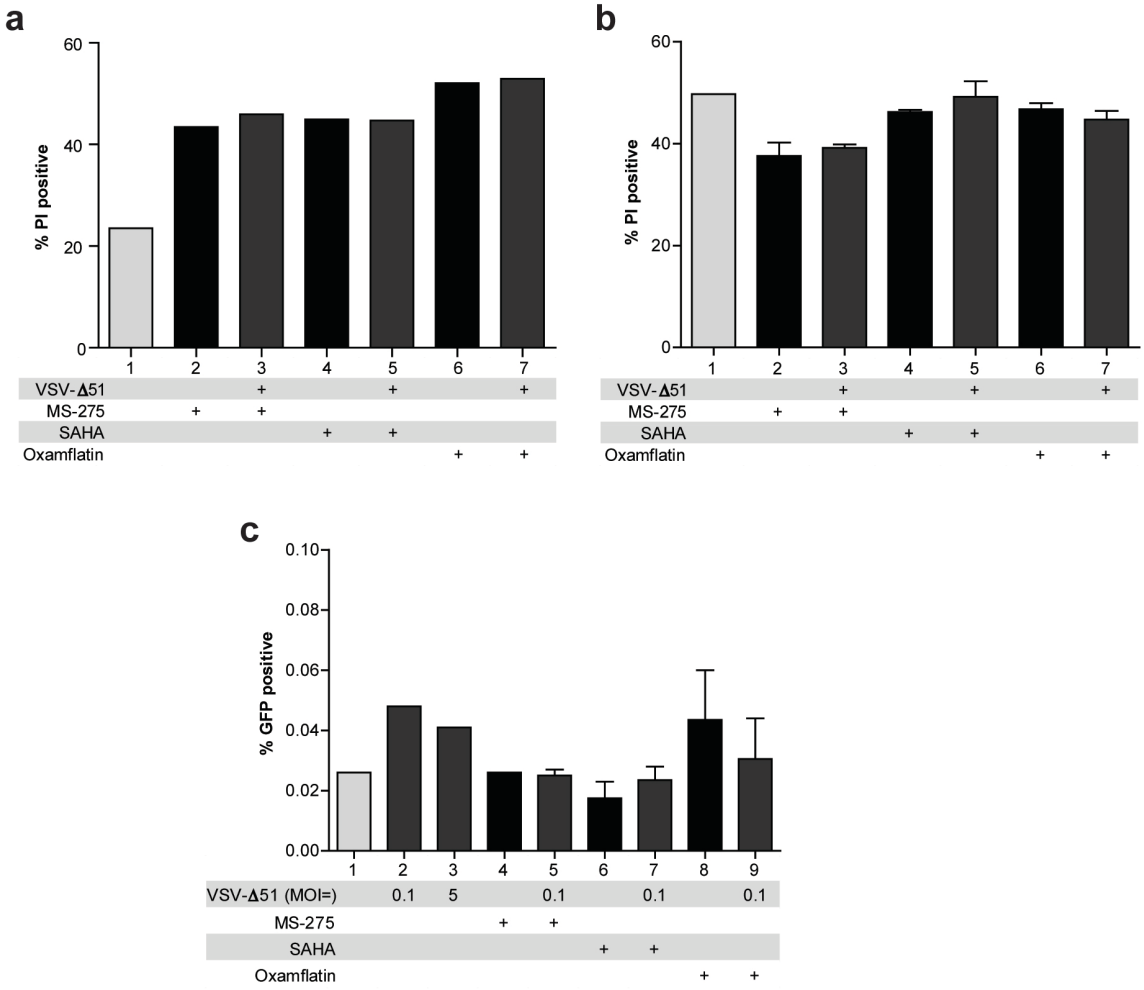
a
% PI positive
60
40
20
0
1 2 3 4 5 6 7
VSV-Δ51 + + +
MS-275 + +
SAHA + +
Oxamflatin + +
b
% PI positive
60
40
20
0
1 2 3 4 5 6 7
VSV-Δ51 + + +
MS-275 + +
SAHA + +
Oxamflatin + +
c
% GFP positive
0.10
0.08
0.06
0.04
0.02
0.00
1 2 3 4 5 6 7 8 9
VSV-Δ51 (MOI=) 0.1 5 0.1 0.1 0.1
MS-275 + +
SAHA + +
Oxamflatin + +

Figure 4.7 – *In vivo* analysis of wtVSV replication in B16-F10 brain tumours

(**a**) B16-F10 cells were implanted intracranially and then treated with $4x10^8$ pfu wtVSV-FLuc 10 days later. Mice received 0.1mg MS-275 or vehicle IP for 5 days as per usual. Groups had 4-5 mice per timepoint. Data points are mean + SEM. (**b**) Mice with 9 day old B16-F10 subcutaneous tumours were given 0.1mg MS-275 or vehicle IP for 5 days as per usual, in addition to $1x10^9$ pfu of wtVSV-GFP IV. Brains were taken out 48 hours after VSV treatment and titered for VSV infectious units on Vero cells.

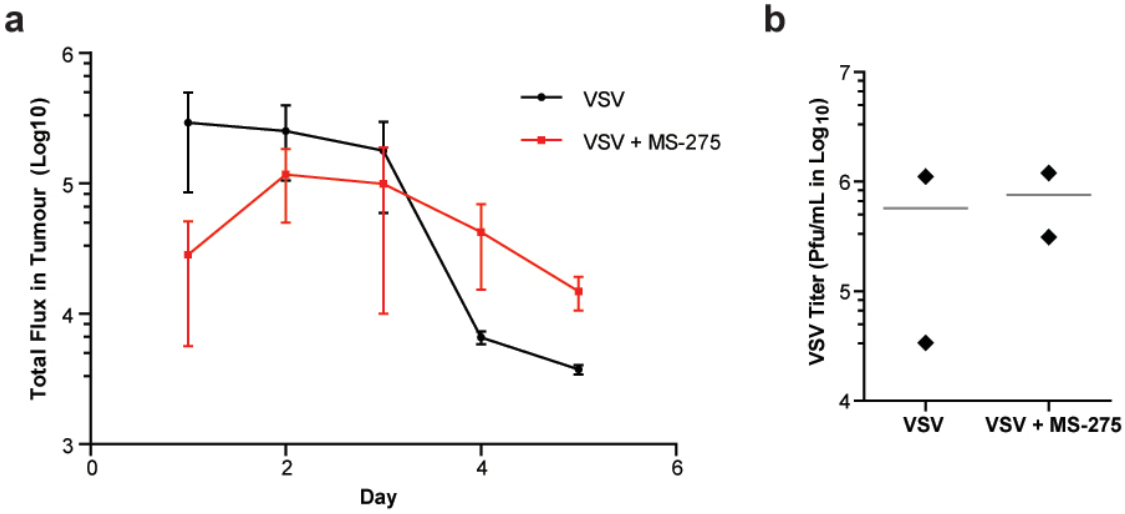
a
Total Flux in Tumour (Log10)
6
5
4
3
0
2
4
6
Day
VSV
VSV + MS-275
b
VSV Titer (Pfu/mL in Log10)
7
6
5
4
VSV
VSV + MS-275

Figure 4.8 – HDI treatment of B16-F10 cells *in vitro* inhibits VSV replication

B16-F10 cells were pre-treated for 2 hours with vehicle, 5μM MS-275, or 5μM SAHA and then infected at an MOI of 0.005 with VSV-Δ51-GFP or wtVSV-GFP. HDI treatment continued throughout the experiment. (**a**) GFP pictures from fluorescent microscopy taken 24 and 48 hours after infection, done in duplicate. (**b-c**) Supernatants were harvested at 48 hours post infection and one well per condition was titered on Vero cells by plaque assay.

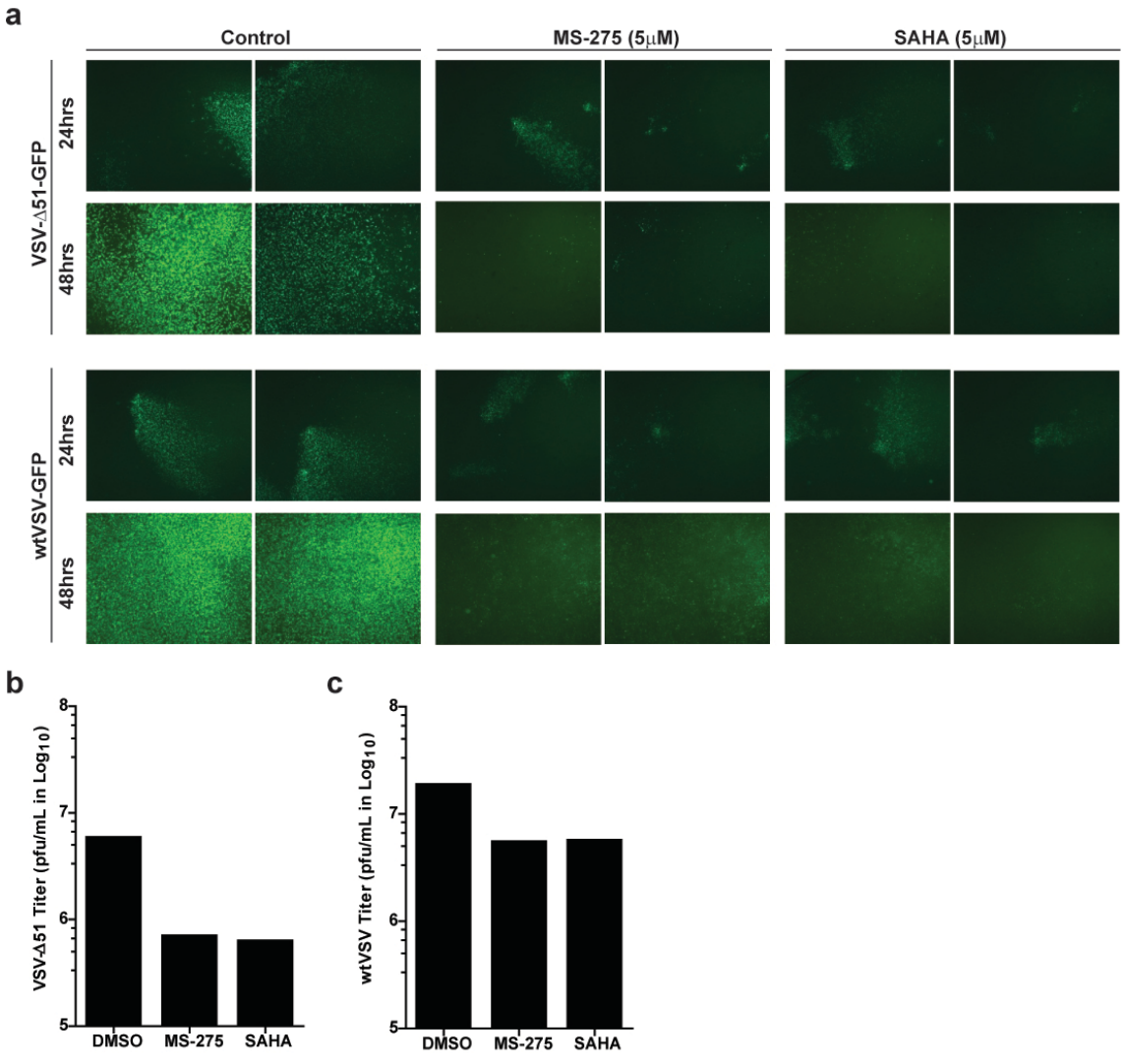
a
Control
MS-275 (5μM)
SAHA (5μM)
VSV-Δ51-GFP
24hrs
48hrs
wtVSV-GFP
24hrs
48hrs
b
VSV-Δ51 Titer (pfu/mL in Log10)
8
7
6
5
DMSO
MS-275
SAHA
c
wtVSV Titer (pfu/mL in Log10)
8
7
6
5
DMSO
MS-275
SAHA

significance was not reached, there was a trend demonstrating an increased lymphocyte presence in the brain following the vaccination protocol, and slightly more following MS-275 treatment (**Appendix IV**). No increase was detected with MS-275 treatment alone.

HDIs have been observed to increase co-stimulatory molecule expression on tumour cells(161). As such, the expression of CD40, CD80, and CD86 was quantified by flow cytometry on B16-F10 cells following MS-275 treatment. BM-DCs were used as controls to verify the staining procedure and antibodies (data not shown). CD40 and CD80 was present on 4 percent of untreated B16-F10 cells, and this doubled to 8 percent following 24hrs of MS-275 (**Figure 4.9a**). In addition, the expression level of all three proteins increased by approximately 30 percent on all cells (**Figure 4.9b**).

4.3.5 A second dose of VSV cannot be delivered in spite of MS-275 suppression of IFN and antiviral antibody

Unpublished observations from the Bell lab have documented that a second dose of VSV delivered IV, two or more days after the initial dose, cannot be detected in the tumour. Various hypotheses have been put forth to explain this apparent block in VSV propagation: the type 1 IFN response, vascular shutdown(18), or even a low level of anti-VSV antibodies.

Balb/C mice with subcutaneous CT26.wt tumours were treated with VSV-Δ51-RFP IV, 6 doses of MS-275 or vehicle, followed by VSV-Δ51-GFP IV (**Figure 4.10a**). 24 hours after the second dose of VSV, tumours were harvested, photographed using a fluorescent dissecting microscope, and titered. Mice that received vehicle between the two VSV doses demonstrated no visible virus, either RFP or GFP positive, by imaging (**Figure 4.10b**). Though the MS-275-treated mice showed much more RFP-positive sections of their tumours,

Figure 4.9 – Co-stimulatory molecule expression increases with MS-275 treatment of B16-F10 cells *in vitro*

B16-F10 cells were incubated for 24 hours with vehicle or 5μM MS-275 *in vitro* and then harvested and stained with antibodies against CD40, CD80, and CD86. (a) Percent of cells staining positive for co-stimulatory molecule and (b) normalized MFI of marker on B16-F10 cells.

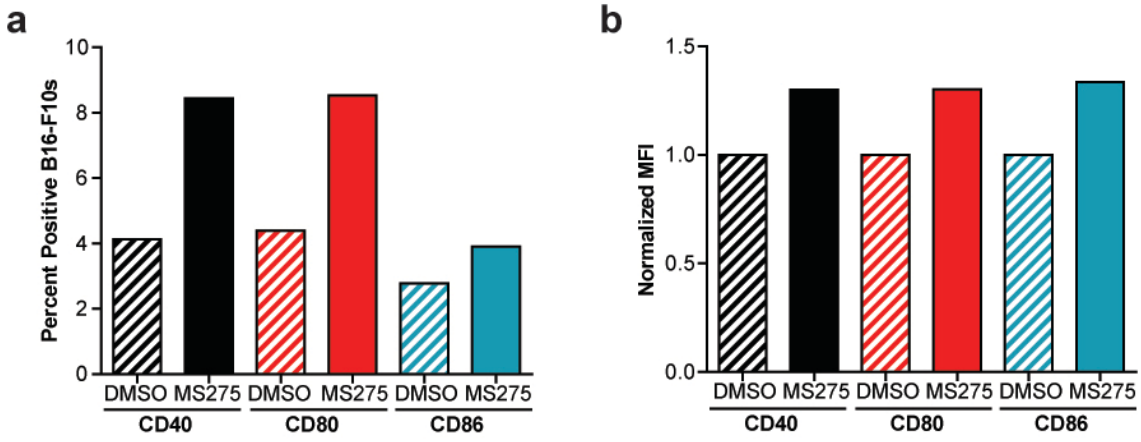
a
Percent Positive B16-F10s
10
8
6
4
2
0
DMSO MS275 DMSO MS275 DMSO MS275
CD40
CD80
CD86
b
Normalized MFI
1.5
1.0
0.5
0.0
DMSO MS275 DMSO MS275 DMSO MS275
CD40
CD80
CD86

Figure 4.10 – MS-275 treatment after initial dose of VSV does not uninhibit a subsequent dose in the CT26.wt model

(**a**) Balb/C mice were implanted with bilateral CT26.wt subcutaneous tumours. Once tumours had grown to approximately 5x5mm animals were treated with 0.1mg MS-275 IP for six days. An initial dose of $5x10^8$ pfu of VSV-Δ51-RFP was given IV on day 0. A second dose of VSV on day 5 was $5x10^8$ pfu of VSV-Δ51-GFP given IV. (**b**) Mice were euthanized on day 6, tumours were harvested, cut in half and quickly imaged, and then frozen on dry ice for later titering. Images were taken with a fluorescent dissecting microscope to visualize GFP, RFP, and brightfield. (**c**) Tumours were homogenized and titered by plaque assay. The bar colour corresponds to the colour of the plaques observed. Bars are mean + SEM.

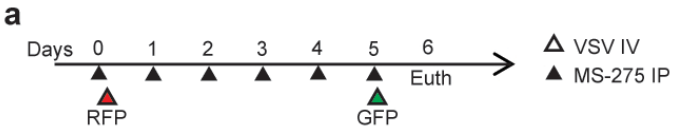
a
Days 0 1 2 3 4 5 6
Euth
VSV IV
MS-275 IP
RFP
GFP

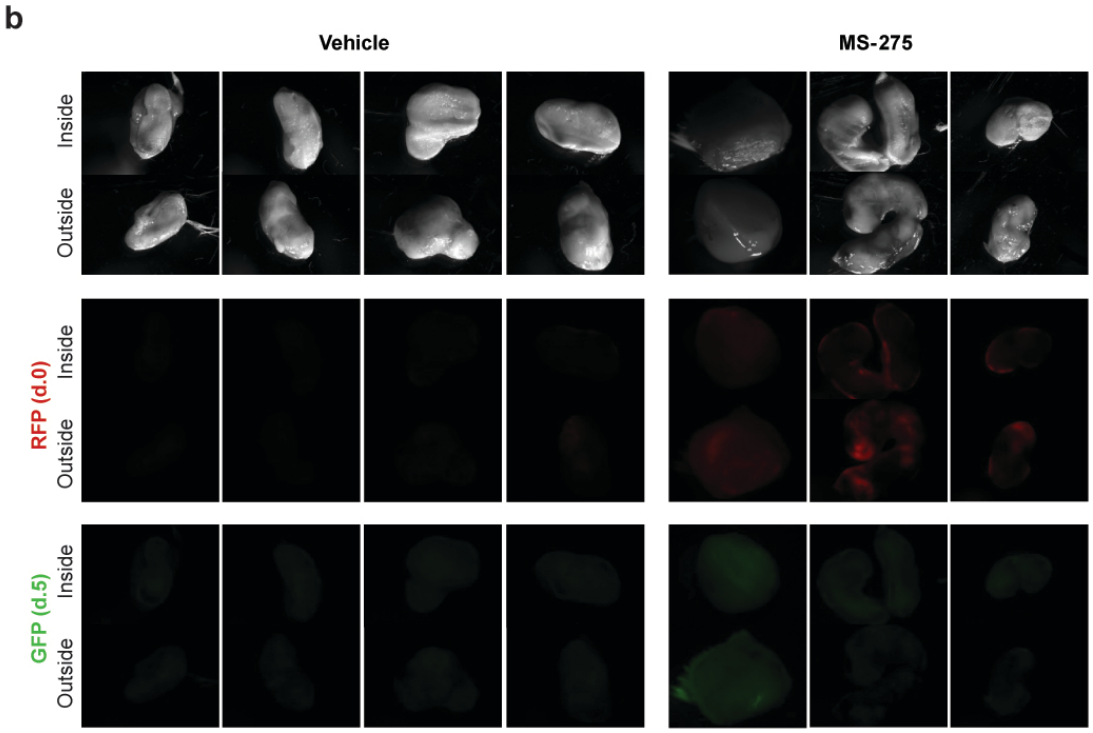
b
Vehicle
MS-275
Inside
Outside
RFP (d.0)
GFP (d.5)

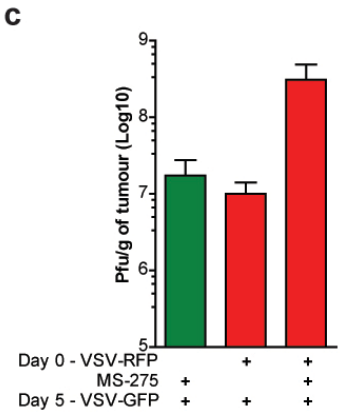
c
Pfu/g of tumour (Log10)
9
8
7
6
5
Day 0 - VSV-RFP
MS-275
Day 5 - VSV-GFP

there were no GFP-positive tumours. The titering data confirm these observations (**Figure 4.10c**). Mice that received only vehicle between the two doses had approximately 1.5 logs lower titer than those that received MS-275. However, neither showed any infection by the second VSV-GFP dose. As a control, the GFP-expressing virus was delivered without the first dose of VSV-RFP. This experiment was repeated in the more permissive CT26.LacZ tumour with similar results (**Figure 4.11**).

Figure 4.11 - MS-275 treatment after initial dose of VSV does not uninhibit a subsequent dose in the permissive CT26.LacZ model

(**a**) Balb/C mice were implanted with bilateral CT26.LacZ subcutaneous tumours. Once tumours had grown to approximately 5x5mm animals were treated with 0.1mg MS-275 IP for six days. An initial dose of $5x10^8$ pfu of VSV-Δ51-GFP was given IV on day 0. A second dose of VSV on day 5 was $5x10^8$ pfu of VSV-Δ51-RFP given IV. (**b**) Tumour images demonstrating GFP and RFP fluorescence from mice receiving both doses of VSV with or without MS-275 treatment. (**c**) Tumour images of mice that only received the second VSV-Δ51-RFP dose and MS-275.

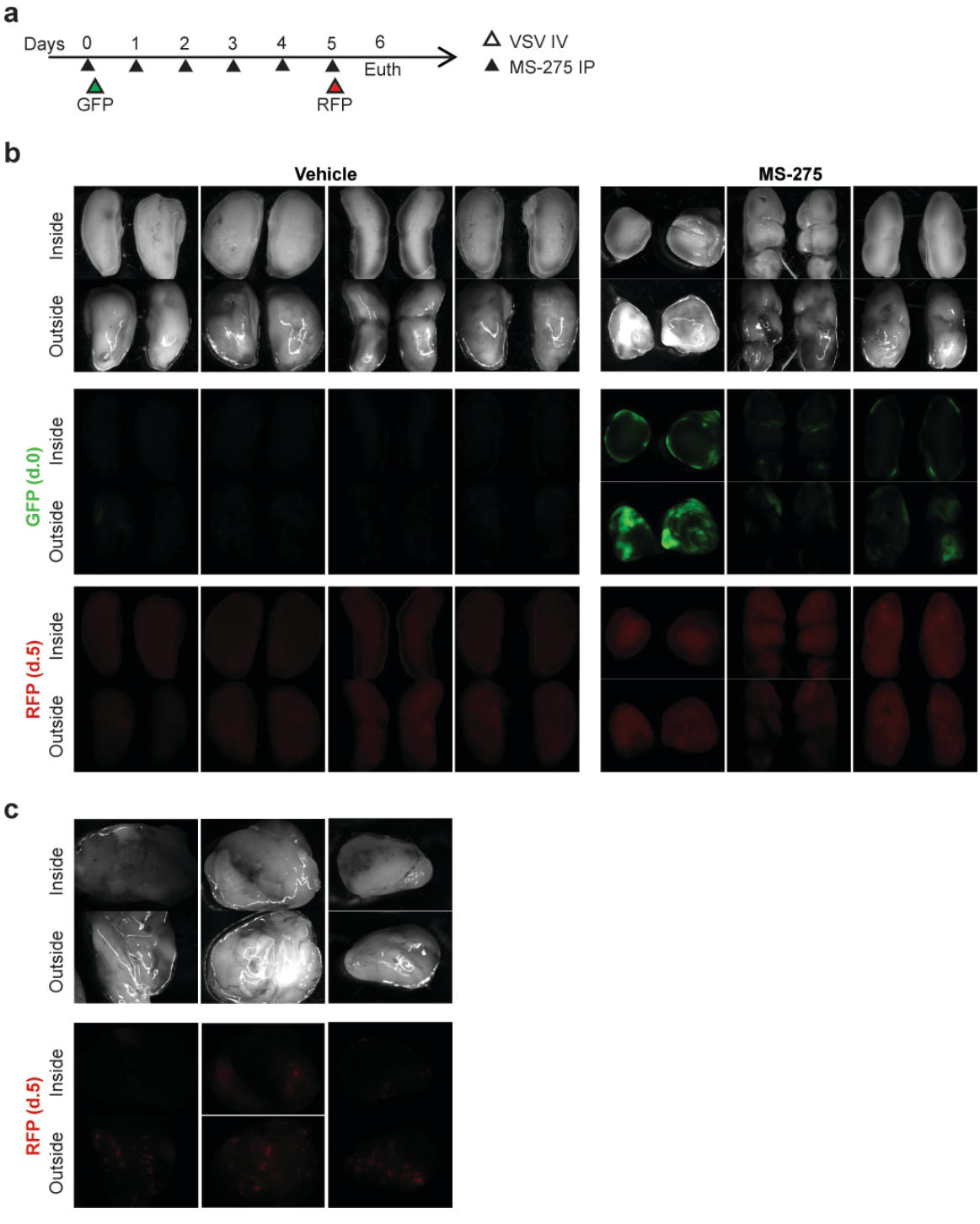
a
Days 0 1 2 3 4 5 6
Euth
VSV IV
MS-275 IP
GFP
RFP
b
Vehicle
MS-275
Inside
Outside
GFP (d.0)
RFP (d.5)
c

4.4 Discussion

MS-275 is a benzamide HDI that inhibits the type I IFN response in most cells, leading to enhanced VSV replication both *in vitro* and *in vivo(116)*. However, research indicates that the impact of HDI treatment on the immune system is neither clear nor consistent between HDIs. Because of the importance of the adaptive immune system in the long-term tumour regressions observed with many OVs, including VSV, the impact of MS-275 on the anti-viral and anti-tumour immune response was examined. In addition, for models with poor *in vivo* permissiveness to VSV, like the B16-F10 melanoma, the enhancement of viral replication by MS-275 may lead to enhanced tumour antigen shedding and DAMP exposure, thereby leading to a stronger anti-tumour immune response.

4.4.1 Initial MS-275 findings

A simple set of experiments in tumour-naïve mice was undertaken to examine the impact of MS-275 treatment on the anti-VSV immune response. Both Balb/C and C57BL/6 mice demonstrate similar responses: decreased spleen cellularity with MS-275 treatment with a moderate decrease in T cells and a strong decrease in B cells (**Figures 4.1 and 4.2**). These observations are coupled with a concomitant decrease in the anti-VSV $CD8^+$ T cell response (**Figures 4.1 and 4.2**) and a strong delay in the anti-VSV neutralizing antibody response (**Figure 4.3**). Conversely, these results were not recapitulated by two hydroxamic acid HDIs, namely SAHA and Oxamflatin (**Figures 4.3 and 4.5**). Further experiments by collaborators indicated that CI994, another benzamide HDI, was able to modestly recapitulate the effects of MS-275 possibly indicating that this effect is a feature of the benzamide class of HDIs. Interpreting these results is not an easy task because benzamides are considered to be much more restricted in the HDACs that they inhibit compared to the

hydroxamic acids, which inhibit all class 1 and 2 HDACs (HDACs 1-10) to varying degrees. MS-275 is thought to inhibit mostly HDACs 1-3(161). However, there have been publications comparing gene expression modulation by MS-275 and SAHA(29, 59), and a close examination of those results might give clues as to the differences in HDAC inhibition profiles between these two drugs.

Important future experiments might further investigate the mechanisms that lead to the selective depletion of naïve lymphocytes by MS-275 treatment. My studies do not indicate that splenocytes are significantly sensitive to HDI treatment *in vitro* (**Figure 4.6**). However, time course of lymphodepletion results delineated in **Figure 4.4** may indicate that the depletion occurs most robustly between 48 and 72 hours. Therefore, my *in vitro* experiments may not have assessed splenocyte HDI sensitivity for a long enough time. Moreover, it is possible that the *in vivo* cytokine environment exacerbates the MS-275-induced phenotype such that experiments that are conducted *in vivo* may lead to more appropriate results.

Though a wide range of cell lines and viruses have been tested for HDI-mediated OV enhancement, B16-F10 cells had not been previously examined. Surprisingly, MS-275 and SAHA treatment of B16-F10 cells inhibited VSV (Δ51 and WT) replication *in vitro* (**Figure 4.8**). This result was substantiated in the B16-F10 brain model (**Figure 4.7**) and led to our hypothesis being revised. Though substantial efficacy enhancement was seen in the B16-F10 oncolytic prime/boost vaccination strategy (**Appendix V**), this could not be attributed to enhanced viral replication. However, there was a longer persistence of VSV in MS-275 treated mice (**Figure 4.7**), which might reflect the delay in neutralizing antibody formation. The enhancement of efficacy observed with the addition of MS-275 appears disproportionate

to the modest increase in viral persistence and is more likely a reflection of the immunological changes that MS-275 imparts.

4.4.2 MS-275-mediated selective lymphodepletion

My collaborators found that MS-275 selectively depletes naïve lymphocytes, both T and B cells, while having no effect on memory T and B cells. In addition, regulatory T cell numbers dropped. Many studies have found that lymphodepletion can help T cell responses by allowing the tumour specific T cells access to important homeostatic cytokines and survival signals, in addition to the depletion of regulatory T cells. This can lead to a more functionally robust anti-tumour T cell expansion(50). Indeed it was observed that the anti-tumour T cells, though not increasing in number, had a significantly enhanced functionality. This was characterized by a higher secretion of the anti-tumour cytokines IFNγ and TNFα and a heightened response in an avidity assay (**Appendix V figure 5**). In addition, the increase in co-stimulatory molecule expression on the B16-F10 cells could lead to better T cell activation(5).

Interestingly, MS-275 has previously been published to enhanced FoxP3 expression in T cells, however, this was only observed after 6 days of treatment, whereas 4 days was not enough(103). Therefore 5 days of treatment may not have induced this phenotype. In addition, although HDIs suppress the deacetylation of lysines, they do not control the acetylation of those proteins. As a result, the signals that the cell receives that lead to the acetylation are also very important in dictating the outcome following HDAC inhibition.

Though these findings of MS-275-mediated selective lymphodepletion have not been described in literature to date, there is evidence that this might be occurring in humans

during clinical trials. It was reported that a dose limiting toxicity for patients treated with MS-275 was a high risk of infection, which may indicate an inability to mount protective immune responses, as we observed. The fact that patients treated with SAHA did not have altered leukocyte counts also validated our findings(83).

4.4.3 Decrease in autoimmune vitiligo

The generation of autoimmune sequelae following cancer immunotherapy has long been thought to be inseparable from the anti-tumour immune response. Though autoimmune vitiligo may not be a life threatening disorder, autoimmune consequences can become severe. Many other cells in the body express melanin, including those of the eye, which can lead to potentially serious consequences(23). We observed a stark decrease in autoimmune vitiligo when the prime/boost vaccination strategy was coupled with MS-275 treatment (**Appendix V: Figure 6**). In spite of the significant decrease in regulatory T cells and a large increase in the reactivity of the anti-DCT T cells, MS-275 conferred protection against autoimmune tissue destruction. As of yet, the mechanisms behind this protection remain elusive, but we hypothesize that it may be related to anti-inflammatory properties that have been previously described for MS-275(96). In addition, research suggests that inflammatory stimuli that upregulate antigen presentation, particularly IFNα, in the target organ play an important role in the generation of autoimmune pathology(90). The autoimmune vitiligo observed in the B16-F10 prime/boost vaccination is dependent upon an inflammatory stimulus like prior skin surgery, so a reduction in pro-inflammatory signals by MS-275 may be protective(20).

4.4.4 Second dose delivery of VSV

The Bell lab has long observed that once a first dose of VSV-Δ51 is delivered to a CT26.LacZ tumour, a second dose can only be seen, through IHC or titering, if it is delivered within 48hours of the first. Beyond that time frame, no virus from the second dose can be found in the tumour(124). Several hypotheses have been put forth to potentially explain this inability to detect virus in the tumour at 72 hours or more after initial infection, including vascular shutdown and tumour hypoxia, the IFN response to the virus, or even perhaps a low level of neutralizing antibodies already in circulation. The anti-VSV neutralizing antibody response was examined as early as day 4 after injection and a significant titer was observed (129). However, the results from **Figure 4.10** and **Figure 4.11** would indicate that neither the type I IFNs response nor the anti-VSV neutralizing antibodies are involved because both of these should have been inhibited by MS-275 treatment. Further studies might look at whether the hypoxia induced following vascular shutdown in VSV-treated tumours affects the delivery of a second dose of VSV(18).

4.4.5 Overall impact of MS-275 treatment in oncolytic prime/boost vaccination

This project originally began to investigate how increased viral replication could impact the anti-tumour immune response. However, the B16-F10 tumour model does not react to MS-275 treatment as is commonly observed with other tumour models, and instead virus replication in this cell line was partially inhibited with HDI treatment. Nonetheless, this allowed us to focus on the immunological changes that were occurring because of MS-275 treatment. Through my research collaboration with Dr. Bridle and Dr. Lichty at McMaster University, we discovered that MS-275 selectively depletes naïve and regulatory lymphocytes. This allows memory T and B cells to expand unconstrained by the usual

regulatory cells and in an environment undepleted of important homeostasis cytokines. This enhanced anti-tumour response is complemented by a reduced anti-VSV response, which may be the cause of the longer viral persistence in the tumour. Perhaps most importantly, there is a concomitant reduction in autoimmune vitiligo, which has been seen in the field as a necessary side-effect of a robust anti-tumour immune response. Important future studies should attempt to further understand the mechanisms that lead to this divergence between cancer immunity and autoimmunity.

General Concluding Remarks

Oncolytic viruses have now been demonstrated to potently kill tumour cells through multiple mechanisms, including specific replication and lysis, tumour vascular collapse, and activation of innate and adaptive immune effectors. Because of the high heterogeneity within tumours and their high adaptability, killing through multiple complementary mechanisms likely allows for a broader susceptibility profile and more robust killing. Although the field of OVs has in the past attempted to inhibit the immune response to allow for better viral replication, it has become clear that the anti-tumour immune response is a vital part of long-term tumour control(108). Consequently, most OV clinical candidates express an immune stimulatory transgene and are being investigated for their ability to induce secondary immune killing of the tumour(19). No matter the anti-cancer agent, eventually it will clear from the body, and if it hasn't killed every cancer cell by then, cancer will recur. An anti-tumour immune response can be the long-term surveillance and effector mechanisms that lead to long-term eradication.

Through the research presented in this thesis it is clear that an anti-tumour immune response induced by VSV infection is paramount to long-term tumour control and that this OV-mediated anti-tumour immune response can be harnessed, even for tumours that are poorly infectable *in vivo* through the use of an infected cell vaccine. This vaccine importantly stimulates multiple arms of the immune system, leading to immediate and long-term tumour killing. In addition, through the proper characterization of innate immune modulators like MS-275, OV replication can be strategically enhanced in the short term while maximizing anti-tumour immune activation and functions. Ultimately, the goal is to create an anti-cancer platform that potently replicates in tumour cells, leading to their killing,

antigen release, and immune stimulation. Through the expression of immune stimulatory transgenes and the use of complementary immunotherapies, OV platforms will be more specific, broadly applicable, and lead to a more successful anticancer weapon.

References

1. 2011. Canadian Cancer Statistics 2011. Canadian Cancer Society, Toronto, ON.
2. **Abdel-Wahab, Z., M. M. Dar, D. Hester, C. Vervaert, R. Gangavalli, J. Barber, T. L. Darrow, and H. F. Seigler.** 1996. Effect of irradiation on cytokine production, MHC antigen expression, and vaccine potential of interleukin-2 and interferon-gamma gene-modified melanoma cells. Cellular immunology **171:**246-254.
3. **Ahmed, M., K. L. Brzoza, and E. M. Hiltbold.** 2006. Matrix protein mutant of vesicular stomatitis virus stimulates maturation of myeloid dendritic cells. Journal of virology **80:**2194-2205.
4. **Alcami, A., and U. H. Koszinowski.** 2000. Viral mechanisms of immune evasion. Trends in microbiology **8:**410-418.
5. **Antonia, S. J., J. Seigne, J. Diaz, C. Muro-Cacho, M. Extermann, M. J. Farmelo, M. Friberg, M. Alsarraj, J. J. Mahany, J. Pow-Sang, A. Cantor, and W. Janssen.** 2002. Phase I trial of a B7-1 (CD80) gene modified autologous tumor cell vaccine in combination with systemic interleukin-2 in patients with metastatic renal cell carcinoma. The Journal of urology **167:**1995-2000.
6. **Apetoh, L., F. Ghiringhelli, A. Tesniere, M. Obeid, C. Ortiz, A. Criollo, G. Mignot, M. C. Maiuri, E. Ullrich, P. Saulnier, H. Yang, S. Amigorena, B. Ryffel, F. J. Barrat, P. Saftig, F. Levi, R. Lidereau, C. Nogues, J. P. Mira, A. Chompret, V. Joulin, F. Clavel-Chapelon, J. Bourhis, F. Andre, S. Delaloge, T. Tursz, G. Kroemer, and L. Zitvogel.** 2007. Toll-like receptor 4-dependent contribution of the immune system to anticancer chemotherapy and radiotherapy. Nature medicine **13:**1050-1059.
7. **Arrowsmith, C. H., C. Bountra, P. V. Fish, K. Lee, and M. Schapira.** 2012. Epigenetic protein families: a new frontier for drug discovery. Nature reviews. Drug discovery **11:**384-400.
8. **Bahar, M. W., S. C. Graham, R. A. Chen, S. Cooray, G. L. Smith, D. I. Stuart, and J. M. Grimes.** 2011. How vaccinia virus has evolved to subvert the host immune response. Journal of structural biology **175:**127-134.
9. **Banchereau, J., F. Briere, C. Caux, J. Davoust, S. Lebecque, Y. J. Liu, B. Pulendran, and K. Palucka.** 2000. Immunobiology of dendritic cells. Annual review of immunology **18:**767-811.
10. **Barreira da Silva, R., and C. Munz.** 2011. Natural killer cell activation by dendritic cells: balancing inhibitory and activating signals. Cellular and molecular life sciences : CMLS **68:**3505-3518.
11. **Bhat, R., S. Dempe, C. Dinsart, and J. Rommelaere.** 2011. Enhancement of NK cell antitumor responses using an oncolytic parvovirus. International journal of cancer. Journal international du cancer **128:**908-919.
12. **Bloor, S., J. Maelfait, R. Krumbach, R. Beyaert, and F. Randow.** 2010. Endoplasmic reticulum chaperone gp96 is essential for infection with vesicular stomatitis virus. Proceedings of the National Academy of Sciences of the United States of America **107:**6970-6975.
13. **Boudreau, J., S. Koshy, D. Cummings, and Y. Wan.** 2008. Culture of myeloid dendritic cells from bone marrow precursors. Journal of visualized experiments : JoVE.
14. **Boudreau, J. E., B. W. Bridle, K. B. Stephenson, K. M. Jenkins, J. Brunelliere, J. L. Bramson, B. D. Lichty, and Y. Wan.** 2009. Recombinant vesicular stomatitis virus transduction of dendritic cells enhances their ability to prime innate and adaptive antitumor immunity. Molecular therapy : the journal of the American Society of Gene Therapy **17:**1465-1472.

15. **Boudreau, J. E., K. B. Stephenson, F. Wang, A. A. Ashkar, K. L. Mossman, L. L. Lenz, K. L. Rosenthal, J. L. Bramson, B. D. Lichty, and Y. Wan.** 2011. IL-15 and type I interferon are required for activation of tumoricidal NK cells by virus-infected dendritic cells. Cancer research **71:**2497-2506.
16. **Braun, S., F. Hepp, H. L. Sommer, and K. Pantel.** 1999. Tumor-antigen heterogeneity of disseminated breast cancer cells: implications for immunotherapy of minimal residual disease. International journal of cancer. Journal international du cancer **84:**1-5.
17. **Breitbach, C. J., J. Burke, D. Jonker, J. Stephenson, A. R. Haas, L. Q. Chow, J. Nieva, T. H. Hwang, A. Moon, R. Patt, A. Pelusio, F. Le Boeuf, J. Burns, L. Evgin, N. De Silva, S. Cvancic, T. Robertson, J. E. Je, Y. S. Lee, K. Parato, J. S. Diallo, A. Fenster, M. Daneshmand, J. C. Bell, and D. H. Kirn.** 2011. Intravenous delivery of a multi-mechanistic cancer-targeted oncolytic poxvirus in humans. Nature **477:**99-102.
18. **Breitbach, C. J., J. M. Paterson, C. G. Lemay, T. J. Falls, A. McGuire, K. A. Parato, D. F. Stojdl, M. Daneshmand, K. Speth, D. Kirn, J. A. McCart, H. Atkins, and J. C. Bell.** 2007. Targeted inflammation during oncolytic virus therapy severely compromises tumor blood flow. Molecular therapy : the journal of the American Society of Gene Therapy **15:**1686-1693.
19. **Breitbach, C. J., S. H. Thorne, J. C. Bell, and D. H. Kirn.** 2011. Targeted and Armed Oncolytic Poxviruses for Cancer: The Lead Example of JX-594. Current pharmaceutical biotechnology.
20. **Bridle, B. W., J. Li, S. Jiang, R. Chang, B. D. Lichty, J. L. Bramson, and Y. Wan.** 2010. Immunotherapy can reject intracranial tumor cells without damaging the brain despite sharing the target antigen. Journal of immunology **184:**4269-4275.
21. **Bridle, B. W., K. B. Stephenson, J. E. Boudreau, S. Koshy, N. Kazdhan, E. Pullenayegum, J. Brunelliere, J. L. Bramson, B. D. Lichty, and Y. Wan.** 2010. Potentiating cancer immunotherapy using an oncolytic virus. Molecular therapy : the journal of the American Society of Gene Therapy **18:**1430-1439.
22. **Buell, J. F., T. G. Gross, and E. S. Woodle.** 2005. Malignancy after transplantation. Transplantation **80:**S254-264.
23. **Caspi, R. R.** 2008. Immunotherapy of autoimmunity and cancer: the penalty for success. Nature reviews. Immunology **8:**970-976.
24. **Castle, J. C., S. Kreiter, J. Diekmann, M. Lower, N. van de Roemer, J. de Graaf, A. Selmi, M. Diken, S. Boegel, C. Paret, M. Koslowski, A. N. Kuhn, C. M. Britten, C. Huber, O. Tureci, and U. Sahin.** 2012. Exploiting the mutanome for tumor vaccination. Cancer research **72:**1081-1091.
25. **Chakraborty, M., S. I. Abrams, C. N. Coleman, K. Camphausen, J. Schlom, and J. W. Hodge.** 2004. External beam radiation of tumors alters phenotype of tumor cells to render them susceptible to vaccine-mediated T-cell killing. Cancer research **64:**4328-4337.
26. **Cheng, M., J. Zhang, W. Jiang, Y. Chen, and Z. Tian.** 2012. Natural killer cell lines in tumor immunotherapy. Frontiers of medicine **6:**56-66.
27. **Chisholm, S. E., and H. T. Reyburn.** 2006. Recognition of vaccinia virus-infected cells by human natural killer cells depends on natural cytotoxicity receptors. Journal of virology **80:**2225-2233.
28. **Choi, I. K., J. S. Lee, S. N. Zhang, J. Park, C. H. Sonn, K. M. Lee, and C. O. Yun.** 2011. Oncolytic adenovirus co-expressing IL-12 and IL-18 improves tumor-specific immunity via differentiation of T cells expressing IL-12Rbeta2 or IL-18Ralpha. Gene therapy **18:**898-909.
29. **Choudhary, C., C. Kumar, F. Gnad, M. L. Nielsen, M. Rehman, T. C. Walther, J. V. Olsen, and M. Mann.** 2009. Lysine acetylation targets protein complexes and co-regulates major cellular functions. Science **325:**834-840.

30. **Clevers, H.** 2004. At the crossroads of inflammation and cancer. Cell **118:**671-674.
31. **Connolly, D. C., R. Bao, A. Y. Nikitin, K. C. Stephens, T. W. Poole, X. Hua, S. S. Harris, B. C. Vanderhyden, and T. C. Hamilton.** 2003. Female mice chimeric for expression of the simian virus 40 TAg under control of the MISIIR promoter develop epithelial ovarian cancer. Cancer research **63:**1389-1397.
32. **Curiel, T. J.** 2007. Tregs and rethinking cancer immunotherapy. The Journal of clinical investigation **117:**1167-1174.
33. **Davies, E., S. Reid, M. F. Medina, B. Lichty, and A. A. Ashkar.** 2010. IL-15 has innate anti-tumor activity independent of NK and CD8 T cells. Journal of leukocyte biology **88:**529-536.
34. **Demaria, S., N. Bhardwaj, W. H. McBride, and S. C. Formenti.** 2005. Combining radiotherapy and immunotherapy: a revived partnership. International journal of radiation oncology, biology, physics **63:**655-666.
35. **Diaz, R. M., F. Galivo, T. Kottke, P. Wongthida, J. Qiao, J. Thompson, M. Valdes, G. Barber, and R. G. Vile.** 2007. Oncolytic immunovirotherapy for melanoma using vesicular stomatitis virus. Cancer research **67:**2840-2848.
36. **Dokmanovic, M., C. Clarke, and P. A. Marks.** 2007. Histone deacetylase inhibitors: overview and perspectives. Molecular cancer research : MCR **5:**981-989.
37. **Dranoff, G., E. Jaffee, A. Lazenby, P. Golumbek, H. Levitsky, K. Brose, V. Jackson, H. Hamada, D. Pardoll, and R. C. Mulligan.** 1993. Vaccination with irradiated tumor cells engineered to secrete murine granulocyte-macrophage colony-stimulating factor stimulates potent, specific, and long-lasting anti-tumor immunity. Proceedings of the National Academy of Sciences of the United States of America **90:**3539-3543.
38. **Drillien, R., D. Spehner, A. Bohbot, and D. Hanau.** 2000. Vaccinia virus-related events and phenotypic changes after infection of dendritic cells derived from human monocytes. Virology **268:**471-481.
39. **Dunn, G. P., L. J. Old, and R. D. Schreiber.** 2004. The three Es of cancer immunoediting. Annual review of immunology **22:**329-360.
40. **Edukulla, R., N. Woller, B. Mundt, S. Knocke, E. Gurlevik, M. Saborowski, N. Malek, M. P. Manns, T. Wirth, F. Kuhnel, and S. Kubicka.** 2009. Antitumoral immune response by recruitment and expansion of dendritic cells in tumors infected with telomerase-dependent oncolytic viruses. Cancer research **69:**1448-1458.
41. **Engelmayer, J., M. Larsson, M. Subklewe, A. Chahroudi, W. I. Cox, R. M. Steinman, and N. Bhardwaj.** 1999. Vaccinia virus inhibits the maturation of human dendritic cells: a novel mechanism of immune evasion. Journal of immunology **163:**6762-6768.
42. **Errington, F., L. Steele, R. Prestwich, K. J. Harrington, H. S. Pandha, L. Vidal, J. de Bono, P. Selby, M. Coffey, R. Vile, and A. Melcher.** 2008. Reovirus activates human dendritic cells to promote innate antitumor immunity. Journal of immunology **180:**6018-6026.
43. **Fehniger, T. A., M. A. Cooper, G. J. Nuovo, M. Cella, F. Facchetti, M. Colonna, and M. A. Caligiuri.** 2003. CD56bright natural killer cells are present in human lymph nodes and are activated by T cell-derived IL-2: a potential new link between adaptive and innate immunity. Blood **101:**3052-3057.
44. **Formenti, S. C., and S. Demaria.** 2009. Systemic effects of local radiotherapy. The lancet oncology **10:**718-726.
45. **Foster, B., C. Prussin, F. Liu, J. K. Whitmire, and J. L. Whitton.** 2007. Detection of intracellular cytokines by flow cytometry. Current protocols in immunology / edited by John E. Coligan ... [et al.] **Chapter 6:**Unit 6 24.

46. **Fournier, P., A. Arnold, and V. Schirrmacher.** 2009. Polarization of human monocyte-derived dendritic cells to DC1 by in vitro stimulation with Newcastle Disease Virus. Journal of B.U.ON. : official journal of the Balkan Union of Oncology **14 Suppl 1:**S111-122.
47. **Fridman, W. H., F. Pages, C. Sautes-Fridman, and J. Galon.** 2012. The immune contexture in human tumours: impact on clinical outcome. Nature reviews. Cancer **12:**298-306.
48. **Gabrilovich, D.** 2004. Mechanisms and functional significance of tumour-induced dendritic-cell defects. Nature reviews. Immunology **4:**941-952.
49. **Galon, J., A. Costes, F. Sanchez-Cabo, A. Kirilovsky, B. Mlecnik, C. Lagorce-Pages, M. Tosolini, M. Camus, A. Berger, P. Wind, F. Zinzindohoue, P. Bruneval, P. H. Cugnenc, Z. Trajanoski, W. H. Fridman, and F. Pages.** 2006. Type, density, and location of immune cells within human colorectal tumors predict clinical outcome. Science **313:**1960-1964.
50. **Gattinoni, L., S. E. Finkelstein, C. A. Klebanoff, P. A. Antony, D. C. Palmer, P. J. Spiess, L. N. Hwang, Z. Yu, C. Wrzesinski, D. M. Heimann, C. D. Surh, S. A. Rosenberg, and N. P. Restifo.** 2005. Removal of homeostatic cytokine sinks by lymphodepletion enhances the efficacy of adoptively transferred tumor-specific CD8+ T cells. The Journal of experimental medicine **202:**907-912.
51. **Gauvrit, A., S. Brandler, C. Sapede-Peroz, N. Boisgerault, F. Tangy, and M. Gregoire.** 2008. Measles virus induces oncolysis of mesothelioma cells and allows dendritic cells to cross-prime tumor-specific CD8 response. Cancer research **68:**4882-4892.
52. **Gerlinger, M., A. J. Rowan, S. Horswell, J. Larkin, D. Endesfelder, E. Gronroos, P. Martinez, N. Matthews, A. Stewart, P. Tarpey, I. Varela, B. Phillimore, S. Begum, N. Q. McDonald, A. Butler, D. Jones, K. Raine, C. Latimer, C. R. Santos, M. Nohadani, A. C. Eklund, B. Spencer-Dene, G. Clark, L. Pickering, G. Stamp, M. Gore, Z. Szallasi, J. Downward, P. A. Futreal, and C. Swanton.** 2012. Intratumor heterogeneity and branched evolution revealed by multiregion sequencing. The New England journal of medicine **366:**883-892.
53. **Ghiringhelli, F., L. Apetoh, F. Housseau, G. Kroemer, and L. Zitvogel.** 2007. Links between innate and cognate tumor immunity. Current opinion in immunology **19:**224-231.
54. **Ghiringhelli, F., L. Apetoh, A. Tesniere, L. Aymeric, Y. Ma, C. Ortiz, K. Vermaelen, T. Panaretakis, G. Mignot, E. Ullrich, J. L. Perfettini, F. Schlemmer, E. Tasdemir, M. Uhl, P. Genin, A. Civas, B. Ryffel, J. Kanellopoulos, J. Tschopp, F. Andre, R. Lidereau, N. M. McLaughlin, N. M. Haynes, M. J. Smyth, G. Kroemer, and L. Zitvogel.** 2009. Activation of the NLRP3 inflammasome in dendritic cells induces IL-1beta-dependent adaptive immunity against tumors. Nature medicine **15:**1170-1178.
55. **Ghose, A., E. Iakhnina, D. Spaner, J. Tartaglia, and N. L. Berinstein.** 2000. Immunogenicity of whole-cell tumor preparations infected with the ALVAC viral vector. Human gene therapy **11:**1289-1301.
56. **Gil, M., M. Bieniasz, A. Wierzbicki, B. J. Bambach, H. Rokita, and D. Kozbor.** 2009. Targeting a mimotope vaccine to activating Fcgamma receptors empowers dendritic cells to prime specific CD8+ T cell responses in tumor-bearing mice. Journal of immunology **183:**6808-6818.
57. **Gilboa, E.** 2007. DC-based cancer vaccines. The Journal of clinical investigation **117:**1195-1203.
58. **Gilboa, E.** 2004. The promise of cancer vaccines. Nature reviews. Cancer **4:**401-411.
59. **Glaser, K. B., M. J. Staver, J. F. Waring, J. Stender, R. G. Ulrich, and S. K. Davidsen.** 2003. Gene expression profiling of multiple histone deacetylase (HDAC) inhibitors: defining a common gene set produced by HDAC inhibition in T24 and MDA carcinoma cell lines. Molecular cancer therapeutics **2:**151-163.

60. **Glozak, M. A., and E. Seto.** 2007. Histone deacetylases and cancer. Oncogene **26:**5420-5432.
61. **Goldman, B., and L. DeFrancesco.** 2009. The cancer vaccine roller coaster. Nature biotechnology **27:**129-139.
62. **Gross, S., and P. Walden.** 2008. Immunosuppressive mechanisms in human tumors: why we still cannot cure cancer. Immunology letters **116:**7-14.
63. **Gujar, S. A., P. Marcato, D. Pan, and P. W. Lee.** 2010. Reovirus virotherapy overrides tumor antigen presentation evasion and promotes protective antitumor immunity. Molecular cancer therapeutics **9:**2924-2933.
64. **Gulley, J. L., P. M. Arlen, A. Bastian, S. Morin, J. Marte, P. Beetham, K. Y. Tsang, J. Yokokawa, J. W. Hodge, C. Menard, K. Camphausen, C. N. Coleman, F. Sullivan, S. M. Steinberg, J. Schlom, and W. Dahut.** 2005. Combining a recombinant cancer vaccine with standard definitive radiotherapy in patients with localized prostate cancer. Clinical cancer research : an official journal of the American Association for Cancer Research **11:**3353-3362.
65. **Hanahan, D., and R. A. Weinberg.** 2000. The hallmarks of cancer. Cell **100:**57-70.
66. **Hanahan, D., and R. A. Weinberg.** 2011. Hallmarks of cancer: the next generation. Cell **144:**646-674.
67. **Hand, P. H., M. Nuti, D. Colcher, and J. Schlom.** 1983. Definition of antigenic heterogeneity and modulation among human mammary carcinoma cell populations using monoclonal antibodies to tumor-associated antigens. Cancer research **43:**728-735.
68. **Hatfield, P., A. E. Merrick, E. West, D. O'Donnell, P. Selby, R. Vile, and A. A. Melcher.** 2008. Optimization of dendritic cell loading with tumor cell lysates for cancer immunotherapy. Journal of immunotherapy **31:**620-632.
69. **Heo, J., C. J. Breitbach, A. Moon, C. W. Kim, R. Patt, M. K. Kim, Y. K. Lee, S. Y. Oh, H. Y. Woo, K. Parato, J. Rintoul, T. Falls, T. Hickman, B. G. Rhee, J. C. Bell, D. H. Kirn, and T. H. Hwang.** 2011. Sequential therapy with JX-594, a targeted oncolytic poxvirus, followed by sorafenib in hepatocellular carcinoma: preclinical and clinical demonstration of combination efficacy. Molecular therapy : the journal of the American Society of Gene Therapy **19:**1170-1179.
70. **Hou, W., J. S. Gibbs, X. Lu, C. B. Brooke, D. Roy, R. L. Modlin, J. R. Bennink, and J. W. Yewdell.** 2012. Viral infection triggers rapid differentiation of human blood monocytes into dendritic cells. Blood.
71. **Humrich, J. Y., P. Thumann, S. Greiner, J. H. Humrich, M. Averbeck, C. Schwank, E. Kampgen, G. Schuler, and L. Jenne.** 2007. Vaccinia virus impairs directional migration and chemokine receptor switch of human dendritic cells. European journal of immunology **37:**954-965.
72. **Ilett, E. J., R. J. Prestwich, T. Kottke, F. Errington, J. M. Thompson, K. J. Harrington, H. S. Pandha, M. Coffey, P. J. Selby, R. G. Vile, and A. A. Melcher.** 2009. Dendritic cells and T cells deliver oncolytic reovirus for tumour killing despite pre-existing anti-viral immunity. Gene therapy **16:**689-699.
73. **Janke, M., B. Peeters, O. de Leeuw, R. Moorman, A. Arnold, P. Fournier, and V. Schirrmacher.** 2007. Recombinant Newcastle disease virus (NDV) with inserted gene coding for GM-CSF as a new vector for cancer immunogene therapy. Gene therapy **14:**1639-1649.
74. **Janke, M., B. Peeters, H. Zhao, O. de Leeuw, R. Moorman, A. Arnold, Y. Ziouta, P. Fournier, and V. Schirrmacher.** 2008. Activation of human T cells by a tumor vaccine infected with recombinant Newcastle disease virus producing IL-2. International journal of oncology **33:**823-832.

75. **Jarahian, M., C. Watzl, P. Fournier, A. Arnold, D. Djandji, S. Zahedi, A. Cerwenka, A. Paschen, V. Schirrmacher, and F. Momburg.** 2009. Activation of natural killer cells by newcastle disease virus hemagglutinin-neuraminidase. Journal of virology **83:**8108-8121.
76. **Jones, S., X. Zhang, D. W. Parsons, J. C. Lin, R. J. Leary, P. Angenendt, P. Mankoo, H. Carter, H. Kamiyama, A. Jimeno, S. M. Hong, B. Fu, M. T. Lin, E. S. Calhoun, M. Kamiyama, K. Walter, T. Nikolskaya, Y. Nikolsky, J. Hartigan, D. R. Smith, M. Hidalgo, S. D. Leach, A. P. Klein, E. M. Jaffee, M. Goggins, A. Maitra, C. Iacobuzio-Donahue, J. R. Eshleman, S. E. Kern, R. H. Hruban, R. Karchin, N. Papadopoulos, G. Parmigiani, B. Vogelstein, V. E. Velculescu, and K. W. Kinzler.** 2008. Core signaling pathways in human pancreatic cancers revealed by global genomic analyses. Science **321:**1801-1806.
77. **Ju, D. W., X. Cao, and B. Acres.** 1996. Active specific immunotherapy of pulmonary metastasis with vaccinia melanoma oncolysate prepared from granulocyte/macrophage-colony-stimulating-factor-gene-encoded vaccinia virus. Journal of cancer research and clinical oncology **122:**716-722.
78. **Kaplan, D. H., V. Shankaran, A. S. Dighe, E. Stockert, M. Aguet, L. J. Old, and R. D. Schreiber.** 1998. Demonstration of an interferon gamma-dependent tumor surveillance system in immunocompetent mice. Proceedings of the National Academy of Sciences of the United States of America **95:**7556-7561.
79. **Kato, H., S. Sato, M. Yoneyama, M. Yamamoto, S. Uematsu, K. Matsui, T. Tsujimura, K. Takeda, T. Fujita, O. Takeuchi, and S. Akira.** 2005. Cell type-specific involvement of RIG-I in antiviral response. Immunity **23:**19-28.
80. **Kelly, E., and S. J. Russell.** 2007. History of oncolytic viruses: genesis to genetic engineering. Molecular therapy : the journal of the American Society of Gene Therapy **15:**651-659.
81. **Khan, O., and N. B. La Thangue.** 2008. Drug Insight: histone deacetylase inhibitor-based therapies for cutaneous T-cell lymphomas. Nature clinical practice. Oncology **5:**714-726.
82. **Kianizad, K., L. A. Marshall, N. Grinshtein, D. Bernard, R. Margl, S. Cheng, F. Beermann, Y. Wan, and J. Bramson.** 2007. Elevated frequencies of self-reactive CD8+ T cells following immunization with a xenoantigen are due to the presence of a heteroclitic CD4+ T-cell helper epitope. Cancer research **67:**6459-6467.
83. **Kim, H. J., and S. C. Bae.** 2011. Histone deacetylase inhibitors: molecular mechanisms of action and clinical trials as anti-cancer drugs. American journal of translational research **3:**166-179.
84. **Kim, J. H., I. Skountzou, R. Compans, and J. Jacob.** 2009. Original antigenic sin responses to influenza viruses. Journal of immunology **183:**3294-3301.
85. **Koebel, C. M., W. Vermi, J. B. Swann, N. Zerafa, S. J. Rodig, L. J. Old, M. J. Smyth, and R. D. Schreiber.** 2007. Adaptive immunity maintains occult cancer in an equilibrium state. Nature **450:**903-907.
86. **Kohno, S. I., C. Luo, A. Nawa, Y. Fujimoto, D. Watanabe, F. Goshima, T. Tsurumi, and Y. Nishiyama.** 2007. Oncolytic virotherapy with an HSV amplicon vector expressing granulocyte-macrophage colony-stimulating factor using the replication-competent HSV type 1 mutant HF10 as a helper virus. Cancer gene therapy **14:**918-926.
87. **Kottke, T., R. M. Diaz, K. Kaluza, J. Pulido, F. Galivo, P. Wongthida, J. Thompson, C. Willmon, G. N. Barber, J. Chester, P. Selby, S. Strome, K. Harrington, A. Melcher, and R. G. Vile.** 2008. Use of biological therapy to enhance both virotherapy and adoptive T-cell therapy for cancer. Molecular therapy : the journal of the American Society of Gene Therapy **16:**1910-1918.
88. **Kottke, T., F. Errington, J. Pulido, F. Galivo, J. Thompson, P. Wongthida, R. M. Diaz, H. Chong, E. Ilett, J. Chester, H. Pandha, K. Harrington, P. Selby, A. Melcher, and R. Vile.** 2011.

Broad antigenic coverage induced by vaccination with virus-based cDNA libraries cures established tumors. Nature medicine **17:**854-859.

89. **Kretzschmar, E., L. Buonocore, M. J. Schnell, and J. K. Rose.** 1997. High-efficiency incorporation of functional influenza virus glycoproteins into recombinant vesicular stomatitis viruses. Journal of virology **71:**5982-5989.
90. **Lang, K. S., M. Recher, T. Junt, A. A. Navarini, N. L. Harris, S. Freigang, B. Odermatt, C. Conrad, L. M. Ittner, S. Bauer, S. A. Luther, S. Uematsu, S. Akira, H. Hengartner, and R. M. Zinkernagel.** 2005. Toll-like receptor engagement converts T-cell autoreactivity into overt autoimmune disease. Nature medicine **11:**138-145.
91. **Lapteva, N., M. Aldrich, D. Weksberg, L. Rollins, T. Goltsova, S. Y. Chen, and X. F. Huang.** 2009. Targeting the intratumoral dendritic cells by the oncolytic adenoviral vaccine expressing RANTES elicits potent antitumor immunity. Journal of immunotherapy **32:**145-156.
92. **Le Boeuf, F., J. S. Diallo, J. A. McCart, S. Thorne, T. Falls, M. Stanford, F. Kanji, R. Auer, C. W. Brown, B. D. Lichty, K. Parato, H. Atkins, D. Kirn, and J. C. Bell.** 2010. Synergistic interaction between oncolytic viruses augments tumor killing. Molecular therapy : the journal of the American Society of Gene Therapy **18:**888-895.
93. **Le, D. T., D. M. Pardoll, and E. M. Jaffee.** 2010. Cellular vaccine approaches. Cancer journal **16:**304-310.
94. **Li, J., M. O'Malley, J. Urban, P. Sampath, Z. S. Guo, P. Kalinski, S. H. Thorne, and D. L. Bartlett.** 2011. Chemokine expression from oncolytic vaccinia virus enhances vaccine therapies of cancer. Molecular therapy : the journal of the American Society of Gene Therapy **19:**650-657.
95. **Li, P., N. Wang, D. Zhou, C. S. Yee, C. H. Chang, R. R. Brutkiewicz, and J. S. Blum.** 2005. Disruption of MHC class II-restricted antigen presentation by vaccinia virus. Journal of immunology **175:**6481-6488.
96. **Lin, H. S., C. Y. Hu, H. Y. Chan, Y. Y. Liew, H. P. Huang, L. Lepescheux, E. Bastianelli, R. Baron, G. Rawadi, and P. Clement-Lacroix.** 2007. Anti-rheumatic activities of histone deacetylase (HDAC) inhibitors in vivo in collagen-induced arthritis in rodents. British journal of pharmacology **150:**862-872.
97. **Lindenmann, J., and P. A. Klein.** 1967. Viral oncolysis: increased immunogenicity of host cell antigen associated with influenza virus. The Journal of experimental medicine **126:**93-108.
98. **Lindsey, W. B., M. W. Lowdell, G. E. Marti, F. Abbasi, V. Zenger, K. M. King, and L. S. Lamb, Jr.** 2007. CD69 expression as an index of T-cell function: assay standardization, validation and use in monitoring immune recovery. Cytotherapy **9:**123-132.
99. **Liu, M., S. Guo, J. M. Hibbert, V. Jain, N. Singh, N. O. Wilson, and J. K. Stiles.** 2011. CXCL10/IP-10 in infectious diseases pathogenesis and potential therapeutic implications. Cytokine & growth factor reviews **22:**121-130.
100. **Liu, T. C., T. Hwang, B. H. Park, J. Bell, and D. H. Kirn.** 2008. The targeted oncolytic poxvirus JX-594 demonstrates antitumoral, antivascular, and anti-HBV activities in patients with hepatocellular carcinoma. Molecular therapy : the journal of the American Society of Gene Therapy **16:**1637-1642.
101. **Livingston, P. O., A. P. Albino, T. J. Chung, F. X. Real, A. N. Houghton, H. F. Oettgen, and L. J. Old.** 1985. Serological response of melanoma patients to vaccines prepared from VSV lysates of autologous and allogeneic cultured melanoma cells. Cancer **55:**713-720.
102. **Ljunggren, H. G., and K. J. Malmberg.** 2007. Prospects for the use of NK cells in immunotherapy of human cancer. Nature reviews. Immunology **7:**329-339.

103. **Lucas, J. L., P. Mirshahpanah, E. Haas-Stapleton, K. Asadullah, T. M. Zollner, and R. P. Numerof.** 2009. Induction of Foxp3+ regulatory T cells with histone deacetylase inhibitors. Cellular immunology **257:**97-104.
104. **MacTavish, H., J. S. Diallo, B. Huang, M. Stanford, F. Le Boeuf, N. De Silva, J. Cox, J. G. Simmons, T. Guimond, T. Falls, J. A. McCart, H. Atkins, C. Breitbach, D. Kirn, S. Thorne, and J. C. Bell.** 2010. Enhancement of vaccinia virus based oncolysis with histone deacetylase inhibitors. PloS one **5:**e14462.
105. **Malhotra, S., T. Kim, J. Zager, J. Bennett, M. Ebright, M. D'Angelica, and Y. Fong.** 2007. Use of an oncolytic virus secreting GM-CSF as combined oncolytic and immunotherapy for treatment of colorectal and hepatic adenocarcinomas. Surgery **141:**520-529.
106. **Martin-Fontecha, A., L. L. Thomsen, S. Brett, C. Gerard, M. Lipp, A. Lanzavecchia, and F. Sallusto.** 2004. Induced recruitment of NK cells to lymph nodes provides IFN-gamma for T(H)1 priming. Nature immunology **5:**1260-1265.
107. **Mastrangelo, M. J., H. C. Maguire, Jr., L. C. Eisenlohr, C. E. Laughlin, C. E. Monken, P. A. McCue, A. J. Kovatich, and E. C. Lattime.** 1999. Intratumoral recombinant GM-CSF-encoding virus as gene therapy in patients with cutaneous melanoma. Cancer gene therapy **6:**409-422.
108. **Melcher, A., K. Parato, C. M. Rooney, and J. C. Bell.** 2011. Thunder and lightning: immunotherapy and oncolytic viruses collide. Molecular therapy : the journal of the American Society of Gene Therapy **19:**1008-1016.
109. **Mellman, I., G. Coukos, and G. Dranoff.** 2011. Cancer immunotherapy comes of age. Nature **480:**480-489.
110. **Miller, J., S. M. Bidula, T. M. Jensen, and C. S. Reiss.** 2009. Cytokine-modified VSV is attenuated for neural pathology, but is both highly immunogenic and oncolytic. International journal of interferon, cytokine and mediator research : IJIM **1:**15-32.
111. **Naik, J. D., C. J. Twelves, P. J. Selby, R. G. Vile, and J. D. Chester.** 2011. Immune recruitment and therapeutic synergy: keys to optimizing oncolytic viral therapy? Clinical cancer research : an official journal of the American Association for Cancer Research **17:**4214-4224.
112. **Nakakubo, Y., M. Miyamoto, Y. Cho, Y. Hida, T. Oshikiri, M. Suzuoki, K. Hiraoka, T. Itoh, S. Kondo, and H. Katoh.** 2003. Clinical significance of immune cell infiltration within gallbladder cancer. British journal of cancer **89:**1736-1742.
113. **Namm, J. P., Q. Li, X. Lao, D. M. Lubman, J. He, Y. Liu, J. Zhu, S. Wei, and A. E. Chang.** 2012. B lymphocytes as effector cells in the immunotherapy of cancer. Journal of surgical oncology **105:**431-435.
114. **Nausch, N., and A. Cerwenka.** 2008. NKG2D ligands in tumor immunity. Oncogene **27:**5944-5958.
115. **Neff, J., J. Modlin, G. S. Birkhead, G. Poland, R. M. Robertson, K. Sepkowitz, C. Yancy, P. Gardner, G. C. Gray, T. Maurer, J. Siegel, F. A. Guerra, T. Berger, W. D. Flanders, R. Shope, P. Advisory Committee on Immunization, and B. Armed Forces Epidemiological.** 2008. Monitoring the safety of a smallpox vaccination program in the United States: report of the joint Smallpox Vaccine Safety Working Group of the advisory committee on immunization practices and the Armed Forces Epidemiological Board. Clinical infectious diseases : an official publication of the Infectious Diseases Society of America **46 Suppl 3:**S258-270.
116. **Nguyen, T. L., H. Abdelbary, M. Arguello, C. Breitbach, S. Leveille, J. S. Diallo, A. Yasmeen, T. A. Bismar, D. Kirn, T. Falls, V. E. Snoulten, B. C. Vanderhyden, J. Werier, H. Atkins, M. J. Vaha-Koskela, D. F. Stojdl, J. C. Bell, and J. Hiscott.** 2008. Chemical targeting of the innate antiviral response by histone deacetylase inhibitors renders refractory cancers sensitive to

viral oncolysis. Proceedings of the National Academy of Sciences of the United States of America **105:**14981-14986.

117. **Obeid, M., T. Panaretakis, N. Joza, R. Tufi, A. Tesniere, P. van Endert, L. Zitvogel, and G. Kroemer.** 2007. Calreticulin exposure is required for the immunogenicity of gamma-irradiation and UVC light-induced apoptosis. Cell death and differentiation **14:**1848-1850.
118. **Obeid, M., A. Tesniere, F. Ghiringhelli, G. M. Fimia, L. Apetoh, J. L. Perfettini, M. Castedo, G. Mignot, T. Panaretakis, N. Casares, D. Metivier, N. Larochette, P. van Endert, F. Ciccosanti, M. Piacentini, L. Zitvogel, and G. Kroemer.** 2007. Calreticulin exposure dictates the immunogenicity of cancer cell death. Nature medicine **13:**54-61.
119. **Okano, S., Y. Yonemitsu, K. Shirabe, Y. Kakeji, Y. Maehara, M. Harada, Y. Yoshikai, M. Inoue, M. Hasegawa, and K. Sueishi.** 2011. Provision of continuous maturation signaling to dendritic cells by RIG-I-stimulating cytosolic RNA synthesis of Sendai virus. Journal of immunology **186:**1828-1839.
120. **Otsuki, A., A. Patel, K. Kasai, M. Suzuki, K. Kurozumi, E. A. Chiocca, and Y. Saeki.** 2008. Histone deacetylase inhibitors augment antitumor efficacy of herpes-based oncolytic viruses. Molecular therapy : the journal of the American Society of Gene Therapy **16:**1546-1555.
121. **Parato, K. A., C. J. Breitbach, F. Le Boeuf, J. Wang, C. Storbeck, C. Ilkow, J. S. Diallo, T. Falls, J. Burns, V. Garcia, F. Kanji, L. Evgin, K. Hu, F. Paradis, S. Knowles, T. H. Hwang, B. C. Vanderhyden, R. Auer, D. H. Kirn, and J. C. Bell.** 2011. The Oncolytic Poxvirus JX-594 Selectively Replicates in and Destroys Cancer Cells Driven by Genetic Pathways Commonly Activated in Cancers. Molecular therapy : the journal of the American Society of Gene Therapy.
122. **Park, B. H., T. Hwang, T. C. Liu, D. Y. Sze, J. S. Kim, H. C. Kwon, S. Y. Oh, S. Y. Han, J. H. Yoon, S. H. Hong, A. Moon, K. Speth, C. Park, Y. J. Ahn, M. Daneshmand, B. G. Rhee, H. M. Pinedo, J. C. Bell, and D. H. Kirn.** 2008. Use of a targeted oncolytic poxvirus, JX-594, in patients with refractory primary or metastatic liver cancer: a phase I trial. The lancet oncology **9:**533-542.
123. **Park, S., Z. Jiang, E. D. Mortenson, L. Deng, O. Radkevich-Brown, X. Yang, H. Sattar, Y. Wang, N. K. Brown, M. Greene, Y. Liu, J. Tang, S. Wang, and Y. X. Fu.** 2010. The therapeutic effect of anti-HER2/neu antibody depends on both innate and adaptive immunity. Cancer cell **18:**160-170.
124. **Paterson, J. M.** 2005. Investigation of the oncolytic activity of Vesicular stomatitis virus in murine cancer models. University of Ottawa.
125. **Paulos, C. M., A. Kaiser, C. Wrzesinski, C. S. Hinrichs, L. Cassard, A. Boni, P. Muranski, L. Sanchez-Perez, D. C. Palmer, Z. Yu, P. A. Antony, L. Gattinoni, S. A. Rosenberg, and N. P. Restifo.** 2007. Toll-like receptors in tumor immunotherapy. Clinical cancer research : an official journal of the American Association for Cancer Research **13:**5280-5289.
126. **Penafuerte, C., and J. Galipeau.** 2008. TGF beta secreted by B16 melanoma antagonizes cancer gene immunotherapy bystander effect. Cancer immunology, immunotherapy : CII **57:**1197-1206.
127. **Pitsios, C., A. Dimitrakopoulou, K. Tsalimalma, T. Kordossis, and H. Choremi-Papadopoulou.** 2008. Expression of CD69 on T-cell subsets in HIV-1 disease. Scandinavian journal of clinical and laboratory investigation **68:**233-241.
128. **Poschke, I., D. Mougiakakos, and R. Kiessling.** 2011. Camouflage and sabotage: tumor escape from the immune system. Cancer immunology, immunotherapy : CII **60:**1161-1171.
129. **Power, A. T., J. Wang, T. J. Falls, J. M. Paterson, K. A. Parato, B. D. Lichty, D. F. Stojdl, P. A. Forsyth, H. Atkins, and J. C. Bell.** 2007. Carrier cell-based delivery of an oncolytic virus

circumvents antiviral immunity. Molecular therapy : the journal of the American Society of Gene Therapy **15:**123-130.

130. **Prestwich, R. J., F. Errington, E. J. Ilett, R. S. Morgan, K. J. Scott, T. Kottke, J. Thompson, E. E. Morrison, K. J. Harrington, H. S. Pandha, P. J. Selby, R. G. Vile, and A. A. Melcher.** 2008. Tumor infection by oncolytic reovirus primes adaptive antitumor immunity. Clinical cancer research : an official journal of the American Association for Cancer Research **14:**7358-7366.
131. **Prestwich, R. J., F. Errington, L. P. Steele, E. J. Ilett, R. S. Morgan, K. J. Harrington, H. S. Pandha, P. J. Selby, R. G. Vile, and A. A. Melcher.** 2009. Reciprocal human dendritic cell-natural killer cell interactions induce antitumor activity following tumor cell infection by oncolytic reovirus. Journal of immunology **183:**4312-4321.
132. **Qiao, S. W., K. Kobayashi, F. E. Johansen, L. M. Sollid, J. T. Andersen, E. Milford, D. C. Roopenian, W. I. Lencer, and R. S. Blumberg.** 2008. Dependence of antibody-mediated presentation of antigen on FcRn. Proceedings of the National Academy of Sciences of the United States of America **105:**9337-9342.
133. **Ramsburg, E., J. Publicover, L. Buonocore, A. Poholek, M. Robek, A. Palin, and J. K. Rose.** 2005. A vesicular stomatitis virus recombinant expressing granulocyte-macrophage colony-stimulating factor induces enhanced T-cell responses and is highly attenuated for replication in animals. Journal of virology **79:**15043-15053.
134. **Randall, R. E., and S. Goodbourn.** 2008. Interferons and viruses: an interplay between induction, signalling, antiviral responses and virus countermeasures. The Journal of general virology **89:**1-47.
135. **Rintoul, J. L., C. G. Lemay, L. H. Tai, M. M. Stanford, T. J. Falls, C. T. de Souza, B. W. Bridle, M. Daneshmand, P. S. Ohashi, Y. Wan, B. D. Lichty, A. A. Mercer, R. C. Auer, H. L. Atkins, and J. C. Bell.** 2012. ORFV: A Novel Oncolytic and Immune Stimulating Parapoxvirus Therapeutic. Molecular therapy : the journal of the American Society of Gene Therapy.
136. **Riond, J., S. Rodriguez, M. L. Nicolau, T. al Saati, and J. E. Gairin.** 2009. In vivo major histocompatibility complex class I (MHCI) expression on MHCIlow tumor cells is regulated by gammadelta T and NK cells during the early steps of tumor growth. Cancer immunity **9:**10.
137. **Roberts, A., L. Buonocore, R. Price, J. Forman, and J. K. Rose.** 1999. Attenuated vesicular stomatitis viruses as vaccine vectors. Journal of virology **73:**3723-3732.
138. **Rosenberg, S. A., N. P. Restifo, J. C. Yang, R. A. Morgan, and M. E. Dudley.** 2008. Adoptive cell transfer: a clinical path to effective cancer immunotherapy. Nature reviews. Cancer **8:**299-308.
139. **Santini, S. M., C. Lapenta, M. Logozzi, S. Parlato, M. Spada, T. Di Pucchio, and F. Belardelli.** 2000. Type I interferon as a powerful adjuvant for monocyte-derived dendritic cell development and activity in vitro and in Hu-PBL-SCID mice. The Journal of experimental medicine **191:**1777-1788.
140. **Sato, E., S. H. Olson, J. Ahn, B. Bundy, H. Nishikawa, F. Qian, A. A. Jungbluth, D. Frosina, S. Gnjatic, C. Ambrosone, J. Kepner, T. Odunsi, G. Ritter, S. Lele, Y. T. Chen, H. Ohtani, L. J. Old, and K. Odunsi.** 2005. Intraepithelial CD8+ tumor-infiltrating lymphocytes and a high CD8+/regulatory T cell ratio are associated with favorable prognosis in ovarian cancer. Proceedings of the National Academy of Sciences of the United States of America **102:**18538-18543.
141. **Scagliarini, A., L. Gallina, F. Dal Pozzo, M. Battilani, S. Ciulli, and S. Prosperi.** 2004. Heparin binding activity of orf virus F1L protein. Virus research **105:**107-112.
142. **Schierer, S., A. Hesse, I. Knippertz, E. Kaempgen, A. S. Baur, G. Schuler, A. Steinkasserer, and D. M. Nettelbeck.** 2012. Human dendritic cells efficiently phagocytose adenoviral

oncolysate but require additional stimulation to mature. International journal of cancer. Journal international du cancer **130:**1682-1694.

143. **Schirrmacher, V.** 2005. Clinical trials of antitumor vaccination with an autologous tumor cell vaccine modified by virus infection: improvement of patient survival based on improved antitumor immune memory. Cancer immunology, immunotherapy : CII **54:**587-598.
144. **Seet, B. T., J. B. Johnston, C. R. Brunetti, J. W. Barrett, H. Everett, C. Cameron, J. Sypula, S. H. Nazarian, A. Lucas, and G. McFadden.** 2003. Poxviruses and immune evasion. Annual review of immunology **21:**377-423.
145. **Shanafelt, A. B., K. E. Johnson, and R. A. Kastelein.** 1991. Identification of critical amino acid residues in human and mouse granulocyte-macrophage colony-stimulating factor and their involvement in species specificity. The Journal of biological chemistry **266:**13804-13810.
146. **Sharma, P., Y. Shen, S. Wen, S. Yamada, A. A. Jungbluth, S. Gnjatic, D. F. Bajorin, V. E. Reuter, H. Herr, L. J. Old, and E. Sato.** 2007. CD8 tumor-infiltrating lymphocytes are predictive of survival in muscle-invasive urothelial carcinoma. Proceedings of the National Academy of Sciences of the United States of America **104:**3967-3972.
147. **Shin, E. J., G. B. Wanna, B. Choi, D. Aguila, 3rd, O. Ebert, E. M. Genden, and S. L. Woo.** 2007. Interleukin-12 expression enhances vesicular stomatitis virus oncolytic therapy in murine squamous cell carcinoma. The Laryngoscope **117:**210-214.
148. **Sica, A., and V. Bronte.** 2007. Altered macrophage differentiation and immune dysfunction in tumor development. The Journal of clinical investigation **117:**1155-1166.
149. **Sivendran, S., B. Glodny, M. Pan, M. Merad, and Y. Saenger.** 2010. Melanoma immunotherapy. The Mount Sinai journal of medicine, New York **77:**620-642.
150. **Smyth, M. J., Y. Hayakawa, K. Takeda, and H. Yagita.** 2002. New aspects of natural-killer-cell surveillance and therapy of cancer. Nature reviews. Cancer **2:**850-861.
151. **Sobol, P. T., J. E. Boudreau, K. Stephenson, Y. Wan, B. D. Lichty, and K. L. Mossman.** 2011. Adaptive antiviral immunity is a determinant of the therapeutic success of oncolytic virotherapy. Molecular therapy : the journal of the American Society of Gene Therapy **19:**335-344.
152. **Steer, H. J., R. A. Lake, A. K. Nowak, and B. W. Robinson.** 2010. Harnessing the immune response to treat cancer. Oncogene **29:**6301-6313.
153. **Stojdl, D. F., B. D. Lichty, B. R. tenOever, J. M. Paterson, A. T. Power, S. Knowles, R. Marius, J. Reynard, L. Poliquin, H. Atkins, E. G. Brown, R. K. Durbin, J. E. Durbin, J. Hiscott, and J. C. Bell.** 2003. VSV strains with defects in their ability to shutdown innate immunity are potent systemic anti-cancer agents. Cancer cell **4:**263-275.
154. **Sun, J. C., and L. L. Lanier.** 2011. NK cell development, homeostasis and function: parallels with CD8 T cells. Nature reviews. Immunology **11:**645-657.
155. **Teng, M. W., J. B. Swann, C. M. Koebel, R. D. Schreiber, and M. J. Smyth.** 2008. Immune-mediated dormancy: an equilibrium with cancer. Journal of leukocyte biology **84:**988-993.
156. **Thorne, S. H., T. H. Hwang, W. E. O'Gorman, D. L. Bartlett, S. Sei, F. Kanji, C. Brown, J. Werier, J. H. Cho, D. E. Lee, Y. Wang, J. Bell, and D. H. Kirn.** 2007. Rational strain selection and engineering creates a broad-spectrum, systemically effective oncolytic poxvirus, JX-963. The Journal of clinical investigation **117:**3350-3358.
157. **Tietze, J. K., D. E. Wilkins, G. D. Sckisel, M. N. Bouchlaka, K. L. Alderson, J. M. Weiss, E. Ames, K. W. Bruhn, N. Craft, R. H. Wiltrout, D. L. Longo, L. L. Lanier, B. R. Blazar, D. Redelman, and W. J. Murphy.** 2012. Delineation of antigen-specific and antigen-nonspecific CD8+ memory T-cell responses after cytokine-based cancer immunotherapy. Blood **119:**3073-3083.

158. **Tirapu, I., A. Lewis, M. Kreutz, H. McLinden, and S. S. Diebold.** 2008. Freeze-and-thaw-disrupted tumour cells impair the responsiveness of DC to TLR stimulation. European journal of immunology **38:**2740-2750.
159. **Trinchieri, G.** 2010. Type I interferon: friend or foe? The Journal of experimental medicine **207:**2053-2063.
160. **Vesely, M. D., M. H. Kershaw, R. D. Schreiber, and M. J. Smyth.** 2011. Natural innate and adaptive immunity to cancer. Annual review of immunology **29:**235-271.
161. **Villagra, A., E. M. Sotomayor, and E. Seto.** 2010. Histone deacetylases and the immunological network: implications in cancer and inflammation. Oncogene **29:**157-173.
162. **Vivier, E., D. H. Raulet, A. Moretta, M. A. Caligiuri, L. Zitvogel, L. L. Lanier, W. M. Yokoyama, and S. Ugolini.** 2011. Innate or adaptive immunity? The example of natural killer cells. Science **331:**44-49.
163. **Vivier, E., E. Tomasello, M. Baratin, T. Walzer, and S. Ugolini.** 2008. Functions of natural killer cells. Nature immunology **9:**503-510.
164. **Vogelstein, B., and K. W. Kinzler.** 2004. Cancer genes and the pathways they control. Nature medicine **10:**789-799.
165. **Wall, E. M., K. Milne, M. L. Martin, P. H. Watson, P. Theiss, and B. H. Nelson.** 2007. Spontaneous mammary tumors differ widely in their inherent sensitivity to adoptively transferred T cells. Cancer research **67:**6442-6450.
166. **Wallack, M. K., Z. Steplewski, H. Koprowski, E. Rosato, J. George, B. Hulihan, and J. Johnson.** 1977. A new approach in specific, active immunotherapy. Cancer **39:**560-564.
167. **Weber, J.** 2011. Immunotherapy for melanoma. Current opinion in oncology **23:**163-169.
168. **Weber, O., A. Siegling, A. Friebe, A. Limmer, T. Schlapp, P. Knolle, A. Mercer, H. Schaller, and H. D. Volk.** 2003. Inactivated parapoxvirus ovis (Orf virus) has antiviral activity against hepatitis B virus and herpes simplex virus. The Journal of general virology **84:**1843-1852.
169. **Weiner, L. M., R. Surana, and S. Wang.** 2010. Monoclonal antibodies: versatile platforms for cancer immunotherapy. Nature reviews. Immunology **10:**317-327.
170. **Wendel, M., I. E. Galani, E. Suri-Payer, and A. Cerwenka.** 2008. Natural killer cell accumulation in tumors is dependent on IFN-gamma and CXCR3 ligands. Cancer research **68:**8437-8445.
171. **Whitmire, J. K.** 2011. Induction and function of virus-specific CD4+ T cell responses. Virology **411:**216-228.
172. **Woller, N., S. Knocke, B. Mundt, E. Gurlevik, N. Struver, A. Kloos, B. Boozari, P. Schache, M. P. Manns, N. P. Malek, T. Sparwasser, L. Zender, T. C. Wirth, S. Kubicka, and F. Kuhnel.** 2011. Virus-induced tumor inflammation facilitates effective DC cancer immunotherapy in a Treg-dependent manner in mice. The Journal of clinical investigation **121:**2570-2582.
173. **Wongthida, P., R. M. Diaz, F. Galivo, T. Kottke, J. Thompson, J. Pulido, K. Pavelko, L. Pease, A. Melcher, and R. Vile.** 2010. Type III IFN interleukin-28 mediates the antitumor efficacy of oncolytic virus VSV in immune-competent mouse models of cancer. Cancer research **70:**4539-4549.
174. **Wongthida, P., R. M. Diaz, C. Pulido, D. Rommelfanger, F. Galivo, K. Kaluza, T. Kottke, J. Thompson, A. Melcher, and R. Vile.** 2011. Activating systemic T-cell immunity against self tumor antigens to support oncolytic virotherapy with vesicular stomatitis virus. Human gene therapy **22:**1343-1353.
175. **Yang, Y., C. T. Huang, X. Huang, and D. M. Pardoll.** 2004. Persistent Toll-like receptor signals are required for reversal of regulatory T cell-mediated CD8 tolerance. Nature immunology **5:**508-515.

176. **Yates, N. L., and M. A. Alexander-Miller.** 2007. Vaccinia virus infection of mature dendritic cells results in activation of virus-specific naive CD8+ T cells: a potential mechanism for direct presentation. Virology **359:**349-361.
177. **Yu, P., Y. Lee, W. Liu, R. K. Chin, J. Wang, Y. Wang, A. Schietinger, M. Philip, H. Schreiber, and Y. X. Fu.** 2004. Priming of naive T cells inside tumors leads to eradication of established tumors. Nature immunology **5:**141-149.
178. **Zhang, H., Q. Wang, K. T. Montone, J. E. Peavey, J. A. Drebin, M. I. Greene, and R. Murali.** 1999. Shared antigenic epitopes and pathobiological functions of anti-p185(her2/neu) monoclonal antibodies. Experimental and molecular pathology **67:**15-25.
179. **Zhang, Q. J., R. P. Seipp, S. S. Chen, T. Z. Vitalis, X. L. Li, K. B. Choi, A. Jeffries, and W. A. Jefferies.** 2007. TAP expression reduces IL-10 expressing tumor infiltrating lymphocytes and restores immunosurveillance against melanoma. International journal of cancer. Journal international du cancer **120:**1935-1941.
180. **Zitvogel, L., A. Tesniere, and G. Kroemer.** 2006. Cancer despite immunosurveillance: immunoselection and immunosubversion. Nature reviews. Immunology **6:**715-727.
181. **Zou, W.** 2006. Regulatory T cells, tumour immunity and immunotherapy. Nature reviews. Immunology **6:**295-307.

Contributions of Collaborators

The following colleagues are recognized as contributing to the work detailed in this thesis. Dr. Kelley Parato undertook the splenocyte transfer experiment from figure 3.1e in addition to the experiment comparing the various VSV recombinants in figure 3.3d. The IHC in figure 3.1f and 3.3a are from experiments performed by Jennifer Paterson. Figure 3.5c is a weighted average of many experiments, one of which was performed by Dr. Kelley Parato, two were performed by Lisa MacKenzie, and one was performed by Agnieszka Kus. Julia Rintoul provided the ORFV for experiments in figures 3.25 and 3.27. Dr. Jean-Simon Diallo was a close collaborator on the entire project involving HDIs, in addition to the group at McMaster University lead by Dr. Brian Lichty and Dr. Yonghong Wan.

Appendices

Appendix I – Optimizing the subcutaneous B16-F10 therapeutic VSVgm-ICV

(**a, c**) B16-F10 tumour-bearing mice were treated with the VSVgm-ICV IP or relevant controls according to the indicated timeline. (**b, d**) Growth of the subcutaneous tumour overtime was monitored. (**a-b**) The number of mice per group was as follows, PBS n=2, irrB16 n=3, VSVgm n=5, VSVgm-ICV n=6. (**c-d**) There were 5 mice per group. *P* Values; **P*<0.05 PBS compared to VSVgm-ICV, #*P*<0.05 PBS compared to VACVgm-ICV→VSVgm-ICV. Data points are all mean + SEM.

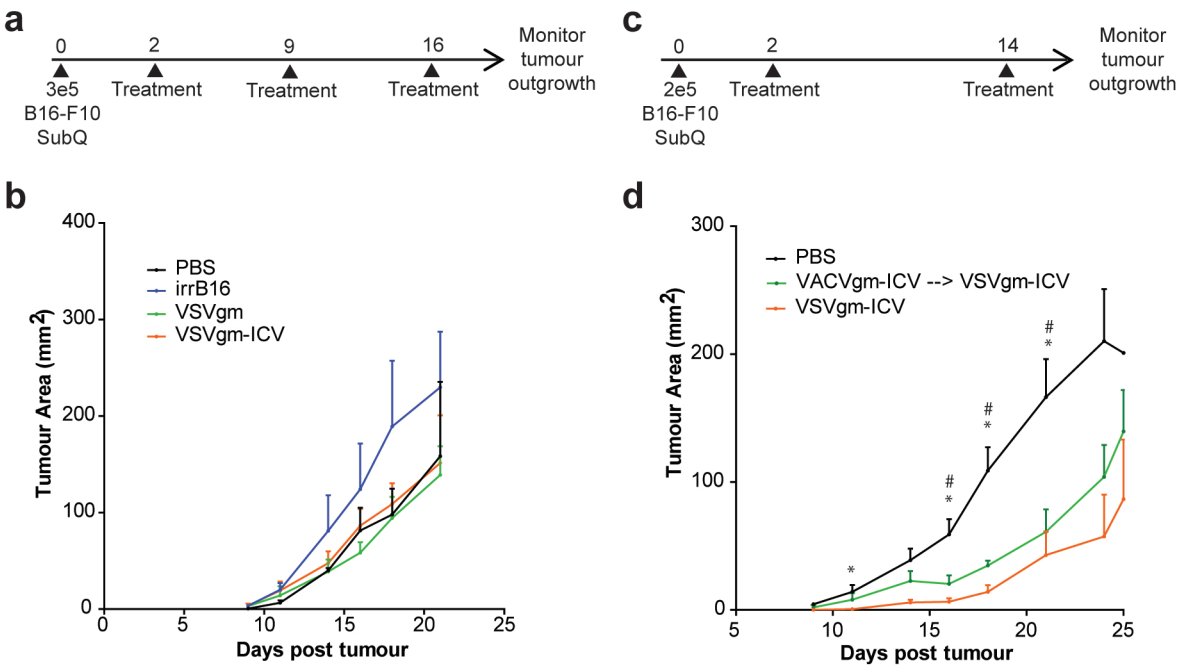
a
0
2
9
16
Monitor tumour outgrowth
3e5 B16-F10 SubQ
Treatment
Treatment
Treatment
c
0
2
14
Monitor tumour outgrowth
2e5 B16-F10 SubQ
Treatment
Treatment
b
Tumour Area (mm2)
Days post tumour
PBS
irrB16
VSVgm
VSVgm-ICV
d
Tumour Area (mm2)
Days post tumour
PBS
VACVgm-ICV --> VSVgm-ICV
VSVgm-ICV

Appendix II – Optimizing the VACV-ICV in therapeutic models of B16-F10

(**a**) B16-F10 tumour-bearing mice were treated with the VACVgm-ICV IP or relevant controls according to the indicated timeline. (**b**) The PBS and irrB16 groups are the same as in Appendix Ia/b. VACVgm had 5 mice and VACVgm-ICV had 6. Tumour area over time is plotted with data points as mean + SEM. (**c**) C57BL/6 mice were injected with 1x105 B16-F10 cells IV on day 0 and then treated according to the timeline. On day 14 animals were euthanized and lung tumours enumerated. (**d**) Number of lung tumours per animal with mean. ICVs were made according to the legend below the graph. One variable was altered from one condition to the next and is highlighted in red. (**e**) C57BL/6 mice were treated according to the timeline provided. (**f**) Lung tumours were enumerated at day 14.

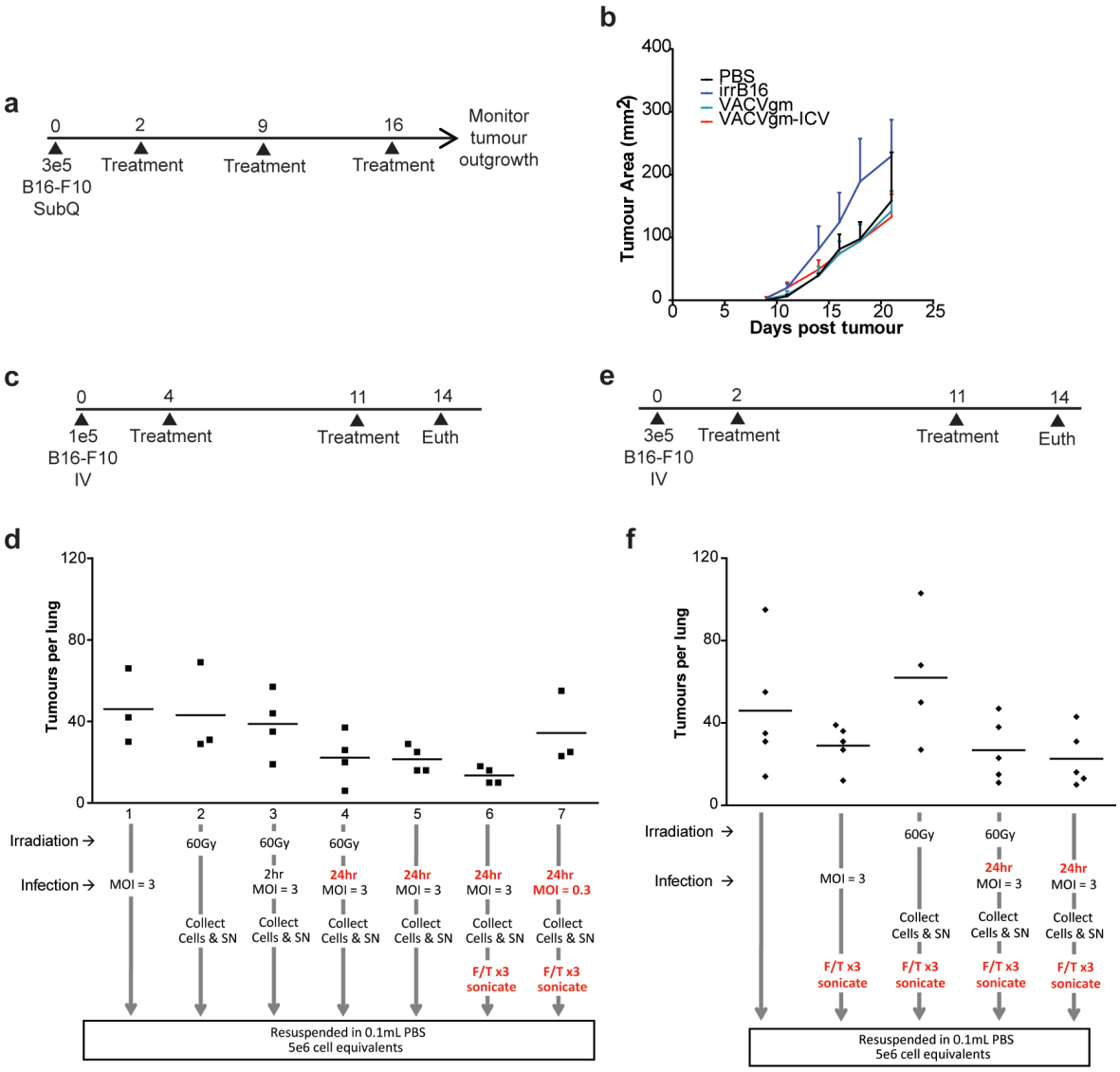
a
0
2
9
16
3e5
B16-F10
SubQ
Treatment
Treatment
Treatment
Monitor
tumour
outgrowth
b
PBS
irrB16
VACVgm
VACVgm-ICV
Tumour Area (mm2)
Days post tumour
c
0
4
11
14
1e5
B16-F10
IV
Treatment
Treatment
Euth
e
0
2
11
14
3e5
B16-F10
IV
Treatment
Treatment
Euth
d
Tumours per lung
Irradiation →
Infection →
MOI = 3
60Gy
Collect
Cells & SN
60Gy
2hr
MOI = 3
60Gy
24hr
MOI = 3
24hr
MOI = 3
24hr
MOI = 3
24hr
MOI = 0.3
F/T x3
sonicate
Resuspended in 0.1mL PBS
5e6 cell equivalents
f
Tumours per lung
Irradiation →
Infection →
MOI = 3
60Gy
24hr
MOI = 3
F/T x3
sonicate
Collect
Cells & SN
Resuspended in 0.1mL PBS
5e6 cell equivalents

Appendix III – The VACV-ICV over-rides the VSV-ICV in the prophylactic subcutaneous B16-F10 model

C57BL/6 mice were immunized with the $5x10^6$ VSV-ICV + $5x10^6$ irrB16 (n=6), $5x10^6$ VACV-ICV + $5x10^6$ irrB16 (n=6), or $5x10^6$ VSV-ICV + $5x10^6$ VACV-ICV (n=7). Both components of the ICVs were mixed right before injection. Mice were immunized on days 0 and 10and then challenged with $3x10^5$ B16-F10 cells subcutaneously on day 20. Mice were deemed positive for a tumour if a nodule equal or larger than $4mm^2$ could be palpated.

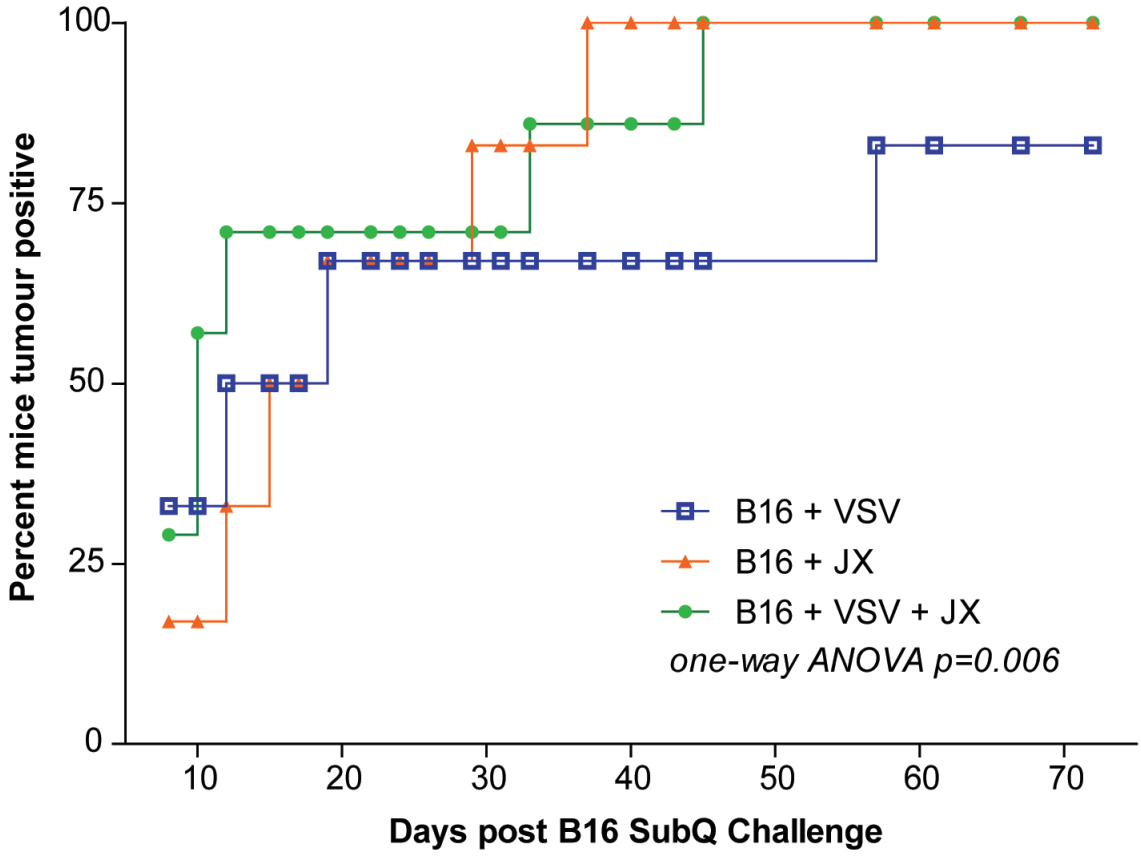
100
75
50
25
0
Percent mice tumour positive
10
20
30
40
50
60
70
Days post B16 SubQ Challenge
B16 + VSV
B16 + JX
B16 + VSV + JX
one-way ANOVA p=0.006

Appendix IV – Effect of MS-275 on lymphocyte recruitment

One group of mice was tumour and vaccination naïve and the other was given B16-F10 intracranial tumours followed by Ad-hDCT on day 1 and VSV-hDCT on day 15. All mice got either vehicle or MS-275 IP on days 15 to 19 and were euthanized on day 22. The same area of each brain was dissected, dissagregated, and examined by flow cytometry for the infiltration of (**a**) CD3+ cells or (**b**) NK1.1+ cells. (**a,b**) Percent of all cells that are positive for indicated marker, grey bar denotes mean. No statistical significant achieved.

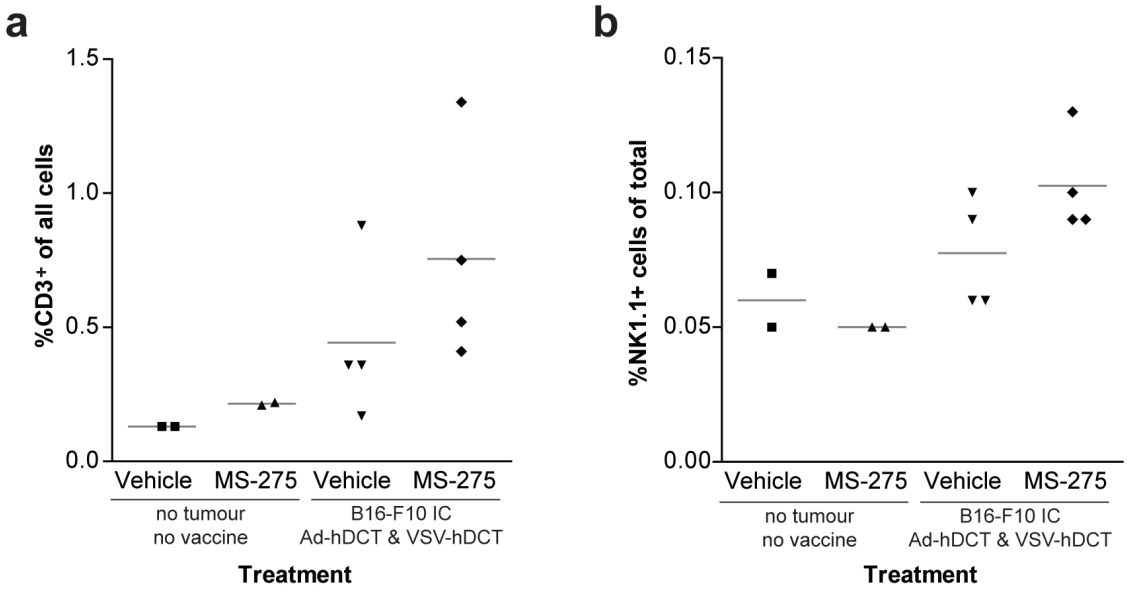
a
%CD3+ of all cells
1.5
1.0
0.5
0.0
Vehicle
MS-275
Vehicle
MS-275
no tumour
no vaccine
B16-F10 IC
Ad-hDCT & VSV-hDCT
Treatment
b
%NK1.1+ cells of total
0.15
0.10
0.05
0.00
Vehicle
MS-275
Vehicle
MS-275
no tumour
no vaccine
B16-F10 IC
Ad-hDCT & VSV-hDCT
Treatment

Appendix V - Combination of an oncolytic vaccine with an immunosuppressive HDACi leads to enhanced tumor destruction and mitigated autoimmunity

Contribution of author: CG Lemay was an ongoing collaborator on this project, contributing to discussions and experiment design. In addition, CG Lemay performed the mouse experiment in Figure 2d, however JS Diallo performed the neutralizing antibody assay. CG Lemay performed the experiment and analysis in supplemental Figure 1.

Submitted: Nature Medicine, May 2012

HDAC inhibition can suppress primary immune responses and enhance secondary immune responses during tumour immunotherapy while abrogating autoimmunity.

Byram W. Bridle[1], Lan Chen[2], Chantal G. Lemay[3], Jean-Simon Diallo[3], Jonathan Pol[1], Andrew Nguyen[1], Alfredo Capretta[4], Jonathan L. Bramson[1], John C. Bell[3], Brian D. Lichty[1,5] and Yonghong Wan[1,5,6]

[1]McMaster Immunology Research Centre, Department of Pathology and Molecular Medicine, McMaster University, Hamilton, ON, Canada, L8N 3Z5
[2]State Key Laboratory of Brain and Cognitive Sciences, Institute of Biophysics, Chinese Academy of Sciences, Beijing, China
[3]Ottawa Health Research Institute, University of Ottawa, Ottawa, ON, K1Y 4E9
[4]Department of Chemistry and Chemical Biology, McMaster University, Hamilton, ON, Canada, L8N 3Z5
[5]last two authors contributed equally

Short title: MS-275 separates anti-tumor immunity and autoimmunity

Keywords: **histone deacetylase, MS-275, oncolytic virus, vaccine, cancer therapy**

Abstract

Histone deacetylase inhibitors (HDACi) can modulate innate antiviral responses and render tumors more susceptible to oncolytic viruses; however, their effects on adaptive immunity in this context are largely unknown. Our present study reveals an unexpected property of the HDACi MS-275 that enhances viral vector-induced lymphopenia leading to selective depletion of bystander lymphocytes and Treg while allowing expansion of antigen-specific secondary responses. The net effect of vaccine plus drug co-administration during the boosting phase is a differential suppression of the primary response and enhancement of the desired boosted response thereby focusing the immune response on the tumor. Furthermore, improvement of T cell functionality was evident suggesting that MS-275 can orchestrate a complex array of effects that synergize immunotherapy and viral oncolysis. Surprisingly, while MS-275 dramatically enhanced efficacy, it suppressed autoimmune pathology, profoundly improving the therapeutic index.

Introduction

Oncolytic viruses are promising therapeutics applicable to a variety of malignancies. One of the mechanisms defining the tumor-selectivity of oncolytic viruses is the fact that cancer cells frequently acquire defects in cellular innate antiviral responses, such as the type-I interferon (IFN) pathway [1-3]. As a result, it has been shown that IFN sensitive viruses such as vesicular stomatitis virus (VSV) are highly effective in targeting and killing tumor cells while sparing normal tissues [4, 5]. However, the extent of IFN non-responsiveness is variable in cancer cell lines and patient tumors, which represents an obstacle to effective OV therapy[6, 7]. Histone deacetylase inhibitors (HDACi) are small molecules that are currently being evaluated clinically for the treatment of cancer but are also known to prevent the transcriptional activation of antiviral genes after IFN stimulation or virus infection[8-10]. We have recently demonstrated that several HDACi can markedly enhance the susceptibility of tumor cells to VSV killing, providing a pharmacological strategy to potentially increase the spectrum of malignancies amenable to oncolytic virus therapy[11].

However, HDACi are also under investigation as anti-inflammatory and immunosuppressive drugs. Evidence from different animal models indicates that HDACi therapy ameliorates inflammatory/autoimmune diseases, enhances allograft survival and induces immune tolerance in GVHD [12-15]. Thus, although HDACi may enhance viral oncolysis, it is unclear whether such a benefit would be at the expense of the optimal development of anti-tumor immunity that may be required to synergize and/or sustain virus-induced tumor regression.

We have recently demonstrated that oncolytic viruses can be engineered to express tumor-associated antigens and used as oncolytic vaccines in tumor-bearing hosts [16]. In particular, when combined with a priming vaccine that expresses the same tumor antigen, oncolytic vaccines can lead to both tumor debulking by the virus and a large boost of tumor-specific cytotoxic T lymphocytes (CTL) in primed animals. Furthermore, the replicating oncolytic vector is amplified in the tumor leading to a larger boost in tumor-bearing animals leading to significantly enhanced numbers of antigen-specific tumor-infiltrating lymphocytes (TILs). We reasoned that the combination of HDACi and oncolytic vaccines would allow

simultaneous investigation of the impact of HDACi on viral oncolysis and adaptive immunity against the virus and the tumor.

In the current study, we confirmed that MS-275, an inhibitor of class I HDACs, led to modestly prolonged viral replication in the tumor but dramatically enhanced tumor-free survival. Surprisingly this drug was able to impair primary immune responses directed at the oncolytic vaccine vector while allowing for potent secondary immune responses focused on the tumor antigen transgene. In fact co-administration of MS-275 with an oncolytic VSV booster vaccine led to a severe but selective lymphopenia leaving the boosted anti-tumor lymphocytes intact while depleting both conventional lymphocytes and regulatory T cells (Treg). More strikingly, this combination therapy not only led to enhanced therapeutic efficacy but also suppressed vaccine-associated autoimmune pathology, yielding a profound improvement of the therapeutic index. Our data indicate that immunomodulation by HDACi occurs at multiple levels and their therapeutic benefit depends on the context and timing.

Results

MS-275 extends oncolytic VSV activity in tumors

We have previously demonstrated that MS-275 can facilitate VSV replication in different types of tumors by modifying IFN-responsiveness both *in vitro* and *in vivo*[11]. To test for such an activity in our current tumor model, we treated mice bearing 5-day-old intracranial B16-F10 melanomas with intravenous (i.v.) injection of an oncolytic VSV expressing the Firefly luciferase (VSV-Luc). MS-275 or vehicle was given intraperitoneally (i.p.) on a daily basis for 5 days as described previously[11]. This confirmed that MS-275 co-administration extended VSV-luc activity in these tumors (Fig S1).

MS-275 dramatically improves the therapeutic outcome in combination with an oncolytic booster vaccine

We have recently demonstrated that by engineering VSV to express human dopachrome tautomerase (VSV-hDCT) we could turn it into a very potent booster vaccine while retaining its oncolytic properties *in vivo*[16]. Combining a recombinant adenoviral vector (Ad) expressing hDCT (Ad-hDCT) and VSV-hDCT in a prime-boost manner dramatically enhanced therapeutic efficacy. The potency of this combination strategy prompted us to investigate whether co-administration of MS-275 with the oncolytic vaccine could further enhance this therapeutic strategy. Five days after intracranial inoculation of B16-F10 cells, mice were treated sequentially with Ad-hDCT and VSV-hDCT at a 14-day interval as described previously[16]. MS-275 was administered 2 h before the VSV-hDCT oncolytic vaccine and then given once daily for 5 consecutive days, which coincided with the persistence of VSV and the peak of the boosted CTL response [16, 17]. Vaccination with the Ad-hDCT vaccine alone prolonged animal survival to a median of 25 days and this therapeutic effect was further enhanced by VSV-hDCT boosting (Fig 1). Despite the improvement of the survival rate, however, most animals treated with the prime-boost regimen ultimately succumbed to tumor progression. MS-275 alone had no therapeutic

effect in this cancer model. Remarkably, concomitant treatment with MS-275 at the time of VSV-hDCT delivery dramatically enhanced the efficacy of the combination treatment and cured 64% (n=11) of the mice.

MS-275 preserves secondary tumor-specific CTL and antibody responses but attenuates primary adaptive immunity against VSV

As MS-275 co-administration provided a rather mild extension of VSV-luc activity in these tumors we hypothesized that the drug might be serving to enhance the vaccine effects of our treatments which are key to efficacy in this model[16]. We first examined the secondary immune response boosted by VSV by quantifying DCT-specific, IFN-γ-producing $CD8^+$ T cells in the circulation at days 5 and 12 post-VSV-hDCT booster vaccination. These time points were chosen based on our previous observation where the secondary T cell response induced by VSV-hDCT reached its peak at day 5 and declined after 12 days [16]. Surprisingly, the magnitude of the DCT-specific $CD8^+$ T cell response boosted by VSV vaccine was not further increased in the presence of MS-275 (Fig. 2a). Similarly, DCT-specific IgG antibodies in plasma were significantly boosted regardless of MS-275 treatment (Fig. 2b). Thus MS-275 co-administration did not increase the secondary immune response to the tumour antigen transgene boosted by our oncolytic vaccine.

However, in the course of our immune analysis we discovered that primary responses against the oncolytic vaccine vector were largely disabled by co-administration of drug. To evaluate this, we first measured $CD8^+$ T cell responses against an immunodominant epitope from the N-protein of VSV at day 7 post-VSV-hDCT inoculation. Consistent with our previous report, pre-immunization with Ad-hDCT allowed a dramatic boost of DCT-specific secondary T cell response while decreasing the primary response against VSV (Fig. 2c). VSV-reactive $CD8^+$ T cells were further reduced in the presence of MS-275 confirming that MS-275 differentially influences expansion of memory and naïve $CD8^+$ T cells. Importantly neutralizing antibodies against VSV were strongly inhibited by MS-275 co-administration where induction of antibodies against the virus was delayed until after drug administration was halted (Fig 2d).

Altogether these results highlight a very curious property of this drug as it is able to impede the generation of primary immune responses while leaving secondary responses entirely intact. This differential immunosuppression appears to allow for an immune response following oncolytic vaccine administration largely focused on the tumour antigen transgene.

To further assess the impact of MS-275 on primary immune responses we co-administered the drug with our Ad-hDCT vector to measure any immunosuppressive properties apparent during a standard vaccination. When co-administered with our Ad-based vaccine vector MS-275 significantly reduced the T cell response against DCT (Fig 3a) leading to loss of therapeutic effect in the B16F10 melanoma model (Fig 3b). Thus the drug displays clear immunosuppressive properties that impair the induction of a primary immune response to vaccination.

MS-275 enhances and sustains lymphopenia induced by VSV booster vaccination

It is well known that intravenous administration of VSV induces a transient lymphopenia [18, 19]. We have also noted that intravenous injection with VSV induced a rapid and severe lymphopenia with cell counts hitting a minimum at 24 h (Fig. 4a) as reported by others [18]. The lymphocyte counts recovered in 3-5 days and often led to a transient increase over the normal level. Surprisingly, although MS-275 alone had a moderate effect on lymphocyte numbers, it dramatically delayed the reconstitution when concomitantly administered with VSV (Fig. 4a). Using an inactive analogue of MS-275[20] (Fig. S2) we confirmed that the exacerbation of VSV-induced lymphopenia required HDAC inhibition. As VSV-induced lymphopenia has been shown to depend on type I IFN signalling in lymphocytes [18, 21], and we have shown that this HDACi skews this signalling pathway we hypothesized that polyIC, a classic inducer of type I IFN, would also generate this effect when combined with MS-275 and indeed polyIC + MS-275 yielded an identical, extended lymphopenia (Fig S3).

A closer examination indicated that both CD4 and CD8 T cell subsets and the B cell population were profoundly affected by addition of MS-275 (Fig. 4b-d). T cells largely recovered in 2 weeks, but B cell recovery was much slower suggesting that B cells are more sensitive to the combination therapy. This treatment significantly reduced CD4+CD8+ double positive T cells in the thymus (Fig S4a). Further analysis in the bone marrow indicated that pre-B and immature B cells were almost completely eliminated by the combination treatment as early as day 3 (Fig S4b). These results suggest that MS-275 and VSV may have a synergistic effect on the survival of precursors leading to the delayed reconstitution of the peripheral T cells and B cells and a significantly extended lymphopenia in response to IFN.

MS-275 improves CTL quality

We next sought to determine whether lymphopenia might actually provide a favourable environment (e.g., more cytokines) which would be predicted to promote the functionality of boosted CTL. Indeed, compared to Ad:VSV prime:boost alone, the addition of MS-275 significantly increased the frequency of $CD8^+$ T cells that co-expressed TNF-α and IFN-γ (Fig. 5a) and the increased intensity of their production (Fig. 5b and c), indicating a heightened response to stimulatory peptide. To further determine the impact of MS-275 on CTL functionality, we tested the avidity of $CD8^+$ T cells from mice boosted with or without MS-275. Figure 5d shows that approximately six-fold more $CD8^+$ T cells could respond to the lowest concentration of the immunodominant peptide from DCT when mice had received MS-275 treatment, confirming that CTL developed in this environment displayed an enhanced functionality.

MS-275 reduces Tregs, especially those that express a high level of Foxp3

The lymphopenia, especially the reduction of total $CD4^+$ T cells, induced by MS-275 plus virus led us to assess its direct impact on $CD4^+Foxp3^+$ Tregs. The number of Tregs was significantly decreased during booster immunization and it took 2 weeks for them to recover

(Fig S5a). Notably, the intensity of Foxp3 expression by Tregs was significantly lower in mice co-administered MS-275 (Fig S5b) suggesting the drug may selectively remove Foxp3 high Tregs thought to have a stronger suppressive function [22, 23]. Down-regulation of Treg in the context of an oncolytic booster vaccine increases the ratio of effectors to Tregs (Fig S5c) and may allow the secondary $CD8^+$ T cell responses induced to function in a less stringently regulated environment.

MS-275 prevents vaccine-induced autoimmune vitiligo

We have noted that mice treated with the our oncolytic vaccine prime:boost regimen targeting DCT developed severe systemic vitiligo (depigmentation), an indication of autoimmune destruction of normal melanocytes expressing DCT. Remarkably, however, the induction of systemic vitiligo was almost completely abolished by concomitant treatment with MS-275, in contrast to its effect on the enhancement of anti-tumor efficacy (Fig. 6).

Discussion

We have previously reported that HDACi can modulate IFN signalling pathways to enhance the susceptibility of tumor cells to oncolytic virus killing but their effect on the systemic immune responses in this context is unknown (Nguyen PNAS 2008; MacTavish PLoS ONE 2010). Our current study demonstrates that co-administration of MS-275, a class I HDACi that is currently in clinical trials as anticancer agent, inhibits both the cellular and humoral immune responses against the viral vector further supporting the combination strategy of HDACi and oncolytic therapy. However, MS-275 also down-regulates the primary response against tumor antigens compromising the induction of anti-tumor immunity. This compromising effect can be avoided if co-administration of HDACi and oncolytic vaccine is carefully timed, namely at boosting phase, leading to synergy between oncolysis and T cell responses. Such a combination results in a selective lymphopenia that selectively reduces Tregs and naïve lymphocytes providing a favourable environment allowing a focused expansion of highly functional anti-tumor CTLs. As a consequence, enhanced oncolytic activity and anti-tumor immunity lead to a more than 60% durable cure rate in a very challenging cancer model. Most strikingly, while MS-275 dramatically enhanced efficacy, it suppressed autoimmune pathology, profoundly improving the therapeutic index.

It is well known that intravenous delivery of VSV induces a transient lymphopenia that has been attributed to the coincident induction of type I IFNs (Schattner Cell Immunol 1983; Kamphuis Blood 2006). Some studies suggest that memory $CD8^+$ T cells are more sensitive to IFN-dependent early attrition than naive $CD8^+$ T cells but others have argued that memory T cells have lowered expression of IFN receptor and STAT1, leading to reduced sensitivity to IFN-mediated depletion (Marshall JV 2011; Peacock JI 2003; JV 2010; Gil Blood 2006; Dondi JI 2003). Another group reported that both naïve and memory $CD8^+$ T cells could be sensitized by IFN at the early stage of viral infection but antigen-specific T cells were rescued by subsequent antigenic stimulation while bystander T cells died after initial non-specific activation (Jiang JI 2003; 171: 4352-4358). Our demonstration that pre-existing tumor antigen-specific T cells could be dramatically boosted by oncolytic vaccine during

lymphopenia appears to support the latter two possibilities. Interestingly, co-administration of MS-275 prolonged the lymphopenia without affecting the expansion of secondary T cell responses, further extending a favourable environment for the development of anti-tumor immunity while reducing/delaying antiviral responses. The drug alone did not significantly affect circulating lymphocytes suggesting that its effect may lie in the delay of reconstitution. This speculation is supported by the observations that the virus:drug combo selectively eliminated lymphocyte precursors in the bone marrow and thymus, consistent with an important role for HDAC1/2 in lymphocyte development (Yamaguchi Genes Dev. 2010;24:455-69).

It has been demonstrated in other cancer immunotherapeutic settings that elimination of unwanted immune cells can provide supportive cytokines for the functional development of tumor antigen-specific $CD8^+$ T cells particularly during adoptive cell therapy (ACT) [28-30]. The fact that a higher frequency of $CD8^+$ T cells that can produce more IFN-γ and TNF-α was found in animals co-treated with MS-275 supports this notion [31]. It is notable that these T cells with enhanced cytokine profiles performed better in the functional avidity assay. Having CTL that respond more strongly to cognate antigen should lead to a more potent anti-tumor immune response. Our finding may also have important implications for adoptive cellular therapy because this interferon:drug combo is able to generate a transient lymphopenia while preserving the desired immune responses [32].

Treg play an important role in maintaining immunological tolerance to self/tumor antigens and depletion of Treg is a key mechanism underlying the effectiveness of cancer immunotherapy [34, 35]. In contrast to SAHA and VPA, which expand Tregs, MS-275 can down-regulate Treg function (PLoS One. 2012;7(1):e30815). We demonstrate that in the context of VSV infection, MS-275 reduces the number of Treg, especially those that express high levels of Foxp3[22, 23], revealing a novel aspect of MS-275 as a strong immunomodulator. It is likely that the removal of Treg-mediated immune suppression contributes to the enhanced anti-tumor efficacy following the combination therapy. Among all cell populations, B cell depletion appeared to be most profound. This correlated with a reduction of neutralizing antibodies against the oncolytic vector, likely contributing to the enhanced viral replication that was observed in the tumor by *in vivo* imaging on days 4 and 5 post-infection when neutralizing antibodies have begun to appear in the absence of drug. Interestingly, tumor-specific antibodies could still be boosted in the presence of the HDACi, suggesting that memory B cells must be resistant to elimination. Several recent studies suggest that naïve B cells or certain subsets of B cells negatively regulate anti-tumor immunity and depletion of B cells increases the efficacy of cancer vaccination [37, 38]. We speculate that removal of B cells together with Treg reduction may further antagonize inhibitory networks [39].

Another novel and very important finding in this study is the prevention of vaccine-induced vitiligo by MS-275. Autoimmune pathology has been observed in both pre-clinical and clinical studies and has been considered an unavoidable outcome following cancer immunotherapy against a self/tumor antigen[40-42]. In fact the association of autoimmune pathology with enhanced clinical responses has even led to it being identified as a positive prognostic factor[43, 44]. Using vitiligo as a read-out we have previously demonstrated that inflammatory signals in the skin are essential to the recruitment of these DCT-specific T

cells and to render normal melanocytes more susceptible to destruction (up-regulation of MHC/self antigens or stress molecules)[45, 46]. Strikingly, disseminated vitiligo was dramatically diminished when MS-275 was co-delivered with virus. To the best of our knowledge, this represents the first time that anti-melanoma efficacy was dramatically enhanced with a simultaneous reduction in vitiligo. Type I IFN has been implicated as a key factor in triggering autoimmune tissue damage[47] and the ability of MS-275 to modify IFN signalling may contribute to reduced autoimmunity. MS-275 also has known anti-inflammatory properties [27, 48, 49] and we speculate that MS-275 administration may suppress these inflammatory signals and thus reduce the recruitment of effector cells into the skin. This notion is supported by other observations where MS-275 has a strong anti-inflammatory effect in ameliorating arthritis through inhibition of pro-inflammatory cytokines and immune cell recruitment[26]. Our finding may offer a pharmacological strategy to enhance anti-tumoral immunity while preventing unwanted autoimmune sequelae.

In summary, we sought to combine an oncolytic vaccine therapy with an HDACi previously demonstrated to enhance viral oncolysis by modifying IFN signalling and found that this combination also mediated significant modification of both anti-viral and anti-tumoral acquired immunity. By reducing anti-viral responses while focusing the immune response on the tumor we were able to extend viral oncolysis, enhance anti-tumor destruction and even reduce autoimmune sequelae. The selective immunosuppressive actions of this drug imply that it should not be combined with therapies aimed at generating primary immune responses including not only vaccination but potentially also viral oncolysis as the drug may impair *in situ* vaccine effects even while enhancing viral replication. Our results provide evidence that MS-275 can function as a selectively immunosuppressive drug that can enhance the potency of an oncolytic vaccine booster. Importantly, this differential immunosuppression can be induced in combination with non-viral IFN inducers such as Poly I:C. This study highlights the importance of monitoring immunity while combining chemotherapy and biologics as unexpected interactions may occur.

Acknowledgements: This work was supported by grants to Y.W. from the Canadian Institutes of Health Research [MOP-67066] and the Ontario Institute for Cancer Research. The authors thank Natasha Khazdan for producing the rVSV vectors.

Figure Legends

Figure 1. MS-275 dramatically enhances the efficacy of oncolytic booster vaccination in a very stringent therapeutic intracranial melanoma model. C57BL/6 mice were injected intracranially with 1,000 B16-F10 cells. Five days later, they were vaccinated with $1x10^8$ pfu of Ad-hDCT i.m. Following a 14-day interval, mice were boosted with $1x10^9$ pfu of VSV-hDCT i.v., with or without 5 consecutive daily treatments with 100 μg of MS-275 or vehicle i.p. beginning 6 hrs prior to injection of VSV. Controls either received Ad-BHG (empty vector) or Ad-hDCT alone on day 5. An additional control group received 5 consecutive daily treatments with MS-275 alone beginning on day 5.

Figure 2. MS-275 inhibits primary immune responses while leaving secondary immune responses intact. B16-F10 tumor-bearing C57BL/6 mice were primed with $1x10^8$ pfu of Ad-hDCT i.m. and boosted 14 days later with $1x10^9$ pfu of VSV-hDCT i.v. with or without 5 consecutive daily treatments with 100 μg of MS-275 i.p. beginning 6 hrs prior to injection of VSV. (a) On indicated days, tumor-specific $CD8^+$ T cell responses were quantified in blood by flow cytometry after *in vitro* re-stimulation with the immunodominant epitope $DCT_{180-188}$ and intracellular cytokine staining for IFN-γ. (b) Using an in-cell Western assay, IgG anti-hDCT antibodies were quantified in plasma. (c) $CD8^+$ T cell responses against the immunodominant viral epitope were compared to the immunodominant DCT epitope and (d) anti-VSV neutralizing antibodies were monitored.

Figure 3. MS-275 impairs induction of primary immune responses via vaccination. C57BL/6 mice were intracranially with 1,000 B16-F10. Five days later, they were vaccinated with $1x10^8$ pfu of Ad-hDCT i.m., with or without 5 consecutive daily treatments with 100 μg of MS-275 or vehicle i.p. beginning 6 hrs prior to injection of the adenoviral vaccine. (a) The impact of drug on induction of primary $CD8^+$ T cell responses against DCT was measured by ICS. (b) Survival data was collected.

Figure 4. VSV induces a transient lymphopenia that is significantly extended by MS-275 co-administration. C57BL/6 mice were exposed to VSV, MS-275, MS-275 analogue or MS-275:VSV combo. (a) Numbers of cells per μl of blood are displayed over a 30-day period post-treatment. Horizontal dotted line represents average count for untreated mice. $CD4^+$ (b), $CD8^+$ T cell and B cell (d) counts are also indicated.

Figure 5. Co-administration of MS-275 with oncolytic vaccine booster generates more functional tumor antigen-specific T cells. Blood-derived $DCT_{180-188}$-specific $CD8^+$ T cells were obtained 5 days post-VSV boosting and their cytokine production and avidity were assessed. (a) The frequency capable of simultaneous production of IFN-γ and TNF-α and the amount of (b) IFN-γ and (c) TNF-α produced per cell (measured as mean fluorescence intensity). (d) The functional avidity of $DCT_{180-188}$-specific $CD8^+$ splenocytes was assessed by flow cytometric detection of intracellular IFN-γ after *in vitro* re-stimulation with different dilutions of cognate peptide.

Figure 6. Co-administration of MS-275 during boosting dramatically reduces autoimmunity. Tumor-bearing C57BL/6 mice were treated with Ad-hDCT + VSV-hDCT in the presence or absence of MS-275 and their vitiligo development was recorded. The left panel displays five mice two months post Ad-hDCT + VSV-hDCT vaccination. The right panel displays five mice having been treated with Ad-hDCT + VSV-hDCT + MS-275 also two months post-boosting. Note that MS-275 was administered during boosting and therefore failed to prevent vitiligo at surgical site on the head where Ad-hDCT priming alone was able to induce vitiligo localized to the site of surgical.

Methods

Mice

Female, age-matched (8-10 weeks old at initiation of experiments) C57BL/6 were purchased from Charles River Laboratories (Wilmington, MA) and housed in a controlled environment in the Central Animal Facility at McMaster University with food and water provided *ad libitum*. All animal experimentation was approved by McMaster University's Animal Research Ethics Board and complied with the Canadian Council on Animal Care guidelines.

Viral vectors

Ad-hDCT is a replication-deficient, E1/E3-deleted adenoviral vector containing the full-length hDCT transgene[46]. Replication-competent VSV-hDCT and VSV-Luc carry transgenes encoding hDCT and firefly luciferase, respectively, and have been described [16, 50]. The Ad-BHG and VSV-MT were control vectors, lacking a transgene.

Cells and culture conditions

B16-F10 cells were grown at 37^{o}C in a humidified atmosphere with 5% CO_2 in F11-MEM containing 10% FBS, 2mM L-glutamine, 5 ml sodium pyruvate, 5 ml MEM non-essential amino acids, 5 ml vitamin solution, 55μM 2-mercaptoethanol and antibiotics (all cell culture reagents from Invitrogen, Grand Island, NY, USA).

Prime-boost protocol

Mice were primed by intramuscular injection of $1x10^8$ pfu of Ad. For boosting, $1x10^9$ pfu of VSV was injected intravenously 14 days later.

Cancer Model

To establish intracranial tumors, mice received intracranial injections of $1x10^3$ B16-F10 cells in 1 μl of PBS. Under anesthetic, mice were placed in a stereotactic instrument (Xymotech Biosystems Inc, Quebec, Canada) and an incision made in the scalp to expose the skull. A small burr hole was drilled through the skull at the injection site. Cells were injected with a 26-gauge needle mounted on a 10 μl Hamilton syringe (Hamilton Company, Reno, NV) at the following site in the right hemisphere of the brain (relative to bregma): 0.62 mm anterior, 2.25 mm lateral and 4.0 mm deep. Cells were injected over a period of 1 minute and the needle was left in place for 2 minutes prior to withdrawal to minimize reflux along the

injection tract. The scalp incision was closed with stainless steel clips that were removed 7-10 days later.

Peptides

The immunodominant peptide from DCT that binds to H-2K^b ($DCT_{180-188}$, SVYDFFVWL) was synthesized by PepScan Systems (Lelystad, The Netherlands). The H-2K^b-restricted epitope from the N protein of VSV (RGYVYQGL) was purchased from Biomer Technologies (Hayward, CA).

Antibodies/Tetramers

Monoclonal antibodies recognizing the following targets were used for flow cytometry assays: CD16/CD32 (Fc Block), CD3 (clone 145-2C11), CD4 (RM4-5), CD8 (53-6.7), IFN-γ (XMG1.2), TNF-α (MP6-XT22), CD19 (1D3), B220 (RA3-6B2) (BD Biosciences, Mississauga, ON, Canada) and Foxp3 (FJK-16s) (eBioscience, San Diego, CA).

Detection of antigen-specific T cell responses

Peripheral lymphocytes were re-stimulated with peptides (1μg/ml) at 37^{o}C for 5 h with brefeldin A (Golgi Plug, 1μg/ml; BD Biosciences) added after 1 h. Cells were treated with Fc block, stained for surface expression of CD3 and CD8 and then fixed, permeabilized (Cytofix/Cytoperm, BD Biosciences) and stained for intracellular IFN-γ and TNF-α. Data were acquired using a FACSCanto with FACSDiva software (BD Biosciences) and analyzed with FlowJo software (Tree Star, Ashland, OR).

T cell functional avidity assay

The functional avidity of T cells was determined with the same method used to assess antigen-specific responses (above) with modifications. Specifically, lymphocytes were stimulated in vitro with 10-fold serial peptide dilutions ranging from 1 μg/ml to 10 pg/ml. The frequency of CD8$^+$ T cells that produced IFN-γ at each peptide concentration was determined. These results were then plotted as the proportion of cell responding relative to the response induced by the highest concentration (i.e. 1 μg/ml) of peptide.

Detection of VSV-neutralizing antibodies

Serum or plasma samples were acquired from blood. Vero cells were seeded into a flat-bottom 96-well culture plate (BD Biosciences) at a density of 12,500 cells/well. Twenty-four hours later, serum or plasma samples were diluted 1/50 in serum-free medium. This, plus subsequent 1:2 serial dilutions were made in a separate 96-well plate (50 μl per well). To each well, 2x10^5 pfu of VSV in 50 mpfu of VSV in 50 uted 1/50 in serum-free medium. This, plus subseq 37^{o}C. Each aliquot of serum/plasma + VSV was then transferred to a well of confluent Vero cells and incubated for 48 h at 37^{o}C. Cell viability was assessed by alamar blue staining (Invitrogen) and detection using a fluoroskan reader (Thermo). The neutralizing antibody titer was defined as the serum/plasma dilution at which cell viability remained 50% of the cells-only positive control.

Quantification of DCT-specific antibodies

DCT-specific antibodies were detected using an in-cell Western blotting assay. U-2OS cells were seeded into a 96-well flat-bottom culture plate and cultured at 37^{o}C. Once confluent, they were infected with a vaccinia vector expressing hDCT at a multiplicity of infection of 5 for 6 h. Infected cells were fixed in the plates with 100 µl of 4% paraformaldehyde for 15 min at 37^{o}C, followed by the addition of 100 µl of ice-cold acetone:methanol (1:1) for 5 min at room temperature. Cells were rehydrated with PBS. Plates were blocked with 1% BSA (w/v) in PBS overnight at 4^{o}C or for 1 h at room temperature. Blocking solution was removed and the plates washed three times with 0.1% Tween-20 (v/v) in PBS. Serum/plasma samples were diluted (6 serial dilutions per sample, done in duplicate) in a separate 96-well plate and then transferred onto the fixed cells for 1 h at room temperature on a shaker or overnight at 4^{o}C. Plates were washed 3 times and Alexa Fluor 680-conjugated goat anti-mouse secondary antibody diluted 1:2000 in PBS was added to each well for 1 h at room temperature on a shaker. Plates were washed 3 times and fluorescence detected using an Odyssey Imaging System (LI-COR Biosciences, Lincoln, NE, USA). Average background fluorescence (cells + secondary antibody only) was subtracted from values obtained from samples. The adjusted optical density values were then plotted for all dilutions for each sample. The area under the curve was determined for each sample and used to plot the magnitude of the antibody response.

In vivo imaging of VSV infection

Mice bearing 5-day-old B16-F10 intracranial melanomas received i.v. injections of $4x10^{8}$ pfu of VSV-Luc with or without co-treatment with MS-275. Each of the 4 days following treatment with VSV, mice were injected with 3 mg of d-luciferin (Molecular Imaging Products Company, Ann Arbor, MI) intraperitoneally. Under anesthetic, VSV infection was visualized with a 200 Series Imaging System (Xenogen Corporation, Hopkinton, MA). Data acquisition and analysis were performed using Living Image v2.5 software. Images were captured under identical exposure, aperture and pixel binning settings.

Statistical analyses

GraphPad Prism for Windows (GraphPad Software, San Diego, CA) was used for graphing. For statistical analyses, GraphPad Prism and Minitab Statistical Software (Minitab Inc., State College, PA) were used. If required, data were normalized by log transformation. Student's two-tailed t-test, one- or two-way ANOVA or general linear modeling was used to query immune response data**.** Differences between means were considered significant at $p \leq 0.05$. Means plus standard error bars are shown. Survival data were analyzed using the Kaplan-Meier method and the logrank test.

References

1. Barber, G.N. VSV-tumor selective replication and protein translation. *Oncogene* 24, 7710-7719 (2005).

2. Dunn, G.P., Koebel, C.M. & Schreiber, R.D. Interferons, immunity and cancer immunoediting. *Nature reviews. Immunology* 6, 836-848 (2006).

3. Parato, K.A., Senger, D., Forsyth, P.A. & Bell, J.C. Recent progress in the battle between oncolytic viruses and tumours. *Nature reviews* 5, 965-976 (2005).

4. Stojdl, D.F. et al. Exploiting tumor-specific defects in the interferon pathway with a previously unknown oncolytic virus. *Nat Med* 6, 821-825 (2000).

5. Stojdl, D.F. et al. VSV strains with defects in their ability to shutdown innate immunity are potent systemic anti-cancer agents. *Cancer Cell* 4, 263-275 (2003).

6. Alain, T. et al. Vesicular stomatitis virus oncolysis is potentiated by impairing mTORC1-dependent type I IFN production. *Proceedings of the National Academy of Sciences of the United States of America* 107, 1576-1581 (2010).

7. Diallo, J.S. et al. A high-throughput pharmacoviral approach identifies novel oncolytic virus sensitizers. *Mol Ther* 18, 1123-1129 (2010).

8. Chang, H.M. et al. Induction of interferon-stimulated gene expression and antiviral responses require protein deacetylase activity. *Proc Natl Acad Sci U S A* 101, 9578-9583 (2004).

9. Minucci, S. & Pelicci, P.G. Histone deacetylase inhibitors and the promise of epigenetic (and more) treatments for cancer. *Nature reviews. Cancer* 6, 38-51 (2006).

10. Nusinzon, I. & Horvath, C.M. Positive and negative regulation of the innate antiviral response and beta interferon gene expression by deacetylation. *Molecular and cellular biology* 26, 3106-3113 (2006).

11. Nguyen, T.L. et al. Chemical targeting of the innate antiviral response by histone deacetylase inhibitors renders refractory cancers sensitive to viral oncolysis. *Proceedings of the National Academy of Sciences of the United States of America* 105, 14981-14986 (2008).

12. Blanchard, F. & Chipoy, C. Histone deacetylase inhibitors: new drugs for the treatment of inflammatory diseases? *Drug discovery today* 10, 197-204 (2005).

13. Choi, S. & Reddy, P. HDAC inhibition and graft versus host disease. *Molecular medicine* 17, 404-416 (2011).

14. Haberland, M., Montgomery, R.L. & Olson, E.N. The many roles of histone deacetylases in development and physiology: implications for disease and therapy. *Nat Rev Genet* 10, 32-42 (2009).

15. Shakespear, M.R., Halili, M.A., Irvine, K.M., Fairlie, D.P. & Sweet, M.J. Histone deacetylases as regulators of inflammation and immunity. *Trends in immunology* 32, 335-343 (2011).

16. Bridle, B.W. et al. Potentiating cancer immunotherapy using an oncolytic virus. *Mol Ther* 18, 1430-1439 (2010).

17. Lun, X. et al. Effects of intravenously administered recombinant vesicular stomatitis virus (VSV(deltaM51)) on multifocal and invasive gliomas. *J Natl Cancer Inst* 98, 1546-1557 (2006).

18. Kamphuis, E., Junt, T., Waibler, Z., Forster, R. & Kalinke, U. Type I interferons directly regulate lymphocyte recirculation and cause transient blood lymphopenia. *Blood* 108, 3253-3261 (2006).

19. McNally, J.M. et al. Attrition of bystander CD8 T cells during virus-induced T-cell and interferon responses. *Journal of virology* 75, 5965-5976 (2001).

20. Suzuki, T. et al. Synthesis and histone deacetylase inhibitory activity of new benzamide derivatives. *Journal of medicinal chemistry* 42, 3001-3003 (1999).

21. Schattner, A., Meshorer, A. & Wallach, D. Involvement of interferon in virus-induced lymphopenia. *Cellular Immunology* 79, 11-25 (1983).

22. Chauhan, S.K., Saban, D.R., Lee, H.K. & Dana, R. Levels of Foxp3 in regulatory T cells reflect their functional status in transplantation. *Journal of immunology* 182, 148-153 (2009).

23. d'Hennezel, E., Yurchenko, E., Sgouroudis, E., Hay, V. & Piccirillo, C.A. Single-cell analysis of the human T regulatory population uncovers functional heterogeneity and instability within FOXP3+ cells. *Journal of immunology* 186, 6788-6797 (2011).

24. Parato, K.A., Lichty, B.D. & Bell, J.C. Diplomatic immunity: turning a foe into an ally. *Curr Opin Mol Ther* 11, 13-21 (2009).

25. Prestwich, R.J. et al. The case of oncolytic viruses versus the immune system: waiting on the judgment of Solomon. *Human gene therapy* 20, 1119-1132 (2009).

26. Lin, H.S. et al. Anti-rheumatic activities of histone deacetylase (HDAC) inhibitors in vivo in collagen-induced arthritis in rodents. *Br J Pharmacol* 150, 862-872 (2007).

27. Zhang, Z.Y., Zhang, Z. & Schluesener, H.J. MS-275, an histone deacetylase inhibitor, reduces the inflammatory reaction in rat experimental autoimmune neuritis. *Neuroscience* 169, 370-377 (2010).

28. Cui, Y. et al. Harnessing the physiology of lymphopenia to support adoptive immunotherapy in lymphoreplete hosts. *Blood* 114, 3831-3840 (2009).

29. Gattinoni, L. et al. Removal of homeostatic cytokine sinks by lymphodepletion enhances the efficacy of adoptively transferred tumor-specific CD8+ T cells. *The Journal of experimental medicine* 202, 907-912 (2005).

30. Melchionda, F. et al. Adjuvant IL-7 or IL-15 overcomes immunodominance and improves survival of the CD8+ memory cell pool. *The Journal of clinical investigation* 115, 1177-1187 (2005).

31. Seder, R.A., Darrah, P.A. & Roederer, M. T-cell quality in memory and protection: implications for vaccine design. *Nature reviews. Immunology* 8, 247-258 (2008).

32. Weber, J. et al. White paper on adoptive cell therapy for cancer with tumor-infiltrating lymphocytes: a report of the CTEP subcommittee on adoptive cell therapy. *Clinical cancer research : an official journal of the American Association for Cancer Research* 17, 1664-1673 (2011).

33. Vlasakova, J. et al. Histone deacetylase inhibitors suppress IFNalpha-induced up-regulation of promyelocytic leukemia protein. *Blood* 109, 1373-1380 (2007).

34. Antony, P.A. et al. CD8+ T cell immunity against a tumor/self-antigen is augmented by CD4+ T helper cells and hindered by naturally occurring T regulatory cells. *Journal of immunology* 174, 2591-2601 (2005).

35. Curiel, T.J. et al. Specific recruitment of regulatory T cells in ovarian carcinoma fosters immune privilege and predicts reduced survival. *Nature medicine* 10, 942-949 (2004).

36. Wang, L., de Zoeten, E.F., Greene, M.I. & Hancock, W.W. Immunomodulatory effects of deacetylase inhibitors: therapeutic targeting of FOXP3+ regulatory T cells. *Nat Rev Drug Discov* 8, 969-981 (2009).

37. Bouaziz, J.D., Yanaba, K. & Tedder, T.F. Regulatory B cells as inhibitors of immune responses and inflammation. *Immunological reviews* 224, 201-214 (2008).

38. Mizoguchi, A. & Bhan, A.K. A case for regulatory B cells. *Journal of immunology* 176, 705-710 (2006).

39. Andreu, P. et al. FcRgamma activation regulates inflammation-associated squamous carcinogenesis. *Cancer cell* 17, 121-134 (2010).

40. Caspi, R.R. Immunotherapy of autoimmunity and cancer: the penalty for success. *Nature reviews. Immunology* 8, 970-976 (2008).

41. Gilboa, E. The risk of autoimmunity associated with tumor immunotherapy. *Nature immunology* 2, 789-792 (2001).

42. Koon, H. & Atkins, M. Autoimmunity and immunotherapy for cancer. *The New England journal of medicine* 354, 758-760 (2006).

43. Nanda, N.K. & Sercarz, E.E. Induction of anti-self-immunity to cure cancer. *Cell* 82, 13-17 (1995).

44. Overwijk, W.W. & Restifo, N.P. Autoimmunity and the immunotherapy of cancer: targeting the "self" to destroy the "other". *Crit Rev Immunol* 20, 433-450 (2000).

45. Bridle, B.W. et al. Immunotherapy can reject intracranial tumor cells without damaging the brain despite sharing the target antigen. *J Immunol* 184, 4269-4275 (2010).

46. Lane, C. et al. Vaccination-induced autoimmune vitiligo is a consequence of secondary trauma to the skin. *Cancer Res* 64, 1509-1514 (2004).

47. Lang, K.S. et al. Toll-like receptor engagement converts T-cell autoreactivity into overt autoimmune disease. *Nature medicine* 11, 138-145 (2005).

48. Adcock, I.M. Histone deacetylase inhibitors as novel anti-inflammatory agents. *Curr Opin Investig Drugs* 7, 966-973 (2006).

49. Nencioni, A. et al. Histone deacetylase inhibitors affect dendritic cell differentiation and immunogenicity. *Clinical cancer research : an official journal of the American Association for Cancer Research* 13, 3933-3941 (2007).

50. Power, A.T. et al. Carrier Cell-based Delivery of an Oncolytic Virus Circumvents Antiviral Immunity. *Mol Ther* 15, 123-130 (2007).

Fig 1

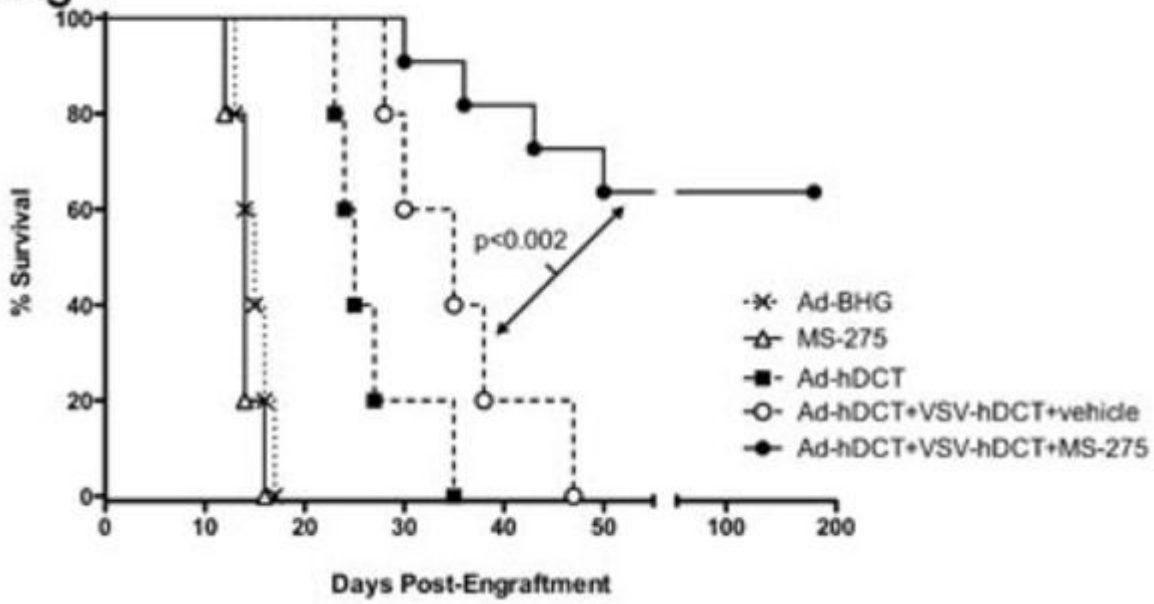
% Survival
100
80
60
40
20
0
0
10
20
30
40
50
100
200
Days Post-Engraftment
p<0.002
Ad-BHG
MS-275
Ad-hDCT
Ad-hDCT+VSV-hDCT+vehicle
Ad-hDCT+VSV-hDCT+MS-275

Fig 2

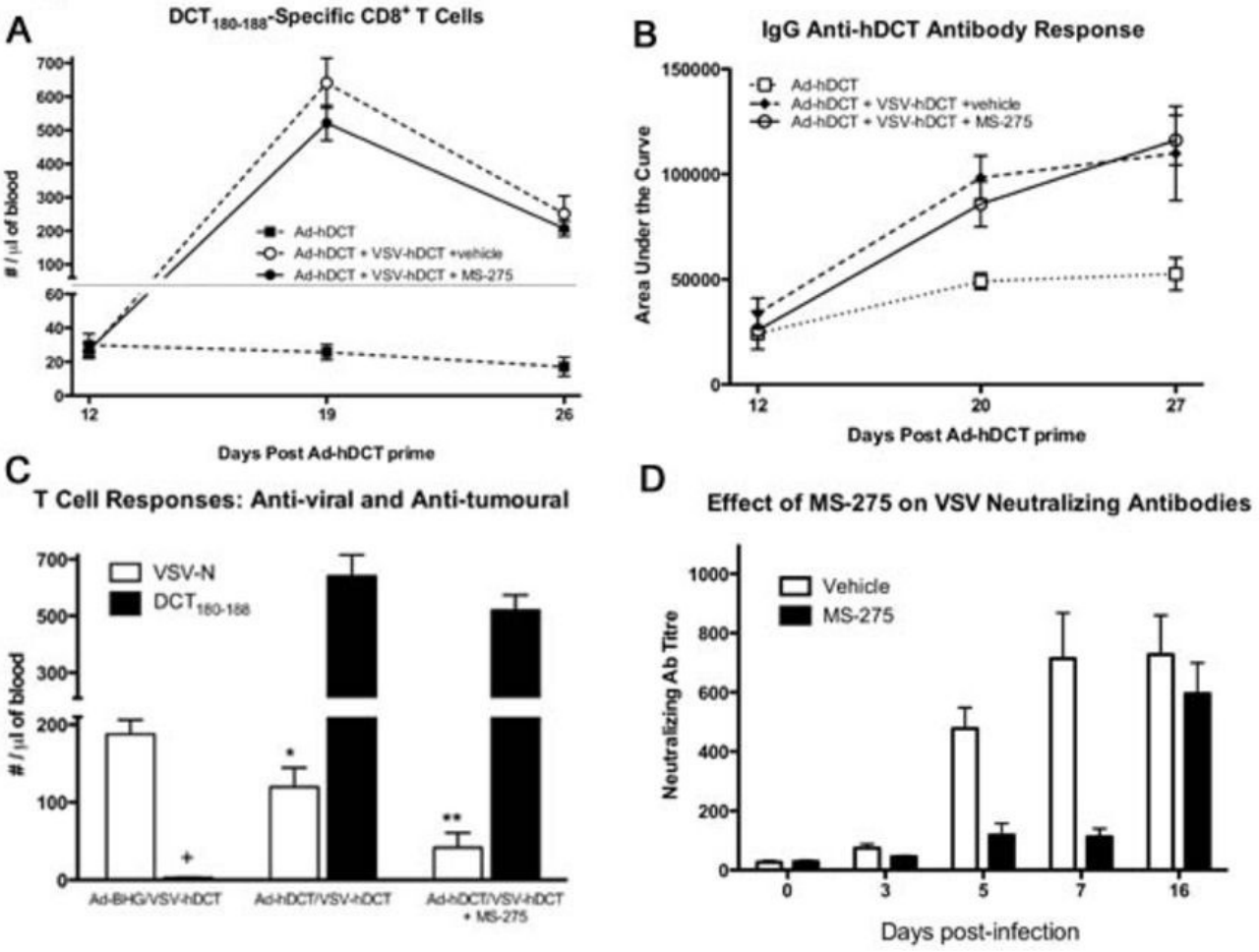
A
DCT180-188-Specific CD8+ T Cells
/ µl of blood
Ad-hDCT
Ad-hDCT + VSV-hDCT +vehicle
Ad-hDCT + VSV-hDCT + MS-275
Days Post Ad-hDCT prime
B
IgG Anti-hDCT Antibody Response
Area Under the Curve
Ad-hDCT
Ad-hDCT + VSV-hDCT +vehicle
Ad-hDCT + VSV-hDCT + MS-275
Days Post Ad-hDCT prime
C
T Cell Responses: Anti-viral and Anti-tumoural
/ µl of blood
VSV-N
DCT180-188
Ad-BHG/VSV-hDCT
Ad-hDCT/VSV-hDCT
Ad-hDCT/VSV-hDCT + MS-275
D
Effect of MS-275 on VSV Neutralizing Antibodies
Neutralizing Ab Titre
Vehicle
MS-275
Days post-infection

Fig 3

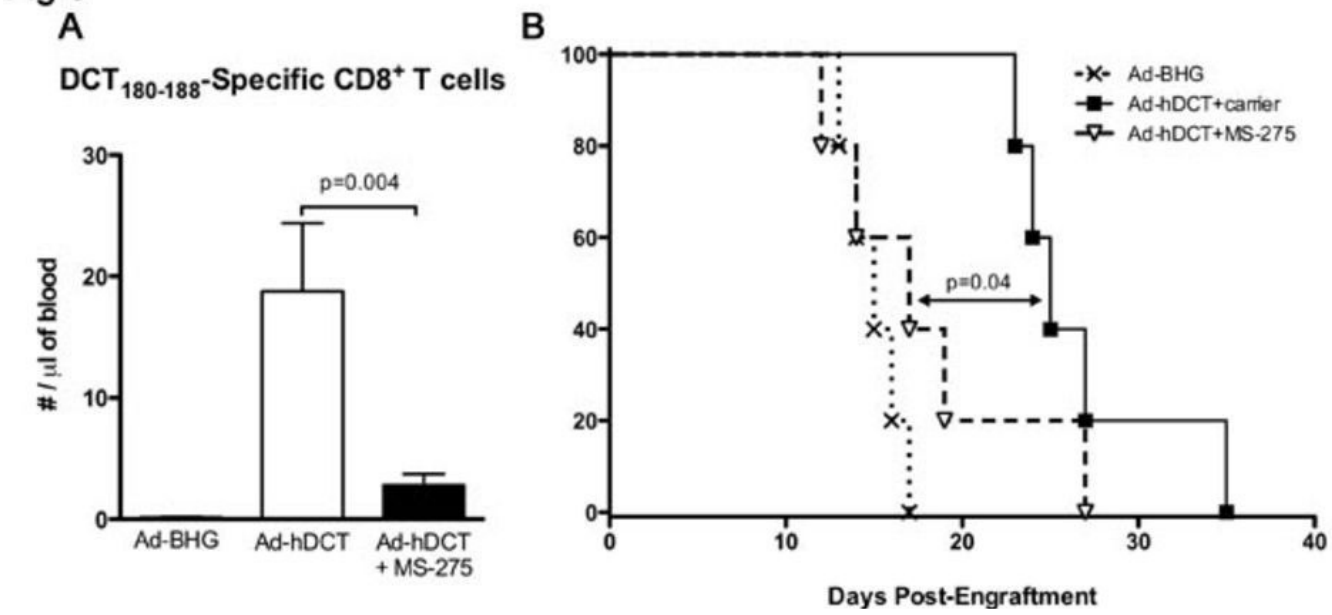
A
DCT180-188-Specific CD8+ T cells
/ μl of blood
30
20
10
0
p=0.004
Ad-BHG
Ad-hDCT
Ad-hDCT + MS-275
B
100
80
60
40
20
0
0
10
20
30
40
p=0.04
Ad-BHG
Ad-hDCT+carrier
Ad-hDCT+MS-275
Days Post-Engraftment

Fig 4

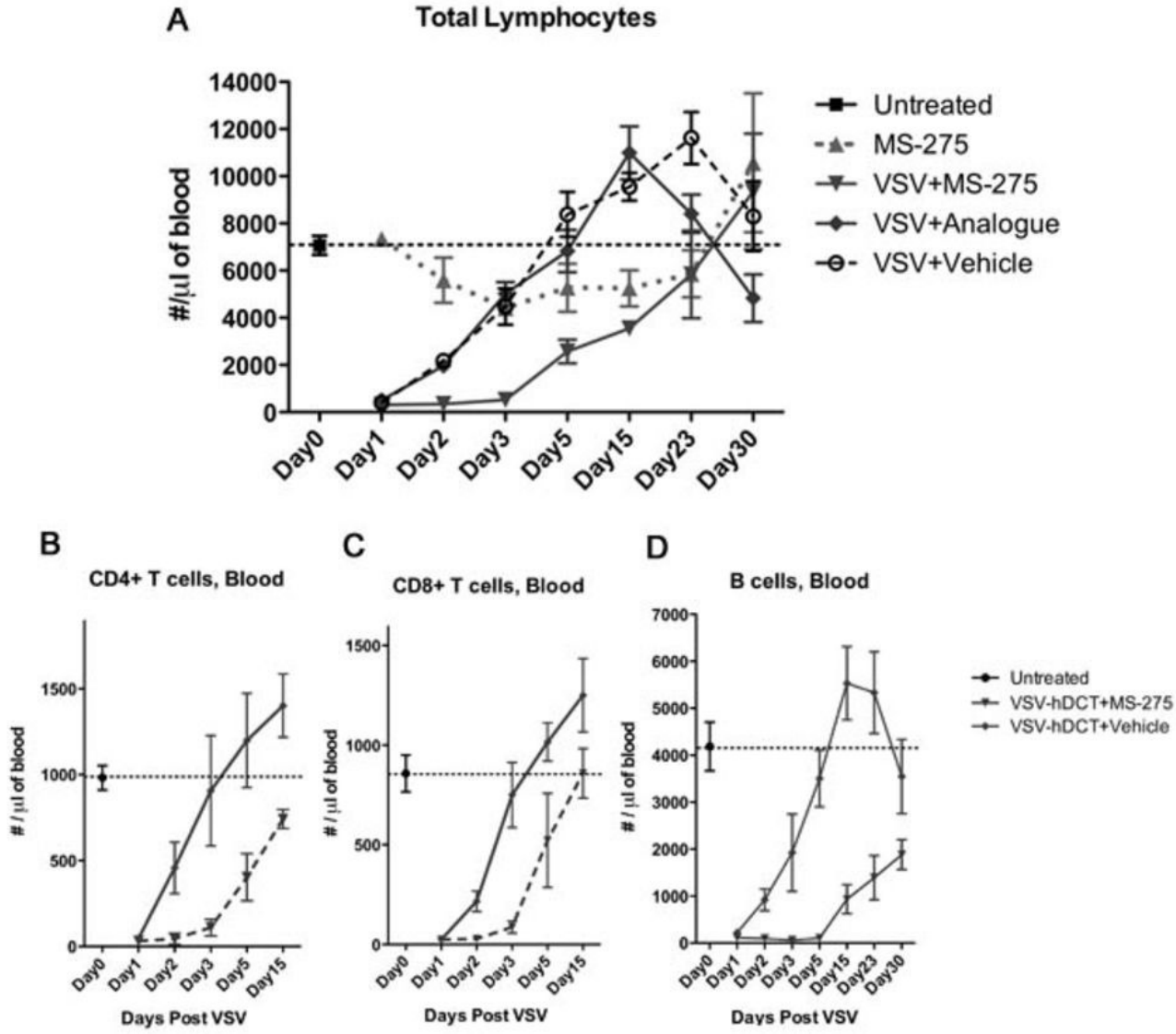
A
Total Lymphocytes
#/µl of blood
14000
12000
10000
8000
6000
4000
2000
0
Day0
Day1
Day2
Day3
Day5
Day15
Day23
Day30
Untreated
MS-275
VSV+MS-275
VSV+Analogue
VSV+Vehicle
B
CD4+ T cells, Blood
C
CD8+ T cells, Blood
D
B cells, Blood
/ µl of blood
Days Post VSV
Untreated
VSV-hDCT+MS-275
VSV-hDCT+Vehicle

Fig 5

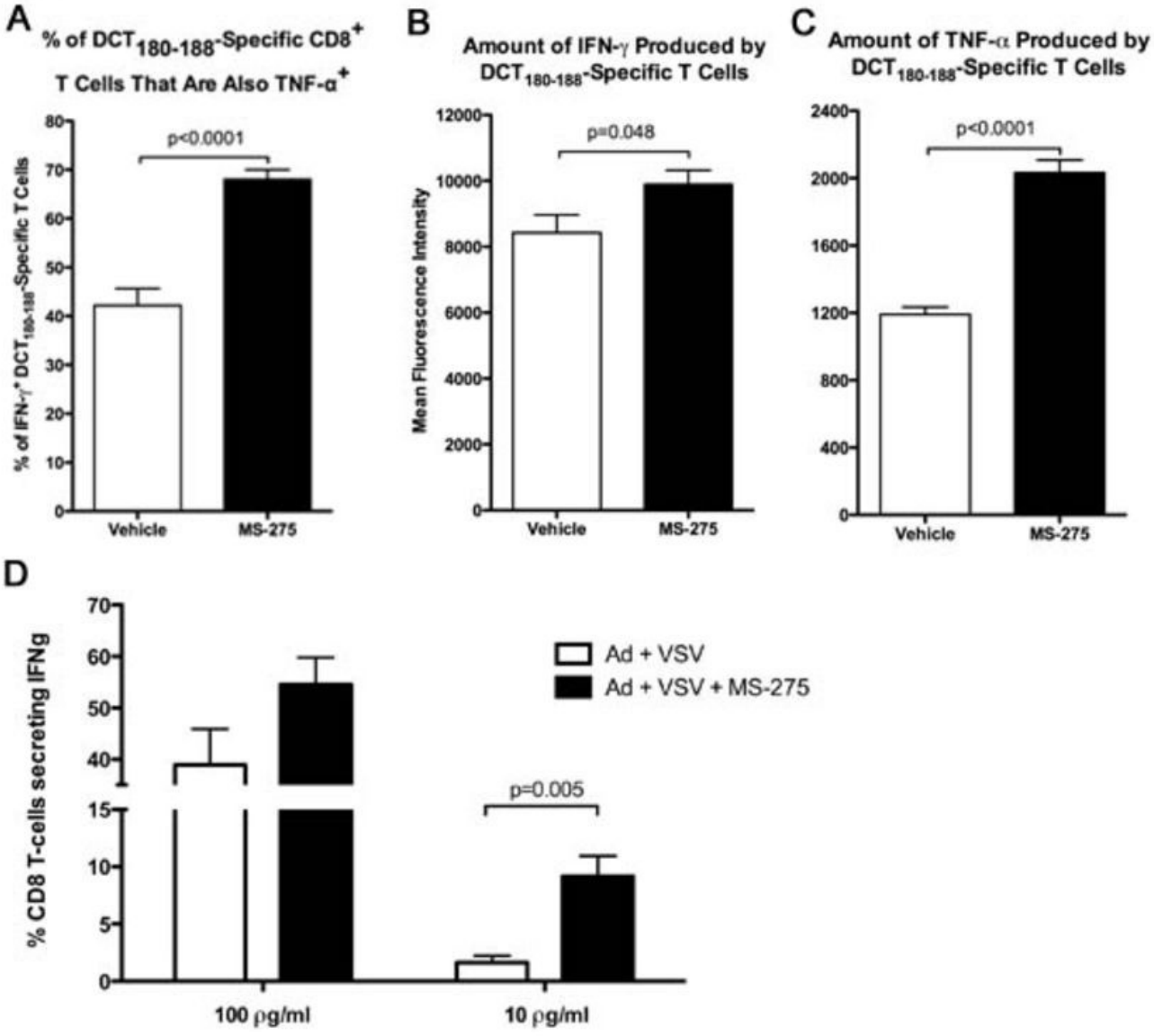
A
% of DCT180-188-Specific CD8+ T Cells That Are Also TNF-α+
% of IFN-γ+ DCT180-188-Specific T Cells
p<0.0001
Vehicle
MS-275
B
Amount of IFN-γ Produced by DCT180-188-Specific T Cells
Mean Fluorescence Intensity
p=0.048
Vehicle
MS-275
C
Amount of TNF-α Produced by DCT180-188-Specific T Cells
p<0.0001
Vehicle
MS-275
D
% CD8 T-cells secreting IFNg
Ad + VSV
Ad + VSV + MS-275
p=0.005
100 pg/ml
10 pg/ml

Fig 6

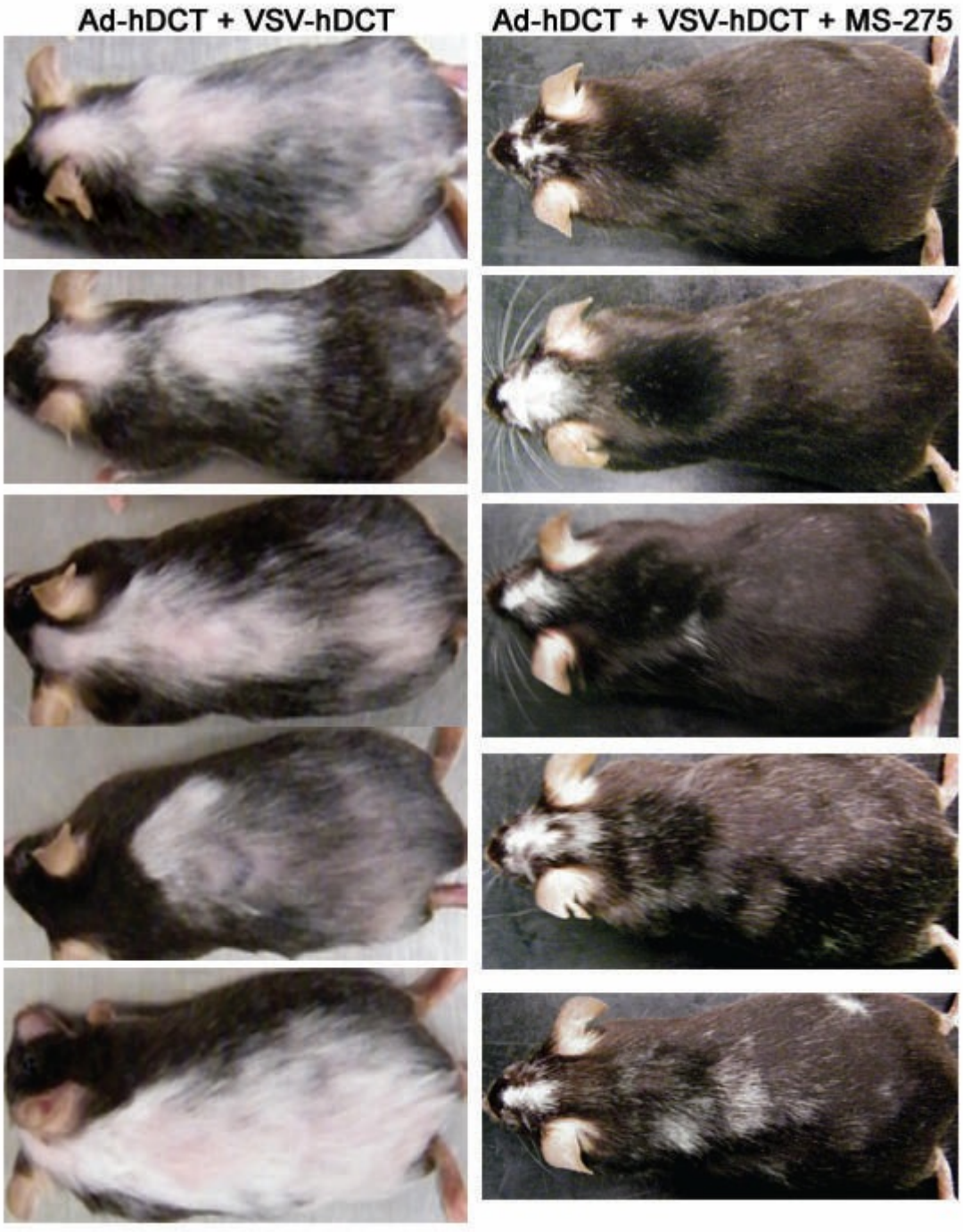

Supplemental Figure Legends

Figure S1 Co-administration of MS-275 extends VSV-luc activity in B16F10 tumours. Mice bearing 5-day-old B16-F10 intracranial melanomas received i.v. injections of $4x10^8$ pfu of VSV-Luc with or without co-treatment with MS-275. Each of the 4 days following treatment with VSV, mice were injected with 3 mg of d-luciferin (Molecular Imaging Products Company, Ann Arbor, MI) intraperitoneally. Under anesthetic, VSV infection was visualized with a 200 Series Imaging System (Xenogen Corporation, Hopkinton, MA). Data acquisition and analysis were performed using Living Image v2.5 software. Images were captured under identical exposure, aperture and pixel binning settings.

Figure S2 Structure of MS-275 and inactive analogue.

The active compound is displayed on the left, while the structure of a highly similar compound lacking HDAC inhibitory activity used in these studies is shown on the right.

Figure S3 PolyI:C induces a lymphopenia that is extended by MS-275 co- administration.8-10 weeks old C57BL/6 female mice were treated with a single dose of PolyI:C (200 μg in 100 μl of phosphate-buffered saline, Sigma) and were treated with 0.1 mg of MS-275 once a day for 5 days via intraperitoneal injection as PolyI:C combination MS-275 treatment group. Mice treated with a single dose of PolyI:C only were regarded as PolyI:C treatment group, whereas mice treated with five doses of MS-275 for 5 days represent the drug only treatment group. Blood was taken from the periorbital sinus and red blood cells were lysed with ACK lysis buffer. Peripheral blood lymphocyte counts were assessed at 2h, 6h, 24h, 48h, 72h and 120h after PolyI:C injection (N=3). Data were collected by a FACSCanto flow cytometer with FACSDiva 5.0.2 software (BD Pharmingen) and analyzed with FlowJo Mac (Treestar, Ashland, OR).

Figure S4 Co-administration of VSV and MS-275 depleted immature lymphocyte precursors in bone marrow and thymus.8-10 weeks old C57BL/6 female mice were infected with a single tail-vein injection (i.v.) dose of VSV (2×10^9 PFU VSV in 200 µl of phosphate-buffered saline) and were treated with 0.1mg of MS-275 via intraperitoneal injection once a day for 3 days as VSV combination MS-275 treatment group. Mice infected with a single dose of VSV only were regarded as VSV treatment group, whereas mice treated with three doses MS-275 or MS-275 analogue for 3 days were drug only or analogue only treatment groups respectively, naïve mice were not treated with virus or drug. (N=3) Lymphocytes from thymus or bone marrow (femur and tibia) were harvested 3 days after VSV injection. Cells were then treated with anti-CD16/32 and surface markers fluorescently labelled by antibodies for (A) CD4/CD8 or (B) B220/IgM (BD Pharmingen). Representative plots are shown. (C) Diagram indicating the location on the B cell plots occupied by B cell precursors.

Figure S5 Co-administration of VSV and MS-275 depleted Treg numbers leaving residual Tregs with lower FoxP3 expression levels.8-10 weeks old C57BL/6 female mice were treated with a single dose of VSV-hDCT (2x109 PFU given i.v.) and were treated with 0.1 mg of MS-275 once a day for 5 days via intraperitoneal injection. Blood was taken from the periorbital sinus and red blood cells were lysed with ACK lysis buffer. Cells were surface stained for CD4 (RM4-5, BD Biosciences, Mississauga, ON, Canada), fixed and permeabilized and stained for Foxp3 (FJK-16s, eBioscience, San Diego, CA). (A) The number of CD4+/FoxP3+ Tregs in blood following treatment. (B) The level of Treg expression of FoxP3 as measured by mean fluorescence intensity. (C) The ratio of DCT-specific CD8+ T cells to CD4+/FoxP3+ Tregs in vaccinated animals plus/minus MS-275.

Fig S1

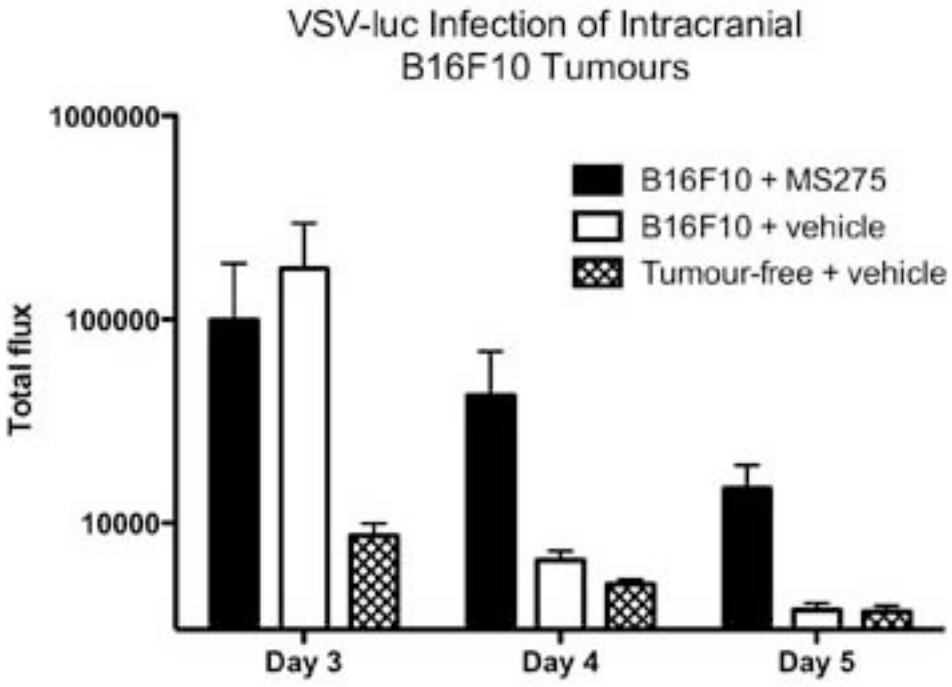
VSV-luc Infection of Intracranial
B16F10 Tumours
1000000
100000
10000
Total flux
B16F10 + MS275
B16F10 + vehicle
Tumour-free + vehicle
Day 3
Day 4
Day 5

Fig S2

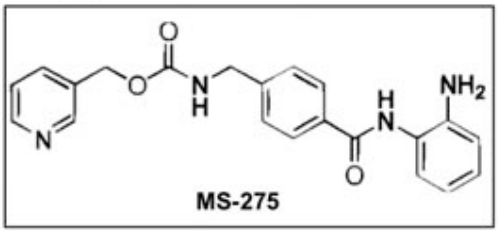
O
O
N
H
N
H
NH2
N
O
MS-275

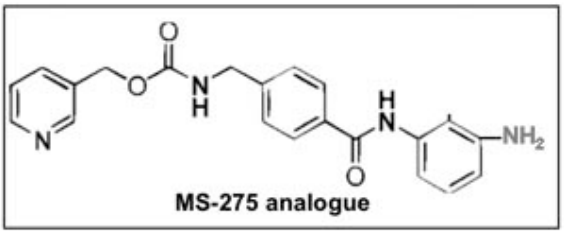
O
O
N
H
N
H
NH2
N
O
MS-275 analogue

Fig S3

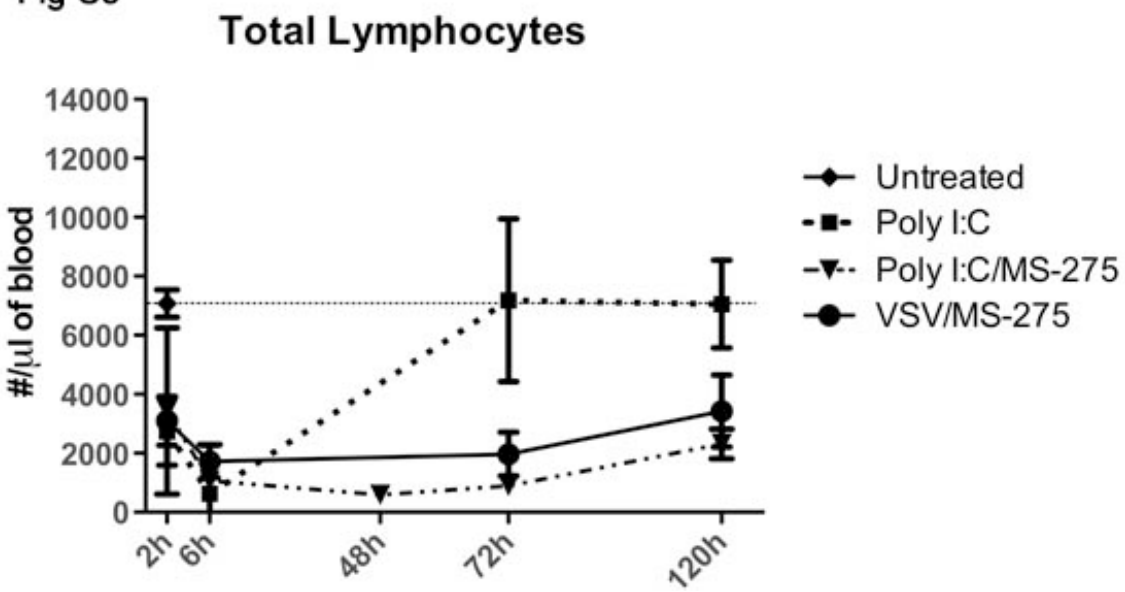
Total Lymphocytes
#/μl of blood
14000
12000
10000
8000
6000
4000
2000
0
2h
6h
48h
72h
120h
Untreated
Poly I:C
Poly I:C/MS-275
VSV/MS-275

Fig S4

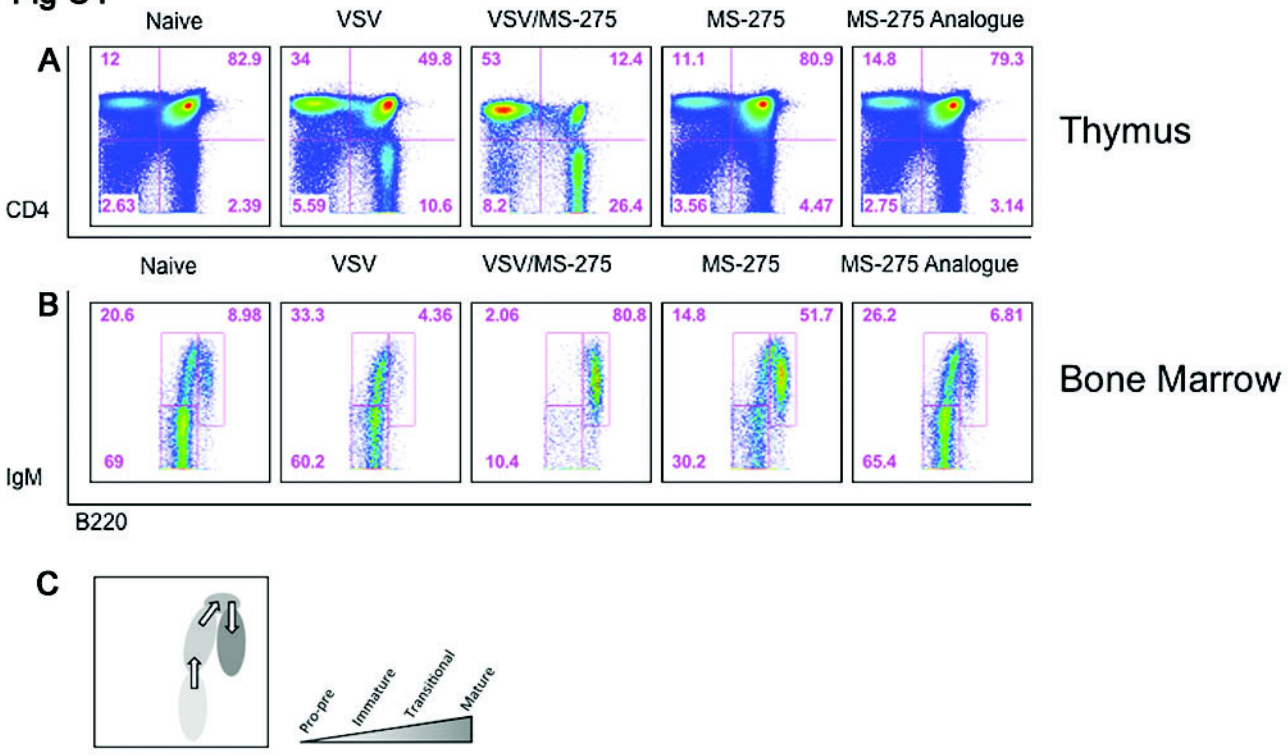
Naive
VSV
VSV/MS-275
MS-275
MS-275 Analogue
A
12
82.9
2.63
2.39
34
49.8
5.59
10.6
53
12.4
8.2
26.4
11.1
80.9
3.56
4.47
14.8
79.3
2.75
3.14
CD4
Thymus
Naive
VSV
VSV/MS-275
MS-275
MS-275 Analogue
B
20.6
8.98
69
33.3
4.36
60.2
2.06
80.8
10.4
14.8
51.7
30.2
26.2
6.81
65.4
IgM
B220
Bone Marrow
C
Pro-pre
Immature
Transitional
Mature

Fig S5

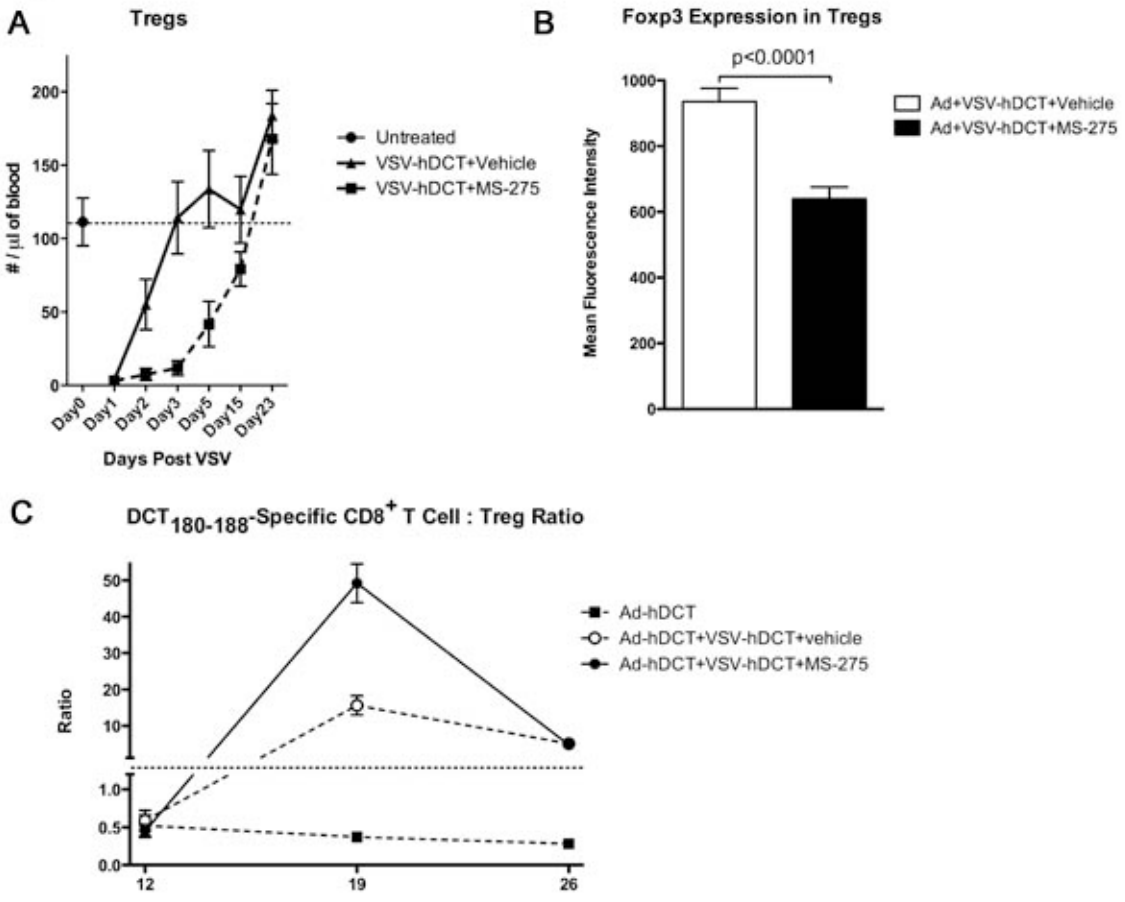
A
Tregs
/ μl of blood
Days Post VSV
Day0
Day1
Day2
Day3
Day5
Day15
Day23
Untreated
VSV-hDCT+Vehicle
VSV-hDCT+MS-275
B
Foxp3 Expression in Tregs
p<0.0001
Mean Fluorescence Intensity
Ad+VSV-hDCT+Vehicle
Ad+VSV-hDCT+MS-275
C
DCT180-188-Specific CD8+ T Cell : Treg Ratio
Ratio
Ad-hDCT
Ad-hDCT+VSV-hDCT+vehicle
Ad-hDCT+VSV-hDCT+MS-275

Appendix VI – Harnessing oncolytic virus-mediated anti-tumour immunity in an infected cell vaccine

Contribution of author:

KA Parato undertook the splenocyte transfer experiment from figure 1e in addition to the experiment comparing the various VSV recombinants in supplental figure S1b. The IHC in figure 1f and 2a are from experiments performed by JM Paterson. Figure 3c is a weighted average of many experiments, one of which was performed by KA Parato, two were performed by L Ferreira, and one was performed by A Kus. The three other experiments included in figure 3c were performed by CG Lemay. V Garcia did the MOI of 10 infection in supplemental figure S1a. JL Rintoul provided technical with large flow cytometry experiments.

TJ Falls and L Ferreira did the intravenous animal injections and helped with large animal experiments. K Garson and BC Vanderhyden provided the transgenic MISIIRTAg mice and the 6048R cell line.

KA Parato, VA Tang, JS Diallo, R Arulanandam, and F LeBoeuf read over the manuscript and provided revisions. All other authors provided guidance and feedback over the course of the work.

All other experiments were performed by CG Lemay in addition to making the figures and writing the paper.

Mol Ther. 2012 Sep;20(9):1791-9. doi: 10.1038/mt.2012.128. Epub 2012 Jul 3.

PMID: 22760544

Harnessing Oncolytic Virus-mediated Antitumor Immunity in an Infected Cell Vaccine

Chantal G Lemay[1,2], Julia L Rintoul[1,2], Agnieszka Kus[1,2], Jennifer M Paterson[1,2], Vanessa Garcia[1,2], Theresa J Falls[2], Lisa Ferreira[2], Byram W Bridle[3], David P Conrad[1,2], Vera A Tang[2], Jean-Simon Diallo[1,2], Rozanne Arulanandam[1,2], Fabrice Le Boeuf[1,2], Kenneth Garson[2], Barbara C Vanderhyden[2], David F Stojdl[2], Brian D Lichty[4], Harold L Atkins[1,2], Kelley A Parato[2], John C Bell[1,2] and Rebecca C Auer[1,2]

[1]Department of Biochemistry, Microbiology and Immunology, University of Ottawa, Ottawa, Ontario, Canada; [2]Ottawa Hospital Research Institute, Centre for Innovative Cancer Therapeutics, Ottawa, Ontario, Canada; [3]Department of Pathobiology, University of Guelph, Guelph, Ontario, Canada; [4]Department of Pathology and Molecular Medicine, Centre for Gene Therapeutics, McMaster University, Faculty of Health Sciences, Hamilton, Ontario, Canada

Treatment of permissive tumors with the oncolytic virus (OV) VSV-Δ51 leads to a robust antitumor T-cell response, which contributes to efficacy; however, many tumors are not permissive to *in vivo* treatment with VSV-Δ51. In an attempt to channel the immune stimulatory properties of VSV-Δ51 and broaden the scope of tumors that can be treated by an OV, we have developed a potent oncolytic vaccine platform, consisting of tumor cells infected with VSV-Δ51. We demonstrate that prophylactic immunization with this infected cell vaccine (ICV) protected mice from subsequent tumor challenge, and expression of granulocyte–monocyte colony stimulating factor (GM-CSF) by the virus (VSVgm-ICV) increased efficacy. Immunization with VSVgm-ICV in the VSV-resistant B16-F10 model induced maturation of dendritic and natural killer (NK) cell populations. The challenge tumor is rapidly infiltrated by a large number of interferon γ (IFNγ)-producing T and NK cells. Finally, we demonstrate that this approach is robust enough to control the growth of established tumors. This strategy is broadly applicable because of VSV's extremely broad tropism, allowing nearly all cell types to be infected at high multiplicities of infection *in vitro,* where the virus replication kinetics outpace the cellular IFN response. It is also personalized to the unique tumor antigen(s) displayed by the cancer cell.

Received 14 February 2012; accepted 1 June 2012; advance online publication 3 July 2012. doi:10.1038/mt.2012.128

INTRODUCTION

The current standard of care for cancer treatment is associated with severe off-target effects due to poor selectivity of the agent for cancer cells. New targeted therapeutics often target only one gene or pathway in a cell, allowing for resistance to easily evolve.[1] Likewise, cancer immunotherapies, though making great strides in recent years, are still focused on identifying one or very few tumor-associated antigens that can be targeted. However, tumors can rapidly evolve immune evasion and immune suppression mechanisms countering these therapies, leading to treatment failure.[2,3] As well, tumors are antigenically heterogeneous[4,5] as a result of high genetic instability.[6] In theory, a vaccine presenting the spectrum of tumor antigens could allow for the *in vivo* selection of the optimum epitope(s) to target.

Oncolytic viruses (OVs) have emerged as a promising anticancer treatment platform, able to specifically replicate in and kill cancer cells while leaving normal cells unharmed. Though engineered for tumor-specific lysis, the multimodal nature of this platform is currently being revealed. Many of these viruses can be delivered systemically to reach distant tumor beds,[7] be targeted to tumor vasculature to induce tumor vascular shutdown,[8,9] and be engineered to carry genetic payloads. Importantly, preclinical and clinical evidence for OV-mediated antitumor immunity is emerging.[10] Recent results from a phase II clinical trial with OncoVex$^{GM\text{-}CSF}$, an oncolytic HSV expressing granulocyte–monocyte colony stimulating factor (GM-CSF), have demonstrated that patients treated with this platform have a very different tumor immune landscape. These tumors had significantly lower regulatory T cells and higher $CD8^+$ effector T cells in the tumor.[11]

Previous research by our lab has demonstrated that a vesicular stomatitis virus (VSV) harboring a deletion in the M protein at position 51 (VSV-Δ51) is very sensitive to interferon (IFN)[12] and neutralizing antibody,[13] which act to clear virus from the host. Antitumor immune stimulation may be important for the ongoing tumor destruction once the virus is cleared, and offers the potential to restore immune surveillance mechanisms that can lead to complete responses and prevent recurrence. Wild-type VSV has been observed to induce antitumor immune responses in models expressing exogenous antigens[14] and has now been demonstrated to be a potent boost in an elegant prime/boost oncolytic vaccination model.[15,16] Strategies that allow us to exploit the antitumor immunity induced through virus replication and lysis will be vital to using the full potential of these viruses. Herein we describe an infected cell vaccine (ICV) platform that presents a multitude of tumor antigens in the context of a robust OV infection.

The last two authors contributed equally to this work.

We demonstrate that this leads to potent immune stimulation and ultimately activates both natural killer (NK) cells and T cells for tumor debulking and long-term cancer surveillance. In addition, no prior knowledge on the tumor antigens is required to make this vaccine.

RESULTS

T cells are required for VSV-mediated long-term tumor regression

Many OV platforms have been observed to induce antitumor immune responses.[17–20] We examined the role of the T cell compartment in oncolytic VSV-Δ51 treatment of cancer. A VSV-sensitive clone of colon carcinoma tumors (CT26.LacZ) was established in immunocompetent and athymic nude mice. When tumors were palpable, mice were treated with six intravenous (i.v.) doses of VSV-Δ51-GFP, UV-inactivated VSV, or phosphate-buffered saline (PBS). In the immune-competent mice, only those treated with VSV-Δ51-GFP had measurable responses, with 60% of the mice demonstrating complete tumor clearance (**Figure 1a,b**). The athymic nude mice initially responded to VSV treatment, demonstrating stable tumor sizes, but showed marginal long-term efficacy, with only 1 out of 10 mice having a durable response (**Figure 1c,d**). This suggests that the T-cell compartment is required for long-term tumor eradication following systemic VSV therapy in this model.

Subsequently, immune-competent mice demonstrating long-term complete responses were used as splenocyte donors in an adoptive cell transfer. Naive immune-competent mice that received splenocytes from VSV-treated and cured mice were not susceptible to CT26.LacZ tumor growth, but were susceptible to syngeneic 4T1 growth (**Figure 1e**). Splenocytes from naive mice and CT26.LacZ tumor-bearing untreated mice were not able to protect against subsequent tumor challenge. Therefore, a specific and long-lived antitumor immune response is generated through treatment with oncolytic VSV.

UV-inactivated VSV was not able to induce any efficacy in the CT26 subcutaneous model (**Figure 1a**). This leads us to reason that VSV replication in the tumor cells is required for immune stimulation. CT26.LacZ tumors are very sensitive to VSV and demonstrate robust infection by immunohistochemistry at 24 hours following i.v. administration (**Figure 1f**). Conversely, B16-F10 cells do not demonstrate any VSV replication in i.v.-treated tumors (**Figure 2a**) and B16-F10 tumor-bearing mice have no response to VSV-treatment (**Figure 2b,c**), further demonstrating the importance of replication in efficacy. Previous research by Breitbach *et al.*[8] demonstrates that after i.v. administration, UV-inactivated VSV is undetectable in tumor sections using the methods described in the current manuscript. The viral proteins found in the tumor sections in **Figures 1** and **2** must result from productive virus replication and spread and not simply tumor-specific accumulation of viral particles.

VSV infection is a potent immune stimulator in a prophylactic ICV

We have so far demonstrated that VSV replication in a permissive tumor can elicit a therapeutic antitumor T-cell response. We postulated whether we could generate a sufficiently robust

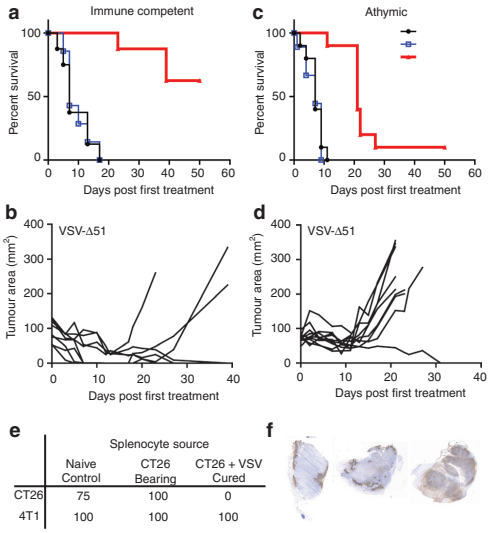

Figure 1 Vesicular stomatitis virus (VSV) treatment induces a potent antitumor immune response, on which treatment is dependent. (**a**,**b**) Balb/C or (**c**,**d**) athymic nude mice were injected subcutaneously with CT26.LacZ cells. Immune-competent Balb/C mice were treated starting on day 14 post-tumor implantation and nude mice were treated on day 10 to reflect a slightly faster onset of tumor development. Mice were injected six times with 5×10^8 plaque-forming unit (pfu) of VSV-Δ51-GFP intravenous (i.v.) or equivalent amount of UV-inactivated VSV-Δ51 or phosphate-buffered saline (PBS). (**a**) Kaplan–Meier survival analysis of VSV-Δ51-GFP treatment in Balb/C mice. $N = 8$ per group. Statistical significance verified by the log rank test, where $P < 0.0001$. (**b**) Tumor area growth over time plotted only for VSV-Δ51-GFP-treated mice. (**c**) Kaplan–Meier survival analysis of VSV-Δ51-GFP treatment in nude mice. $N = 10$ for each group. Statistical significance verified by the log rank test, where $P < 0.0001$. (**d**) Tumor area growth over time plotted only for VSV-Δ51-GFP-treated mice. (**e**) Splenocytes were harvested from either naive mice, CT26.LacZ tumor-bearing mice, or CT26.LacZ tumor-bearing mice cured with six doses of VSV-Δ51-GFP. These splenocytes were injected i.v. into naive Balb/C mice, which were challenged subcutaneously 48 hours later with CT26.LacZ cells and 4T1 cells on the contralateral flank. (**f**) Balb/C mice-bearing CT26.LacZ subcutaneous tumors were injected i.v. with 5×10^8 plaque-forming unit (pfu) of VSV-Δ51. Two days later, mice were euthanized; tumors were harvested, and frozen. Sections were stained by immunohistochemistry (IHC) for VSV.

therapeutic response in VSV-resistant B16-F10 cells by infecting them *ex vivo* and presenting this cocktail as an ICV. This would bypass the necessity for *in vivo* replication to mount an antitumor immune response. Though B16-F10 cells are not readily permissive to VSV following i.v. delivery, we can achieve complete infection by infecting the cells *in vitro* at a high multiplicity of infection (**Supplementary Figure S1a**).

As a means of determining the immunogenicity of such a vaccine, γ-irradiated tumor cells were infected and assessed for their ability to provide protection against a future tumor challenge (**Figure 3a**). This VSV-ICV was administered intraperitoneally (i.p.) to mice on days 0 and 7, with a tumor challenge on day 14 (**Figure 3b**).

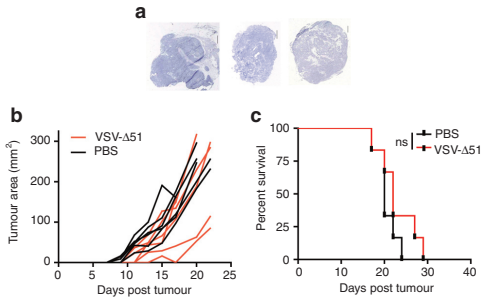

Figure 2 Vesicular stomatitis virus (VSV) replication is poor in B16-F10 tumors and leads to no efficacy. (**a**) C57BL/6 mice-bearing B16-F10 subcutaneous tumors were injected intravenously (i.v.) with 5×10^8 plaque-forming unit (pfu) of VSV-Δ51. Two days later, mice were euthanized, and tumors were harvested and frozen. Sections were stained by immunohistochemistry (IHC) for VSV. (**b**) C57BL/6 mice-bearing B16-F10 subcutaneous tumors were injected three times a week starting on day 6 for a total of six doses of VSV-Δ51 i.v. Tumor area growth over time plotted for PBS (in black) and VSV-Δ51 treated (in red). $N = 6$ per group. (**c**) Kaplan–Meier survival analysis with statistics examined by log rank test where $P > 0.2$.

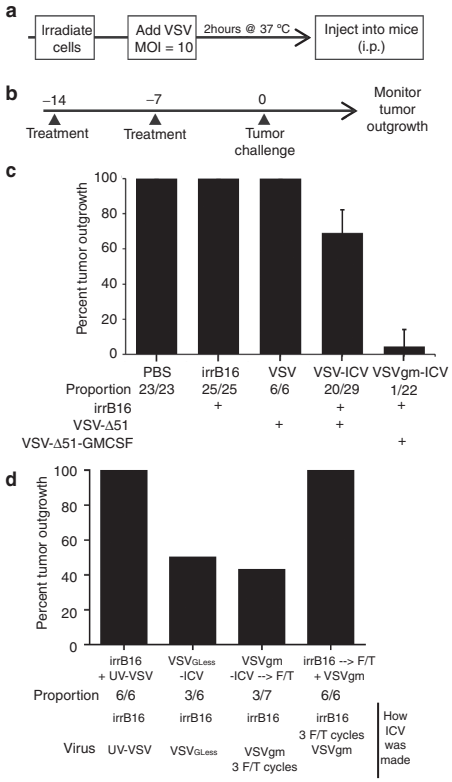

Figure 3 Vesicular stomatitis virus (VSV) acts as a potent adjuvant in a prophylactic B16-F10 infected cell vaccine. (**a**) Schematic representing preparation of infected cell vaccine (ICV). (**b**) Prophylactic ICV treatment timeline in days. (**c**–**d**) C57BL/6 mice were immunized with various control or vaccine preparations according to the timeline in (**b**). They were then challenged with 1×10^5 B16-F10 cells subcutaneously and tumor outgrowth was monitored. (**c**) Shown is the weighted mean + weighted standard deviation of final tumor outgrowth for each group, averaged from results from multiple experiments. The total number of mice tested, with the fraction exhibiting tumor growth is listed below the graph. (**d**) Shown is the percent outgrowth from the one experiment in which that condition was tested.

The immunization of mice with γ-irradiated B16-F10 cells infected with VSV-Δ51-GFP was able to completely protect 30% of mice tested (9 protected/29) from later live cell challenge (**Figure 3c**). Control groups immunized with PBS or γ-irradiated B16-F10 cells demonstrate complete susceptibility to the tumor challenge. These results were also verified in a different mouse strain with the parental CT26.wt cell line (**Supplementary Figure S2**). Like the B16-F10 cells, and unlike the clone CT26. LacZ, the parental CT26.wt cells are not permissive to *in vivo* VSV infection.

GM-CSF expression by VSV enhances immune activation by the VSV-ICV

GM-CSF is a potent immunostimulating cytokine able to increase monocyte and macrophage migration and activation.[21] To increase the immune stimulation properties of our vaccine, GM-CSF was cloned into the VSV-Δ51 genome and expression was confirmed by western blot (data not shown). The ICV made with VSV-Δ51-GMCSF (VSVgm-ICV) prevented B16-F10 tumor engraftment in over 95% of mice tested (21 protected/22) (**Figure 3c**). Due to the heightened efficacy of this approach, we chose the VSV-Δ51-GMCSF virus for further characterization. The VSV-Δ51-GMCSF virus was tested as a direct oncolytic alongside VSV-Δ51-GFP in the B16-F10 subcutaneous model and it demonstrated no increased efficacy (**Supplementary Figure S1b**).

Replication beyond the infected cells of the vaccine is not required for full ICV efficacy

We examined whether virus replication and spread or tumor cell integrity were important for ICV efficacy. UV-inactivated VSV lacks the ability to express gene products and was unable to confer any protection (**Figure 3d**). G-Less VSV is a recombinant that lacks the gene encoding the glycoprotein, but is grown in cells expressing VSV G. This virus infects cells and expresses N, M, L, and P genes. It can package new virions, though these are not infectious.[22] This virus was able to protect the same proportion of mice as the VSV-ICV in this experiment (**Supplementary Figure S3**). These viruses are compared to VSV-Δ51-GFP because neither UV-inactivated nor G-Less virus expresses GM-CSF. To determine the importance of cellular integrity to the efficacy of the vaccine, vaccine preparations were attempted in two other methods. γ-Irradiated B16-F10 cells were first freeze/thawed multiple times before being mixed with VSV-Δ51-GMCSF (irrB16 –> F/T + VSVgm). Compared to the regular VSVgm-ICV, this preparation was not able to protect any of the six mice treated. Alternatively,

the VSVgm-ICV was made as per usual but freeze/thawed multiple times before injection (VSVgm-ICV –> F/T). This preparation protected only four out of seven mice.

Taken together, these results indicate that in two VSV-resistant cancer models tumor cells infected with VSV-Δ51 can stimulate an antitumor immune response that is capable of protecting mice from a later tumor challenge. In addition, the expression of GM-CSF from infected cells greatly increased the immunization capabilities of the ICV in the B16-F10 model. Interestingly, it seems that cellular integrity is important in conferring immunological protection from this vaccine but virus only needs basal replication within the cells constituting the vaccine, as demonstrated by the VSV_{GLess}-ICV. Whether it is simply transcription or genome replication that is required is not presently clear.

VSVgm-ICV induces rapid innate immune activation

We next examined the activation of early innate cells following VSVgm-ICV treatment. Splenocytes were harvested at 24 hours post-treatment and dendritic cells (DCs) evaluated for markers of activation. Mice treated with either VSVgm alone or VSVgm-ICV had a higher proportion of activated DCs. This is demonstrated by a higher frequency of cells expressing MHC II and CD86, as well as higher expression levels of these activation markers (**Figure 4a–c**).

In addition, splenic lymphocytes were examined for early activation through CD69 expression early after treatment with the VSVgm-ICV. CD69 is a marker of early lymphocyte activation and is not found on naive lymphocyte populations.[23,24] Lymphocytes from VSVgm-ICV-treated mice demonstrate dramatically higher degrees of early activation than control animals (**Figure 4d**). In keeping with this finding, at 24 hours post-treatment, a higher frequency of blood NK cells from VSVgm or VSVgm-ICV-treated mice express IFNγ and more of the cytokine is expressed per cell (**Supplementary Figure S4a,b**). However, not surprisingly, NK cells are no longer expressing IFNγ in the blood on the day of tumor challenge (**Supplementary Figure S4c,d**).

VSVgm-ICV increases tumor infiltration by activated T and NK cells

To understand what cell types are responsible for tumor rejection in the B16-F10 model following VSVgm-ICV treatment, we implanted the challenge flank tumor in matrigel, thereby allowing us to easily resect and disaggregate the tumor (**Figure 5a**). Mice were injected with Brefeldin A 6 hours before tumor harvest. This allows us to determine the expression profiles of tumor infiltrating cells while they are in the tumor environment. We determined that T cells are 10 times more numerous in the tumor following vaccination with the VSVgm-ICV than with irradiated cells alone or VSVgm (**Figure 5c**). This difference is even larger when compared to the PBS-treated mice, with 30 times more T cells in the treated tumor. Indeed, over 8% of the tumor cellular content is T cells, equal to a ratio of one T cell for every 12.5 tumor cells (**Supplementary Figure S5a**). Importantly, there is also a much greater number of $CD3^+$ $IFN\gamma^+$ cells in the tumor following VSVgm-ICV than in any control group (**Figure 5b,d** and **Supplementary Figure S5b**).

In addition to a significant increase in T cells in the challenge tumor, VSVgm-ICV-immunized mice have 4–13-fold more NK cells (**Figure 5e**). Importantly, there are more NK cells producing either IFNγ or Granzyme B (**Figure 5g**), and there are more NK cells expressing both IFNγ and Granzyme B (**Figure 5f**).

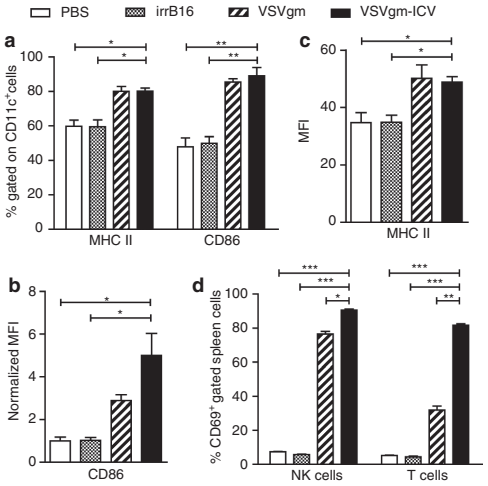

Figure 4 The VSVgm-infected cell vaccine (ICV) leads to dendritic cell and lymphocyte early activation in the spleen within 24 hours of vaccination. C57BL/6 mice were immunized with the VSVgm-ICV or relevant controls i.p. and euthanized 24 hours later. Splenocytes were stained and examined by flow cytometry for dendritic cell markers of activation. (**a**) Percent of $CD11c^+$ cells that express MHC II and/or CD86. (**b**) Mean fluorescence intensity of MHC II staining on $CD11c^+$ cells. (**c**) Mean fluorescence intensity of CD86 staining on $CD11c^+$ cells normalized to phosphate-buffered saline (PBS) levels. $N = 3$ mice per group, except for VSVgm-ICV that had four mice. (**d**) C57BL/6 mice were immunized with the VSVgm-ICV or relevant controls i.p. and euthanized 15 hours later. Splenocytes were stained and examined by flow cytometry for NK and T cells markers in addition to CD69. Percent of indicated cells that express CD69. All data presented as mean + SEM with three mice per group. P values, $^*P < 0.05$, $^{**}P < 0.005$, $^{***}P \leq 0.0001$.

A VSVgm-ICV reduces tumor burden in the therapeutic setting

Having demonstrated that a VSVgm-ICV can protect mice from a tumor challenge, we sought to examine the vaccine's potency in more relevant therapeutic models, through the treatment of mice that have already been inoculated with tumors. C57BL/6 mice bearing B16-F10 subcutaneous tumors were treated i.p. with VSVgm-ICV, irrB16, VSVgm, or PBS control (**Figure 6a**). Animals treated with the VSVgm-ICV had a dramatic delay in tumor growth (**Figure 6b**). In contrast, treatment with oncolytic VSV-Δ51-GMCSF had similar tumor growth to PBS-treated animals. Treatment with γ-irradiated B16-F10 cells led to marginally delayed tumor growth compared to the other control groups, though this is not statistically significant.

A systemic dissemination model was also undertaken to examine the effectiveness of this vaccine. Mice were given B16-F10 cells i.v., leading to tumor seeding mostly in the lung, though macroscopic tumors can also occur in the thymus, kidneys,

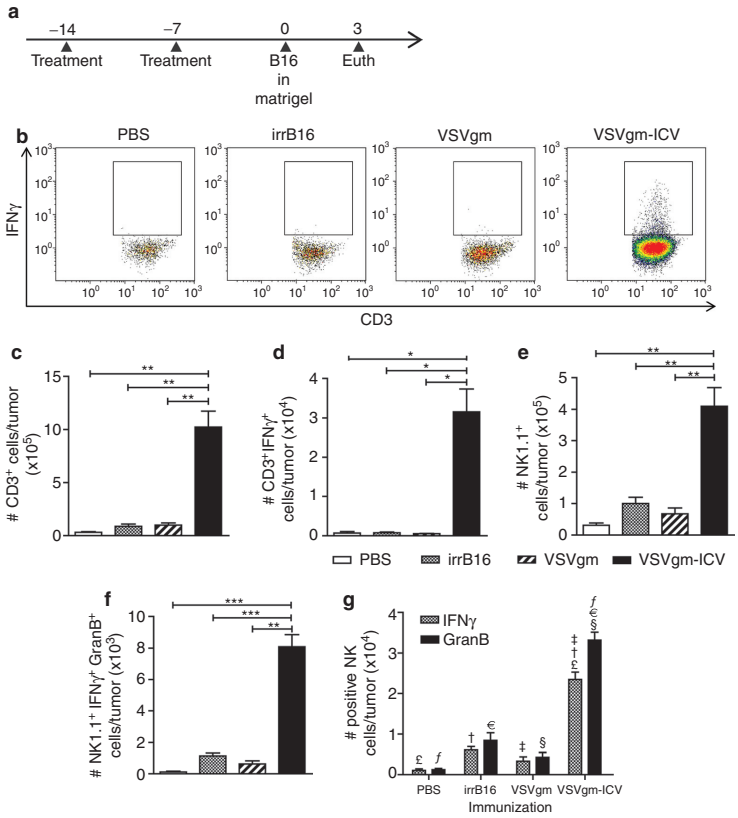

Figure 5 Prophylactic immunization with the VSVgm-infected cell vaccine (ICV) leads to robust activated T cell and NK cell infiltration of the challenge tumor. (**a**) C57BL/6 mice were prophylactically immunized as described earlier with VSVgm-ICV or controls. B16-F10 cells in matrigel were subcutaneously injected on day 0. On day 3, mice were injected intravenously (i.v.) with brefeldin A, then 6 hours later were euthanized. Tumors were resected on day 3 for enzymatic disaggregation and flow cytometric analysis. (**b**) Representative dot plots demonstrating $CD3^+$ cells expressing IFNγ. (**c**) The average total number of $CD3^+$ cells per tumor in each group. (**d**) The average total number of $CD3^+$ $IFN\gamma^+$ cells per tumor in each group. (**e**) The average total number of $NK1.1^+$ cells per tumor in each group. (**f**) The average total number of $NK1.1^+IFN\gamma^+GranzymeB^+$ cells per tumor in each group. (**g**) The total number of $NK1.1^+IFN\gamma^+$ cells and $NK1.1^+GranzymeB^+$ cells per tumor in each group. *P* values, £, †, ‡, ∫, §, and ∈ are all $P \leq 0.005$. All data are presented as mean + SEM with five mice per group. *P* values, * $P < 0.05$, ** $P < 0.005$, *** $P \leq 0.0005$.

and ovaries. Treatments were initiated the following day and all mice were euthanized on day 22 to examine tumor burden (**Figure 6c**). Treatment with VSVgm-ICV demonstrated undetectable tumor burden at the time of sacrifice in 80% of mice and no other tumors were found in any of the animals (**Figure 6e,d**). In contrast, control-treated mice demonstrated heavy tumor burden: 3 PBS-treated mice, 1 VSVgm-treated mouse, and 1 irrB16-treated mouse had large growths in locations other than the lung. Another PBS-treated mouse was found dead before scheduled euthanizing. Lung weights demonstrated that the VSVgm-ICV-treated mice had a much lower tumor burden than controls, identical to non-tumor–bearing mouse lungs. As a more stringent test of the VSVgm-ICV's therapeutic potential, treatments were started on days 3 or 4 after tumor seeding. In both cases two of four VSVgm-ICV-treated mice had no visible lung tumors at the time of sacrifice, whereas all irrB16-treated mice had significant tumor burden (**Supplementary Figure S6**). Treatments beginning later than day 4 were not attempted and so it remains to be seen if efficacy can be achieved while delaying treatments further.

A spontaneous model of ovarian cancer also demonstrated therapeutic benefit from the VSVgm-ICV (**Supplementary Figure S7**). These transgenic mice develop spontaneous bilateral ovarian tumors driven by the SV40 TAg.[25] The vaccine was made with the 6048R cell line that had been previously established from one such tumor. Though normal ovary weights were not quantified, one VSVgm-ICV-treated mouse had normal appearing ovaries and these weighed 0.05 g in total.

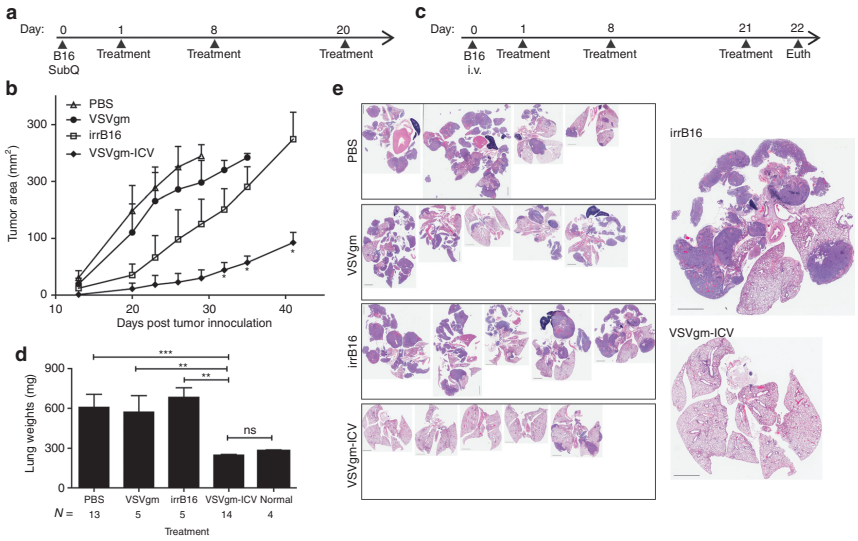

Figure 6 Treatment with the VSVgm-infected cell vaccine (ICV) can significantly impact tumor growth in subcutaneous and systemic models. (**a**) C57BL/6 mice were implanted with B16-F10 subcutaneous tumors and treated according to the presented timeline. (**b**) Tumor area was monitored and is shown in days following tumor implantation as mean + SEM with five mice per group, except for the VSVgm only group that had four. (**c**) C57BL/6 mice were injected intravenously (i.v.) with B16-F10 cells and treated according to presented timeline with the VSVgm-ICV or controls. Mice were euthanized on day 22, and their lungs were weighed and fixed in 10% formalin. Lungs were then sliced and analyzed by hematoxylin and eosin (H&E) staining. (**d**) Lung weights shown are pooled from two separate experiments and presented as mean + SEM with variance analysis by Mann–Whitney test. Normal lungs are those from mice that have not received any lung tumors or treatments. (**e**) Hematoxylin and eosin (H&E) staining of all mice in one experiment with representative sections demonstrating tumor burden at endpoint. All lungs are on the same scale, with black bar indicating 2 mm. A higher magnification of a representative vaccine and control-treated lung are presented on the right. One phosphate-buffered saline (PBS) mouse had the heart buried in tumor, and so the organ could not be removed. A few control mice had tumors in their thymus and so these organs were kept in the H&Es and weights. *P* values, * $P < 0.05$, ** $P < 0.005$, *** $P \leq 0.0001$.

These results highlight the potency of this vaccine platform; able to initiate antitumor immune responses that can single-handedly slow the progression of highly aggressive and VSV-resistant tumors.

DISCUSSION

Several recent studies have reported the very important role the immune system plays in tumor clearance. Indeed the quantity and quality of $CD8^+$ T cells found in the tumor is one of the strongest favorable prognostic markers in many cancer types.[25] Not surprisingly, cancers evolve multiple mechanisms of immune evasion and suppression.[26]

OVs are emerging as promising clinical candidates that target tumors at multiple fronts. Importantly, many have been observed to stimulate antitumor immune responses when replicating in permissive tumors.[10] However, not all tumors are permissive to these viruses. We sought to optimize and test an OV vaccine that could be used with all tumor types, regardless of *in vivo* permissivity; harnessing the antitumor immune response generated when an immunogenic virus replicates in tumor cells.

We observed that the efficacy obtained with VSV-Δ51 in the permissive CT26.LacZ colon cancer model is largely dependent on an intact T-cell compartment and that mice cured with this OV treatment generate a robust antitumor immune response (**Figure 1**). However, this efficacy does not translate to tumor models that are resistant to the viral doses achieved in systemic delivery of VSV (**Figure 2**). We propose that the deficit in efficacy due to the lack of *in vivo* replication could be overcome by infecting γ-irradiated tumor cells *in vitro*, and then injecting this ICV into the mouse. Indeed an ICV using VSV-Δ51-GFP was able to protect 30% of mice from future B16-F10 tumor challenge in a prophylactic setting (**Figure 3c**). Interestingly, cloning the cytokine GM-CSF into the viral genome greatly increased the potency of the ICV. The VSVgm-ICV protects 95% of mice from future tumor challenge. GM-CSF enhances the recruitement and activation of antigen presenting cells.[21] However, further studies are required to fully elucidate the role of GM-CSF in this vaccine.

Though UV-inactivated VSV does not lead to sufficient immune stimulation, a G-Less VSV was able to recapitulate the tumor protection achieved with fully replication competent virus (**Figure 3d**). Therefore a basal level of viral transcription/replication is required, though it need not replicate beyond the initially infected cells that constitute the vaccine. We also observed a requirement for cellular integrity, thus, it is reasonable to hypothesize that this vaccine does not simply present viral danger signals in the context of tumor antigens. Instead, we speculate that viral infection of cells initiates critical immunogenic processes that,

coupled with tumor-associated antigens, lead to robust immune activation. In addition, viral infection of an intact cell is quite immunogically relevant, offering persistent toll-like receptor ligation required for a robust immune response.[27]

Treatment with the VSVgm-ICV leads to rapid innate immune activation seen in the spleen and blood (**Figure 4**, and **Supplementary Figure S4**). In many cases, VSVgm leads to the same level of early immune activation as does the vaccine. VSV injected i.p. will productively infect the first cells it encounters, thereby initiating similar immune activation due to viral infection. However, no antitumor immune responses were detected at late timepoints with VSVgm alone (**Figures 5** and **6**) and importantly no auto-immune sequelae have ever been observed with VSVgm treatment, whether i.p. or i.v. (data not shown).

Though the VSVgm-ICV is demonstrated to activate NK cells 24 hours after prophylactic vaccination, they do not likely play a role in challenge tumor rejection as tumor implantation occurs after NK cells have returned to baseline (**Supplementary Figure S4**). Importantly, NK cell activation following VSVgm-ICV should have a significant role in a therapeutic setting, through the early debulking of the existing tumor and through the induction of inflammation at the tumor site. Though seemingly related to the vaccination, we believe that the NK cell infiltration and activation observed in the challenge tumor following VSVgm-ICV is in fact a consequence of activated T cell infiltration (**Figure 5**). Previous research indicates that T cells can activate NK cells in this manner.[28] NK cells have been demonstrated to be important mediators of early tumor debulking and in cytokine secretion, which further amplifies Th1 responses.[29–31] Certainly, the large quantity and activated nature of the T cells observed infiltrating the B16-F10 challenge tumor only 3 days after implantation indicates that the VSVgm-ICV initiates an effective Th1 T cell response.

The activity of this vaccine is highlighted by its impact in therapeutic models of cancer (**Figure 6** and **Supplementary Figures S6** and **S7**). Importantly, therapy could be delayed to 4 days after systemic dissemination, while still providing a therapeutic benefit. In some cases, the vaccine is delivered in a completely separate anatomical compartment and yet leads to significant tumor clearance. Further studies will focus on better understanding the critical immunological components that lead to this efficacy.

The concept of using virally infected cells as a cancer vaccine has been previously investigated in both mouse models and human patients[32–35] with some success, though few have investigated the immunological basis for this efficacy. Clinical trials using NDV-infected autologous and allogeneic melanoma cells demonstrated impressive 10 and 15-year survival data.[36,37] However, many of these approaches used inactivated virus, replication-defective, or non-lytic strains. Of note, Livingston *et al.* used wild-type VSV to infect melanoma cell lines to create a vaccine, though observed very limited responses. However, in this case the infected cells were swelled, homogenized, enucleated, and the virus UV-inactivated before treatment.[38] The results we have presented in this manuscript suggest that intact cells and replication competent lytic virus is much more immunogenic. We used an oncolytic strain of VSV so as to minimize toxicity, while allowing us to keep actively, yet locally, replicating virus as part of the vaccine. In addition, in virus-permissive tumor models, there might be an added benefit of tumor debulking and local inflammation in the tumor microenvironment provided by the OV.

Though other immunotherapies have also achieved therapeutic efficacy in the B16-F10 tumor model, the VSVgm-ICV achieves this while requiring no previous knowledge about the relevant tumor antigens[15] or the immunosuppressive mechanisms employed by the tumor. Importantly, the ICV is relatively simple to prepare, requiring no long-term *ex vivo* manipulations.[39,40]

The ICV platform would be best coupled to a debulking treatment that might also stimulate the immune system. Local tumor irradiation may help with tumor debulking and has been demonstrated to increase inflammation in the tumor environment,[41] leading to enhanced immunotherapeutic responses.[42,43] An ideal scenario might include first surgically removing the tumor, using this tumor bulk to create the VSV-ICV, and then treating the patient to reduce metastatic recurrence.

The ICV is a promising immunotherapeutic platform that achieves the stimulation of both innate and adaptive immune cells. The potency of the ICV is highlighted by the significant impact it has on the progression of an aggressive and immunosuppressive tumor. In addition, the use of autologous tumor leads to a personalized vaccine that can potentially present the full range of a patient's unique tumor antigens. Recently, Castle *et al.*[44] have shown that the B16-F10 tumor cell line has acquired over 500 somatic mutations that could, in principle, encode numerous novel immunogenic epitopes. Despite this, γ-irradiated B16-F10 cells, on their own, are ineffective in stimulating antitumor immunity, probably due to the lack of danger signals. Here, we show that infection of B16-F10 cells makes them a very potent vaccine platform that has the capacity to induce both a protective and therapeutic immune response. Since the B16-F10 cell line expresses a vast array of potential neo-antigens, perhaps many of these could now be made visible to the immune system when presented as an ICV. It is possible that because of this, the ICV has the potential to induce a broadly active T-cell response against a spectrum of neo-antigens. Currently, we have no data to support this notion, however studies are underway to determine the number and nature of mutant epitopes that the cellular immune system recognizes in B16-F10 cells following infected cell vaccination. It remains possible that our ICV approach simply focuses a robust response on a single or limited number of tumor antigens.

MATERIALS AND METHODS

Cell lines and mice. CT26.WT and CT26.LacZ (also known as CT26.CL25) colon carcinoma, 4T1 breast cancer, and B16-F10 melanoma cells were purchased from the American Type Culture Collection (Manassas, VA) and the B16-F10.LacZ were a gift from Dr Ann F Chambers. All were cultured in HyQ Dulbecco's modified Eagle's medium (high glucose) (HyClone, Logan, UT) supplemented with 10% fetal calf serum (CanSera, Etobicoke, Ontario, Canada). 6048R cells (gift from Dr Vanderhyden) were grown in αMEM with 10% fetal bovine serum, 2.08 μg/ml epidermal growth factor (R&D Systems, Minneapolis, MN), 1× of ITSS (Roche, Montreal, CA), gentamicin, and penicillin/streptomycin (Invitrogen, Burlington, CA).

Female 6-week-old Balb/C, C57BL/6, and CD1 nude mice were purchased from Charles River Laboratories (Wilmington, MA). Female 8-week-old FVB/N MISIIRTAg transgenic mice (line tg4568—a gift from Dr Vanderhyden) were generated using the transgene described by Connolly *et al.*[45] These mice develop bilateral ovarian tumors of epithelial origin with full penetrance and typically endpoint at 14 weeks of age.

All experiments were conducted with the approval of the University of Ottawa Animal Care and Veterinary Service. Tumor Area is calculated by multiplying the width by the length of the tumor.

Virus. VSV-Δ51-GFP and VSV-Δ51-GMCSF were grown in Vero cells and purified by centrifugation or sucrose gradient banding and centrifugation. VSV-GLess was grown on 293G cells. Virus stocks were aliquoted in PBS, kept at –80 °C, used once, and then discarded. VSV-Δ51-GMCSF was cloned using PCR primers to murine GM-CSF and amplified off the pcDNA4.1-GMCSF vector. GM-CSF was cloned into the VSV-Δ51 vector at the *Xho*I and *Nhe*I sites between the G and L genes.

Direct treatment model and immunohistochemistry. Subcutaneous tumors were established by injecting 3×10^5 CT26.LacZ or B16-F10 cells in PBS on the hind flank of the mouse. Tumors were allowed to grow until palpable, six treatments were then administered i.v. for 2 weeks, every monday, wednesday, and friday, unless otherwise stated. VSV-Δ51 was used at 5×10^8 plaque-forming unit (pfu)/100 µl. To analyze VSV replication in CT26.LacZ and B16-F10 tumors following i.v. delivery, Balb/c or C57BL/6 mice were implanted with tumors subcutaneously and tumors were allowed to grow until reaching a sufficient size to dissect. Mice were then injected i.v. with 5×10^8 pfu/100 µl. Forty eight hours after injection, mice were euthanized, tumors were excised, and frozen in Shandon Cryomatrix freezing medium (TermoElectron, Waltham, MA) in liquid nitrogen. Five microgram sections were stained by immunohistochemistry with rabbit anti-serum raised against VSV (gift of Dr Earl Brown) at a 1/5,000 dilution for 30 min. Secondary antibody and ABC reagents were used as directed from the Vectastain ABC kit and Horseradish peroxidase activity was assessed using a Diaminobenzene-HRP kit (KPL Biosciences, Guelph, Ontario, Canada). Nuclei were counterstained with hematoxylin. Images were obtained using an Epson Perfection 2450 Photo Scanner.

Rechallenge and splenocyte transfer. Mice were treated as in the direct oncolysis model with six doses of VSV at 5×10^8 pfu/100 µl i.v. Once tumors were palpable. Mice that had complete responses were kept for at least 3 months to ensure long-term responses. Splenocytes were harvested and purified by Lympholyte-M gradient from mice that were naive, had a tumor but received no treatment, or cured by VSV treatment. 5×10^7 of these isolated splenocytes were transferred to naive mice i.v., and these mice were then challenged 48 hours later with 3×10^5 CT26.LacZ cells on the right hind flank or 4T1 cells on the left flank. Tumor outgrowth was monitored.

ICV. Tumor cells were harvested from tissue culture and aliquoted in Eppendorf tubes at 2×10^7 cells/200 µl in PBS. These were γ-irradiated for 30Gy (CT26.wt), 45Gy (6048R), or 60Gy (B16-F10) in a Pantak HF320 X-Ray machine. Virus or PBS was added to the tubes at 2×10^8 pfu in 200 µl of PBS and incubated at 37 °C for 2 hours. The mixture was then injected in mice, 100 µl i.p.; therefore giving each mouse 5×10^6 γ-irradiated cells and 5×10^7 pfu of virus per dose. For **Figure 3f**, the "irrB16 → F/T + VSVgm" sample was γ-irradiated, then subjected to 3 freeze/thaw cycles in a dry ice bath and 42 °C water bath. Cells were then mixed with VSVgm before injection into the animal. Conversely, for the "VSVgm-ICV → F/T" sample, the ICV was made as usual and following the 2 hour infection the mixture was subjected to 3 freeze/thaw cycles before injection as detailed above. In the prophylactic model, mice were immunized on days –14 and –7, and then challenged with 1×10^5 live tumor cells subcutaneously on day 0. For the therapeutic model, mice were given 1×10^5 B16-F10 cells subcutaneously on day 0 or 7×10^4 B16-F10 cells i.v., and then vaccinated on days 1, 8, and 20 i.p. For the 3 and 4 day B16-F10 i.v. model, mice were treated on days 3, 10, and 22 or 4, 11, and 23, and then euthanized on day 28 to determine lung tumor burden.

In subcutaneous models, tumor measurements were determined with callipers until end point was reached. In i.v. model, endpoint was reached when mouse demonstrated severe respiratory distress, had a mass larger than 15 mm, or predetermined experimental endpoint was reached. Lungs were removed and fixed in 10% formalin for at least 3 days. These were then blotted dry and weighed. Lungs were then paraffin embedded and slices were analyzed by hematoxylin and eosin staining. Pictures were taken on the Aperio ScanScope (Axiovision Technologies, Toronto, Ontario, Canada) and analyzed using Aperio ImageScope software (Axiovision Technologies, Toronto, Ontario, Canada).

Flow cytometry. Spleens and blood were harvested from mice at indicated timepoints, red blood cells were lysed using ACK lysis buffer, and resuspended in RPMI + 10% fetal bovine serum. For examination of DC maturation, cells were stained with cell surface antibodies for CD11c-PE-Cy7 (clone N418; eBioscience), CD86/B7-1 (clone GL1; eBioscience, San Diego, CA), and MHC class II-FITC (clone M5/114.15.2l eBioscience). For early lymphocyte activation, splenocytes were stained with CD3-PerCP (clone 17A2; R&D Systems), DX5-PE (BD Bioscience), and CD69-FITC (clone H1.2F3; BD Biosciences). All flow cytometry was performed on a Beckman Coulter CyAn and data analyzed with Kaluza v1.1 software. For the examination of NK cell activation splenocytes were restimulated for 1.5 hours with PMA and ionomycin, during the last hour GolgiPlug (BD Biosciences) was added. These cells were then stained with CD3-PerCP (clone 17A2; R&D Systems), DX5-PE, Granzyme-B-PE-Cy7 (clone 16G6; eBioscience), and IFNγ-FITC (clone XMG1.2; eBiosciences) and examined by flow cytometry.

Examination of cellular infiltrate of matrigel challenge tumor. Following the regular prophylactic immunization schedule mice were challenged with 3×10^5 B16-F10 cells resuspended in 300 µl of matrigel (BD Biosciences). 6 hours before euthanasia, mice were treated i.v. with 0.25 mg Brefeldin A (Sigma, Oakville, Canada) as previously published.[46] Mice were euthanized and matrigel plugs were excised from the flank and disaggregated using a cocktail of collagenase type IV (Cooper Biomedical, Malvern, PA), Dispase, and DNase I (Invitrogen) resuspended in HBSS. This mixture was then washed and stained with surface antibodies: anti-CD3-PE (clone 17A2; BD Biosciences) or anti-NK1.1-PE (clone PK136; BD Biosciences). Cells were then permeabilized and fixed (BD Cytofix/Cytoperm; BD Biosciences) and stained with intracellular antibodies: IFNγ-FITC (clone XMG1.2; eBiosciences) and Granzyme B-PE-Cy7 (16G6; eBioscience).

Statistical analysis. All statistical analyses were determined using GraphPad Prism 5.0 software. Where applicable, data are presented as mean + SEM and significance of variance was determined by *T*-test with Welch's correction, unless otherwise stated.

SUPPLEMENTARY MATERIAL

Figure S1 . VSV infection of B16-F10 cells at a high MOI can overcome replication issues.
Figure S2. VSV acts as a potent adjuvant in a prophylactic CT26.wt-infected cell vaccine.
Figure S3. The VSV_{GLess}-ICV performs identically as the VSV-ICV.
Figure S4. Prophylactic immunization with the VSVgm-ICV leads to early NK cell activation; however activation is not maintained until tumor challenge.
Figure S5. A significant increase in the proportion of T and NK cells is observed within the challenge tumor.
Figure S6. Treatment with the VSVgm-ICV reduces tumor burden even when treatment is delayed to day 3 or 4 after tumor inoculation.
Figure S7. The VSVgm-ICV has therapeutic efficacy in the MISIIRTAg spontaneous ovarian cancer model.

ACKNOWLEDGMENTS

C.G.L. and J.L.R. are supported by CIHR Doctoral awards: Frederick Banting and Charles Best Canada Graduate Scholarship. J.C.B. is supported by the Terry Fox Foundation, the Ontario Institute for Cancer Research, the Ottawa Regional Cancer Foundation, the Ottawa Hospital Foundation, and the Canadian Institute for Health Research. The authors declared no conflict of interest.

REFERENCES

1. Jones, S, Zhang, X, Parsons, DW, Lin, JC, Leary, RJ, Angenendt, P *et al.* (2008). Core signaling pathways in human pancreatic cancers revealed by global genomic analyses. *Science* **321**: 1801–1806.
2. Alpizar, YA, Chain, B, Collins, MK, Greenwood, J, Katz, D, Stauss, HJ *et al.* (2011). Ten years of progress in vaccination against cancer: the need to counteract cancer evasion by dual targeting in future therapies. *Cancer Immunol Immunother* **60**: 1127–1135.
3. Singer, K, Gottfried, E, Kreutz, M and Mackensen, A (2011). Suppression of T-cell responses by tumor metabolites. *Cancer Immunol Immunother* **60**: 425–431.
4. Hand, PH, Nuti, M, Colcher, D and Schlom, J (1983). Definition of antigenic heterogeneity and modulation among human mammary carcinoma cell populations using monoclonal antibodies to tumor-associated antigens. *Cancer Res* **43**: 728–735.
5. Gerlinger, M, Rowan, AJ, Horswell, S, Larkin, J, Endesfelder, D, Gronroos, E *et al.* (2012). Intratumor heterogeneity and branched evolution revealed by multiregion sequencing. *N Engl J Med* **366**: 883–892.
6. Braun, S, Hepp, F, Sommer, HL and Pantel, K (1999). Tumor-antigen heterogeneity of disseminated breast cancer cells: implications for immunotherapy of minimal residual disease. *Int J Cancer* **84**: 1–5.
7. Breitbach, CJ, Burke, J, Jonker, D, Stephenson, J, Haas, AR, Chow, LQ *et al.* (2011). Intravenous delivery of a multi-mechanistic cancer-targeted oncolytic poxvirus in humans. *Nature* **477**: 99–102.
8. Breitbach, CJ, Paterson, JM, Lemay, CG, Falls, TJ, McGuire, A, Parato, KA *et al.* (2007). Targeted inflammation during oncolytic virus therapy severely compromises tumor blood flow. *Mol Ther* **15**: 1686–1693.
9. Liu, TC, Hwang, T, Park, BH, Bell, J and Kirn, DH (2008). The targeted oncolytic poxvirus JX-594 demonstrates antitumoral, antivascular, and anti-HBV activities in patients with hepatocellular carcinoma. *Mol Ther* **16**: 1637–1642.
10. Melcher, A, Parato, K, Rooney, CM and Bell, JC (2011). Thunder and lightning: immunotherapy and oncolytic viruses collide. *Mol Ther* **19**: 1008–1016.
11. Kaufman, HL, Kim, DW, DeRaffele, G, Mitcham, J, Coffin, RS and Kim-Schulze, S (2010). Local and distant immunity induced by intralesional vaccination with an oncolytic herpes virus encoding GM-CSF in patients with stage IIIc and IV melanoma. *Ann Surg Oncol* **17**: 718–730.
12. Stojdl, DF, Lichty, BD, tenOever, BR, Paterson, JM, Power, AT, Knowles, S *et al.* (2003). VSV strains with defects in their ability to shutdown innate immunity are potent systemic anti-cancer agents. *Cancer Cell* **4**: 263–275.
13. Power, AT, Wang, J, Falls, TJ, Paterson, JM, Parato, KA, Lichty, BD *et al.* (2007). Carrier cell-based delivery of an oncolytic virus circumvents antiviral immunity. *Mol Ther* **15**: 123–130.
14. Diaz, RM, Galivo, F, Kottke, T, Wongthida, P, Qiao, J, Thompson, J *et al.* (2007). Oncolytic immunovirotherapy for melanoma using vesicular stomatitis virus. *Cancer Res* **67**: 2840–2848.
15. Bridle, BW, Stephenson, KB, Boudreau, JE, Koshy, S, Kazdhan, N, Pullenayegum, E *et al.* (2010). Potentiating cancer immunotherapy using an oncolytic virus. *Mol Ther* **18**: 1430–1439.
16. Bridle, BW, Boudreau, JE, Lichty, BD, Brunellière, J, Stephenson, K, Koshy, S *et al.* (2009). Vesicular stomatitis virus as a novel cancer vaccine vector to prime antitumor immunity amenable to rapid boosting with adenovirus. *Mol Ther* **17**: 1814–1821.
17. Prestwich, RJ, Errington, F, Ilett, EJ, Morgan, RS, Scott, KJ, Kottke, T *et al.* (2008). Tumor infection by oncolytic reovirus primes adaptive antitumor immunity. *Clin Cancer Res* **14**: 7358–7366.
18. Gauvrit, A, Brandler, S, Sapede-Peroz, C, Boisgerault, N, Tangy, F and Gregoire, M (2008). Measles virus induces oncolysis of mesothelioma cells and allows dendritic cells to cross-prime tumor-specific CD8 response. *Cancer Res* **68**: 4882–4892.
19. Gujar, SA, Marcato, P, Pan, D and Lee, PW (2010). Reovirus virotherapy overrides tumor antigen presentation evasion and promotes protective antitumor immunity. *Mol Cancer Ther* **9**: 2924–2933.
20. Sobol, PT, Boudreau, JE, Stephenson, K, Wan, Y, Lichty, BD and Mossman, KL (2011). Adaptive antiviral immunity is a determinant of the therapeutic success of oncolytic virotherapy. *Mol Ther* **19**: 335–344.
21. Sivendran, S, Glodny, B, Pan, M, Merad, M and Saenger, Y (2010). Melanoma immunotherapy. *Mt Sinai J Med* **77**: 620–642.
22. Roberts, A, Buonocore, L, Price, R, Forman, J and Rose, JK (1999). Attenuated vesicular stomatitis viruses as vaccine vectors. *J Virol* **73**: 3723–3732.
23. Lindsey, WB, Lowdell, MW, Marti, GE, Abbasi, F, Zenger, V, King, KM *et al.* (2007). CD69 expression as an index of T-cell function: assay standardization, validation and use in monitoring immune recovery. *Cytotherapy* **9**: 123–132.
24. Pitsios, C, Dimitrakopoulou, A, Tsalimalma, K, Kordossis, T and Choremi-Papadopoulou, H (2008). Expression of CD69 on T-cell subsets in HIV-1 disease. *Scand J Clin Lab Invest* **68**: 233–241.
25. Galon, J, Costes, A, Sanchez-Cabo, F, Kirilovsky, A, Mlecnik, B, Lagorce-Pagès, C *et al.* (2006). Type, density, and location of immune cells within human colorectal tumors predict clinical outcome. *Science* **313**: 1960–1964.
26. Stewart, TJ and Abrams, SI (2008). How tumours escape mass destruction. *Oncogene* **27**: 5894–5903.
27. Yang, Y, Huang, CT, Huang, X and Pardoll, DM (2004). Persistent Toll-like receptor signals are required for reversal of regulatory T cell-mediated CD8 tolerance. *Nat Immunol* **5**: 508–515.
28. Fehniger, TA, Cooper, MA, Nuovo, GJ, Cella, M, Facchetti, F, Colonna, M *et al.* (2003). CD56bright natural killer cells are present in human lymph nodes and are activated by T cell-derived IL-2: a potential new link between adaptive and innate immunity. *Blood* **101**: 3052–3057.
29. Vivier, E, Raulet, DH, Moretta, A, Caligiuri, MA, Zitvogel, L, Lanier, LL *et al.* (2011). Innate or adaptive immunity? The example of natural killer cells. *Science* **331**: 44–49.
30. Smyth, MJ, Hayakawa, Y, Takeda, K and Yagita, H (2002). New aspects of natural-killer-cell surveillance and therapy of cancer. *Nat Rev Cancer* **2**: 850–861.
31. Martín-Fontecha, A, Thomsen, LL, Brett, S, Gerard, C, Lipp, M, Lanzavecchia, A *et al.* (2004). Induced recruitment of NK cells to lymph nodes provides IFN-gamma for T(H)1 priming. *Nat Immunol* **5**: 1260–1265.
32. Heicappell, R, Schirrmacher, V, von Hoegen, P, Ahlert, T and Appelhans, B (1986). Prevention of metastatic spread by postoperative immunotherapy with virally modified autologous tumor cells. I. Parameters for optimal therapeutic effects. *Int J Cancer* **37**: 569–577.
33. Bohle, W, Schlag, P, Liebrich, W, Hohenberger, P, Manasterski, M, Möller, P *et al.* (1990). Postoperative active specific immunization in colorectal cancer patients with virus-modified autologous tumor-cell vaccine. First clinical results with tumor-cell vaccines modified with live but avirulent Newcastle disease virus. *Cancer* **66**: 1517–1523.
34. Liebrich, W, Schlag, P, Manasterski, M, Lehner, B, Stöhr, M, Möller, P *et al.* (1991). *In vitro* and clinical characterisation of a Newcastle disease virus-modified autologous tumour cell vaccine for treatment of colorectal cancer patients. *Eur J Cancer* **27**: 703–710.
35. Sivanandham, M, Shaw, P, Bernik, SF, Paoletti, E and Wallack, MK (1998). Colon cancer cell vaccine prepared with replication-deficient vaccinia viruses encoding B7.1 and interleukin-2 induce antitumor response in syngeneic mice. *Cancer Immunol Immunother* **46**: 261–267.
36. Cassel, WA and Murray, DR (1992). A ten-year follow-up on stage II malignant melanoma patients treated postsurgically with Newcastle disease virus oncolysate. *Med Oncol Tumor Pharmacother* **9**: 169–171.
37. Batliwalla, FM, Bateman, BA, Serrano, D, Murray, D, Macphail, S, Maino, VC *et al.* (1998). A 15-year follow-up of AJCC stage III malignant melanoma patients treated postsurgically with Newcastle disease virus (NDV) oncolysate and determination of alterations in the CD8 T cell repertoire. *Mol Med* **4**: 783–794.
38. Livingston, PO, Albino, AP, Chung, TJ, Real, FX, Houghton, AN, Oettgen, HF *et al.* (1985). Serological response of melanoma patients to vaccines prepared from VSV lysates of autologous and allogeneic cultured melanoma cells. *Cancer* **55**: 713–720.
39. Kottke, T, Errington, F, Pulido, J, Galivo, F, Thompson, J, Wongthida, P *et al.* (2011). Broad antigenic coverage induced by vaccination with virus-based cDNA libraries cures established tumors. *Nat Med* **17**: 854–859.
40. Kottke, T, Diaz, RM, Kaluza, K, Pulido, J, Galivo, F, Wongthida, P *et al.* (2008). Use of biological therapy to enhance both virotherapy and adoptive T-cell therapy for cancer. *Mol Ther* **16**: 1910–1918.
41. Demaria, S, Bhardwaj, N, McBride, WH and Formenti, SC (2005). Combining radiotherapy and immunotherapy: a revived partnership. *Int J Radiat Oncol Biol Phys* **63**: 655–666.
42. Chakraborty, M, Abrams, SI, Coleman, CN, Camphausen, K, Schlom, J and Hodge, JW (2004). External beam radiation of tumors alters phenotype of tumor cells to render them susceptible to vaccine-mediated T-cell killing. *Cancer Res* **64**: 4328–4337.
43. Gulley, JL, Arlen, PM, Bastian, A, Morin, S, Marte, J, Beetham, P *et al.* (2005). Combining a recombinant cancer vaccine with standard definitive radiotherapy in patients with localized prostate cancer. *Clin Cancer Res* **11**: 3353–3362.
44. Castle, JC, Kreiter, S, Diekmann, J, Löwer, M, van de Roemer, N, de Graaf, J *et al.* (2012). Exploiting the mutanome for tumor vaccination. *Cancer Res* **72**: 1081–1091.
45. Connolly, DC, Bao, R, Nikitin, AY, Stephens, KC, Poole, TW, Hua, X *et al.* (2003). Female mice chimeric for expression of the simian virus 40 TAg under control of the MISIIR promoter develop epithelial ovarian cancer. *Cancer Res* **63**: 1389–1397.
46. Foster, B, Prussin, C, Liu, F, Whitmire, JK and Whitton, JL (2007). Detection of intracellular cytokines by flow cytometry. *Curr Protoc Immunol* Chapter 6: Unit 6.24.

Appendix VII – Oncolytic viruses: the best is yet to come

Contribution of author: CG Lemay researched and wrote the manuscript with guidance from JC Bell. M Abei wrote the last section on "eradicating the root of cancer, the cancer stem cells".

Review was requested by the journal Current Cancer Drug Targets for a special issue on OVs. It has been accepted.

Title: Oncolytic Virus: The Best is Yet to Come

Running title: Future of Oncolytic Viruses

Authors: Chantal G Lemay[1,2], Masato Abei[3], John C Bell[1,2]

Affiliations:
[1]Faculty of Medicine, University of Ottawa, ON, Canada. [2]Center for Innovative Cancer Therapeutics, Ottawa Hospital Research Institute, ON, Canada, [3]Division of Gastroenterology, Faculty of Medicine, University of Tsukuba, Ibaraki, Japan.

Abstract:
Oncolytic viruses are a promising anti-cancer platform that has achieved great pre-clinical and clinical milestones in recent years. A full arsenal of selective, safe, and effective viruses has been developed and from here, pre-clinical research has focused on a new horizon. These viruses face many challenges both in the bloodstream and in the tumour microenvironment. Herein we discuss the recent progress in pre-clinical virotherapy research, with special focus on innovative strategies that seek to complement the current strengths of virotherapy, ensuring an optimal multi-faceted attack on cancer. We highlight the research areas that we believe provide the most potential to increase the efficacy of this exciting biotherapy platform: cell carriers, tumour vascular destruction, microenvironment modulation, combination therapies, and virus-mediated anti-tumour immune responses.

Keywords:
Cancer Therapy
Combination Therapy
Immunity
Oncolytic Viruses

Conflict of Interest: John C Bell is a co-founder of Jennerex Biotherapeutics

Acknowledgements: JB is supported by the OICR, CIHR, and the Terry Fox Foundation. CL is supported by a CIHR Canada Graduate Scholarship. MA is supported by a grant from Ministry of Education, Science and Technology of Japan.

Introduction

The oncolytic virus field developed in fits and starts since the early 1950s but the last 10-15 years has seen a concerted effort from the scientific and medical communities to really test the efficacy and potential of this class of therapeutics. We now know that OVs are very safe therapeutics and there have been tantalizing signs of efficacy in the clinic. These early studies have taught us a lot about the platform and perhaps most importantly that our initial concept of creating a virus machine that would eat through tumours like the videogame hero *"Pac-Man"* are probably incorrect. It's becoming clear from both pre-clinical and clinical studies that viruses have important hurdles to overcome within the tumour and the patient. But just as important we are beginning to realize that viruses are attacking cancers in multiple different ways. This new understanding of *virus:patient* interactions is opening our eyes to novel ways to arm viruses or combine therapies to safely enhance virus spread and tumour killing.

Herein we discuss the recent progress in pre-clinical and clinical virotherapy research, with special focus on innovative strategies that seek to complement the current strengths of virotherapy, ensuring an optimal multi-faceted attack on cancer. We highlight the research areas that we believe provide the most potential to increase the efficacy of this exciting biotherapy platform. The last five decades of cancer research and treatment has clearly shown that monotherapy approaches will never be successful for the treatment of metastatic cancers and so a multi-faceted therapeutic(s) is necessary if significant improvements in patient outcomes are to be achieved. Combination therapies incorporating oncolytic viruses have potential to deal with rapidly evolving and heterogeneous human cancers.

A. Riding the Trojan Horse to Maximize Intravenous Delivery

Systemic delivery of oncolytic viruses (OVs) offers the prospect of targeting distant tumour beds and undiscovered micrometastasis. However, the blood stream is a very hostile environment where innate and adaptive components can neutralize virus particles and significantly decrease the effective dose. Carrier cells offer a "Trojan Horse" approach to OV delivery, cloaking the virus from blood components and potentially allowing for tumour homing. It has been clearly demonstrated that they enhance efficacy in immune hosts, thereby allowing for dosing in pre-immune patients and for repeat dosing [*1-4*]. Interestingly, in a study using adenovirus in osteosarcoma, carrier cells were demonstrated to abolish virus uptake by the liver [*5*]. Therefore, these carrier cells not only offer the prospect of protection from neutralising blood components, but might also reduce virus uptake by the reticulo-endothelial system, again increasing the effective dose that is delivered to the tumour.

Many carrier cells have now been used not only for shielding virus but also for their homing potential. An observation that macrophages were frequently found within plasmacytomas of myeloma patients led to the testing of CD14+ macrophages and dendritic cells (DCs) as cell carriers for an oncolytic measles virus. The group demonstrated that these can be used in mice to deliver measles virus to tumours and extend survival [*6*]. Macrophages have also been investigated for their ability to migrate to, and extravasate into, hypoxic tumour cores. In this model, macrophages were first transfected with a hypoxia-driven E1A plasmid and then infected with a prostate-specific E1A-dependent adenovirus. In this way, the macrophages, upon entering the hypoxic tumour core, become productively infected with the adenovirus and release progeny into the neighbouring tumour cells [*7*].

Mesenchymal stem cells (MSCs) are also promising as cancer therapy carriers because they naturally migrate to most solid tumours and are easily harvested and expanded, allowing for autologous treatment [*3*, *8*]. As such, they have now been shown to efficiently deliver measles virus and adenoviruses to various solid tumours [*3*, *9*]. In a small exploratory study, four children with treatment-refractory stage IV neuroblastoma received MSCs loaded with an Rb-specific adenovirus. Of these, one child demonstrated an impressive response to the treatment, having complete disappearance of metastatic disease after the final infusion and maintenance of this disease-free state for 4 years [*10*].

Another interesting avenue for carrier cell research involves the use of immune cells, as these have the potential to not only evade blood components but also home to tumour sites and lead to anti-tumour immune responses. The homing and carrier abilities of T cells have been evaluated by many groups with promising results. Naive T cells were used to deliver WT-VSV to lymphoid tissues to purge these organs of their metastatic burden. Interestingly, the group found that these naive T cells do not become productively infected by VSV, but instead carry the virus on their cell surface [*11*]. In addition, work has been performed with *in vitro* activated human T cells as carriers for oncolytic measles virus. This work has demonstrated that although these cells do not preferentially accumulate in the tumour, approximately 1.5% of them do traffic to the tumour tissue and are able to deliver virus to tumour cells [*12*]. This research serves as a stepping stone towards using anti-tumour T cells or T cells that are engineered *ex vivo* to have chimeric antigen receptors. Adoptive cell therapies have gained momentum as a valuable cancer treatment, especially in malignant melanoma, which has had several clinical trials to optimize the collection, selection, and expansion of tumour-reactive T cells. These trials boast a 50% response rate, an impressive number for an aggressive disease with few treatments available. However, these protocols are extremely expensive and laborious, often taking over a month of processing and expansion. In addition, patients receive lymphodepletion regimens to reduce regulatory and naive T cell numbers, which carries a heavy side effect burden [*13*]. Owing to the induction of a large inflammatory response, oncolytic virotherapy may increase the production of systemic homeostatic cytokines and may naturally suppress regulatory T cells. In this way, combining an OV with adoptive cell transfer may decrease the requirement for dangerous lymphodepletion and cytokine regimens. Indeed a recent paper from the Journal of Immunology has demonstrated that using an oncolytic vaccinia that expresses a tumour antigen is just as effective as a therapeutic DC vaccination protocol, but, unlike the DC vaccination, the vaccinia protocol does not require whole body irradiation to achieve the same efficacy [*14*].

Along these lines, cytokine induced killer (CIK) cells have been examined for their ability to deliver oncolytic vaccinia to tumours while maintaining their innate ability to target tumours. These cells also have the added advantage of being easier to develop than antigen-specific T cells. Strikingly, these cells deliver virus to the tumour more efficiently than virus alone and are still able to exert their own anti-tumour destruction. This led to very efficient tumour clearance in multiple cancer models [*15*].

Carrier cell research is moving towards using cells that not only provide shielding from antibodies and complement but also detarget from off-target organs, home to tumour sites, and even potentially exert their own anti-tumour effector functions. In this way, these cells can be complete biological platforms, designed to maximize their output of virus specifically at the tumour site. In addition, cells could be manipulated to secrete cytokines or viral enhancers that would boost the anti-tumour effect of the treatment.

B. Virus-Mediated Tumour-Specific Asphyxiation

Angiogenesis is a necessary process for any tumour that has grown beyond a minimal size. This process is tightly regulated by pro and anti-angiogenic factors that oppose each other to fine tune the process. This tuning is called the "angiogenic switch" [*16*]. Though targeting this pathway to reinstate a more normal balance has demonstrated promise in pre-clinical models, clinical results have been disappointing, partly due to a high incidence of side effects at high doses [*16*]. However, the normalization of tumour vasculature through the antagonism of the VEGF system has proven to reduce interstitial tumour pressure, allowing for better delivery of other anti-cancer agents [*17*]. This offers an interesting avenue for combination therapy, as vascular disruption may further lead to cancer cell death, and vascular normalization may enhance viral distribution in the tumour.

Several groups have begun incorporating antiangiogenic proteins into their viruses in the hopes of further destabilizing the tumour and increasing cell death. For example, endostatin inhibits endothelial cell proliferation and migration, in addition to inducing apoptosis or G1 arrest. There have been over 750 reports describing the role of endostatin in cancer; it demonstrates tumour growth inhibition in over 20 different cancer models [*18*]. This gene has been engineered, either alone or as a fusion with angiostatin (another well characterized endogenous inhibitor of angiogenesis), into both adenovirus and vaccinia virus [*18-21*]. Other groups have used similar approaches, blocking VEGF signalling by encoding proteins like vascular endothelial cell growth inhibitor (VEGI) [*22*], or a soluble vascular endothelial growth factor receptor 1 (VEGFR-1) fused to an immunoglobulin domain [*23*], or a single-chain antibody against VEGF [*24*]. Other strategies have incorporated TIMP2 [*25*], an inhibitor of matrix metalloproteinases and angiogenesis, or vasculostatin, which, among other antiangiogenic properties, antagonizes the $\alpha v\beta 5$ integrin family [*26*]. Interestingly, the group investigating the effect of a vaccinia virus expressing a single-chain antibody against VEGF (VACV-scAb-VEGF) also compared this to treatment with bevacizumab (aka Avastin) after VACV treatment. Bevacizumab is a clinical antibody against VEGF approved for use in multiple cancer types, but it has demonstrated potentially dangerous side-effects such as hypertension and proteinuria. Encoding the antibody against VEGF in an oncolytic virus offers the possibility of decreasing these side effects; since the molecule should only be produced in the tumour environment, off-target effects should decrease. The group demonstrated that efficacy was comparable in either scenario, but did observe that vessel density was much lower in areas infected with the VACV-scAb-VEGF compared to vaccinia and bevacizumab treatment [*24*]. Further studies might incorporate both treatments together, first treating VACV-scAb-VEGF, followed by maintenance doses of bevacizumab.

All of these research groups have observed marked decreases in vessel density in the infected tumours and demonstrated increased efficacy when used in *in vivo* cancer models. However, it is not clear if efficacy is due to the direct inhibition of tumour growth through inhibition of angiogenesis or if the decrease in interstitial pressure through vascular normalization is playing a role in increased viral spread. Examining the basis for this efficacy will inform the treatment protocol and lead to better combination therapy platforms with rational timing and dosing.

One paper did examine the impact on viral replication in bevacizumab pre-treated tumours infected with an oncolytic adenovirus. They observed that bevacizumab does not have any effect on virus replication or cell death when combined *in*

vitro, but does lead to significantly higher viral expression and genome copies *in vivo*. This lends strength to the idea that vascular normalization through antiangiogenic manipulation can increase viral distribution and spread through a tumour [*27*].

Another strategy for vascular disruption is the use of the virus itself as the disruption agent. Tumour stroma is much more genetically stable, so it is less likely to evolve around the negative selection that the virus imposes, and endothelial cells are easy for the virus to access from the blood stream. This has been attempted through the use of RGD peptides [*28-30*] or echistatin motifs [*30*, *31*] that bind to integrins upregulated on newly formed and tumour vasculature. However, these motifs also bind integrins that are commonly upregulated on some tumours; therefore, it is difficult to attribute increased efficacy solely to endothelial cell killing. One study performed multiple assays to determine the binding and infection efficacy of oncolytic measles virus expressing various RGD motifs or echistatin. This group was able to observe these targeted viruses infecting blood vessels from chick chorioallantoic membranes, neovasculature in an ear pinnae model, as well as tumour blood vessels after intravenous delivery of virus [*30*].

Chen *et* al developed an elegant system for targeting their oncolytic adenovirus to the tumour endothelium while also enhancing viral movement into the tumour. They engineered their virus to express a fusogenic glycoprotein under the control of an endothelial-specific promoter. This led to heterofusion events between endothelial cells and neighbouring tumour cells, facilitating transendothelial migration [*32*]. Though not investigated, this approach may also lead to eventual vascular collapse if enough endothelial cells become infected and fused.

In addition, it has been demonstrated by our lab and others that some viruses naturally disrupt or infect tumour vasculature. Saito *et al* demonstrated that the adenovirus (Ad) E1A protein inhibits HIF1a-mediated induction of VEGF and suppresses angiogenesis *in* vivo [*33*]. Similarly, it was demonstrated that VSV-Δ51 infection of tumours leads to rapid and potent shutdown of the tumour vasculature through the recruitment of neutrophils [*34*]. It was later observed that VSV-Δ51 could specifically infect tumour endothelial cells [*35*], though the impact of this infection is difficult to ascertain. In addition, the clinical candidate JX-594 vaccinia virus has been observed to decrease VEGF levels and vascular perfusion by CT scan in patients [*36*].

Conversely, some groups have found that using VEGF can also enhance viral infection of tumours. However, this was attributed to acute vascular leakiness [*37*] and a fortuitous observation that VEGF-pulsed endothelial cells become sensitive to viral infection by both reovirus and VSV [*38*].

Vascular disruption combined with OVs is a promising modality because it could lead to vascular normalization, which decreases interstitial pressure and has been demonstrated to increase viral distribution in the tumour. In addition, these agents target an important part of a growing tumour that is often forgotten: the stroma. The tumour stroma is generally more genetically stable, and therefore, less likely to have time to adapt to the stress inflicted by the vascular disrupting therapy.

C. Manipulating the Tumour Microenvironment to Improve Virotherapy

Although a virus faces multiple barriers on its journey to the tumour, it does not get much easier once it has reached its destination. The tumour microenvironment is composed of a dense network of extracellular matrix (ECM) that effectively blocks virus from disseminating throughout the tumour bed. The ECM is a complex, entangled array of glycoproteins, collagens, glycosaminoglycans, and proteoglycans that are modulated by multiple endogenous proteases, such as matrix metalloproteinases (MMPs) and heparanase [*39*]. In many tumours, the ECM restricts tissue diffusion to only allow molecules smaller than 60nm [*40*].

Innovative studies using replication-deficient Ad gene transfer examined the use of elastase, trypsin, or a mix of collagenase/dispase in increasing transduction of smooth muscle cells or gliomas. These studies all observed marked increase in infection efficiency [*41*, *42*]. As a means to enhance oncolytic viral distribution and spread within the tumour,

many groups have employed ECM degrading enzymes. Relaxin is a peptide hormone that decreases the secretion of collagen and has been shown to induce MMP expression [*43*]. It has been used in conjunction with oncolytic Ads to successfully increase transduction efficiency, viral spread, and viral persistence, leading to increased survival. Importantly, these studies examined the effect of relaxin on metastasis and observed no increase in lung metastasis upon treatment [*43*, *44*].

Collagen has been investigated for its role in preventing viral dissemination through tumours and has been shown to inhibit oncolytic Ad [*45*] and HSV [*46*]. However, many other ECM components have been observed to hinder hydraulic flow through tissue, such as hyaluronicacid (HA), sulphated glycosaminoglycans, and glycoproteins [*47*]. As a means to degrade these ECM components, groups have tested various MMPs; MMP-1, MMP-8 [*45*, *47*], and MMP-9 [*48*] have all been demonstrated to lead to ECM degradation and increased viral distribution in tumours. MMP-1 and -8 increase hydraulic conductivity and significantly increase viral infection of the tumour core, whereas control tumours only demonstrate virus staining on the tumour rim [*47*]. Other groups have successfully increased viral spread and *in vivo* efficacy by co-injecting the virus with a bacterial collagenase [*46*] or hyaluronidase [*49*], or by encoding hyaluronidase in the virus itself [*50*]. An Ad expressing decorin [*51*], an endogenous inhibitor of collagen assembly that induces MMP-1, and an HSV expressing chondroitinase ABC [*52*], a bacterial enzyme that removes chondroitin sulphate glycosaminoglycans from proteoglycans, also increase virus spread and in vivo efficacy.

However, it is important to note that tumour invasion and metastasis also utilizes ECM degradation. The gravity of this assertion is highlighted by most groups investigating treatment impact on metastasis or invasion. Importantly, all groups that examined these factors observed no increase in metastatic spread or invasion, and indeed most groups noted a decrease in metastasis following these combination therapies.

Diop-frimpong *et al* postulated that Losartan might have a more favourable safety profile, as it is already an approved drug for controlling hypertension and does not demonstrate high grade toxicity to normal tissues [*53*]. It is a prototype nonpeptide angiotensin II receptor antagonist with antihypertensive functions. In addition, Losartan inhibits collagen-stimulated platelet aggregation through its interaction with glycoprotein VI [*54*]. In this study, the authors demonstrate that Losartan is able to reduce collagen I levels in 4 distinct tumour models, enhance tumour penetration of nanoparticles, and improve HSV spread and efficacy in two models of cancer [*53*].

Interestingly, degradation of ECM is also postulated to decrease interstitial pressure in the tumour, which might also lead to enhanced viral delivery to the tumour core [*55*]. However, the matrix composition of each tumour will likely determine the effectiveness of each of these treatments. Also, the gravity of possible impacts on metastatic spread and invasion will require careful consideration into the method of ECM degradation and close follow-up of patients treated with such therapies. However, the dramatic increase in viral spread and efficacy does warrant further research for this combination treatment.

D. Choosing your Side-Kick Wisely: Manipulations of Cell Signalling Pathways

Combinations with radiotherapy

From a pragmatic point of view, implementing a new viral therapy in combination with the current standard of care, like chemotherapy or radiotherapy, makes most sense. Radiation therapy has been demonstrated to synergize with oncolytic Ad [*56-61*] in multiple models, and this phenomenon is shown to rely on a radiation-mediated increase in dynamin-2, a membrane associated protein required for Ad cell entry [*59*]. However, it was later reported that synergy was only seen in subcutaneous and *in vitro* models and was not observed in orthotopic glioma models [*62*]. This may be a result of poor timing between treatment because Liu *et al* observed that a high dose of radiation before adenoviral treatment was much more efficacious than a continuous low-dose after viral treatment [*63*].

Herpes simplex virus (HSV) has also been observed to synergize with radiotherapy [*64-67*]. Further studies implicated several factors in this process: radiation-induced GADD34, the enhancement of viral promoters by p38 [*68*], and HSV-mediated inhibition of DNA repair [*69*]. The γ_1 34.5 gene of HSV is a homologue of GADD34 and is frequently deleted in oncolytic mutants. Therefore, radiation-induced upregulation of GADD34 leads to increased replication of γ_1 34.5-deleted HSV [*70*]. However, another group reported no additive effects with a γ_1 34.5-deleted HSV combined with radiation when tested *in vivo*, suggesting that this interaction may not be ubiquitous [*71*].This highlights the importance of fully understanding the underlying mechanism of synergy to best sculpt a combination therapy that takes full advantage of the interactions at play. Radiation has also been successfully combined with VSV-Δ51 [*72*], reovirus [*73*], and measles [*74*].

Recently, there has been interest in using the sodium iodide symporter (NIS) for imaging and radiotherapy by coupling the NIS-expressing virus with radionuclide therapy. Measles-NIS has been demonstrated to be safe and effective for *in vivo* imaging of viral replication, and it significantly enhances tumour killing when combined with radionuclides [*75-77*]. VSV-Δ51 [*78*] and vaccinia virus [*79*] have also been successfully engineered with the human NIS gene and are able to induce uptake of radionuclides for imaging [*79*] and therapy [*78*].

Combinations with chemotherapy

Standard chemotherapeutics have also been investigated for possible synergism with various kinds of virotherapy. Ad has been successfully combined with cisplatin [*80*, *81*], 5-fluorouracil [*82*], temozolomide [*83*], irinotecan [*84*], paclitaxel [*81*, *85*], and others; their inclusions all demonstrate a degree of increased tumour cell death. In the case of temozolomide, the Ad-Δ24-RGD decreased levels of MGMT, a DNA repair protein commonly used by gliomas to evade temozolomide-induced death [*83*]. For paclitaxel and cisplatin, the responses from different cell lines vary from synergistic to antagonistic [*81*, *86*].

Similar to radiotherapy, cisplatin induces GADD34 expression, which synergizes with γ_1 34.5-deleted HSV vectors [*87*]. Reovirus is observed to synergize with docetaxel, and this is hypothesized to rely on docetaxel-mediated microtubule stabilization [*88*]. Vaccinia virus demonstrates synergy in combination with paclitaxel, and this interaction was demonstrated to stem from a more cooperative relationship: Paclitaxel forces cells into the S-phase of their cell cycle, a point where vaccinia virus preferentially infects cells. In addition, type 1 IFNs and HMGB1 released from vaccinia-infected cells sensitizes these cells to paclitaxel-induced cell death [*89*].

However, combining virotherapy with conventional chemotherapy can also risk abrogating important virus-stimulated anti-tumour immune responses. Sung *et al* combined cisplatin with a fusogenic VSV (rVSV-F) and an IL-12-secreting VSV (rVSV-IL12). Although both demonstrate enhanced cytotoxicity *in vitro* in combination with cisplatin, there is an increase in *in vivo* efficacy with the rVSV-F but a dramatic decrease in combination with the rVSV-IL12 virus [*90*]. Rational design of platforms should take into consideration this effect and design treatment regimens that fully take advantage of the benefits OV therapy has to offer, including possible long term tumour control from anti-tumour immune responses. This topic will be discussed in more detail in the last section of this review.

With the growing capacity of computational biology, one way of rationally designing treatment schedules is to model possible interactions *in silico* followed by validation in animal models. This was successfully performed with Ad ONYX-015 and the MEK inhibitor CI1040 [*91*].

Combinations with histone deacetylase inhibitors

Histone deacetylase inhibitors (HDIs) are a class of small molecule that inhibit protein deacetylation and demonstrate inhibitory effects on the type 1 IFN pathway. These drugs are currently being clinically tested for use in cancer and have demonstrated some promise in haematologic malignancies. Due to their antagonism of the IFN pathway, they have also been shown to highly potentiate the killing and replication of many OVs: VSV-Δ51 with SAHA and MS-275 [*92*], oncolytic HSV G47Δ and strain R849 with Trichostatin A (TSA) [*93*, *94*] and the rQNestin34.5 strain with Valproic Acid (VPA) [*95*], and the oncolytic double deleted strain of vaccinia with TSA [*96*]. However, all HDIs are not equal and they each demonstrate unique protein targets. Consequently, Ad has been observed to synergize in some cell lines with the HDI

FR901228 [*97*] and TSA [*98*] but is antagonized by VPA [*99*]. HDIs modulate a myriad of cellular pathways [*100*] and viruses have complex interactions with cellular pathways, therefore understanding the full scope of this combination is nearly impossible and requires careful consideration.

High through-put screens

Because of the complex interactions a virus has with its host cell, the most efficient way to discover viral enhancers may be to blindly screen large libraries of chemicals. This technique involves no bias, and novel interactions can be identified. Diallo *et al* identified several new chemicals that enhance replication of VSV-Δ51, with their lead candidate VSe1 enhancing replication by a factor of 1000 [*101*]. Passer *et al* also performed a similar screen for compounds that enhance oncolytic HSV and found two such small molecules that greatly enhanced replication by antagonizing the endogenous protein ENT1 [*102*].

It is worth mentioning that virus dissemination through a tumour is also hindered by the narrow spaces between cells. Nagano *et al* demonstrated that the simple act of inducing some cell death in a tumour dramatically increases the ease with which HSV can spread throughout the tumour and leads to much higher titers [*103*]. Therefore, some of the aforementioned interactions could possibly stem from the cell death induction of the chemical or radiotherapy. This also implies that chemicals that are able to specifically enhance a phase of the viral life cycle, while also inducing some cell death, will lead to strong synergy.

Of note, our group has also examined the ability of two viruses to complement each other. In this case, vaccinia virus is used to specifically decrease type 1 IFN levels in the tumour through induction of its B18R gene product. This paves the way for VSV-Δ51 to robustly replicate in the tumour days after the vaccinia injection [*104*]. One could also imagine a scenario where VSV is endowed with a vaccinia-stimulating gene, allowing for co-complementation to occur. Because both viruses are tumour specific, this enhanced viral replication need not increase the toxicity to normal cells.

Though combining OV therapy with the current standard of care is tempting due to the immediate applicability and feasibility, it may not always be the most appropriate for the development of the best possible cancer treatment. Current cancer therapies carry a heavy burden of side-effects and may modulate OV efficacy differently depending on the underlying cellular genetic abnormalities. Using computational biology, high-throughput screens, and intense validation and characterization, we may be able to discover new compounds that have fewer side effects and boost viral potency in a much more robust and specific manner.

E. Virally-Induced Immunotherapy – Long-Term Surveillance That Wins the War

Our immune system has evolved to recognize and kill pathogenic intruders. Through the use of many pattern recognition receptors, the presence of a virus is rapidly recognized and a strong inflammatory response ensues [*105*]. The premise of using OVs to generate a long-term anti-tumour immune response is to usurp these viral "danger signals" to activate the immune system against the cancer. The immune system requires two signals; signal one is the foreign antigen, which in this case is the tumour associated antigen (TAA). Signal two is a molecular signal that warns of tissue stress or pathogen invasion through the ligation of pattern recognition receptors. Through the encouragement of phagocytosis of dying, infected cancer cells, both signals can be satisfied and immune-mediated tumour destruction can proceed [*106*].

OVs create the "perfect inflammatory storm"

Many OVs have demonstrated the ability to stimulate dendritic cell (DC) maturation upon incubation with infected tumour cells [*107-111*]. Likewise, many OVs have been found to stimulate T cell activation [*108*, *109*, *112*] and, in some cases, to depend on T cells for efficacy *in vivo* [*113*, *114*].

In addition, some groups have begun investigating the role and efficacy of oncolytic viruses in stimulating natural killer (NK) cells, with encouraging results. Reovirus-stimulated DCs are able to activate NK cells to secrete IFNγ and to become cytotoxic towards tumour cells [*115*]. Importantly, reovirus treatment induces NK and T cell homing to the tumour [*116*,

117]. NDV infection of multiple tumour types induces NK activating receptors to be upregulated on the tumour cell, leading to NK secretion of IFNγ and TNFα and NK-mediated killing of these infected tumour cells [*118*]. An elegant study by Wongthida *et al* demonstrates the importance of IL-28 in inducing NK-mediated *in vivo* efficacy of WT-VSV in the B16 melanoma model. They observed that only IL-28R-expressing variants of B16 respond to VSV treatments *in vivo,* though no difference in *in vitro* susceptibility is seen. Upon further examination, it was determined that innate cells secrete IL-28 upon VSV infection, and this IL-28 acting upon IL-28R-expressing tumour cells leads to NK-mediated lysis. Forced expression of IL-28R in the non-expressing variants leads to *in vivo* efficacy when treated with VSV [*119*]. In addition, Boudreau *et al* further demonstrated a crucial role for type 1 IFNs and IL-15 from VSV-infected DCs in stimulating NK cells which leads to *in vivo* efficacy [*120*]. The oncolytic parvovirus H-1PV and vaccinia virus have also been observed to enhance NK cell killing of infected tumour cells [*121*, *122*].

Pouring Gas on the Fire

A popular strategy for boosting the virotherapy-induced anti-tumour immune response is to engineer the virus to express a cytokine or chemokine. Granulocyte/monocyte colony-stimulating factor (GM-CSF) has been the most commonly used, having been engineered into VSV [*123*], NDV [*124*], oncolytic HSV HF10 [*125*] and NV1034 [*126*], vaccinia strain JX963 [*127*], and the telomerase promoter controlled Ad TOA02 [*128*], among others. GM-CSF is potent in the recruitment, maturation, and activation of antigen presenting cells and has been used extensively in vaccine protocols [*123*, *129*]. However, many other cytokines and chemokines have been successfully introduced into the oncolytic viral genomes, such as interleukin-12 (IL-12) [*130-132*], a potent Th1-promoting cytokine that activates NK and T cells, as well as IL-2 [*133*], the T cell chemokine RANTES (CCL5) [*134*, *135*], MIP-1α, FLT3L [*136*], and interleukin-23 [*137*]. These viruses are all found to be more robust than their parental counterparts. This strategy manages to harness the strength of the immune system while mitigating side effects that might arise from systemic administration of the cytokine, as seen with IL-2 and vascular leak syndrome [*133*]. OVs will only express these cytokines where they can productively replicate, *ie* in the tumour microenvironment.

In addition, OV treatment has been used in conjunction with DC vaccination and adoptive T cell therapy. When preceding DC vaccination, hTERT-Ad is able to induce tumour specific IFNγ production by splenocytes and lead to better tumour control. This OV-induced inflammation could not be substituted with TLR ligands, demonstrating the strength of the inflammatory response generated by replicating viruses. Surprisingly, this treatment protocol also led to a decreased antibody response against the virus [*138*]. Similar findings are observed when DC vaccination is preceded by an oncolytic Ad expressing both IL-12 and GM-CSF [*139*]. Boudreau *et al* demonstrated that VSV-Δ51 is a potent activator of DCs, and that these VSV-transduced DCs can lead to tumour regression when injected into a tumour-bearing animal. This protocol is even more efficient when VSV is engineered to express the model tumour antigen OVA, and efficacy can be abrogated by the depletion of CD8+ T cells or NK cells [*111*]. As alluded to previously, T cell adoptive therapies are gaining ground as a profound cancer treatment. Though more recent work from Dr. Vile's lab used T cells as carriers for VSV, previous work demonstrates that intratumoural delivery of VSV in conjunction with intravenously delivered tumour-specific T cells could lead to significant tumour control and 75% of mice demonstrating long term responses [*114*].

A novel strategy that is gaining momentum is the encoding of TAAs into the OV genome [*14*, *111*, *140*]. This strategy has been elegantly utilized by Bridle *et al*, in which WT-VSV expressing the human melanoma antigen dopachrome tautomerase (hDCT) is used to boost a pre-existing anti-DCT response generated with a replication deficient adenovirus. This heterologous, antigen-specific, boost with an oncolytic vector leads to enormous anti-tumour T cell responses that control the growth of aggressive B16F10 brain tumours [*141*]. In addition, by specifically boosting the anti-DCT response with VSV-hDCT, the anti-VSV response is decreased. Another interesting take on this strategy is offered by Kottke *et al*. They have incorporated a cDNA library from a normal human prostate into VSV. Surprisingly, this virus does not induce long term autoimmunity against the prostate, and it does lead to significant prostate tumour control [*142*]. In addition, both Bridle *et al* and Kottke *et al* use xenogenic antigens in order to more successfully break tolerance.

F. Eradicating the Root of Cancer, the Cancer Stem Cells

Recent studies on hematologic and solid malignancies have indicated that there is significant heterogeneity with respect to tumor-forming ability and only a subpopulation of cells is responsible for tumorigenesis. These cells have been referred to as cancer stem cells (CSC) or cancer-initiating cells (CICs)[143-145]. CICs have been shown to be relatively resistant to conventional anti-cancer therapies including chemotherapy and radiotherapy and they are considered to play a role in both disease relapse and metastasis. Therefore, these are critical therapeutic targets [145].

Recently, accumulating evidence are supporting the idea that OVs are ideal candidates for targeting CICs, since they kill cancer cells through mechanisms different from conventional therapies and they are not subject to typical mechanism of drug resistance [146, 147]. Indeed, Eriksson, et al. [148] have demonstrated that capsid-modified E1A mutated Ads, Ad5/3-Δ24 which enters through the serotype 3 Ad receptor and Ad5.pk7-Δ24 which uses heparin sulfate proteoglycans, were able to kill $CD44^{+}/CD24^{-}$ breast CICs. The same group has also reported that Ad5/3 variants that are controlled by tissue specific promoters, such as cyclooxygenase-2, telomerase (hTERT) and multidrug resistance (mdr) protein promoters, also target breast CICs [149]. Jiang, et al. [150] have also reported on the ability of RGD-fiber modified Δ24 Ad to kill brain tumor stem cells through autophagy, as indicated by accumulation of autophagic vacuoles, Atg5, and LC3II in the infected cells. In addition, Skog, et al. [151] have found that Ad16 and chimpanzee Ad CV23 effectively target glioblastoma CICs, while Zhang, et al. [152], who engineered a telomerase-specific oncolytic Ad expressing the tumor necrosis factor-related apoptosis-inducing ligand (TRAIL), showed that this OV preferentially targets radioresistant esophageal CSC-like cells. Meanwhile, Marcato, et al. [153] were able to show that oncolytic reovirus also kills breast CICs. Likewise, Wakimoto, et al. [154] showed that an HSV-1 mutant, G47Δ (γ34.5Δ, $ICP6^{-}$, ICP47/Us11proΔ), can target glioblastoma CICs. The same group has also reported on the synergy of G47Δ with chemotherapy [155] and also on the synergy of MG18L, a novel oncolytic HSV which deletes U_S3 and has inactivated U_L39, with phosphoinositide 3-kinase/Akt pathway inhibitors [156] in killing glioblastoma CICs *in vitro* and *in vivo*. Finally, Parato, et al. have recently reported that an oncolytic vaccinia virus, JX-594, could kill lung and colon CICs *in vitro* [157].

How this promising basic data for OV-mediated CIC killiing translates into clinical benefit await the results of clinical trials. Total killing of CICs may require further refinement of OVs including their arming with appropriate genes targeting CICs. However, this data strongly supports the idea that OVs offer important new benefits that conventional cancer therapeutics could never provide.

G. Where Are We Heading?

The field of oncolytic virotherapy has developed exponentially in the last decade, seeing dozens of viruses being developed that have impressive safety profiles and tumour-specificity. For these first generation viruses, clinical development is well underway with notable milestones having been achieved. The rapid evolution of this burgeoning field has identified both new hurdles and therapeutic opportunities and the challenge facing us now is to capitalize on the latest scientific developments. To create a multi-faceted platform viruses will have to avoid anti-viral immunity, home to tumours, replicate and spread, and initiate long-term anti-tumour immune responses. Currently, virotherapy is heading towards a new horizon of cancer therapy that will ultimately see OVs become the ultimate biological tumour killing machines.

References

[1] Power, A. T., Wang, J., Falls, T. J., Paterson, J. M., Parato, K. A., Lichty, B. D., Stojdl, D. F., Forsyth, P. A. J., Atkins, H., and Bell, J. C. Carrier Cell-based Delivery of an Oncolytic Virus Circumvents Antiviral Immunity. *Mol. Ther*. **2007**, *15*, 123-130.

[2] Liu, C., Russell, S. J., and Peng, K. W. Systemic Therapy of Disseminated Myeloma in Passively Immunized Mice Using Measles Virus-infected Cell Carriers. *Mol Ther*. **2009**, *18*, 1155-1164.

[3] Mader, E. K., Maeyama, Y., Lin, Y., Butler, G. W., Russell, H. M., Galanis, E., Russell, S. J., Dietz, A. B., and Peng, K.-whye. Mesenchymal Stem Cell Carriers Protect Oncolytic Measles Viruses from Antibody Neutralization in an Orthotopic Ovarian Cancer Therapy Model. *Clin. Cancer Res*. **2009**, *15*, 7246-7255.

[4] Ilett, E. J., and Errington-mais, F. Internalization of Oncolytic Reovirus by Human Dendritic Cell Carriers Protects the Virus from Neutralization. *Clin. Cancer Res*. **2011**, *17*, 2767-2776.

[5] Alcayaga-miranda, F., Cascallo, M., Rojas, J. J., Pastor, J., and Alemany, R. Osteosarcoma cells as carriers to allow antitumor activity of canine oncolytic adenovirus in the presence of neutralizing antibodies. *Cancer Gene Ther*. **2010**, *17*, 792-802.

[6] Peng, K.-whye, Dogan, A., Vrana, J., Liu, C., Ong, H. T., Kumar, S., Dispenzieri, A., Dietz, A. B., and Russell, S. J. Tumor-associated macrophages infiltrate plasmacytomas and can serve as cell carriers for oncolytic measles virotherapy of disseminated myeloma. *Am. J. Hematol*. **2009**, 401-407.

[7] Muthana, M., Giannoudis, A., Scott, S. D., and Tumors, H. P. Use of Macrophages to Target Therapeutic Adenovirus to Human Prostate Tumors. *Cancer Res*. **2011**, 1805-1815.

[8] Garcia-Gomez, I., Elvira, G., Zapata, A., Lamana, M. L., Ramirez, M., Garcia-Castro, J., Garcia Arranz, M., Vicente, A., Bueren, J. A., and Garcia-Olmo, D. Mesenchymal stem cells : biological properties and clinical applications. *Expert Opinion Biol. Ther*. **2010**, *10*, 1453-1468.

[9] Yong, R. L., Shinojima, N., Fueyo, J., Gumin, J., Vecil, G. G., Marini, F. C., Bogler, O., Andreeff, M., and Lang, F. F. Human bone marrow−derived mesenchymal stem cells for intravascular delivery of oncolytic adenovirus Δ 24-RGD to Human Gliomas. *Cancer Res*. **2009**, *69*, 8932-8940.

[10] Garcia-Castro, J., Alemany, R., Cascallo, M., Martinez-Quintanilla, J., Mar Arriero, M. del, Lassaletta, A., Madero, L., and Ramırez, M. Treatment of metastatic neuroblastoma with systemic oncolytic virotherapy delivered by autologous mesenchymal stem cells : an exploratory study. *Cancer Gene Ther*. **2010**, 476-483.

[11] Qiao, J., Kottke, T., Willmon, C., Galivo, F., Wongthida, P., Diaz, R. M., Thompson, J., Ryno, P., Barber, G. N., Chester, J., Selby, P., Harrington, K., Melcher, A., and Vile, R. G. Purging metastases in lymphoid organs using a combination of antigen-nonspecific adoptive T cell therapy, oncolytic virotherapy and immunotherapy. *Nat. Med*. **2008**, *14*, 37-44.

[12] Ong, H. T., Hasegawa, K., Dietz, A. B., Russell, S. J., and Peng, K.-w. Evaluation of T cells as carriers for systemic measles virotherapy in the presence of antiviral antibodies. *Gene Ther*. **2007**, *14*, 324-333.

[13] Hershkovitz, L., Schachter, J., Treves, A. J., and Besser, M. J. Focus on Adoptive T Cell Transfer Trials in Melanoma. *Clin. Develop. Immunol*. **2010**, *2010*, 1-11.

[14] Gil, M., Bieniasz, M., Wierzbicki, A., Bambach, B. J., Rokita, H., and Kozbor, D. Targeting a mimotope vaccine to activating Fcgamma receptors empowers dendritic cells to prime specific CD8+ T cell responses in tumor-bearing mice. *J. Immunol*. **2009**, *183*, 6808-6818.

[15] Thorne, S. H., Negrin, R. S., and Contag, C. H. Synergistic Antitumor Effects of immune cell-viral biotherapy. *Science*. **2006**, *311*, 1780.

[16] Dvorak, H. F., Weaver, V. M., Tlsty, T. D., and Bergers, G. Tumor Microenvironment and Progression. *J. Surg. Oncol*. **2011**, 468-474.

[17] Jain, R. K. Lessons from multidisciplinary translational trials on anti-angiogenic therapy of cancer. *Nat. Rev. Cancer*. **2008**, *8*, 309-316.

[18] Ribatti, D. Endogenous inhibitors of angiogenesis A historical review. *Biochim. Biophys. Acta*. **2009**, *33*, 638-644.

[19] Fang, L., Pu, Y.-yan, Hu, X.-cui, Sun, L.-jun, Luo, H.-mei, Pan, S.-kun, Gu, J.-zhong, Cao, X.-rong, and Su, C.-qing. Antiangiogenesis gene armed tumor-targeting adenovirus yields multiple antitumor activities in human HCC xenografts in nude mice. *Hepatol. Res*. **2010**, *40*, 216-228.

[20] Tysome, J. R., Briat, A., Alusi, G., Cao, F., Gao, D., Yu, J., Wang, P., Yang, S., Dong, Z., Wang, S., Deng, L., Francis, J., Timiryasova, T., Fodor, I., Lemoine, N. R., and Wang, Y. Lister strain of vaccinia virus armed with endostatin – angiostatin fusion gene as a novel therapeutic agent for human pancreatic cancer. *Gene Ther*. **2009**, 1223-1233.

[21] Tysome, J. R., Wang, P., Alusi, G., Briat, A., Wang, J., Bhakta, V., Fodor, I., Lemoine, N. R., and Wang, Y. Lister Vaccine Strain of Vaccinia Virus Armed with the Endostatin – Angiostatin Fusion Gene: An oncolytic virus superior to dl1520 (ONYX-015) for human head and neck cancer. *Human Gene Ther*. **2011**, *8*, 1-8.

[22] Xiao, T., Fan, J. K., Huang, H. L., Gu, J. F., Li, L.-yuan, and Liu, X. Y. VEGI-armed oncolytic adenovirus inhibits tumor neovascularization and directly induces mitochondria-mediated cancer cell apoptosis, *Cell Res*. **2009**, *20*, 367-378.

[23] Guse, K., Sloniecka, M., Diaconu, I., Ottolino-perry, K., Tang, N., Ng, C., Boeuf, F. L., Bell, J. C., Mccart, J. A., Ristima, A., and Pesonen, S. Antiangiogenic Arming of an Oncolytic Vaccinia Virus Enhances Antitumor Efficacy in Renal Cell Cancer Models. *J. Virol*. **2010**, *84*, 856-866.

[24] Frentzen, A., Yu, Y. A., Chen, N., Zhang, Q., Weibel, S., Raab, V., and Szalay, A. A. Anti-VEGF single-chain antibody GLAF-1 encoded by oncolytic vaccinia virus significantly enhances antitumor therapy. *Proc. Nat. Accad. Sci*. **2009**, *106*, 12915-12920.

[25] Yang, S. W., Cody, J. J., Rivera, A. A., Waehler, R., Wang, M., Kimball, K. J., Alvarez, R. A., Siegal, G. P., Douglas, J. T., and Ponnazhagan, S. Conditionally replicating adenovirus expressing TIMP2 for ovarian cancer therapy. *Clin. Cancer Res*. **2011**, *17*, 538-549.

[26] Hardcastle, J., Kurozumi, K., Dmitrieva, N., Sayers, M. P., Ahmad, S., Waterman, P., Weissleder, R., Chiocca, E. A., and Kaur, B. Enhanced antitumor efficacy of vasculostatin (Vstat120) expressing oncolytic HSV-1. *Mol. Ther*. **2009**, *18*, 285-294.

[27] Libertini, S., Iacuzzo, I., Perruolo, G., Scala, S., and Ierano, C. Bevacizumab increases viral distribution in human anaplastic thyroid carcinoma xenografts and enhances the effects of E1A-defective adenovirus dl 922-947. *Clin. Cancer Res*. **2008**, *14*, 6505-6514.

[28] Tyler, M. a, Ulasov, I. V., Borovjagin, A., Sonabend, A. M., Khramtsov, A., Han, Y., Dent, P., Fisher, P. B., Curiel, D. T., and Lesniak, M. S. Enhanced transduction of malignant glioma with a double targeted Ad5/3-RGD fiber-modified adenovirus. *Mol. Cancer Ther*. **2006**, *5*, 2408-16.

[29] Kim, J., Yeong, H., Kim, T.-il, Kim, P.-hwan, Ryu, J., Yun, C.-ok, and Wan, S. Active targeting of RGD-conjugated bioreducible polymer for delivery of oncolytic adenovirus expressing shRNA against IL-8 mRNA. *Biomaterials*. **2011**, *32*, 5158-5166.

[30] Ong, H. T., Trejo, T. R., Pham, L. D., Oberg, A. L., Russell, S. J., and Peng, K.-whye. Intravascularly Administered RGD-Displaying Measles Viruses Bind to and Infect Neovessel Endothelial Cells In Vivo, *Mol. Ther*. **2009**, *17*, 1012-1021.

[31] Hallak, L. K., Merchan, J. R., Storgard, C. M., Loftus, J. C., and Russell, S. J. Targeted measles virus vector displaying echistatin infects endothelial cells via alpha(v)beta3 and leads to tumor regression., *Cancer Res*. **2005**, *65*, 5292-300.

[32] Chen, H. H., Cawood, R., Sherbini, Y. E., Purdie, L., Peregrino, M. B., Seymour, L. W., and Carlisle, R. C. Active Adenoviral Vascular Penetration by Targeted Formation of Heterocellular Endothelial – epithelial Syncytia. *Mol. Ther*. **2009**, *19*, 67-75.

[33] Saito, Y., Sunamura, M., Motoi, F., Abe, H., Egawa, S., Duda, D. G., Hoshida, T., Fukuyama, S., Hamada, H., and Matsuno, S. Oncolytic replication-competent adenovirus suppresses tumor angiogenesis through preserved E1A region. *Cancer Gene Ther*. **2006**, *13*, 242-52.

[34] Breitbach, C. J., Paterson, J., Lemay, C. G., Falls, T., McGuire, A., Parato, K. A., Stojdl, D. F., Daneshmand, M., Speth, K., Kirn, D. H., McCart, J. A., Atkins, H., and Bell, J. C. Targeted inflammation during oncolytic virus therapy severely compromises tumor blood flow. *Mol. Ther*. **2007**, *15*, 1686-93.

[35] Breitbach, C. J., Silva, N. S. D., Falls, T. J., Aladl, U., Evgin, L., Paterson, J., Sun, Y. Y., Roy, D. G., Rintoul, J. L., Daneshmand, M., Parato, K., Stanford, M. M., Lichty, B. D., Fenster, A., Kirn, D., Atkins, H., and Bell, J. C. Targeting Tumor Vasculature With an Oncolytic Virus. *Mol. Ther*. **2009**, *19*, 886-894.

[36] Liu, T.-C., Hwang, T., Park, B.-H., Bell, J. C., and Kirn, D. H. The targeted oncolytic poxvirus JX-594 demonstrates antitumoral, antivascular, and anti-HBV activities in patients with hepatocellular carcinoma., *Mol. Ther*. **2008**, *16*, 1637-42.

[37] Tseng, J.-C., Granot, T., DiGiacomo, V., Levin, B., and Meruelo, D. Enhanced specific delivery and targeting of oncolytic Sindbis viral vectors by modulating vascular leakiness in tumor. *Cancer Gene Ther*. **2010**, *17*, 244-55.

[38] Kottke, T., Hall, G., Pulido, J., Diaz, R. M., Thompson, J., Chong, H., Selby, P., Coffey, M., Pandha, H., Chester, J., Melcher, A., Harrington, K., and Vile, R. Antiangiogenic cancer therapy combined with oncolytic virotherapy leads to regression of established tumors in mice. *J. Clin. Invest*. **2010**, *120*, 1551-1560.

[39] Kim, S.-H., Turnbull, J. E., and Guimond, S. E. Extracellular matrix and cell signalling: the dynamic cooperation of integrin, proteoglycan and growth factor receptor. *J. Endocrinol*. **2011**, *209*, 139-151.

[40] Jain, R. K., and Stylianopoulos, T. Delivering nanomedicine to solid tumors. *Nat. Rev. Clin. Oncol*. **2010**, *7*, 653-664.

[41] Maillard, L., Ziol, M., Tahlil, O., Feuvre, C. Le, Feldman, L. J., Branellec, D., Bruneval, P., and Steg, P. Pre-treatment with elastase improves the efficiency of percutaneous adenovirus-mediated gene transfer to the arterial media. *Gene Ther*. **1998**, *5*, 1023-30.

[42] Kuriyama, N., Kuriyama, H., Julin, C. M., Lamborn, K., and Israel, M. a. Pretreatment with protease is a useful experimental strategy for enhancing adenovirus-mediated cancer gene therapy. *Human Gene Ther*. **2000**, *11*, 2219-30.

[43] Kim, J.-H., Lee, Y.-S., Kim, H., Huang, J.-H., Yoon, A.-R., and Yun, C.-O. Relaxin expression from tumor-targeting adenoviruses and its intratumoral spread, apoptosis induction, and efficacy. *J. Nat. Cancer Inst*. **2006**, *98*, 1482-93.

[44] Ganesh, S., Gonzalez Edick, M., Idamakanti, N., Abramova, M., Vanroey, M., Robinson, M., Yun, C.-O., and Jooss, K. Relaxin-expressing, fiber chimeric oncolytic adenovirus prolongs survival of tumor-bearing mice. *Cancer Res*. **2007**, *67*, 4399-407.

[45] Cheng, J., Sauthoff, H., Huang, Y., Kutler, D. I., Bajwa, S., Rom, W. N., and Hay, J. G. Human matrix metalloproteinase-8 gene delivery increases the oncolytic activity of a replicating adenovirus. *Mol. Ther*. **2007**, *15*, 1982-90.

[46] McKee, T. D., Grandi, P., Mok, W., Alexandrakis, G., Insin, N., Zimmer, J. P., Bawendi, M. G., Boucher, Y., Breakefield, X. O., and Jain, R. K. Degradation of fibrillar collagen in a human melanoma xenograft improves the efficacy of an oncolytic herpes simplex virus vector. *Cancer Res*. **2006**, *66*, 2509-13.

[47] Mok, W., Boucher, Y., and Jain, R. K. Matrix metalloproteinases-1 and -8 improve the distribution and efficacy of an oncolytic virus. *Cancer Res*. **2007**, *67*, 10664-8.

[48] Hong, C.-s, Fellows, W., Niranjan, A., Alber, S., Watkins, S., Cohen, J. B., Glorioso, J. C., and Grandi, P. Ectopic matrix metalloproteinase-9 expression in human brain tumor cells enhances oncolytic HSV vector infection, *Gene Ther*. **2010**, *17*, 1200-1205.

[49] Ganesh, S., Gonzalez-Edick, M., Gibbons, D., Roey, M. Van, and Jooss, K. Intratumoral coadministration of hyaluronidase enzyme and oncolytic adenoviruses enhances virus potency in metastatic tumor models. *Clin. Cancer Res*. **2008**, *14*, 3933-41.

[50] Guedan, S., Rojas, J. J., Gros, A., Mercade, E., Cascallo, M., and Alemany, R. Hyaluronidase expression by an oncolytic adenovirus enhances its intratumoral spread and suppresses tumor growth. *Mol. Ther*. **2010**, *18*, 1275-83.

[51] Choi, I.-k, Lee, Y.-s, Yoo, J. Y., Yoon, A.-r, Kim, H., Kim, D.-s, Seidler, D. G., Kim, J.-h, and Yun, C.-o. Effect of decorin on overcoming the extracellular matrix barrier for oncolytic virotherapy. *Gene Ther*. **2009**, *17*, 190-201.

[52] Dmitrieva, N., Yu, L., Viapiano, M., Cripe, T. P., Chiocca, E. A., Glorioso, J. C., and Kaur, B. Chondroitinase ABC I−mediated enhancement of oncolytic virus spread and antitumor efficacy. *Clin. Cancer Res*. **2011**, *17*, 1362-1372.

[53] Diop-frimpong, B., Chauhan, V. P., Krane, S., Boucher, Y., and Jain, R. K. Losartan inhibits collagen I synthesis and improves the distribution and efficacy of nanotherapeutics in tumors. *Proc. Nat. Accad. Sci*. **2011**, *108*, 2909-2914.

[54] Naik, P., Murumkar, P., Giridhar, R., and Yadav, M. R. Angiotensin II receptor type 1 (AT1) selective nonpeptidic antagonists-a perspective. *Bioorg. Medicin. Chemist*. **2010**, *18*, 8418-56.

[55] Brekken, C., Bruland, Ø. S., and Lange Davies, C. de. Interstitial fluid pressure in human osteosarcoma xenografts: significance of implantation site and the response to intratumoral injection of hyaluronidase, *Anticancer Res*. **2000**, *20*, 3503-12.

[56] Chen, Y., Deweese, T., Dilley, J., Zhang, Y., Li, Y., Ramesh, N., Lee, J., Pennathur-das, R., Radzyminski, J., Wypych, J., Brignetti, D., Scott, S., Stephens, J., Karpf, D. B., Henderson, D. R., and Yu, D.-chao. CV706 , a prostate cancer-specific adenovirus variant in combination with radiotherapy produces synergistic antitumor efficacy without increasing toxicity. *Cancer Res*. **2001**, *61*, 5453-5460.

[57] Lamfers, M. L. M., Grill, J., Dirven, C. M. F., Beusechem, V. W. V., Geoerger, B., Berg, J. V. D., Alemany, R., Fueyo, J., Curiel, D. T., Vassal, G., Pinedo, H. M., Vandertop, W. P., and Gerritsen, W. R. Potential of the conditionally replicative adenovirus Ad5-Δ24RGD in the treatment of malignant gliomas and its enhanced effect with radiotherapy. *Cancer Res*. **2002**, *62*, 5736-5742.

[58] Geoerger, B., Grill, J., Opolon, P., Morizet, J., Aubert, G., Lecluse, Y., Beusechem, V. W. van, Gerritsen, W. R., Kirn, D. H., and Vassal, G. Potentiation of radiation therapy by the oncolytic adenovirus dl1520 (ONYX-015) in human malignant glioma xenografts. *Br. J. Cancer*. **2003**, *89*, 577-84.

[59] Qian, J., Yang, J., Dragovic, A. F., Abu-Isa, E., Lawrence, T. S., and Zhang, M. Ionizing radiation-induced adenovirus infection is mediated by Dynamin 2. *Cancer Res*. **2005**, *65*, 5493-7.

[60] Dilley, J., Reddy, S., Ko, D., Nguyen, N., Rojas, G., Working, P., and Yu, D.-C. Oncolytic adenovirus CG7870 in combination with radiation demonstrates synergistic enhancements of antitumor efficacy without loss of specificity. *Cancer Gene Ther*. **2005**, *12*, 715-22.

[61] Idema, S., Lamfers, M. L. M., Beusechem, V. W. V., Noske, D. P., Heukelom, S., and Dirven, C. M. F. AdΔ24 and the p53-expressing variant AdΔ24-p53 achieve potent anti-tumor activity in glioma when combined with radiotherapy. *J. Gene Med*. **2007**, *9*, 1046-1056.

[62] Lamfers, M. L. M., Idema, S., Bosscher, L., Heukelom, S., Moeniralm, S., Meulen-Muileman, I. H. van der, Overmeer, R. M., Valk, P. van der, Beusechem, V. W. van, Gerritsen, W. R., Vandertop, W. P., and Dirven, C. M. F. Differential effects of combined Ad5- delta 24RGD and radiation therapy in in vitro versus in vivo models of malignant glioma. *Clin. Cancer Res*. **2007**, *13*, 7451-8.

[63] Liu, C., Zhang, Y., Liu, M. M., Zhou, H., Chowdhury, W., Lupold, S. E., Deweese, T. L., and Rodriguez, R. Evaluation of continuous low dose rate versus acute single high dose rate radiation combined with oncolytic viral therapy for prostate cancer. *Int. J. Rad. Biol*. **2010**, *86*, 220-9.

[64] Adusumilli, P. S., Chan, M.-K., Hezel, M., Yu, Z., Stiles, B. M., Chou, T.-C., Rusch, V. W., and Fong, Y. Radiation-induced cellular DNA damage repair response enhances viral gene therapy efficacy in the treatment of malignant pleural mesothelioma. *Annal. Surg. Oncol*. **2007**, *14*, 258-69.

[65] Advani, S. J., Sibley, G. S., Song, P. Y., Hallahan, D. E., Kataoka, Y., Roizman, B., and Weichselbaum, R. R. Enhancement of replication of genetically engineered herpes simplex viruses by ionizing radiation: a new paradigm for destruction of therapeutically intractable tumors. *Gene Ther*. **1998**, *5*, 160-5.

[66] Bradley, J. D., Kataoka, Y., Advani, S., Chung, S. M., Arani, R. B., Gillespie, G. Y., Whitley, R. J., Markert, J. M., Roizman, B., and Weichselbaum, R. R. Ionizing radiation improves survival in mice bearing intracranial high-grade gliomas injected with genetically modified herpes simplex virus. *Clin. Cancer Res*. **1999**, *5*, 1517-1522.

[67] Blank, S. V., Rubin, S. C., Coukos, G., Amin, K. M., Albelda, S. M., and Molnar-Kimber, K. L. Replication-selective herpes simplex virus type 1 mutant therapy of cervical cancer is enhanced by low-dose radiation. *Human Gene Ther*. **2002**, *13*, 627-39.

[68] Mezhir, J. J., Advani, S. J., Smith, K. D., Darga, T. E., Poon, A. P. W., Schmidt, H., Posner, M. C., Roizman, B., and Weichselbaum, R. R. Ionizing radiation activates late herpes simplex virus 1 promoters via the p38 pathway in tumors treated with oncolytic viruses. *Cancer Res*. **2005**, *65*, 9479-84.

[69] Hadjipanayis, C. G., and DeLuca, N. a. Inhibition of DNA repair by a herpes simplex virus vector enhances the radiosensitivity of human glioblastoma cells. *Cancer Res*. **2005**, *65*, 5310-6.

[70] Adusumilli, P. S., Stiles, B. M., Chan, M.-K., Chou, T.-C., Wong, R. J., Rusch, V. W., and Fong, Y. Radiation therapy potentiates effective oncolytic viral therapy in the treatment of lung cancer. *Annal. Thoracic Surg*. **2005**, *80*, 409-17.

[71] Jorgensen, T. J., Katz, S., Wittmack, E. K., Varghese, S., Todo, T., Rabkin, S. D., and Martuza, R. L. Ionizing radiation does not alter the antitumor activity of herpes simplex virus vector G207 in subcutaneous tumor models of human and murine prostate cancer. *Neoplasia*. **2001**, *3*, 451-6.

[72] Alajez, N. M., Mocanu, J. D., Shi, W., Chia, M. C., Breitbach, C. J., Hui, A. B. Y., Knowles, S., Bell, J. C., Busson, P., Takada, K., Lo, K.-W., O'Sullivan, B., Gullane, P., and Liu, F.-F. Efficacy of systemically administered mutant vesicular stomatitis virus (VSVDelta51) combined with radiation for nasopharyngeal carcinoma. *Clin. Cancer Res*. **2008**, *14*, 4891-7.

[73] Twigger, K., Vidal, L., White, C. L., Bono, J. S. De, Bhide, S., Coffey, M., Thompson, B., Vile, R. G., Heinemann, L., Pandha, H. S., Errington, F., Melcher, A., and Harrington, K. J. Enhanced in vitro and in vivo cytotoxicity of combined reovirus and radiotherapy. *Clin. Cancer Res*. **2008**, *14*, 912-23.

[74] Liu, C., Sarkaria, J. N., Petell, C. a, Paraskevakou, G., Zollman, P. J., Schroeder, M., Carlson, B., Decker, P. a, Wu, W., James, C. D., Russell, S. J., and Galanis, E. Combination of measles virus virotherapy and radiation therapy has synergistic activity in the treatment of glioblastoma multiforme. *Clin. Cancer Res*. **2007**, *13*, 7155-65.

[75] Hasegawa, K., Pham, L., O'Connor, M. K., Federspiel, M. J., Russell, S. J., and Peng, K.-W. Dual therapy of ovarian cancer using measles viruses expressing carcinoembryonic antigen and sodium iodide symporter., *Clin. Cancer Res*. **2006**, *12*, 1868-75.

[76] Msaouel, P., Iankov, I. D., Allen, C., Aderca, I., Federspiel, M. J., Tindall, D. J., Morris, J. C., Koutsilieris, M., Russell, S. J., and Galanis, E. Noninvasive imaging and radiovirotherapy of prostate cancer using an oncolytic measles virus expressing the sodium iodide symporter. *Mol. Ther*. **2009**, *17*, 2041-8.

[77] Li, H., Peng, K.-W., Dingli, D., Kratzke, R. a, and Russell, S. J. Oncolytic measles viruses encoding interferon beta and the thyroidal sodium iodide symporter gene for mesothelioma virotherapy. *Cancer Gene Ther*. **2010**, *17*, 550-8.

[78] Goel, A., Carlson, S. K., Classic, K. L., Greiner, S., Naik, S., Power, A. T., Bell, J. C., and Russell, S. J. Radioiodide imaging and radiovirotherapy of multiple myeloma using VSV(Delta51)-NIS, an attenuated vesicular stomatitis virus encoding the sodium iodide symporter gene. *Blood*. **2007**, *110*, 2342-50.

[79] Haddad, D., Chen, N. G., Zhang, Q., Chen, C.-H., Yu, Y. a, Gonzalez, L., Carpenter, S. G., Carson, J., Au, J., Mittra, A., Gonen, M., Zanzonico, P. B., Fong, Y., and Szalay, A. a. Insertion of the human sodium iodide symporter to facilitate deep tissue imaging does not alter oncolytic or replication capability of a novel vaccinia virus. *J. Translat. Med.* **2011**, *9*, 36.

[80] Yoon, A.-R., Kim, J.-H., Lee, Y.-S., Kim, H., Yoo, J.-Y., Sohn, J.-H., Park, B.-W., and Yun, C.-O. Markedly enhanced cytolysis by E1B-19kD-deleted oncolytic adenovirus in combination with cisplatin., *Human Gene Ther*. **2006**, *17*, 379-90.

[81] Cheong, S. C., Wang, Y., Meng, J.-H., Hill, R., Sweeney, K., Kirn, D., Lemoine, N. R., and Halldén, G. E1A-expressing adenoviral E3B mutants act synergistically with chemotherapeutics in immunocompetent tumor models. *Cancer Gene Ther*. **2008**, *15*, 40-50.

[82] Oncology, U. S., and Scotland, G. A controlled trial of intratumoral ONYX-015 , a selectively- replicating adenovirus , in combination with cisplatin and 5- fluorouracil in patients with recurrent head and neck cancer. *Nat. Med*. **2000**, 879-885.

[83] Alonso, M. M., Gomez-Manzano, C., Bekele, B. N., Yung, W. K. A., and Fueyo, J. Adenovirus-based strategies overcome temozolomide resistance by silencing the O6-methylguanine-DNA methyltransferase promoter. *Cancer Res*. **2007**, *67*, 11499-504.

[84] Gomez-Manzano, C., Alonso, M. M., Yung, W. K. A., McCormick, F., Curiel, D. T., Lang, F. F., Jiang, H., Bekele, B. N., Zhou, X., Alemany, R., and Fueyo, J. Delta-24 increases the expression and activity of topoisomerase I and enhances the antiglioma effect of irinotecan, *Clin. Cancer Res*. **2006**, *12*, 556-62.

[85] Ingemarsdotter, C. K., Baird, S. K., Connell, C. M., Öberg, D., Halldén, G., and McNeish, I. A. Low-dose paclitaxel synergizes with oncolytic adenoviruses via mitotic slippage and apoptosis in ovarian cancer., *Oncogene*. **2010**, *29*, 6051-63.

[86] Ma, G., Kawamura, K., Li, Q., Okamoto, S., Suzuki, N., Kobayashi, H., Liang, M., Tada, Y., Tatsumi, K., Hiroshima, K., Shimada, H., and Tagawa, M. Combinatory cytotoxic effects produced by E1B-55kDa-deleted adenoviruses and chemotherapeutic agents are dependent on the agents in esophageal carcinoma., *Cancer Gene Ther*. **2010**, *17*, 803-13.

[87] Adusumilli, P. S., Chan, M.-K., Chun, Y. S., Hezel, M., Chou, T.-C., Rusch, V. W., and Fong, Y. Cisplatin-induced GADD34 upregulation potentiates oncolytic viral therapy in the treatment of malignant pleural mesothelioma. *Cancer Biol. Ther*. **2006**, *5*, 48-53.

[88] Heinemann, L., Simpson, G. R., Boxall, A., Kottke, T., Relph, K., Vile, R., Melcher, A., Prestwich, R., Harrington, K. J., Morgan, R., and Pandha, H. S. Synergistic effects of oncolytic reovirus and docetaxel chemotherapy in prostate cancer., *BMC Cancer*. **2011**, *11*, 221.

[89] Huang, B., Sikorski, R., Kirn, D. H., and Thorne, S. H. Synergistic anti-tumor effects between oncolytic vaccinia virus and paclitaxel are mediated by the IFN response and HMGB1. *Gene Ther*. **2010**, *18*, 164-172.

[90] Sung, C.-K., Choi, B., Wanna, G., Genden, E. M., Woo, S. L. C., and Shin, E. J. Combined VSV oncolytic virus and chemotherapy for squamous cell carcinoma. *The Laryngoscope*. **2008**, *118*, 237-42.

[91] Bagheri, N., Shiina, M., Lauffenburger, D. a, and Korn, W. M. A Dynamical Systems Model for Combinatorial Cancer Therapy Enhances Oncolytic Adenovirus Efficacy by MEK-Inhibition, *PLoS Computational Biology*. **2011**, (Rao, C. V., Ed.) *7*, e1001085.

[92] Nguyen, T. L.-anh, Abdelbary, H., Arguello, M., Breitbach, C., Leveille, S., Diallo, J.-simon, Yasmeen, A., Bismar, T. A., Kirn, D., Falls, T., Snoulten, V. E., Vanderhyden, B. C., Werier, J., Atkins, H., Vaha-Koskela, M. J. V., Stojdl, D. F., Bell, J. C., and Hiscott, J. Chemical targeting of the innate antiviral response by histone deacetylase inhibitors renders refractory cancers sensitive to viral oncolysis. *Proc. Natl. Accad. Sci*. **2008**, *105*, 14981-14986.

[93] Liu, T.-C., Castelo-Branco, P., Rabkin, S. D., and Martuza, R. L. Trichostatin A and oncolytic HSV combination therapy shows enhanced antitumoral and antiangiogenic effects. *Molecular Ther*. **2008**, *16*, 1041-7.

[94] Katsura, T., Iwai, S., Ota, Y., Shimizu, H., Ikuta, K., and Yura, Y. The effects of trichostatin A on the oncolytic ability of herpes simplex virus for oral squamous cell carcinoma cells. *Cancer Gene Ther*. **2009**, *16*, 237-45.

[95] Otsuki, A., Patel, A., Kasai, K., Suzuki, M., Kurozumi, K., Chiocca, E. A., and Saeki, Y. Histone deacetylase inhibitors augment antitumor efficacy of herpes-based oncolytic viruses. *Mol. Ther*. **2008**, *16*, 1546-55.

[96] Mactavish, H., Diallo, J.-S., Huang, B., Stanford, M., Boeuf, F. Le, Silva, N. De, Cox, J., Simmons, J. G., Guimond, T., Falls, T., McCart, J. A., Atkins, H., Breitbach, C., Kirn, D., Thorne, S., and Bell, J. C. Enhancement of vaccinia virus based oncolysis with histone deacetylase inhibitors. *PloS one*. **2010**, *5*, e14462.

[97] Watanabe, T., Hioki, M., Fujiwara, T., Nishizaki, M., Kagawa, S., Taki, M., Kishimoto, H., Endo, Y., Urata, Y., Tanaka, N., and Fujiwara, T. Histone deacetylase inhibitor FR901228 enhances the antitumor effect of telomerase-specific replication-selective adenoviral agent OBP-301 in human lung cancer cells. *Exp. Cell Res*. **2006**, *312*, 256-65.

[98] Bieler, A., Mantwill, K., Dravits, T., Bernshausen, A., Glockzin, G., Köhler-Vargas, N., Lage, H., Gansbacher, B., and Holm, P. S. Novel three-pronged strategy to enhance cancer cell killing in glioblastoma cell lines: histone deacetylase inhibitor, chemotherapy, and oncolytic adenovirus dl520. *Human Gene Ther*. **2006**, *17*, 55-70.

[99] Hōti, N., Chowdhury, W., Hsieh, J.-T., Sachs, M. D., Lupold, S. E., and Rodriguez, R. Valproic acid, a histone deacetylase inhibitor, is an antagonist for oncolytic adenoviral gene therapy. *Mol. Ther*. **2006**, *14*, 768-78.

[100] Xu, W. S., Parmigiani, R. B., and Marks, P. A. Histone deacetylase inhibitors : molecular mechanisms of action. *Oncogene*. **2007**, 5541-5552.

[101] Diallo, J.-S., Boeuf, F. Le, Lai, F., Cox, J., Vaha-Koskela, M., Abdelbary, H., MacTavish, H., Waite, K., Falls, T., Wang, J., Brown, R., Blanchard, J. E., Brown, E. D., Kirn, D. H., Hiscott, J., Atkins, H., Lichty, B. D., and Bell, J. C. A high-throughput pharmacoviral approach identifies novel oncolytic virus sensitizers, *Mol. Ther*. **2010**, *18*, 1123-9.

[102] Passer, B. J., Cheema, T., Zhou, B., Wakimoto, H., Zaupa, C., Razmjoo, M., Sarte, J., Wu, S., Wu, C.-lee, Noah, J. W., Li, Q., Buolamwini, J. K., Yen, Y., Rabkin, S. D., and Martuza, R. L. Identification of the ENT1 antagonists dipyridamole and dilazep as amplifiers of oncolytic herpes simplex virus-1 replication. *Cancer Res*. **2010**, *70*, 3890-3895.

[103] Nagano, S., Perentes, J. Y., Jain, R. K., and Boucher, Y. Cancer cell death enhances the penetration and efficacy of oncolytic herpes simplex virus in tumors. *Cancer Res*. **2008**, *68*, 3795-802.

[104] Boeuf, F. Le, Diallo, J.-simon, Mccart, J. A., Thorne, S., Falls, T., Stanford, M., Kanji, F., Auer, R., Brown, C. W., Lichty, B. D., Parato, K., Atkins, H., Kirn, D., and Bell, J. C. Synergistic interaction between oncolytic viruses augments tumor killing. *Mol. Ther*. **2010**, *18*, 888-895.

[105] Whitmire, J. K. Induction and function of virus-specific CD4+ T cell responses. *Virology*. **2011**, *411*, 216-28.

[106] Naik, J. D., Twelves, C. J., Selby, P. J., Vile, R. G., and Chester, J. D. Immune recruitment and therapeutic synergy: Keys to optimizing oncolytic viral therapy ? *Clin. Cancer Res*. **2011**, *17*, 4214-24.

[107] Errington, F., Steele, L., Prestwich, R., Harrington, K. J., Pandha, H. S., Vidal, L., Bono, J. de, Selby, P., Coffey, M., Vile, R., and Melcher, A. Reovirus Activates Human Dendritic Cells to Promote Innate Antitumor Immunity. *J. Immunol*. **2008**, *180*, 6018-6026.

[108] Prestwich, R. J., Errington, F., Ilett, E. J., Morgan, R. S. M., Scott, K. J., Kottke, T., Thompson, J., Morrison, E. E., Harrington, K. J., Pandha, H. S., Selby, P. J., Vile, R. G., and Melcher, A. Tumor infection by oncolytic reovirus primes adaptive antitumor immunity. *Clin. Cancer Res*. **2008**, *14*, 7358-66.

[109] Gauvrit, A., Brandler, S., Sapede-Peroz, C., Boisgerault, N., Tangy, F., and Gregoire, M. Measles virus induces oncolysis of mesothelioma cells and allows dendritic cells to cross-prime tumor-specific CD8 response. *Cancer Res*. **2008**, *68*, 4882-92.

[110] Ilett, E. J., Prestwich, R. J., Kottke, T., Errington, F., Thompson, J. M., Harrington, K. J., Pandha, H. S., Coffey, M., Selby, P. J., Vile, R. G., and Melcher, A. Dendritic cells and T cells deliver oncolytic reovirus for tumour killing despite pre-existing anti-viral immunity. *Gene Ther*. **2009**, *16*, 689-99.

[111] Boudreau, J. E., Bridle, B. W., Stephenson, K. B., Jenkins, K. M., Brunellière, J., Bramson, J. L., Lichty, B. D., and Wan, Y. Recombinant Vesicular Stomatitis Virus Transduction of Dendritic Cells Enhances Their Ability to Prime Innate and Adaptive Antitumor Immunity. *Mol. Ther*. **2009**, *17*, 1465-1472.

[112] Gujar, S. A., Marcato, P., and Pan, D. Reovirus virotherapy overrides tumor antigen presentation evasion and promotes protective antitumor immunity evasion and promotes protective antitumor immunity. *Mol. Cancer Ther*. **2010**, *9*, 2924-2933.

[113] Sobol, P. T., Boudreau, J. E., Stephenson, K., Wan, Y., Lichty, B. D., and Mossman, K. L. Adaptive antiviral immunity is a determinant of the therapeutic success of oncolytic virotherapy. *Mol. Ther*. **2011**, *19*, 335-344.

[114] Diaz, R. M., Galivo, F., Kottke, T., Wongthida, P., Qiao, J., Thompson, J., Valdes, M., Barber, G. N., and Vile, R. G. Oncolytic immunovirotherapy for melanoma using vesicular stomatitis virus. *Cancer Res*. **2007**, *67*, 2840-8.

[115] Prestwich, R. J., Errington, F., Steele, L. P., Ilett, E. J., Morgan, R. S. M., Harrington, K. J., Pandha, H. S., Selby, P. J., Vile, R. G., and Melcher, A. Reciprocal human dendritic cell-natural killer cell interactions induce antitumor activity following tumor cell infection by oncolytic reovirus. *J. Immunol*. **2009**, *183*, 4312-4321.

[116] Gujar, S. A., Pan, D., Marcato, P., Garant, K. A., and Lee, P. W. K. Oncolytic rirus-initiated protective immunity against prostate cancer. *Mol. Ther*. **2011**, *19*, 797-804.

[117] Steele, L., Errington, F., Prestwich, R., Ilett, E., Harrington, K., Pandha, H., Coffey, M., Selby, P., Vile, R., and Melcher, A. Pro-inflammatory cytokine/chemokine production by reovirus treated melanoma cells is PKR/NF-kappaB mediated and supports innate and adaptive anti-tumour immune priming. *Mol. Cancer. Ther.* **2011**, *10*, 20.

[118] Jarahian, M., Watzl, C., Fournier, P., Arnold, A., Djandji, D., Zahedi, S., Cerwenka, A., Paschen, A., Schirrmacher, V., and Momburg, F. Activation of natural killer cells by Newcastle disease virus hemagglutinin-neuraminidase. *J. Virol*. **2009**, *83*, 8108.

[119] Wongthida, P., Diaz, R. M., Galivo, F., Kottke, T., Thompson, J., Pulido, J., Pavelko, K., Pease, L., Melcher, A., and Vile, R. Type III IFN interleukin-28 mediates the antitumor efficacy of oncolytic virus VSV in immune-competent mouse models of cancer. *Cancer Res*. **2010**, *70*, 4539.

[120] Boudreau, J. E., Stephenson, K. B., Wang, F., Ashkar, A. A., Mossman, K. L., Lenz, L. L., Rosenthal, K. L., Bramson, J. L., Lichty, B. D., and Wan, Y. IL-15 and type I interferon are required for activation of tumoricidal NK cells by virus-infected dendritic cells. *Cancer Res*. **2011**, *71*, 2497.

[121] Bhat, R., Dempe, S., Dinsart, C., and Rommelaere, J. Enhancement of NK cell antitumor responses using an oncolytic parvovirus. *Int. J. Cancer*. **2011**, *919*, 908-919.

[122] Chisholm, S. E., and Reyburn, H. T. Recognition of vaccinia virus-infected cells by human natural killer cells depends on natural cytotoxicity receptors. *J. Virol*. **2006**, *80*, 2225-2233.

[123] Ramsburg, E., Publicover, J., Buonocore, L., Poholek, A., Robek, M., Palin, A., and Rose, J. K. A vesicular stomatitis virus recombinant expressing granulocyte-macrophage colony-stimulating factor induces enhanced T-cell responses and is highly attenuated for replication in animals. *J. Virol*. **2005**, *79*, 15043.

[124] Janke, M., Peeters, B., Leeuw, O. De, Moorman, R., Arnold, A., Fournier, P., and Schirrmacher, V. Recombinant Newcastle disease virus (NDV) with inserted gene coding for GM-CSF as a new vector for cancer immunogene therapy. *Gene Ther*. **2007**, *14*, 1639–1649.

[125] Kohno, S.-i, Luo, C., Nawa, A., Fujimoto, Y., Watanabe, D., Goshima, F., Tsurumi, T., and Nishiyama, Y. Oncolytic virotherapy with an HSV amplicon vector expressing granulocyte–macrophage colony-stimulating factor using the replication-competent HSV type 1 mutant HF10 as a helper virus. *Cancer Gene Ther*. **2007**, *14*, 918–926.

[126] Malhotra, S., Kim, T., Zager, J., Bennett, J., Ebright, M., D'Angelica, M., and Fong, Y. Use of an oncolytic virus secreting GM-CSF as combined oncolytic and immunotherapy for treatment of colorectal and hepatic adenocarcinomas. *Surgery*. **2007**, *141*, 520–529.

[127] Thorne, S. H., Hwang, T.-ho H., Gorman, W. E. O., Bartlett, D. L., Sei, S., Kanji, F., Brown, C., Werier, J., Cho, J.-han, Lee, D.-ewon, Wang, Y., Bell, J. C., and Kirn, D. H. Rational strain selection and engineering creates a broad-spectrum , systemically effective oncolytic poxvirus , JX-963. *J. Clin. Invest*. **2007**, *117*, 3350-3358.

[128] Lei, N., Shen, F. B., Chang, J. H., Wang, L., Li, H., Yang, C., Li, J., and Yu, D. C. An oncolytic adenovirus expressing granulocyte macrophage colony-stimulating factor shows improved specificity and efficacy for treating human solid tumors. *Cancer Gene Ther*. **2009**, *16*, 33-43.

[129] Sivendran, S., Glodny, B., Pan, M., Merad, M., and Saenger, Y. Melanoma Immunotherapy. *Mount Sinai J. Med*. **2010**, *77*, 620-642.

[130] Choi, I.-k, Lee, J.-s, Zhang, S.-n, Park, J., Lee, K.-m, Sonn, C. H., and Yun, C.-o. Oncolytic adenovirus co-expressing IL-12 and IL-18 improves tumor-specific immunity via differentiation of T cells expressing IL-12Rb2 or IL-18Ra. *Gene Ther*. **2011**, *18*, 898-909.

[131] Shin, E. J., Wanna, G. B., Choi, B., Aguila, D., Ebert, O., Genden, E. M., and Woo, S. L. Interleukin-12 expression enhances vesicular stomatitis virus oncolytic therapy in murine squamous cell carcinoma. *The Laryngoscope*. **2007**, *117*, 210-4.

[132] Ino, Y., Saeki, Y., Fukuhara, H., and Todo, T. Triple combination of oncolytic herpes simplex virus-1 vectors armed with interleukin-12, interleukin-18, or soluble B7-1 results in enhanced antitumor efficacy., *Clin. Cancer Res*. **2006**, *12*, 643-52.

[133] Janke, M., Peeters, B., Zhao, H., Leeuw, O. De, Moorman, R., Arnold, A., Ziouta, Y., Fournier, P., and Schirrmacher, V. Activation of human T cells by a tumor vaccine infected with recombinant Newcastle disease virus producing IL-2. *Int. J. Oncol*. **2008**, *33*, 823–832.

[134] Lapteva, N., Aldrich, M., Weksberg, D., Rollins, L., Goltsova, T., Chen, S.-Y., and Huang, X. F. Targeting the intratumoral dendritic cells by the oncolytic adenoviral vaccine expressing RANTES elicits potent antitumor immunity. *J. Immunother*. **2009**, *32*, 145-56.

[135] Li, J., Malley, M. O., Urban, J., Sampath, P., Guo, Z. S., Kalinski, P., Thorne, S. H., and Bartlett, D. L. Chemokine Expression From Oncolytic Vaccinia Virus Enhances Vaccine Therapies of Cancer. *Mol. Ther*. **2011**, *19*, 650-657.

[136] Ramakrishna, E., Woller, N., Mundt, B., Knocke, S., Gürlevik, E., Saborowski, M., Malek, N., Manns, M. P., Wirth, T., Kühnel, F., and Kubicka, S. Antitumoral immune response by recruitment and expansion of dendritic cells in tumors infected with telomerase-dependent oncolytic viruses. *Cancer Res*. **2009**, *69*, 1448-58.

[137] Miller, J., Bidula, S. M., Jensen, T. M., and Reiss, C. S. cytokine-modified VSV is attenuated for neural pathology, but is both highly immunogenic and oncolytic. *Int. J. Interferon Cytokine Mediator Res*. **2010**, *1*, 15-32.

[138] Woller, N., Knocke, S., Mundt, B., Gurlevik, E., Struver, N., Kloos, A., Boozari, B., Schache, P., Manns, M. P., Malek, N. P., Sparwasser, T., Zender, L., Wirth, T. C., Kubicka, S., and Kuhnel, F. Virus-induced tumor inflammation facilitates effective DC cancer immunotherapy in a Treg-dependent manner in mice. *J. Clin. Invest*. **2011**, *121*, 2570-82.

[139] Zhang, S. N., Choi, I. K., Huang, J. H., Yoo, J. Y., Choi, K. J., and Yun, C. O. Optimizing DC Vaccination by Combination With Oncolytic Adenovirus Coexpressing IL-12 and GM-CSF. *Mol. Ther*. **2011**, *19*, 1558-68.

[140] Wongthida, P., Diaz, R. M., Pulido, C., Rommelfanger, D., Galivo, F., Kaluza, K., Kottke, T., Thompson, J., Melcher, A., and Vile, R. Activating Systemic T-Cell Immunity Against Self Tumor Antigens to Support Oncolytic Virotherapy with Vesicular Stomatitis Virus. *Hum. Gene Ther*. **2011**, *11*, 1-11.

[141] Bridle, B. W., Stephenson, K. B., Boudreau, J. E., Koshy, S., Kazdhan, N., Pullenayegum, E., Brunellière, J., Bramson, J. L., Lichty, B. D., and Wan, Y. Potentiating cancer immunotherapy using an oncolytic virus. *Mol. Ther*. **2009**, *18*, 1430-1439.

[142] Kottke, T., Errington, F., Pulido, J., Galivo, F., Thompson, J., Wongthida, P., Diaz, R. M., Chong, H., Ilett, E., Chester, J., Pandha, H., Harrington, K., Selby, P., Melcher, A., and Vile, R. Broad antigenic coverage induced by vaccination with virus-based cDNA libraries cures established tumors, *Nat. Med*. **2011**, *17*, 854-9.

[143] Jordan, C. T.; Guzman, M. L.; Noble, M. Cancer stem cells. *New Engl. J. Med.* 2006, 355, 1253-61.

[144] Dean, M.; Fojo, T.; Bates, S. Tumor stem cells and drug resistance. *Nat. Rev. Cancer* 2005, 5, 275-84.

[145] Frank, N. Y.; Schatton, T.; Frank, M. H. The therapeutic promise of the cancer stem cell concept. *J. Clin. Invest.* 120, 41-50.

[146] Cripe, T. P.; Wang P-Y.; Marcato, P.; Mahller, Y.Y.; Lee, P.W.K. Targeting cancer-initiating cells with oncolytic viruses. *Mol. Ther.* 2009, 17(10), 1677-82.

[147] Short, J.J.; Curiel, D.T. Oncolytic adenovirus targeted to cancer stem cells. *Mol. Cancer Ther.* 2009; 8(8), 2096-2102.

[148] Eriksson, M.; Guse, K.; Bauerschmitz, G.; Virkkunen, P.; Tarkkanen, M.; Tanner, M.; Hakkarainen, T.; Kanerva, A.; Desmond, R.A.; Personen, S.; Hemminki, A. Oncolytic adenoviruses kill breast cancer initiating $CD44^{+}CD24^{-/low}$ cells. *Mol. Ther.* 2007, 15 (12), 2088-93.

[149] Bauerschmitz, G.J.; Ranki, T.; Kangasniemi, L.; Ribacka, C.; Eriksson, M.; Porten, M.; Herrmann, I.; Ristimaki, A.; Virkkunen, P.; Tarkkanen, M.; Hakkarainen, T.; Kanerva, A.; Rein, D.; Pesonen, S.; Hemminki, A. Tissue-specific promoters active in $CD44^{+}CD24^{-/low}$ breast cancer cells. *Cancer Res.* 2008, 68(14), 5533-9.

[150] Jiang H.; Gomez-Manzano, C.; Aoki, H.; Alonso, M.M.; Kondo, S.; McCormick, F.; Xu, J.; Kondo, Y.; Bekele, N.; Colman, H.; Lang, F.F.; Fueyo, J. Examination of the therapeutic potential of delta-24-RGD in brain tumor stem cells: Role of autophagic cell death. *J. Natl. Cancer Inst.* 2007, 99, 1410-4.

[151] Skog, J.; Edlund, K.; Bergenheim, A.T.; Wadell, G. Adenoviruses 16 and CV23 efficiently transduce human low-passage tumor and cancer stem cells. *Mol .Ther.* 2007; 15: 2140-5.

[152] Zhang, X.; Komaki, R.; Wang, L.; Fang, B.; Chang, J.Y. Treatment of radioresistant stem-like esophageal cancer cells by an apoptotic gene-armed, telomerase-specific oncolyticv adenovirus. *Clin. Cancer Res.* 2008, 14(9), 2813-2823.

[153] Marcato, P.; Dean, C.A.; Giacomantonio, C.A.; Lee, P.W.K. Oncolytic reovirus effectively targets breast cancer stem cells. *Mol. Ther.* 2009, 17(6), 972-79.

[154] Wakimoto, H.; Kesari, S.; Farrell, C.J., Curry, Jr., W.T.; Zaupa, C.; Aghi, M.; Kuroda, T.; Stemmer-Rachamimov, A.; Shah, K.; Liu, T-C., Jeyaretna, D.S.; Debasitis, J.; Pruszak, J.; Martuza, R.L.; Rabkin, S.D. Human glioblastoma-derived cancer stem cells: Establishment of invasive glioma model and treatment with oncolytic herpes simplex virus vectors. *Cancer Res.* 2009, 69(8), 3472-81.

[155] Kanai, R.; Rabkin, S.D.; Yip, S.; Sgubin, D.; Zaupa, C.M.; Hirose, Y.; Louis, D.N.; Wakimoto, H.; Martuza, R.L. Oncolytic virus-mediated manipulation of DNA damage responses: synergy with chemotherapy in killing glioblastoma stem cells. *J. Natl. Cancer Inst.* 2012, 104(1), 42-55.

[156] Kanai, R.; Wakimoto, H.; Martuza, R.L.; Rabkin, S.D. A novel oncolytic herpes simplex virus that synergizes with phosphoinositide 3-kinase/Akt pathway inhibitors to target glioblastoma stem cells. *Clin. Cancer Res.* 2011, 17(11), 3686-96.

[157] Parato, K.A.; Breitbach, C. J.; Le Boeuf, F.; Jiahu Wang, J.; Storbeck, C.; Ilkow, C.; Diallo, J-S., Theresa Falls, T.; Burns, J.; Garcia, V.; Kanji, F.; Evgin, L.; Hu, K.; Paradis, F.; Knowles, S.; Hwang, T-H.; Barbara Vanderhyden, B.C.; Auer, R.; David H Kirn, D.H.; Bell1, J.C. The oncolytic poxvirus JX-594 selectively replicates in and destroys cancer cells driven by genetic pathways commonly activated in cancers. *Mol. Ther.* 2011, in press. doi: 10.1038/mt.2011.276.

Appendix VIII - Targeted inflammation during oncolytic virus therapy severely compromises tumor blood flow.

Breitbach CJ, Paterson JM, **Lemay CG**, Falls TJ, McGuire A, Parato KA, Stojdl DF, Daneshmand M, Speth K, Kirn D, McCart JA, Atkins H, Bell JC.

Mol Ther. 2007 Sep;15(9):1686-93. Epub 2007 Jun 19.

Contribution of author: CG Lemay analyzed the microarray and validated the findings through qPCR as presented in Supplementary Figure 3.

Appendix IX - Vesicular stomatitis virus oncolysis is potentiated by impairing mTORC1-dependent type I IFN production.

Alain T, Lun X, Martineau Y, Sean P, Pulendran B, Petroulakis E, Zemp FJ, **Lemay CG**, Roy D, Bell JC, Thomas G, Kozma SC, Forsyth PA, Costa-Mattioli M, Sonenberg N.

Proc Natl Acad Sci U S A. 2010 Jan 26;107(4):1576-81. Epub 2010 Jan 4.

Contribution of author: CG Lemay did the dissection of brain tissue, homogenization, and RNA extractions, which were then analyzed by qPCR by D Roy.

Appendix X - ORFV: A Novel Oncolytic and Immune Stimulating Parapoxvirus Therapeutic.

Rintoul JL, **Lemay CG**, Tai LH, Stanford MM, Falls TJ, de Souza CT, Bridle BW, Daneshmand M, Ohashi PS, Wan Y, Lichty BD, Mercer AA, Auer RC, Atkins HL, Bell JC.

Mol Ther. 2012 Jan 24. doi: 10.1038/mt.2011.301. [Epub ahead of print]

PMID: 22273579

Contribution of author: CG Lemay provided technical assistance during most flow cytometry experiments, specifically helping with animal dissections, spleen and blood processing, and antibody staining when necessary.

Curriculum Vitae

Work Experience

Consultant, Jennerex Biotherapeutics Inc.
Sept-Nov 2010

- Advised and performed assay development to examine virus-infected cancer cells by flow cytometry to ultimately optimize GMP viral growth conditions.

June 2006-April 2007

- Researched and optimized several protocols for detecting and quantifying virus in clinical samples. Worked closely with government officials and private industry to deliver results in a timely and efficient manner.
- Both assays and results that I generated were integral to a biodistribution study report and new drug submission accepted by the FDA and Health Canada.

Communications Officer (CR-04), Industry Canada, Federal Government
Summer 2003

- Independently organized a training session for over 300 government employees.
- Wrote a post-mortem report on training sessions.

Data Entry Clerk, Industry Canada, Federal Government
Summer 2002

- Worked as part of a team to assemble hundreds of student employment kits.
- Translated French documents to English.

Publications

- **Lemay CG**, *et al*. Harnessing oncolytic virus-mediated anti-tumour immunity in an infected cell vaccine. Accepted at Molecular Therapy, 2012.
- Bridle BW, Chen L, **Lemay CG**, *et al.* Combination of an oncolytic vaccine with an immunosuppressive HDACi leads to enhanced tumor destruction and mitigated autoimmunity. Submitted, May 2012.
- Rintoul J, **Lemay CG**, *et al.* ORFV: a novel oncolytic and immune stimulating parapoxvirus therapeutic. Molecular Therapy. 2012 Jan 24. doi: 10.1038/mt.2011.301
- Alain T, Lun X, Martineau Y, Sean P, Pulendran B, Petroulakis E, Zemp FJ, **Lemay CG**, et al. Vesicular Stomatitis virus oncolysis is potentiated by impairing mTORC1-dependent type 1IFN production. PNAS. 2010. 107 (4): 1576-81
- Breitbach CJ, Paterson JM, **Lemay CG**, *et al*. Targeted inflammation during oncolytic virus therapy severely compromises tumor blood flow. Molecular Therapy. 2007 Sep;15(9):1686-93

Education

PhD Candidate: Sept 2006 – May 2012
University of Ottawa, Faculty of Medicine, Department of Biochemistry

- Supervisor: Dr. John Bell
- Transferred from Masters in May 2008.
- Took 4 graduate classes with an A+ average as part of my doctorate:
  - Molecular Basis of Diseases I
  - Introduction to RNA
  - Advanced Topics in Immunology
  - Molecular Biology of Human Diseases II
- Took several non-compulsory classes:
  - Community Outreach and Media Relations in the Sciences
  - MITACS: Project Management I

University of Ottawa: Bachelors in Biopharmaceuticals – Genomics option (co-op): 2003-2006

- Graduated *magna cum laude* and on the Dean's honour list for all years.
- Honours research performed in Dr. Bell's lab.
- 16 months of co-op placements in Dr. Bell and Dr. Rashmi Kothary labs.

University of Ottawa: Bachelors in Biotechnology (co-op): 2001-2003

- Double degree in chemical engineering and biochemistry.
- On the Dean's honour list as of 2nd year.
- Chose to leave this program and transfer into biopharmaceuticals.

Conferences, Presentations, & Awards

- Some notable conferences attended:
  - Immunopotentiators in Modern Vaccines – Porto, Portugal – Apr 2011
    - Gave an oral presentation on thesis work.
  - 4th-6th International Conferences on Oncolytic Viruses as Cancer Therapeutics (2007-2011)
    - Won a travel award for the 2009 conference
  - 5th Canadian Symposium on Gene Therapy and Vaccines (ATGQ) – 2010
    - Won 1st prize for best poster presentation
  - Ontario Institute for Cancer Research Annual Symposium – Alliston, ON – 2010
  - Keystone Conference on Mobilizing Cellular Immunity for Cancer Therapy (2009)
- Refined presentation skills through 1 oral and 9 poster presentations at conferences.
- Also participated in 5 (2007-2011) Ottawa Hospital Research Institute (OHRI) annual symposia, giving poster presentations at each one.
  - Won 2nd prize in the PhD poster section in 2010.
  - Won the 2011 OHRI IMPACT award (Identification of Marketable Products, Applications and Commercializable Technologies).
- As a graduate student, participated in 6 annual Biochemistry department symposia.
    - Won best PhD poster in 2009 and was elected to represent the University of Ottawa at the national CIHR poster competition.
    - Placed 2nd for my PhD seminar in 2012

Scholarships

- Sept 2008 – Aug 2011 – CIHR Banting and Best Canada Graduate Scholarship
- Sept 2008 – was offered but refused OGS scholarship
- Fall 2008 – Dec 2011 – University of Ottawa Excellence Scholarship
- Sept 2007-Aug 2008 – OGSST
- Winter 2007 – Sceptre Investment Counsel Limited Scholarship of Excellence (OSOFT)
- Fall 2006-Summer 2008 – University of Ottawa Admission Scholarship
- Winter 2005 & Fall 2003 – University of Ottawa Merit scholarship
- Fall 2001-Winter 2002 – Undergrad Admission scholarship

Volunteer Work

- Co-founder and volunteer with the University of Ottawa's chapter of Scientists Without Borders - Sept 2008-2010.
    - Our mandate was to amass working laboratory equipment destined for landfills and send it to developing countries. Successfully shipped over $100,000 worth of equipment to Tanzania.
- Volunteer with "Let's Talk Science" doing activities in grades 2 to 12 helping make science fun, interactive, and interesting. - Sept 2006 to Present
- Learned patience, time management, and organization as assistant coach and trainer for children's ringette teams for 7 years. Developed their skills and improved their confidence.